RESEARCH ARTICLE

A new anchialine *Stephos* Scott from the Yucatan Peninsula with notes on the biogeography and diversity of the genus (Copepoda, Calanoida, Stephidae)

Eduardo Suárez-Morales[1], Martha A. Gutiérrez-Aguirre[2],
Adrián Cervantes-Martínez[2], Thomas M. Iliffe[3]

1 *El Colegio de la Frontera Sur (ECOSUR)-Chetumal, A.P. 424. Chetumal, Quintana Roo 77014, Mexico* **2** *Universidad de Quintana Roo Campus Cozumel. Cozumel, Quintana Roo Mexico* **3** *Department of Marine Biology. Texas A&M University at Galveston, Galveston, TX 77553-1675, USA*

Corresponding author: *Eduardo Suárez-Morales* (esuarez@ecosur.mx)

Citation: Suárez-Morales E, Gutiérrez-Aguirre MA, Cervantes-Martínez A, Iliffe TM (2017) A new anchialine *Stephos* Scott from the Yucatan Peninsula with notes on the biogeography and diversity of the genus (Copepoda, Calanoida, Stephidae). ZooKeys 671: 1–17. https://doi.org/10.3897/zookeys.671.12052

Abstract

Surveys of the anchialine crustacean fauna of the Yucatan Peninsula (YP), Mexico, have revealed the occurrence of calanoid copepods. The genus *Stephos* Scott, 1892, belonging to the family Stephidae is among the most frequent and widely distributed groups in anchialine caves but has not been hitherto recorded from the YP. Recent collections from an anchialine cave in an island off the northern coast of the YP yielded many specimens of a new species of *Stephos*. The new taxon, *S. fernandoi* **sp. n.**, is described here based on male and female specimens. The new species is clearly distinguished from its congeners by the following characters: male left fifth leg with three terminal lamellae plus subdistal process, right leg with distal row of peg-like elements; female fifth leg with single long, acute apical process; genital double-somite with two rows each of 4 long spinules adjacent to operculum; legs 2-4 with articulated setae. The diversity of the genus shows regional differences; the Australia-Western Pacific region is the most diverse (eleven species), followed by the Mediterranean (seven species) and the Northeastern Atlantic (six species); only four species are known from the Northwestern Tropical Atlantic (NWTA). The morphology of the female fifth leg was examined to explore possible biogeographic trends in the genus; patterns suggest multiple colonization events in the highly diverse regions and a relatively recent radiation in the NWTA, characterized by anchialine forms. The introduction of stephid copepods in the region may be a relatively recent event derived from colonization of benthopelagic ancestral forms and subsequent invasion onto cave habitats. The new species appears to be linked to the strictly anchialine *Miostephos*.

Introduction

The primitive calanoid copepod families Epacteriscidae and Ridgewayiidae are the most representative and diverse copepods in anchialine and subterranean environments worldwide (Fosshagen et al. 2001). Other calanoid families with cave-dwelling species are the Arietellidae, Pseudocyclopiidae, Pseudocyclopidae, Fosshageniidae, and Stephidae (Boxshall et al. 1990; Suárez-Morales and Iliffe 1996; Jaume et al. 1999; Fosshagen and Iliffe 2004). The latter family contains marine hyperbenthic forms living in coastal waters and in anchialine habitats. It contains 4 valid genera of which *Stephos* T. Scott, 1892 is the most diverse, currently incorporating 31 species (Bradford-Grieve 1999; Boxshall and Halsey 2004; Moon et al. 2015; Boxshall and Walter 2016). Members of this genus have been reported from tropical to polar latitudes worldwide; *Stephos* has been recognized to frequently inhabit submarine and anchialine caves (Jaume et al. 2008; Kršinić 2012, 2015). The remaining three stephid genera are relatively small, with a restricted distribution; together they contain a total of 6 species (Razouls et al. 2015, 2016). Previous reports of the family Stephidae from the Northwestern Tropical Atlantic (NWTA) include only a few species: *Stephos deichmannae* Fleminger, 1957 from surface plankton in the Gulf of Mexico (Fleminger 1957; Suárez-Morales et al. 2009), *S. lucayensis* Fosshagen, 1970, and *S. exumensis* Fosshagen, 1970, both from bottom samples of the Bahamas (Fosshagen 1970). The two known species of the genus *Miostephos* Bowman, 1976, *M. cubrobex* Bowman, 1976 from Cuba and *M. leamingtonensis* Yeatman, 1980 from Bermuda are other anchialine stephids from the NWTA (Razouls et al. 2015, 2016).

The anchialine crustacean fauna of the Yucatan Peninsula (YP) of Mexico is widely recognized as highly interesting, with many endemic species (Yager 1987; Iliffe 1992; Mercado-Salas et al. 2013; Boxshall et al. 2014). Members of the Ridgewayiidae (Suárez-Morales and Iliffe 2005) and Epacteriscidae (Suárez-Morales et al. 2006) have been hitherto recorded in the YP, but there are no data on the occurrence of other anchialine calanoid families. During a biological survey of the crustacean fauna of an anchialine cave in the island of Cozumel, off the northeastern coast of the YP, many male and female specimens of copepods were collected. A first analysis revealed the presence of a calanoid tentatively identified as belonging to the family Stephidae. A detailed examination revealed that these specimens represent an undescribed species of the genus *Stephos* which is herein described in full and compared with its known congeners. The distribution and diversity of the genus in the NWTA is also analyzed.

Materials and methods

Specimens were collected on 6 July 2014 during a biological survey of an anchialine cave, Cenote Tres Potrillos, on Cozumel Island at 20°27'3.2"N, 86°59'14.4"W, Quintana Roo, Mexico. From a small pool at the cave entrance, a vertical shaft opens into a very large chamber with a halocline at 11 m. Beneath the halocline, sulfidic, fully marine water reaches a maximum depth of 38 m. A 40 m long passage at 12 m depth extends off the side of the main chamber (Mejía et al. 2008, fig. 3). Other anchialine crustaceans from this cave includes the shrimp *Barbouria yanezi* Mejía, Zarza & López, 2008, *Agostocaris* sp., and *Procaris* sp., the isopod *Bahalana* sp., and the amphipod *Mayaweckelia* sp. Plankton specimens were collected in the halocline with the aid of a conical plankton net (50 μm mesh size). The collected material was fixed and preserved in 100% ethanol. The copepods were sorted from the original sample and then transferred to glycerol. Specimens were prepared for taxonomic analysis by dissecting all appendages and light staining them with Methylene blue; the appendages were examined as temporary mounts in glycerine and sealed with Entellan® as permanent mounts. Drawings were prepared using a camera lucida mounted on an E-200 Nikon compound microscope with Nomarski DIC at magnifications of 1000X. Male and female specimens were prepared for SEM examination with a JEOL SM-6010 microscope at facilities of ECOSUR in Chetumal, Mexico. The process included dehydration of specimens in progressively higher ethanol solutions (60, 70, 80, 96, 100%) and drying with a treatment with hexamethyldisilazane (HMDS). Terminology of the body parts and appendages followed Huys and Boxshall (1991). Body length was measured from the anterior margin of the cephalosome to the posterior margin of the caudal rami. The type specimens are deposited in the collection of zooplankton held at El Colegio de la Frontera Sur (ECOSUR), Chetumal, Quintana Roo, Mexico (ECO-CHZ) and in the National Museum of Natural History, Smithsonian Institution (USNM) (MSC, Maryland), United States. Original samples are deposited at the Universidad de Quintana Roo (UQROO) Campus Cozumel, Mexico.

Results

Order Calanoida Sars, 1903
Family Stephidae T. Scott, 1892
Genus *Stephos* T. Scott, 1892

***Stephos fernandoi* sp. n.**
http://zoobank.org/DD961DAC-CECF-49A2-86D7-30A9E13270A1
Figures 1–4

Material examined. Holotype. One adult ♀, collected on 6 July 2014 from the anchialine cave of Cenote Tres Potrillos, Cozumel Island (20°27'3.2"N, 86°59'14.4"W),
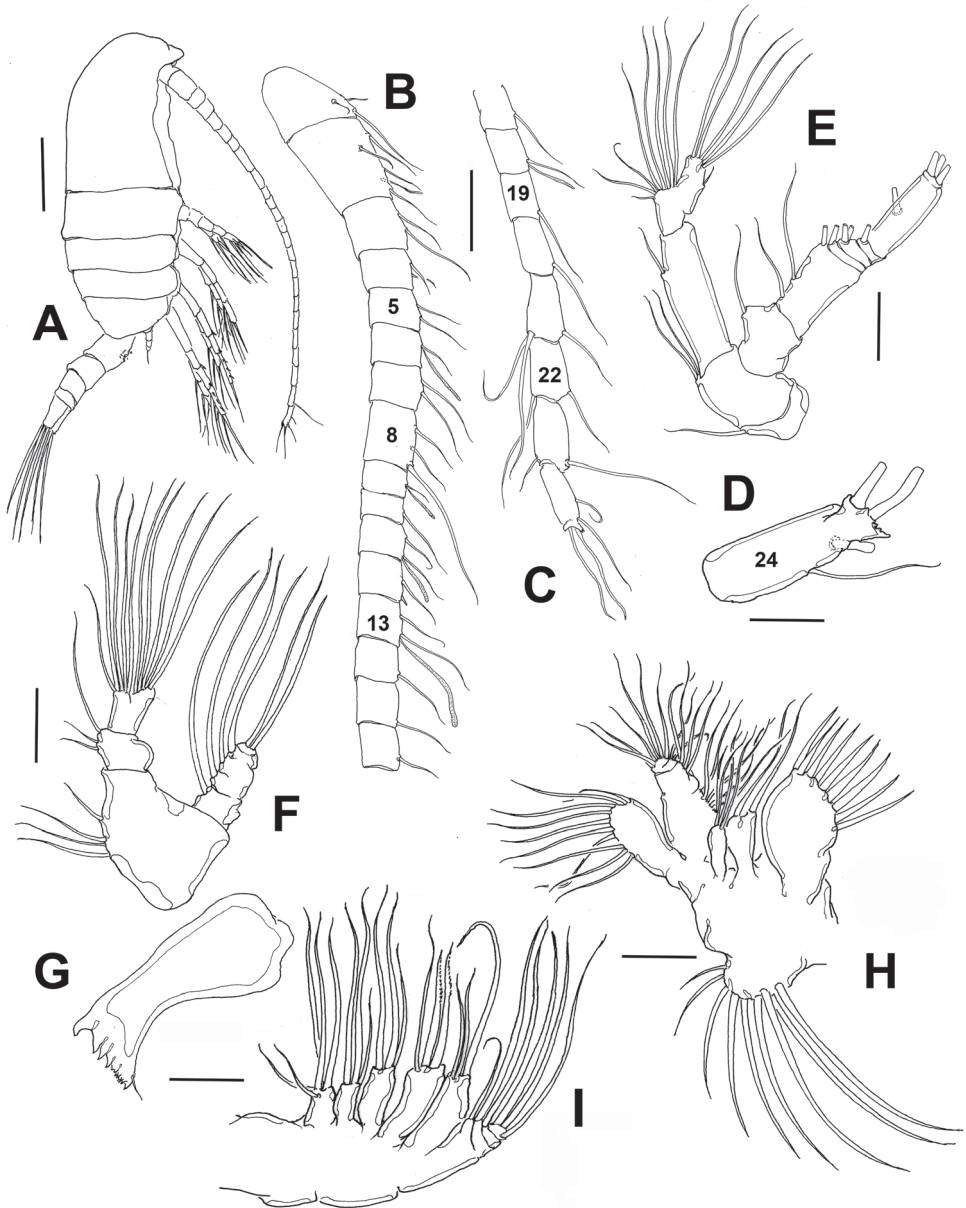
Figure 1. *Stephos fernandoi* sp. n., adult female from Cozumel, Mexico. **A** habitus, lateral view **B** antennule, segments 1–16 **C** antennule segments 17–24 **D** antennule segment 24 showing apical process **E** antenna **F** mandibular palp **G** gnathal base **H** maxillule **I** maxilla. Scale bars: **A** 100 μm; **D** 10 μm; **B, C, E–I** 20 μm.

Quintana Roo, Mexico. Specimen dissected on slide deposited in the collection of Zooplankton of El Colegio de la Frontera Sur (ECOSUR) in Chetumal, Mexico, under number ECO-CHZ-09411. Allotype: one adult ♂, collected on same date and

site, specimen dissected (ECO-CHZ-09412). Paratypes: four dissected adult ♀♀, one dissected adult ♂, slides (ECO-CHZ-09413), two undissected ♀♀, eight undissected ♂♂ (ECO-CHZ-09414), and three undissected ♀♀, three ♂♂ (USNM-1422288), all from same date and site, ethanol-preserved, vials.

Descriptions. *Female*. Mean length of prosome: 0.343 mm (*n* = 13); total length including caudal rami = 0.475 mm (*n* = 13). Body with typical calanoid shape, relatively robust in lateral and dorsal views, prosome 5-segmented, widest at first pedigerous somite (Figs 1A, 4A, B). Cephalosome and first pedigerous somite completely separate, fourth and fifth pedigerous somites fused, with posterolateral corners rounded, moderately produced, symmetrical (Fig. 4A). Rostrum weakly developed, represented by small medial expansion, rostral points absent (Fig. 4C). Urosome 4-segmented, representing 31% of total body length. Genital double-somite relatively long, almost 40% of urosome, barrel-shaped, symmetrical, weakly expanded mid-ventrally, expansion associated with genital field (Fig. 2J). Single gonopore opening ventrally at proximal 1/3 of somite; adjacent ventral surface of somite ornamented with 4 slender spiniform elements (arrowed in Fig. 4E) inserted at each side of simple, transverse genital operculum. Anal somite shortest of urosome, subrectangular, about 10% of urosome length, cuticular ornamentations absent on dorsal and ventral surfaces (Figs 2J, 4F).

Caudal rami subrectangular, symmetrical, length/width ratio = 1.6–1.7, armed with 6 caudal setae (II-VII) (Fig. 4F). Inner margin naked except for displaced dorsal seta (VII) inserted on proximal 1/4 of inner margin, seta reaching beyond distal margin of ramus (Fig. 4F). Caudal seta I absent, seta II (Fig. 4F) reduced, inserted near base of seta III. Terminal setae III-VI well developed. All ramal setae biserially plumose.

Antennule (Fig. 1B–D) 24-segmented, reaching posterior margin of preanal somite. Armature per segments as follows: segmental number (ancestral segment, setae (s) + aesthetasc (ae)): 1(I-II, 3s); 2(III-IV,4s + ae), 3(V, 2s), 4(VI, 2s), 5(VII, 2s), 6(VIII, 1s + ae), 7(IX, 2s), 8(X-XI, 3s), 9 (XII, 1s+ae), 10 (XIII, 1s), 11(XIV, 2s + ae), 12(XV, 2s), 13(XVI, 2s + ae), 14(XVII, 1s), 15(XVIII, 1s), 16(XIX, 1s), 17(XX, 1s), 18(XXI,1s + ae), 19 (XXII,1s), 20(XXIII,1s), 21(XXIV,2s +1s), 22(XXV,1s +1s), 23(XXVI, 1s +1s), 24(XXVII-XXVIII, 3s + ae) (Figs 1B–D). One of the setal elements on segment 12 spiniform (arrow in Fig. 4D). Distal segment with apical acute process present in some specimens (Fig. 1D).

Antenna (Fig. 1E) biramous, with exopod longer than endopod. Coxa armed with one seta. Basis with two distal subequal setae on medial margin. Endopod 2-segmented, first segment long, cylindrical, with short seta inserted at 2/3 of medial margin; distal portion of terminal segment with two lobes, proximal lobe with 8 setae; distal lobe with single short, lateral seta plus five long terminal setae. Exopod indistinctly 7-segmented, first segment with one long seta, second segment longest, armed with three setae, one proximal, one medial and one on distal position. Segments 3–6 with 1, 2, 1, 1 setae, respectively. Distal segment with crown of three long, terminal setae, subequal in length and diameter.

Mandible (Fig. 1G) with gnathobase armed with four large monocuspid ventral teeth plus three smaller bicuspid teeth, dorsal monocuspid tooth, and short dorsal
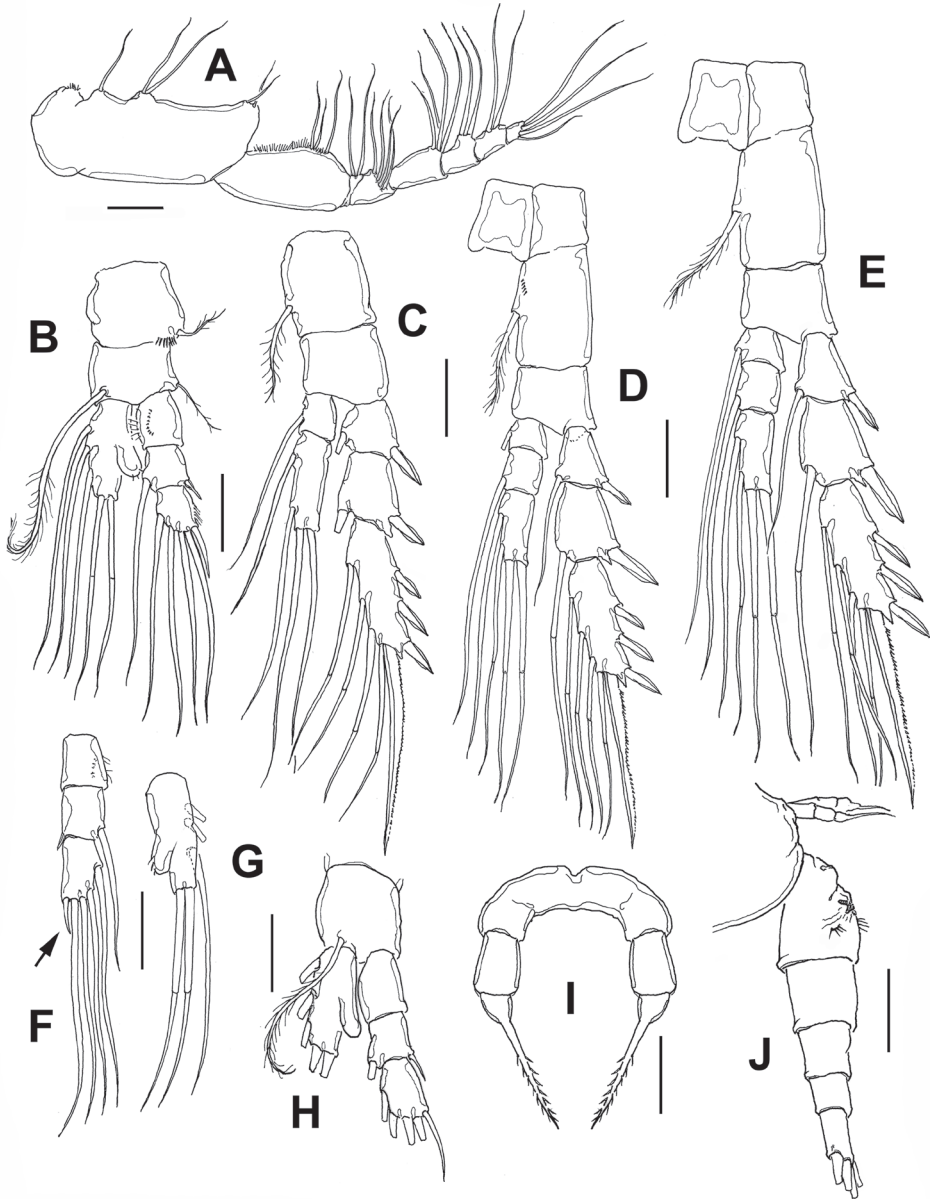
Figure 2. *Stephos fernandoi* sp. n., adult female from Cozumel, Mexico. **A** maxilliped **B** leg 1 **C** leg 2 **D** leg 3 **E** leg 4 **F** leg 1 exopod, another specimen showing reduced outermost apical spine (arrow) **G** leg 1 endopod, another specimen **H** male leg 1 **I** female leg 5, anterior view **J** fifth pedigerous somite and urosome, lateral view. Scale bars: **A–I** 20 μm; **J** 50 μm.

seta. Serial teeth distinctly separated from large ventralmost tooth by diastema. Palp biramous (Fig. 1F), basis robust, armed with four subequal setae inserted on medial margin. Endopod short, 2-segmented; proximal segment with two short and one long

setae, outer margin protuberant; distal segment subrectangular, with 10 setae, one reduced. Exopod indistinctly 5-segmented, armed with 1, 1, 1, 1, 2 setae.

Maxillule (Fig. 1H) with praecoxal arthrite bearing nine spiniform marginal setae. Coxal epipodite with nine setae, coxal endite with two setae. Basis with proximal endite bearing four setae, distal basal endite armed with five setae. Endopod reduced, not articulated to basis, indistinctly 3-segmented, proximal segment with four setae, second segment with two setae, distal segment with six. Exopod oblong, with ten subequal setae.

Maxilla (Fig. 1I) indistinctly 6-segmented including precoxa, coxa, allobasis and 3-segmented endopod. Praecoxal and coxal endites with 5, 3, 3, 3 setae, distal coxal endite with two stout spinulated setae. Basal endite of allobasis with 3 setae, incorporated endopodal segment with single seta. Free endopodal segments armed with 1, 1, 3 setae.

Maxilliped (Fig. 2A) indistinctly nine-segmented, precoxa and coxa partially fused, precoxa unarmed, with cluster of spinules. Coxa with three groups of setae, proximal endite with 1 seta, middle endite with two, distal with two. Basis ornamented with row of short spinules; armed with 3 setae, one shorter than the rest. Endopod six-segmented, armed as follows: 2, 4, 4, 2, 2, 4. Basal and endopodal setae slender, distally attenuated.

Legs 1-4 (Fig. 2B–E) biramous, increasing in size posteriorly. First swimming leg (Fig. 2B) with three-segmented exopod and one-segmented endopod; coxa subrectangular, with short outer coxal seta not reaching distal margin of basal segment; row of spinules at insertion of coxal seta. Basipod with long, recurved inner plumose seta reaching beyond distal margin of third exopodal segment; outer basipodal seta slender. Endopod with outer knob ornamented with 1–3 minute apical setules (Fig. 2B, G). First exopodal segment with row of spinules. Outer spine on third exopodal segment elongate, spine shorter in some specimens (arrowed in Fig. 2F). Second leg with two-segmented endopod (Fig. 2C), legs 3 and 4 with three-segmented exopods and endopods, with articulate setae (Fig. 2D, E). Armature formula of legs 1–4 as in Table 1.

Fifth legs (Fig. 2I) reduced, symmetrical, uniramous, two-segmented with proximal segment cylindrical, distal segment proximally globose, forming long spiniform bipinnate apical process (Figs 2I, 4G, H).

Male. Body slightly longer than female, average total length: 0.493 mm (n =10); length of prosome: 0.31 mm (Fig. 3A). Rostrum as in female. Urosome 5-segmented, representing 32% of total body length. First urosomite symmetrical; anal somite shortest. Caudal rami relatively short, symmetrical, caudal setae as in female.

Left and right antennules 24-segmented, lacking geniculation, slightly longer than in female when extended posteriorly; antennulary armature as in female. Mouthparts and swimming legs 1–4 as in female.

Fifth legs (Figs 3B, 4I–L) uniramous, asymmetrical. Left leg five-segmented, about as long as right counterpart; proximal segment widest of ramus, with inner margin expanded. Second, third, and fourth segments elongate, fourth with triangular plate on distomedial angle; distal segment with three terminal lamellae tapering distally plus subdistal subtriangular process, and with short seta inserted proximally on medial mar-
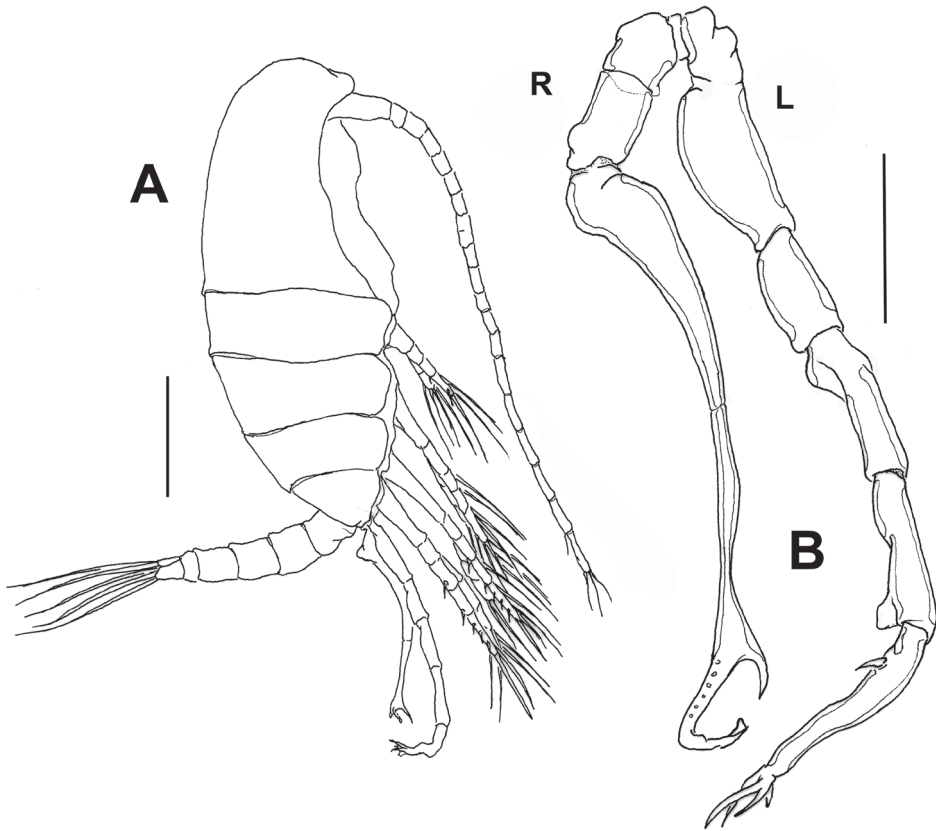
Figure 3. *Stephos fernandoi* sp. n., adult male from Cozumel, Mexico. **A** habitus, lateral view **B** leg 5. L=left ramus, R= right ramus. Scale bars: **A** 100 μm; **B** 50 μm.

Table 1. Armature formula of swimming legs 1-4. Roman numerals indicate spines and Arabic numerals are setae.

	coxa	basis	exopod	endopod
leg 1	0-1	1-1	0-0; I-1; I,2,2	0,2,3
leg 2	0-1	0-0	I-1; I-1; III,I,4	0-1; 0,2,2
leg 3	0-1	0-0	I-1; I-1; III,I,4	0-1; 0-1; 0,2,2
leg 4	0-1	0-0	I-1; I-1; III,I,4	0-1; 0-1; 0,2,2

gin (Fig. 4J). Right fifth leg (Fig. 3B) four-segmented, first and second segments cylindrical, robust, unarmed. Third segment elongate and tapering. Fourth segment very slender and bifurcating distally into "C"-shaped structure furnished with 6–8 peg-like elements along bifurcation (Fig. 4L). End of subdistal process acute, opposite end with apical leaf-like expansion (Fig. 4K).

Etymology. The new species is named after the Mexican carcinologist Dr. Fernando Alvarez (Instituto de Biología, UNAM, Mexico), who has significantly contrib-

uted to the knowledge of the Mexican crustacean fauna, particularly from caves and anchialine habitats.

Remarks. The new species was included in the diverse stephid genus *Stephos* based on its possession of the following characters: 1) cephalosome and first pedigerous somite separate, pedigers 4–5 partially fused, 2) female urosome 4-segmented, male five-segmented; 3) caudal rami with 4 terminal setae (III–VI), dorsal caudal seta VII inserted on inner margin; 4) antennules 24-segmented in male and female, lacking geniculation in male; 5) female leg 5 uniramous, one or two-segmented, distal segment tapering, ornamented; 6) male fifth legs uniramous, strongly asymmetrical, modified into grasping organ, left leg five-segmented, with complex distal segment, right leg slender (Bradford-Grieve 1999).

Based on the morphology of the male fifth legs, Bradford-Grieve (1999) divided the species of *Stephos* into four distinct groups. The new species *S. fernandoi* can be assigned to "group IV" by its possession of a male right leg 5 with a narrow fourth segment. Currently, this group includes nine species: *S. pentacanthos* Chen & Zhang, 1965 from off China, *S. tsuyazakiensis* Tanaka, 1966 from Japan, *S. rustadi* Strömgren, 1969 from Norway, *S. morii* Greenwood, 1977 from Australia, *S. pacificus* Ohtsuka & Hiromi, 1987 from Japan, *S. angulatus* Bradford-Grieve, 1999 from New Zealand, *S. marsalensis* Costanzo, Campolmi & Zagami, 2000 from Italy, *S. vivesi* Jaume, Boxshall & Gràcia, 2008 from the Balearic Islands, and *S. goejinensis* Moon, Yeon & Venmathi Maran, 2015 from Korea (see table 1 in Bradford-Grieve 1999; Jaume et al. 2008; Moon et al. 2015).

The new species is the only one in this group with a right leg 5 ramus combining a distal segment (segment 4) with diverging processes set at right angles with acute tips plus a series of peg-like elements along the longest process (Fig. 4L). It differs from *S. angulatus* because in this species, the processes are both apically rounded and the segment lacks the peg-like elements observed in the new species. The left ramus has a similar structure in both species, with segment 4 bearing a distal lobular process (Bradford-Grieve 1999, fig. 8; Fig. 4L) and three distal lamellae, but the new species has an additional subdistal process (Figs 3B, 4J). In *S. marsalensis,* the distal segment of right male P5 is unbranched (Costanzo et al. 2000, fig. 4d), thus diverging from the bifid condition found in *S. fernandoi*; also, the left leg has five lamellate hyaline processes on the distal segment vs. only three such processes in the new species. The anchialine *S. vivesi* has a left leg with eight narrow lamellae and a relatively simple, spatulate distal segment of the right leg with two proximal processes (Jaume et al. 2008, fig. 2b–d), thus diverging from the pattern observed in the new species. The fifth leg of the new species differs from that of *S. geojinensis* in the number of lamellae on the distal segment of the left leg, three (Fig. 4J) vs. seven long plus 13 short lamellae, and right leg with distal segment bifurcate, with both branches subequally long (Fig. 3B) vs. outer branch extremely long, inner branch reduced (Moon et al. 2015, fig. 4d). The same kind of distally asymmetrical right fifth leg is present in *S. tsuyazakiensis* (Tanaka 1966, fig. 1o), thus differing from the new species. In *S. morii*, the right leg distal segment has a strong inner bulb-like
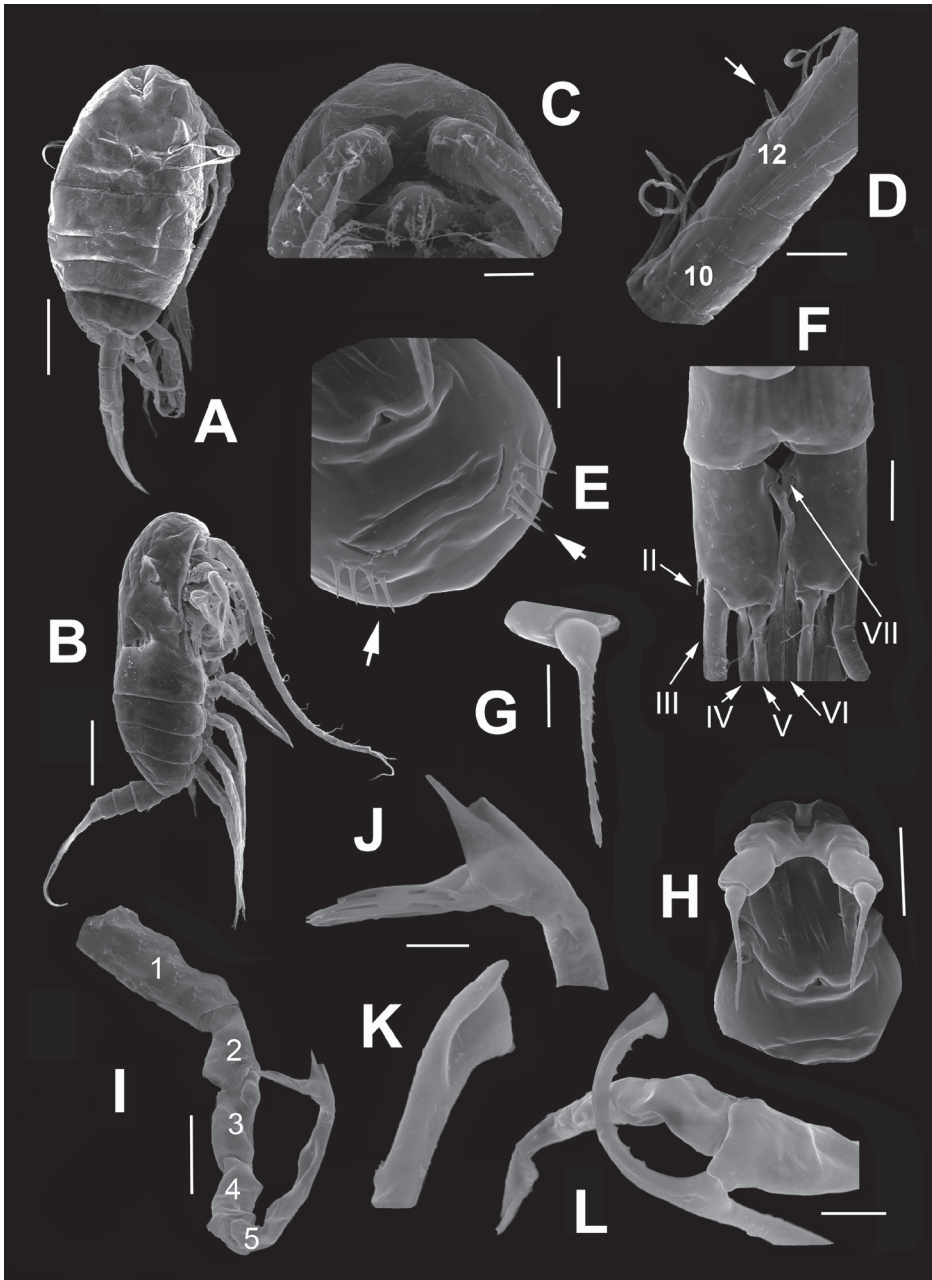
Figure 4. *Stephos fernandoi* sp. n., from Cozumel, Mexico. SEM-processed specimens. Female. **A** habitus, semi-lateral view **B** same, lateral view, another specimen **C** rostrum, ventral view **D** antennule segments 9–13, spiniform seta on segment 12 arrowed **E** genital double-somite, ventral surface showing ornamentation (arrows) **F** caudal rami showing caudal setae II-VII, ventral view **G** distal segment of leg 5 **H** leg 5, ventral view. Male. **I** left leg 5 showing segmentation **J** same, detail of distal segment **K** right leg 5, distal segment, detail of apical end **L** right leg 5, distal segment. Scale bars **A, B** 100 μm; **C, D, H, I** 20 μm, **E–G, L** 10 μm; **J, K** 5 μm.

process (Greenwood 1977, fig. 4g) which is absent in the new species; also, the left leg terminal segment has a long, distinctive spiniform process on subdistal position which is not present in *S. fernandoi* (Fig. 3B). In *S. rustadi*, the right leg distal segment is chela-like, with an expanded inner margin and the left leg is clearly shorter that its right counterpart and has three distinctive hook-like processes (Strömgren 1969, fig. 3f), thus diverging from the fifth leg structure of the new species. In *S. penthacanthos*, the right fifth leg has a spiniform process on the outer margin and the terminal segment is modified into a long, slender claw-like process, curved inwardly (Chen and Zhang 1965, fig. 20.5), thus differing from the spatulate distal segment described in the new species. In *S. pacificus*, the right fifth leg distal segment is relatively simple, represented by an elongate, narrow unbranched structure (Ohtsuka and Hiromi 1987, fig. 3f), different from the pattern observed in the new species, clearly branched (Fig. 3B).

The female fifth leg of *S. fernandoi* differs from that known in most species of *Stephos*, which has a medial seta and/or a row of spinules on the distal segment. It most closely resembles the fifth legs of the two species of *Miostephos*, *M. cubrobex* from Cuba (Bowman 1976, fig. 13) and *M. leamingtonensis* from Bermuda (Yeatman 1980, fig. 5), both with an attenuated unarmed distal segment. The new species differs in the genus characters (i.e. three-segmented female urosome, six-segmented left male fifth leg, reduced male right fifth leg strongly resembling the female fifth leg) (Bowman 1976). In species of *Stephos*, the female genital double-somite has widely different patterns of ornamentation on the ventral and/or lateral surfaces, including rows of spinules with both symmetrical and asymmetrical arrangements (Ohtsuka and Hiromi 1987; Bradford-Grieve 1999; Costanzo et al. 2000), lack of surface ornamentation, as in *S. canariensis* (Boxshall et al., 1990) or *S. grieveae* (Kršinić, 2015) or a highly modified, strongly asymmetrical somite as in *S. exumensis* (Fosshagen, 1970). The new species has a unique pattern combining a symmetrical genital double-somite with an ornamentation pattern represented by a set of 4 spiniform elements at each side of the genital operculum; this pattern has not been observed in any other species of *Stephos*.

Discussion

The distribution of primitive anchialine copepods (i.e., epacteriscids, misophrioids) in the Caribbean, Yucatan, the Canary Islands, and the tropical Pacific has been taken to indicate their Tethyan origin (Fosshagen et al. 2001; Boxshall and Jaume 2000; Boxshall et al. 2014). There are, however, groups whose invasion of cave habitats and subsequent isolation into anchialine waters is related to more recent events. During the Pleistocene, when the eastern coast of the YP emerged (Iturralde-Vinent and MacPhee 1999), some stygobionts which already were established in caves became isolated by the overlying freshwater lens. Cozumel Island is the most recently emerged land of the YP (Vázquez-Domínguez and Arita 2010) so the new species may represent a second-

ary invasion and probably colonized recently the youngest epicontinental anchialine systems of the YP.

In terms of its known geographic distribution, the 32 known species of *Stephos* occur in different regions each harboring its own, distinctive diversity, as follows:

a) Australia-Western Pacific (eleven species): *S. penthacanthos*, *S. morii*, *S. tropicus* Mori, 1942, *S. tsuyazakiensis*, *S. pacificus* Ohtsuka & Hiromi, 1987, *S. angulatus*, *S. robustus*, *S. kurilensis* Kos, 1972, *S. hastatus* Bradford-Grieve, 1999, *S. geojinensis*, *S. projectus* Moon, Youn & Venmathi Maran, 2015.
b) Mediterranean (seven species): *S. gyrans* (Giesbrecht, 1893), *S. margalefi* Riera, Vives & Gili, 1991, *S. vivesi*, *S. cryptospinosus* Zagami, Campolmi & Costanzo, 2000, *S. marsalensis*, *S. boettgerschnackae* Kršinić, 2012, *S. grieveae* Kršinić, 2015.
c) Northeastern Atlantic (six species): *S. canariensis* Boxshall, Stock & Sánchez, 1990, *S. rustadi*, *S. minor* Scott, 1892, *S. scotti* Sars, 1902, *S. fultoni* Scott T. & A., 1898, *S. lamellatus* Sars, 1902.
d) Northwestern Tropical Atlantic (four species): *S. deichmannae*, *S. exumensis*, *S. lucayensis*, *S. fernandoi*.
e) Polar (three species): *S. antarcticum* Wolfenden, 1908, *S. longipes* Giesbrecht, 1902, *S. arcticus* Sars, 1909.
f) Indo-Pacific (one species): *S. maculosus* Andronov, 1974.

The genus is most diverse in the Australia-Western Pacific region, followed by the Northeastern Atlantic and the Mediterranean. There are no records of *Stephos* from the Southwestern and Southeastern Atlantic and the Eastern Pacific (Fig. 5). Regional endemism is high; there are no confirmed records regarding the occurrence of any species of *Stephos* in more than one of these regions (Razouls et al. 2015, 2016). The restricted distribution of the anchialine stephid genera and species in the NWTA region (Fosshagen 1970; Bowman 1976; Yeatman 1980) and in other areas with a rich anchialine fauna (i.e., Mediterranean) suggest that the new species, *S. fernandoi*, is endemic to Cozumel Island. *Stephos fernandoi* is the third species of anchialine calanoid copepod recorded in the YP and represents the second record of the family Stephidae in Mexican waters (Suárez-Morales et al. 2009).

Stephids are in general benthopelagic or anchialine forms, strongly associated with the bottom communities, but some species are known from the plankton (Fleminger 1957; Kos 1972; Ohtsuka and Hiromi 1987; Costanzo et al. 2000; Zagami et al. 2000; Moon et al. 2015). Except for the planktonic *S. deichmannae*, all the stephids found in the NWTA are cave-dwelling anchialine forms (Fosshagen 1970; Bowman 1976; Yeatman 1980). The availability of cave habitats in the NWTA region has favored a highly endemic stephid fauna, likely younger and less speciose but comparable with that of the Mediterranean.
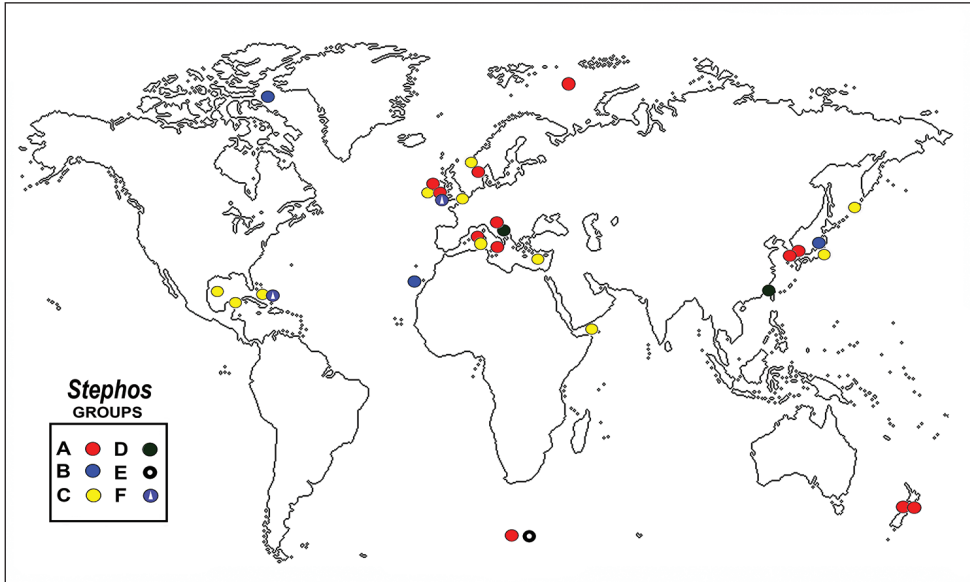
Figure 5. Geographic distribution of *Stephos* female fifth leg groups **A–F**. Group **A** lateral seta present, segment apically elongate **B** lateral seta present, segment not apically elongate, short **C** lateral seta absent, segment apically elongate **D** lateral seta present, segment elongate, with additional segmental processes, branched or bifurcate **E** lateral seta absent, segment elongate, with outer segmental processes **F** lateral seta absent, segment short, apically truncate or blunt, leg rami symmetrical or asymmetrical.

Morphological analysis and biogeography

In *Stephos*, the male fifth legs show at least four different morphological patterns (Bradford-Grieve 1999) but little can be inferred from them in terms of biogeographic patterns. In order to explore possible distributional trends in the genus, we examined and grouped the structural patterns of the female fifth leg of 29 species of *Stephos*. These morphological types were based on the development and armature of the distal segment, as follows: A) lateral seta present, segment apically elongate (*S. boettgerschnackae*, *S. cryptospinosus*, *S. angulatus*, *S. rustadi*, *S. vivesi*, *S. geojinensis*, *S. hastatus*, *S. lamellatus*, *S. minor*, *S. longipes*, *S. projectus*); B) lateral seta present, segment not apically elongate, short (*S. arcticus*, *S. canariensis*, *S. tsuyazakiensis*), C) lateral seta absent, segment apically elongate (*S. exumensis*, *S. deichmannae*, *S. maculosus*, *S. scotti*, *S. fernandoi*, *S. kurilensis*, *S. pacificus*, *S. marsalensis*, *S. gyrans*), D) lateral seta present, segment elongate, with additional segmental processes, branched or bifurcate (*S. grieveae*, *S. penthacanthos*); E) lateral seta absent, segment elongate, with outer segmental processes (*S. antarcticum*); F) lateral seta absent, segment short, apically truncate or blunt, leg rami symmetrical or asymmetrical (*S. margalefi*, *S. lucayensis*, *S. fultoni*).

Pattern D was deemed as the most primitive group, followed by groups A and B, also with a lateral seta and an apically elongate or short segment, respectively. The derived pat-

terns are those lacking a lateral seta (i.e., E, C, and F). The known distribution of records of these six groups is presented in Fig. 5. Group D is restricted to the Mediterranean and Japan; the primitive patterns A and B are the most widespread, distributed in the most diverse regions (i.e., the Mediterranean, northeastern Atlantic) and reaching polar and sub-polar latitudes. The derived groups C and F occur in the most diverse regions but they are the only groups present in the Western Hemisphere, restricted to the NWTA region. The distribution of the species diversity and our interpretation of the female fifth leg types suggest the occurrence of different colonization and speciation events in these coastal demersal copepods resulting from geological changes (i.e., marine regressions and transgressions) in each region (see Fleminger 1986; Por 1986; Suárez-Morales 2003). The genus probably passed through different episodes of diversification mainly in regions such as the western Pacific and the Mediterranean, where both primitive and derived patterns of the female fifth legs co-occur (Fig. 5). The complex biogeographic history of the Mediterranean explains the high diversity and co-occurrence of species belonging to at least three of our groups, suggesting distinct origins, and remarkably characterized by their preference for anchialine and cave habitats (Por 1986; Jaume et al. 2008; Kršinić 2015). Contrastingly, the most recent radiation of *Stephos* appears to have taken place in the NWTA, represented by only four species with a derived female fifth leg; three of them are anchialine (*S. lucayensis*, *S. exumensis*, *S. fernandoi*) (Fosshagen 1970; present data) and one is planktonic (*S. deichmannae*) (Fleminger 1957). Furthermore, the new species, *S. fernandoi*, has clear affinities with the two species of *Miostephos*, mainly in the reduced female fifth leg (as in pattern C) (Bowman 1976; Yeatman 1980); it is thus suggested that *Stephos*-like benthopelagic ancestors invaded the region, colonized the caves and one branch subsequently diverged into the *Miostephos* lineage in the NWTA. Similar colonization processes, with diversity/radiation centers in the western Pacific and congeners distributed in the NWTA have been described for other demersal calanoids like *Tortanus* (Ohtsuka & Reid, 1998) and *Bestiolina* (Suárez-Morales & Almeyda-Artigas, 2016). It is speculated that ancestors of *Stephos* probably originated in the Australian-Western-Pacific region and successively colonized the Mediterranean and the northeastern Atlantic. They probably reached the NWTA either through the Isthmus of Panama during the Middle Miocene-Pliocene (Ohtsuka and Reid 1998) although there are no records of *Stephos* from the eastern Pacific coast, or by passive transportation of planktonic forms onto the NWTA. This analysis should be considered tentative as there are still many missing data; a complete morphological revision of incompletely described species, a confirmation of doubtful records, and a phylogenetic analysis including molecular data is expected to reveal more detailed patterns about this genus.

Acknowledgements

References

Bowman TE (1976) *Miostephos cubrobex*, a n. gen. and sp. of copepod from an anchialine pool in Cuba (Calanoida, Stephidae). Proceedings of the Biological Society of Washington 89: 185–190.

Boxshall GA, Halsey SH (2004) An Introduction to Copepod Diversity. The Ray Society, London, 966 pp.

Boxshall GA, Jaume D (2000) Discoveries of cave misophrioids (Crustacea: Copepoda) shed new light on the origin of anchialine faunas. Zoologischer Anzeiger 239: 1–19.

Boxshall GA, Stock JH, Sánchez E (1990) A new species of *Stephos* Scott, 1892 (Copepoda: Calanoida) from and anchialine lava pool on Lanzarote, Canary Islands. Stygologia 5: 33–41.

Boxshall GA, Walter TC (2016) *Stephos* Scott T., 1892. In: Walter TC, Boxshall G (Eds) World of Copepods database. http://www.marinespecies.org/aphia.php?p=taxdetails&id=104239 [on 2016-12-26]

Boxshall GA, Zylinski S, Jaume D, Iliffe TM, Suárez-Morales E (2014) A new genus of speleophriid copepod (Copepoda: Misophrioida) from a cenote in the Yucatan, Mexico with a phylogenetic analysis at the species level. Zootaxa 3821: 321–336. https://doi.org/10.11646/zootaxa.3821.3.2

Bradford-Grieve J (1999) New species of benthopelagic copepods of the genus *Stephos* (Calanoida: Stephidae) from Wellington Harbour, New Zealand. New Zealand Journal of Marine and Freshwater Research 33: 13–27. https://doi.org/10.1080/00288330.1999.9516853

Chen QC, Zhang SZ (1965) The planktonic copepods of the Yellow Sea and the East China Sea. 1. Calanoida. Studia Marina Sinica 7: 20–131.

Costanzo G, Campolmi M, Zagami G (2000) *Stephos marsalensis* new species (Copepoda, Calanoida, Stephidae) from coastal waters of Sicily, Italy. Journal of Plankton Research 22: 2007–2014. https://doi.org/10.1093/plankt/22.10.2007

Fleminger A (1957) New calanoid copepods of the families Aetideidae, Euchaetidae and Stephidae from the Gulf of Mexico. Fishery Bulletin 57: 355–363.

Fleminger A (1986) The Pleistocene equatorial barrier between the Indian and Pacific oceans and a likely cause for Wallace's line. In: Pierrot-Bults AC, van der Spoel S, Zahuranec BJ, Johnson RK (Eds) Pelagic Biogeography. UNESCO, Paris, 84–97.

Fosshagen A (1970) Marine biological investigations in the Bahamas. 12. Stephidae (Copepoda, Calanoida) from the Bahamas, with remarks on *Stephos sinuatus* Willey and *S. arcticus* Sars. Sarsia 41: 37–48. https://doi.org/10.1080/00364827.1970.10411157

Fosshagen A, Boxshall GA, Iliffe TM (2001) The Epacteriscidae, a cave-living family of calanoid copepods. Sarsia 86: 245–348. https://doi.org/10.1080/00364827.2001.10425520

Fosshagen A, Iliffe TM (2004) New epacteriscids (Copepoda, Calanoida) from anchialine caves in the Bahamas. Sarsia 89: 117–136. https://doi.org/10.1080/00364820410004981

Greenwood JG (1977) Calanoid copepods of Moreton Bay (Queensland). 2. Families Calocalanidae to Centropagidae. Proceedings of the Royal Society of Queensland 88: 49–67.

Huys R, Boxshall GA (1991) Copepod Evolution. The Ray Society, London 159, 468 pp.

Iliffe TM (1992) An annotated list of the troglobitic anchialine and freshwater fauna of Quintana Roo. In: Navarro D, Suárez-Morales E (Eds) Diversidad Biológica en la Reserva de la

Biosfera de Sian Ka'an, Quintana Roo, México. Vol. II. México: Centro de Investigaciones de Quintana Roo (CIQRO)/ Secretaría de Desarrollo Social (SEDESOL), 197–217.

Iturralde-Vinent MA, MacPhee RDF (1999) Paleogeography of the Caribbean region: implications for Cenozoic biogeography. Bulletin of the American Museum of Natural History 238: 1–95.

Jaume D, Boxshall GA, Gràcia F (2008) *Stephos* (Copepoda: Calanoida: Stephidae) from Balearic caves (W Mediterranean). Systematics and Biodiversity 6: 503–520. https://doi.org/10.1017/S1477200008002764

Jaume D, Fosshagen A, Iliffe TM (1999) New cave-dwelling pseudocyclopiids (Copepoda, Calanoida, Pseudocyclopiidae) from the Balearic, Canary, and Philippine archipelagos. Sarsia 84: 391–417. https://doi.org/10.1080/00364827.1999.10807346

Kos MS (1972) A new species of *Stephos* (Copepoda, Calanoida) from coastal waters of the Kuril Islands. Crustaceana 23: 113–118. https://doi.org/10.1163/156854072X00282

Kršinić F (2012) Description of *Stephos boettgerschnackae* sp. nov., a new copepod (Calanoida, Stephidae) from an anchialine cave in the Adriatic Sea. Crustaceana 85: 1525–1539. https://doi.org/10.1163/156854012X651718

Kršinić F (2015) Description of *Stephos grieveae* sp. nov. (Calanoida, Stephidae) from an anchialine cave in the Adriatic Sea. Marine Biodiversity Records 8: e125: 1–10. https://doi.org/10.1017/S1755267215001013

Mejía LM, Zarza E, López M (2008) *Barbouria yanezi* sp. nov., a new species of cave shrimp (Decapoda, Barbouriidae) from Cozumel island, Mexico. Crustaceana 81: 663–672. https://doi.org/10.1163/156854008784513474

Mercado-Salas NF, Morales-Vela B, Suárez-Morales E, Iliffe TM (2013) Conservation status of the inland aquatic crustaceans in the Yucatan Peninsula, Mexico: shortcomings of a protection strategy. Aquatic Conservation of Marine and Freshwater Systems 23(6): 939–951. https://doi.org/10.1002/aqc.2350

Moon SY, Youn SH, Venmathi Maran BA (2015) Two new species of benthopelagic *Stephos* (Copepoda, Calanoida, Stephidae) from Korea. ZooKeys 495: 21–40. https://doi.org/10.3897/zookeys.495.7862

Ohtsuka S, Hiromi J (1987) Calanoid copepods collected from the near-bottom in Tanabe Bay on the Pacific coast of the middle Honshu, Japan. III. Stephidae. Publications of the Seto Marine Biological Laboratory 32: 219–232.

Ohtsuka S, Reid JW (1998) Phylogeny and zoogeography of the planktonic copepod genus *Tortanus* (Calanoida: Tortanidae),with establishment of a new subgenus and descriptions of two new species. Journal of Crustacean Biology 18: 774–807. https://doi.org/10.2307/1549154

Por FD (1986) Crustacean Biogeography of the Late Middle Miocene Middle Eastern Landbridge. In: Gore RH, Heck HL (Eds) Crustacean Biogeography. A. Balkema, Rotterdam, 69–84.

Razouls C, de Bovée F, Kouwenberg J, Desreumaux N (2015–2016) Diversity and geographic distribution of marine planktonic copepods. http://copepodes.obs-banyuls.fr/en [December 22, 2016]

Strömgren T (1969) A new species of *Stephos* (Copepoda, Calanoida) from the Norwegian west coast. Sarsia 37: 1–8. https://doi.org/10.1080/00364827.1969.10411141

Suárez-Morales E (2003) Historical biogeography and distribution of the freshwater calanoid copepods (Crustacea: Copepoda) of the Yucatan Peninsula, Mexico. Journal of Biogeography 30: 1851–1859. https://doi.org/10.1111/j.1365-2699.2003.00958.x

Suárez-Morales E, Almeyda-Artigas RJ (2016) A new species of *Bestiolina* (Copepoda, Calanoida, Paracalanidae) from the Northwestern Atlantic with comments on the distribution of the genus. Revista Mexicana de Biodiversidad 87(2): 301–310. https://doi.org/10.1016/j.rmb.2016.05.002

Suárez-Morales E, Ferrari FD, Iliffe TM (2006) A new epacteriscid copepod (Calanoida: Epacteriscidae) from the Yucatan Peninsula, Mexico, with comments on the biogeography of the family. Proceedings of the Biological Society of Washington 119: 222–238. https://doi.org/10.2988/0006-324X(2006)119[222:ANECCE]2.0.CO;2

Suárez-Morales E, Fleeger JM, Montagna PA (2009) Free-living Copepoda of the Gulf of Mexico. In: Felder DL, Camp DK (Eds) Gulf of Mexico – Its Origins, Waters, and Biota, Biodiversity. Texas A&M University Press, 841–870.

Suárez-Morales E, Iliffe TM (1996) New superfamily of Calanoida (Copepoda) from an anchialine cave in the Bahamas. Journal of Crustacean Biology 16(4): 754–762. https://doi.org/10.2307/1549194

Suárez-Morales E, Iliffe TM (2005) A new *Exumella* Fosshagen (Crustacea: Copepoda: Ridgewayiidae) from anchialine waters of the western Caribbean, with comments on regional biogeography. Bulletin of Marine Science 77(3): 409–423.

Tanaka O (1966) Neritic Copepoda Calanoida from the north-west coast of Kyushu. Journal of the Marine Biological Association of India, Symposium on Crustacea 1: 38–50.

Vázquez-Domínguez E, Arita H (2010) The Yucatan Peninsula: biogeographical history 65 million years in the making. Ecography 33: 212–219. https://doi.org/10.1111/j.1600-0587.2009.06293.x

Yager J (1987) *Speleonectes tulumensis*, n. sp. (Crustacea, Remipedia) from two anchialine cenotes of the Yucatan Peninsula, Mexico. Stygologia 3: 160–166.

Yeatman H (1980) *Miostephos leamingtonensis*, a new species of copepod from Bermuda. Journal of the Tennessee Academy of Science 55: 20–21.

Zagami G, Campolmi M, Costanzo G (2000) A new species of *Stephos* T. Scott, 1892 (Copepoda: Calanoida) from coastal waters of Sicily, Italy. Journal of Plankton Research 22: 15–27. https://doi.org/10.1093/plankt/22.1.15

RESEARCH ARTICLE

First description of the male and redescription of the female of *Parahiranetis salgadoi* Gil-Santana (Hemiptera, Reduviidae, Harpactorinae)

Hélcio R. Gil-Santana[1], Adriana Trevizoli Salomão[2], Jader de Oliveira[3]

1 *Laboratório de Diptera, Instituto Oswaldo Cruz, Av. Brasil, 4365, 21040-360, Rio de Janeiro, RJ, Brazil*
2 *Programa de Pós-graduação em Ecologia, Instituto de Biologia, Universidade Estadual de Campinas, CP 6109, 13083-970, Campinas, SP, Brazil* **3** *Laboratório de Parasitologia, Universidade Estadual Paulista "Julio de Mesquita Filho", Faculdade de Ciências Farmacêuticas UNESP/FCFAR, Rodovia Araraquara Jaú, KM 1, 14801-902, Araraquara, SP, Brazil*

Corresponding author: *Hélcio R. Gil-Santana* (helciogil@uol.com.br; helciogil@ioc.fiocruz.br)

Citation: Gil-Santana HR, Salomão AT, Oliveira J (2017) First description of the male and redescription of the female of *Parahiranetis salgadoi* Gil-Santana (Hemiptera, Reduviidae, Harpactorinae). ZooKeys 671: 19–48. https://doi.org/10.3897/zookeys.671.11985

Abstract

The male of *Parahiranetis salgadoi* Gil-Santana, 2015 is described for the first time, with a redescription of the female of this species based on additional specimens. Comments on possible mimicry and crypsis exhibited by adults and nymphs of this species, respectively, are provided.

Keywords

Graptocleptes, Harpactorini, Heteroptera, *Hiranetis*, Neotropics, sexual dimorphism, wasp mimicry

Introduction

Harpactorinae is the largest subfamily of Reduviidae and is represented by the tribes Apiomerini and Harpactorini in the Neotropical region (Gil-Santana et al. 2015). Harpactorini is the most diversified Reduviidae group with more than 53 recognized genera in the Neotropical region (McPherson and Ahmad 2011, Forero 2011, 2012, Swanson 2012, Gil-Santana 2015, Gil-Santana et al. 2015). Several taxa of Harpactorini

are thought to be involved in mimicry systems with Hymenoptera (Champion 1899, Elkins 1969, Maldonado and Lozada 1992, Hogue 1993, Gil-Santana 2008, Forero and Giraldo-Echeverry 2015, Gil-Santana 2015, 2016). They resemble bees or wasps in general body and wing coloration as well as physical proportions (Haviland 1931, Leathers and Sharkey 2003, Gil-Santana 2008, 2015, 2016). The striking resemblance resulting from this mimicry has frequently led to the confounding of some closely related genera, such as *Hiranetis* Spinola, 1840 and *Graptocleptes* Stål, 1866 (Gil-Santana et al. 2013).

Sexual dimorphism has been recorded in several species of Harpactorini. In a number of species belonging to *Zelus* Fabricius, 1803, for example, males and females differ drastically in size, body configuration, and coloration (Zhang et al. 2016). In addition to the bigger size and larger abdomen of females, males in several genera have larger eyes and/or a basally-thickened third antennal segment. The latter has been considered to be among the diagnostic features at generic level (Stål 1872, Champion 1899, Martin-Park et al. 2012, Gil-Santana et al. 2013, Gil-Santana 2016). However, sexual dimorphism may also be limited to minor differences in coloration and size, as in many species of *Zelus* (Zhang et al. 2016).

Male genitalia have been found to provide useful diagnostic characteristics for distinguishing species within the genera of Harpactorini (e.g. Elkins 1954a,b, Hart 1975, 1986, 1987, Forero et al. 2008, Zhang et al. 2016). The parameres, medial process of the pygophore, dorsal phallothecal plates, and the struts were the main structures with attributes important at the specific level in studies of *Aristathlus* Bergroth, 1913 (Forero et al. 2008), *Atopozelus* Elkins, 1954 (Elkins 1954a), *Atrachelus* Amyot & Serville, 1843 (Elkins 1954b), *Ischnoclopius* Stål, 1868 (Hart 1975) and *Zelus* (Hart 1986, 1987, Zhang et al. 2016). The endosoma contents, such as its processes, were not examined or recorded in most of these studies. Nevertheless, they have been described for one species of *Graptocleptes* (*G. bicolor* (Burmeister, 1838); Gil-Santana et al. 2013) and one of *Hiranetis* (*H. atra* Stål, 1872; Gil-Santana 2016). These genera are considered to be closely related to each other (Stål 1872, Champion 1899) and to *Parahiranetis* Gil-Santana, 2015 (Gil-Santana 2015, 2016), allowing for important comparisons of several diagnostic traits of male genitalia.

Parahiranetis is a monotypic genus containing the wasp-mimicking species *P. salgadoi* Gil-Santana, 2015. This genus was described based on two female specimens collected in the middle of last century (holotype) and in its first half (paratype) in Rio de Janeiro, Brazil (Gil-Santana 2015). Following the publication of the species, the second author (ATS) informed the first author (HRG-S) that she had observed and collected specimens of a wasp-mimicking reduviid in São Paulo, a state neighboring Rio de Janeiro, the type-locality. Surprisingly, the species that she observed was *P. salgadoi.* Through this opportunity, we were able to obtain both males and females, which allowed us to provide the first description of the male and a redescription of the female of this species and also record the morphological variability occurring in this species. We also provide photographs of live immature and adult specimens. The apparent mimicry and crypsis shown by the adults and nymphs, respectively, are also discussed.

Materials and methods

The specimens described here are deposited in the Entomological Collection of the National Museum of the Federal University of Rio de Janeiro (Museu Nacional da Universidade Federal do Rio de Janeiro), Rio de Janeiro, Brazil (**MNRJ**). When citing the text on the labels of a pinned specimen, a slash (/) separates the lines and a double slash (//) different labels. All measurements are in millimeters (mm).

All fieldwork, including observation and collection of the living specimens from the state of São Paulo, was undertaken by the second author (ATS), who also pinned and dried these specimens for subsequent study. She obtained images of live specimens (Figs 43, 59–63) using a Canon EOS 60D digital camera with a Canon EF 100 mm macro lens.

Scanning electron microscopy images (Figs 4–5, 14–16, 18–21, 46–47, 54, 57–58) were obtained by the third author (JO). The male and female adults and adult female external genitalia from *P. salgadoi* were cleaned in an ultrasound machine. Subsequently, the samples were dehydrated in alcohol, dried in an incubator at 45 ºC for 20 min, and fixed in small aluminum cylinders with transparent glaze. Sputtering metallization was then performed on the samples for 2 minutes at 10 mA in an Edwards sputter coater. After this process, the samples were studied and photographed using a Topcon SM-300 scanning electron microscope, as described by Rosa et al. (2010, 2014).

The photo of the female holotype of *Isthmiade braconides* (Perty, 1832) (Coleoptera: Cerambycidae: Cerambycinae: Rhinotragini) (Fig. 64), which is deposited in the Bavarian State Collection of Zoology (Zoologische Staatssammlung München, ZSM), Munich, Germany, was kindly provided by Dr Steve Lingafelter (Arizona, USA).

All remaining figures were produced by the first author (HRG-S). The fixed adults, microscopic preparations and genitalia were photographed using digital cameras (Nikon D5200 with a Nikon Macro Lens 105 mm, Sony DSC-W830 and Sony DSC-HX400V). Drawings were made using a *camera lucida*. For clarity, the vesture (setation) was omitted in the ink drawings of Figs 23 and 24. Images were edited using Adobe Photoshop 7.0.

Observations were made using a stereoscope microscope (Zeiss Stemi) and a compound microscope (Leica CME). Measurements were made using a micrometer eyepiece. The total length of the head was measured excluding the neck, for better uniformity of this measurement. Antennal segments were cleared in 20% NaOH solution for 72 hours for microscopic examination (Figs 6–10, 12–13, 49–52). Dissections of the male genitalia were made by first removing the pygophore from the abdomen with a pair of forceps and then clearing it in 20% NaOH solution for 24 hours. Following this procedure, the phallus was found to have spontaneously and completely inflated in one male (Figs 26–29). In another three specimens, the phallus was almost completely everted by carefully pulling on the dorsal endosomal processes using a pair of fine forceps (Figs 30–33). The dissected structures were studied and photographed in glycerol.

General morphological terminology mainly follows Schuh and Slater (1995). Currently, there is a lack of consensus about the terminology to be applied to female and male genitalia in Reduviidae (e.g. Rédei and Tsai 2011). Therefore, in order to maintain uniformity with previous works about species of Harpactorini, the terminology of the male and female genitalia structures follows Davis (1969), Forero et al. (2008), Gil-Santana et al. (2013) and Gil-Santana (2016).

Taxonomy

Subfamily Harpactorinae
Tribe Harpactorini

Parahiranetis salgadoi Gil-Santana, 2015
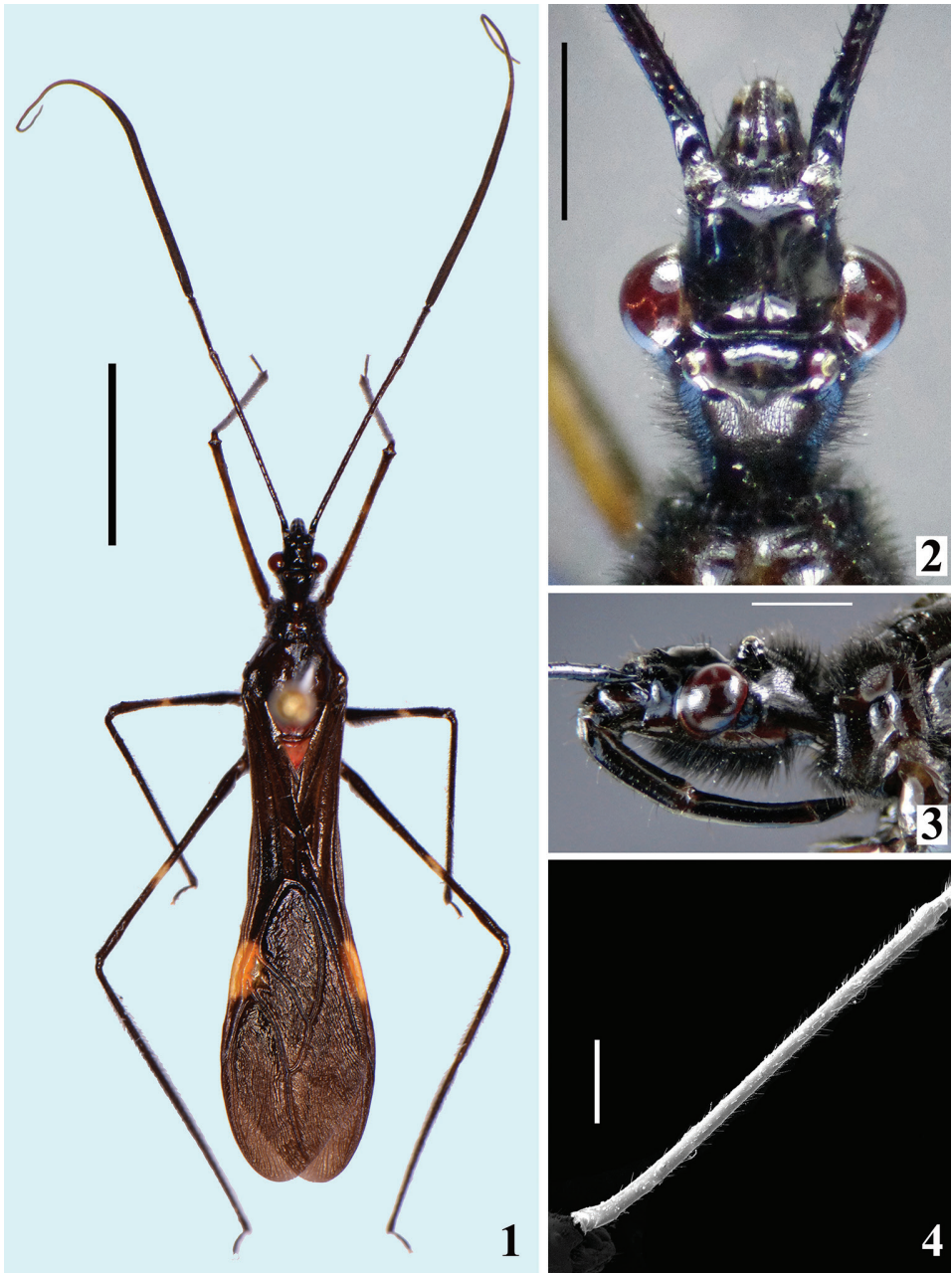Figures 1–63

Parahiranetis salgadoi Gil-Santana, 2015: 32 [description], 33 [Figures 1–4], 34 [Figures
    5–7], 34–35 [description]; Gil-Santana 2016: 93 [citation].

Material examined. *Parahiranetis salgadoi*. **Type material. BRAZIL**, Rio de Janeiro, Rio de Janeiro Municipality, **Holotype** (female): Floresta da Tijuca [Tijuca Forest] / D[istrito] Federal [currently, Rio de Janeiro] / 31.x.1951 / C. A. Campos Seabra [leg.] // [ex] Coleção [Collection] Campos Seabra // 'XXXII' // Holotipo [red label] // *Parahiranetis salgadoi* Gil-Santana, 2015 / Gil-Santana det., (MNRJ); **Paratype** (female): Rio de Janeiro / 20.ix.[19]36 / H. S. Lopes [leg.] // Paratipo [red label] // *Parahiranetis salgadoi* Gil-Santana, 2015 / Gil-Santana det., (MNRJ).

  Additional specimens. BRAZIL, São Paulo, Jundiaí, Serra do Japi, 21.x.2014, 23°13'S, 46°56'W, 1.013 m.a.s.l., 01 female, 01 male, 30.x.2014, 23°14'S, 46°55'W, 900 m.a.s.l., 01 male, 31.x.2014, 23°14'S, 46°55'W, 900 m.a.s.l., 02 males, 03.xi.2014, 23°14'S, 46°55'W, 900 m.a.s.l., 03 females, 01 male, 14.xi.2014, 23°14'S, 46°55'W, 900 m.a.s.l., 01 female, 01 male, 21.xi.2014, 23°13'S, 46°56'W, 1.013 m.a.s.l., 02 males, 1.014 m.a.s.l., 02 females, 01 male, A.T. Salomão leg., (MNRJ).

  Description. MALE. Measurements are given in Table 1.

  Coloration: general coloration black, sometimes brownish, with reddish portions (Figs 1–3). Head, including antennae, black (Figs 2–3). Thorax mostly blackish; in some specimens variable blackish-brown on pleura, sterna and ventral portion of coxae; dark-reddish on anterior half of midline on fore lobe of pronotum, including midlongitudinal sulcus, in most specimens; disc of scutellum bright reddish; hemelytra generally black, sometimes dark brown, with a yellowish spot on external and mid-distal portions of corium (Fig. 1), reaching adjacent part of membrane, especially in basal portion of distal cell of membrane (Fig. 17); in one specimen a small dark-reddish spot present at extreme base of hemelytra, adjacent to propleura. Hind wing mostly brownish-black, with clear area at basal portion and in four lines parallel to veins (Fig. 17).

Figures 1–4. *Parahiranetis salgadoi* Gil-Santana, male. **1** dorsal view **2–3** head **2** dorsal view **3** lateral view **4** antennal segment I, lateral view. Scale bars: 5.0 mm (**1**); 1.0 mm (**2–4**).

Fore femur black to dark brown, frequently with dorsal surface paler, with dark yellowish tinge, and with a yellowish annulus; the latter is as distinct as the annuli on other femora in few specimens, but in most of them, it is very faint, sometimes almost

Table 1. Measurements (mm) of male specimens (N=9) of *P. salgadoi* from São Paulo State.

Measurement	Mean	SD	Maximum	Minimum
Body length to tip of hemelytra	18.0	0.82	19.5	17.0
Body length to tip of abdomen	13.75	0.53	14.7	13.2
Head length (excluding neck)	2.26	0.04	2.3	2.2
Anteocular portion length	0.93	0.04	1.0	0.85
Postocular portion length	0.71	0.03	0.75	0.65
Head width across eyes	1.7	0.05	1.8	1.62
Interocular distance	0.85	0.06	0.9	0.71
Transverse width of eye	0.39	0.01	0.4	0.38
Length of eye	0.61	0.02	0.67	0.60
Antennal segment I length	5.48	0.12	5.7	5.3
Antennal segment II length	1.66	0.06	1.7	1.5
Ant. segment III length **(n = 6)**	9.25	0.35	9.7	8.9
Ant. segment IV length **(n = 3)**	2.03	0.15	2.2	1.9
Max. width ant. seg. III **(n = 6)**	0.26	0.02	0.32	0.24
Labial segment II length	1.33	0.08	1.5	1.25
Labial segment III length	1.33	0.08	1.5	1.25
Labial segment IV length	0.45	0.05	0.5	0.35
Ocellar tubercle width	0.95	0.05	1.0	0.9
Pronotum length	2.57	0.17	2.95	2.4
Pronotum maximum width	2.95	0.14	3.3	2.85
Scutellum length	0.93	0.03	1.0	0.9
Fore femur length	5.62	0.07	5.7	5.6
Fore tibia length	5.97	0.14	6.25	5.8
Fore tarsus length	0.66	0.009	0.67	0.65
Mid femur length	4.9	0.09	5.0	4.8
Mid tibia length	6.3	0.17	6.5	6.0
Mid tarsus length	0.66	0.009	0.67	0.65
Hind femur length	6.7	0.14	6.9	6.5
Hind tibia length	9.4	0.33	9.8	9.0
Hind tarsus length	0.7	0.02	0.75	0.65
Abdomen length	7.78	0.39	8.5	7.2
Abdomen maximum width	2.3	0.36	2.7	1.8

imperceptible, and is situated somewhat distally to midportion of fore femora; this annulus is approximately 1/8 to 1/11 as long as fore femur and its midpoint is about 8 to 11% distal from midpoint of fore femur. Mid and hind femora black, with an evident yellowish annulus situated somewhat distally to midportion of each femur. On mid femora, the annulus is approximately 1/7 to 1/10 as long as the segment and its midpoint is about 5 to 8% distal from midpoint of mid femur, while on hind femora, the same relationships are around 1/8 to 1/11 and 7 to 9%, respectively. In few specimens, the submedian annuli of the mid and hind femora are clearer, almost whitish at midportion of each femur. Tibia and tarsi black; claws clearer, dark-yellowish, sometimes
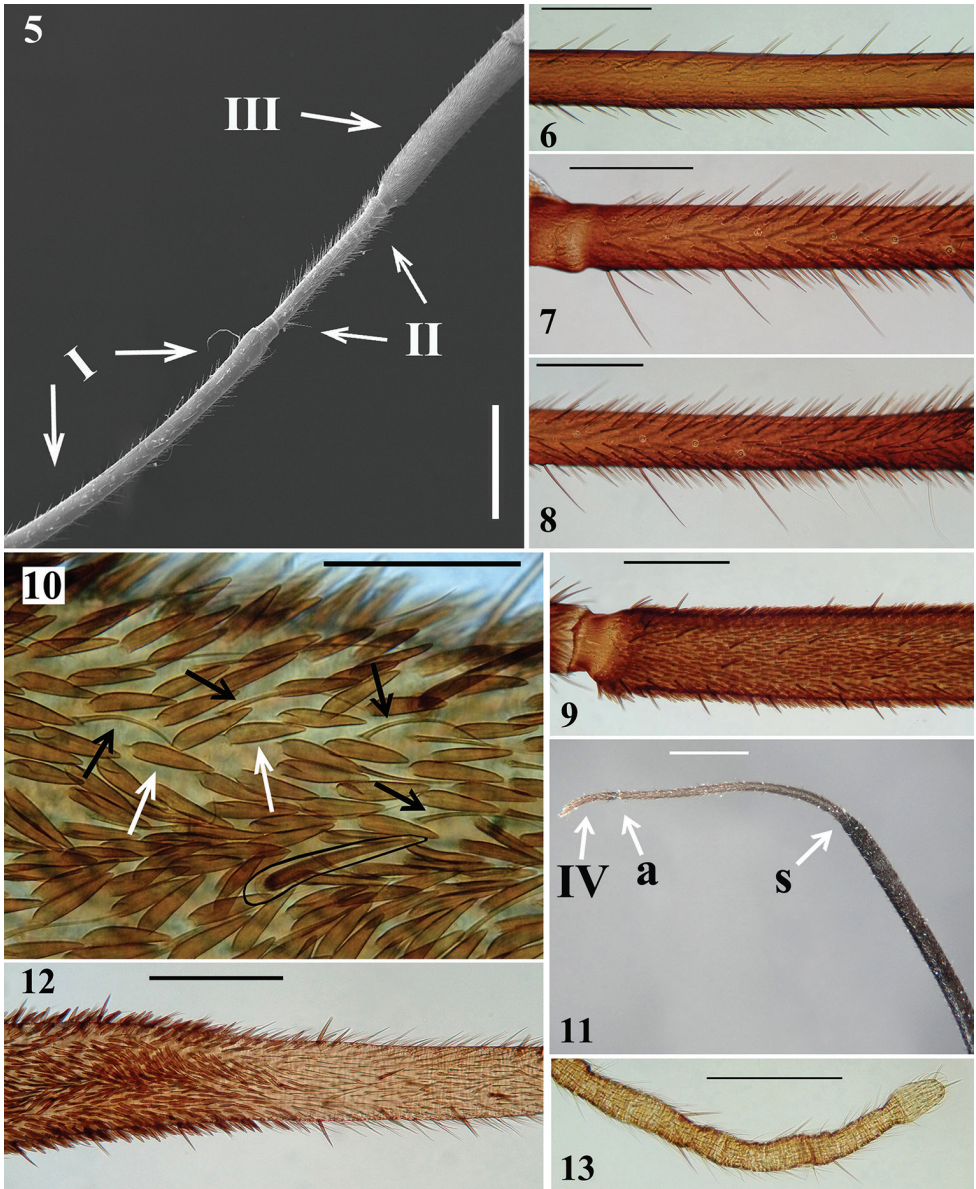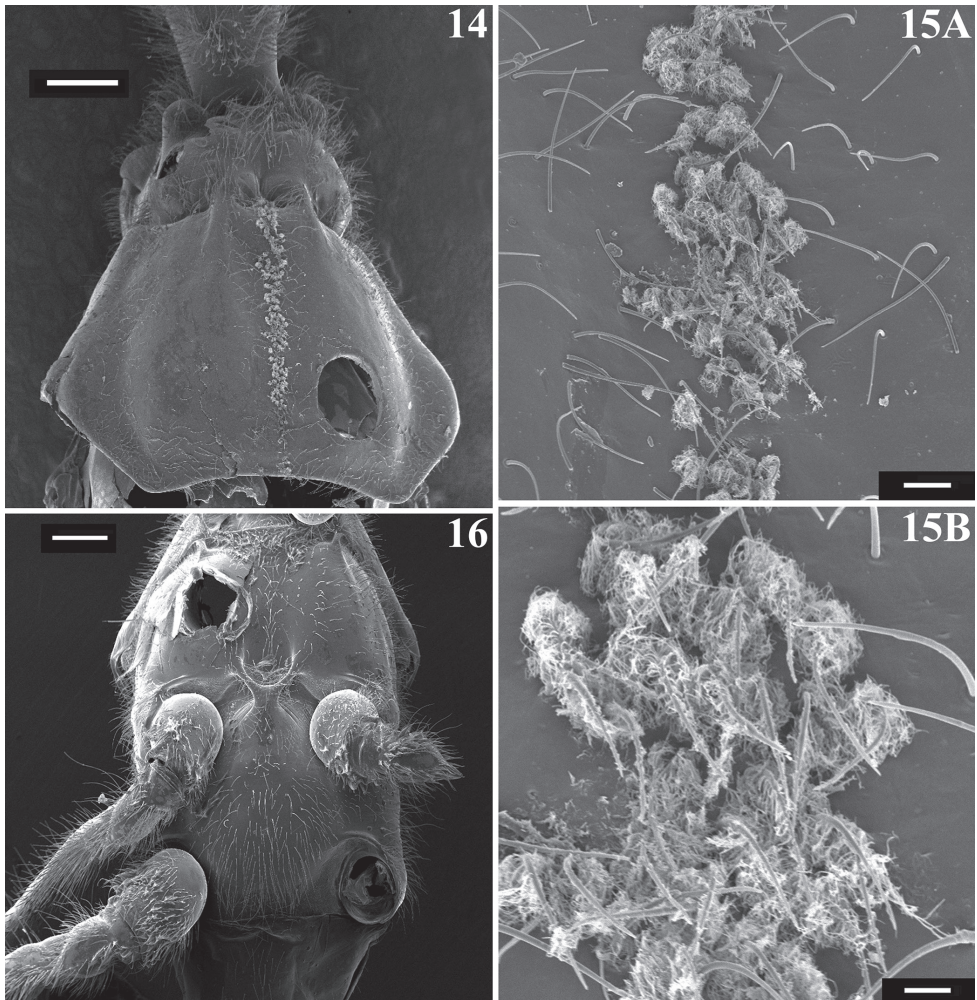
Figures 5–13. *Parahiranetis salgadoi* Gil-Santana, male antenna. **5** apical half of segment I, segment II and basal portion of segment III **6** segment I, midportion **7–8** segment II **7** basal half **8** distal half **9–10** segment III **9** basal portion **10** small area under higher magnification (a stiff darkened seta contoured; black arrows point to thin pale setae; white arrows point to blackish stiff adpressed setae) **11** segments III (distal half) and IV (basal half). (**s**: point of clear separation between the thickened and thinner portions; **a**: articulation between segment III and IV; IV: fourth segment, partially broken) **12** segment III, region of the transition between the thickened and thinner portions **13** segment IV, distal half. Scale bars: 1.0 mm (**5, 11**); 0.3 mm (**6–9, 12, 13**); 0.1 mm (**10**).

with some reddish tinge. Abdomen: segment II (first visible) almost completely reddish; somewhat elevated transverse anterior area on sternite II is clear, light-yellowish to yellowish; in many specimens, there is a very small linear blackish spot on superior portion of anterior margin of sternite II, just below connexivum. Sternite III mostly reddish, with connexivum completely blackish or mostly blackish with only extreme base or basal half reddish, or only with superior margin darkened; in some specimens area near connexivum is also darkened or blackish to a varying extent. Sternite IV mostly blackish, reddish laterally on anterior half; extent of reddish coloration is variable among specimens; remaining sternites and pygophore almost completely blackish; most specimens with a very small reddish spot on posterolateral angle of last sternite, just below connexivum; other small variations in some specimens: reddish faint tinge on inferior portion of connexivum of sternites IV and/or V; median portion of sternites VI and/or VII brownish-black to a varying extent.

Structure and vestiture: integument mostly shiny, smooth. In some specimens, a thin layer or small patches of sticky substance variably cover integument of antennal segment I and legs, especially on femora and tibiae of fore and mid legs, and/or are scattered on thorax and sternites. Head (Figs 2–3): elongate, approximately 1.3 to 1.4 times as long as width across eyes (length measured excluding neck), almost completely glabrous between eyes; integument shiny, with sparse long and short, straight or somewhat curved blackish setae, which are much denser, forming pubescence of long blackish thick setae on postocular portion and gula. Anteocular portion slightly longer than postocular; the latter, in dorsal view, narrowing gradually to form the neck. Postantennal spines small, somewhat acute or slightly rounded. Interocular sulcus deep, well-marked, curved laterally. A very shallow pair of elevations present anterior to interocular sulcus; sometimes, a thin midlongitudinal furrow present between these elevations. Antenna inserted at level of upper third of eye; antennal segments I and II straight (Figs 1, 4–5); segment I approximately 2.5 times longer than head, with shiny and smooth integument and very sparse, short (with variable lengths), stiff, darkened setae, which become more numerous on mesal surface, approximately in distal two-thirds (Figs 4–6); segments II–IV opaque; segment II, except at glabrous extreme base, covered with numerous short, stiff, semi-erect dark setae, intermixed with similar but longer setae, and a few (about eight to ten) very much thinner isolated elements (interpreted as trichobothria), which are present laterally on basal two-thirds and anteriorly on distal third (Figs 5, 7–8); segment III variably curved (Fig. 1), approximately 1.7 times longer than segment I, conspicuously thickened approximately in basal two-thirds (Figs 1, 5, 9, 11); thickened portion clearly separated in relation to the distal thinner portion (Figs 11–12) and, except at extreme base (which is glabrous) (Fig. 9), completely covered with very short, stiff, blackish, adpressed setae, and with scattered stiff, darkened, semi-erect setae (about twice longer) and a pubescence formed by longer, very thin, pale setae, which are almost imperceptible in this portion (Figs 9–10); distal third of segment III (Fig. 12) and segment IV (Fig. 13) covered with dense pubescence formed by short, thin, pale to whitish setae and with scattered short, darkened, stiff, semi-erect setae; the latter somewhat less numerous on segment IV; segment IV thinnest, moder-

ately curved, with its apex rounded; after drying, segment IV commonly appears to be very distorted with some portions shriveled (Fig. 13). Eyes globose, glabrous, projecting laterally, prominent in dorsal view, reaching dorsal margin of head at interocular sulcus, not reaching ventral margin of head, which is far from inferior margin of the eye (Figs 2–3). Ocelli elevated, much closer to eyes than to each other (Fig. 2). Clypeus straight (Fig. 2). Labium stout, curved, with scattered and somewhat curved, longer and thinner dark setae, reaching prosternum at proximal or mid portion; segment II (first apparent) thickest, straight, reaching level of middle portion of eyes, as long as segment III; segment III somewhat curved, reaching or almost reaching level of anterior margin of prosternum; segment IV shortest, triangular, tapering (Fig. 3). Thorax with shiny and mostly smooth integument; prothorax covered with very numerous blackish, thick setae on fore lobe of pronotum and anterior portions of propleura; hind lobe of pronotum with more sparse, shorter and thinner setae on dorsal portion, while on midline thin, short and whitish setae form a midlongitudinal line; basal portion of these setae is frequently covered with rounded, flocky patches of white wax-like substance, enhancing this white stripe (Figs 14–15). Anterior collar inconspicuous; anterolateral angles rounded. Midlongitudinal sulcus on fore lobe of pronotum becoming abruptly deeper at transverse sulcus to form a depression; lateral to the depression, two ill-defined oblique sulci present; transverse sulcus of pronotum not very deep, interrupted before middle by a pair of submedian shallow carina; midlongitudinal furrow on hind lobe very shallow or not evident; lateral longitudinal sulci well marked at posterior half to posterior two-thirds of hind lobe of pronotum (Fig. 14). Humeral angle elevated, rounded at lateral margin (Fig. 14). Scutellum subtriangular, elevated at disc, sometimes somewhat depressed at anterior portion, with scattered, moderately long, dark setae; apex acute, covered with thin, whitish setae, which frequently are basally covered by rounded, flocky patches of white wax-like substance. Posterior portion of propleura, mesopleura, metapleura and thoracic sterna covered with long darkened setae. Mesopleura and metapleura without tubercles. In some specimens, there is a patch of thin whitish setae basally covered with rounded, flocky patches of white wax-like substance, extending from superior margin and posterior portion of mesopleura to anterior portion of metapleura. Mesosternum somewhat elevated laterally, with a median U-shaped carina posteriorly (Fig. 16). Legs: coxae almost to completely glabrous on anterior and basal third portions; fore coxae with scattered, blackish, stout setae posteriorly; mid and hind coxae covered with numerous stout dark setae, including some longer setae on posterior portion and, to a varying extent laterally (Fig. 16). Trochanters densely covered with blackish stout setae and some longer elements ventrally; on ventral surface, one or a pair of fusiform, moderately narrow, glabrous areas. Femora and tibiae slender and elongate. Fore femur slightly longer than or approximately as long as head and pronotum together. All femora slightly dilated subapically, thickened basally, to approximately 1.6 to 1.8 times thicker than narrowest portion of the segment; narrowest portion of femora generally with yellowish annuli (somewhat distally to midportion); apices of all femora with a pair of lateral small tubercles. Femora covered with sparse, long, straight, blackish setae and dense, erect, brush-like setae ven-

Figures 14–16. *Parahiranetis salgadoi* Gil-Santana, male thorax. **14** pronotum, dorsal view **15** setae of the midlongitudinal line of the pronotum with flocky patches of wax-like substance **A–B** under progressively higher magnification **16** meso- and metathorax, ventral view. Scale bars: : 0.5 mm (**14, 16**); 0.05 mm (**15A**); 0.02 mm (**15B**).

trally, which are longer on basal portion and restricted to basal portion on hind femur. Fore tibiae somewhat enlarged at apex, where there is a dorsal spur and a mesal comb; mid tibiae with uniform thickness; hind tibiae somewhat enlarged in basal half and narrowing a little to apex; all tibiae with scattered, long, thick, blackish setae and dense, shorter, erect, brush-like blackish setae on ventral surface, which become progressively more numerous towards apex; hind tibiae along all portions densely covered with these erect, brush-like blackish setae, which are somewhat longer in slightly enlarged basal half; tarsi with dark shorter setae. Hemelytra long, surpassing abdomen by about half length of membrane; corium covered with curved, adpressed, short dark setae, which
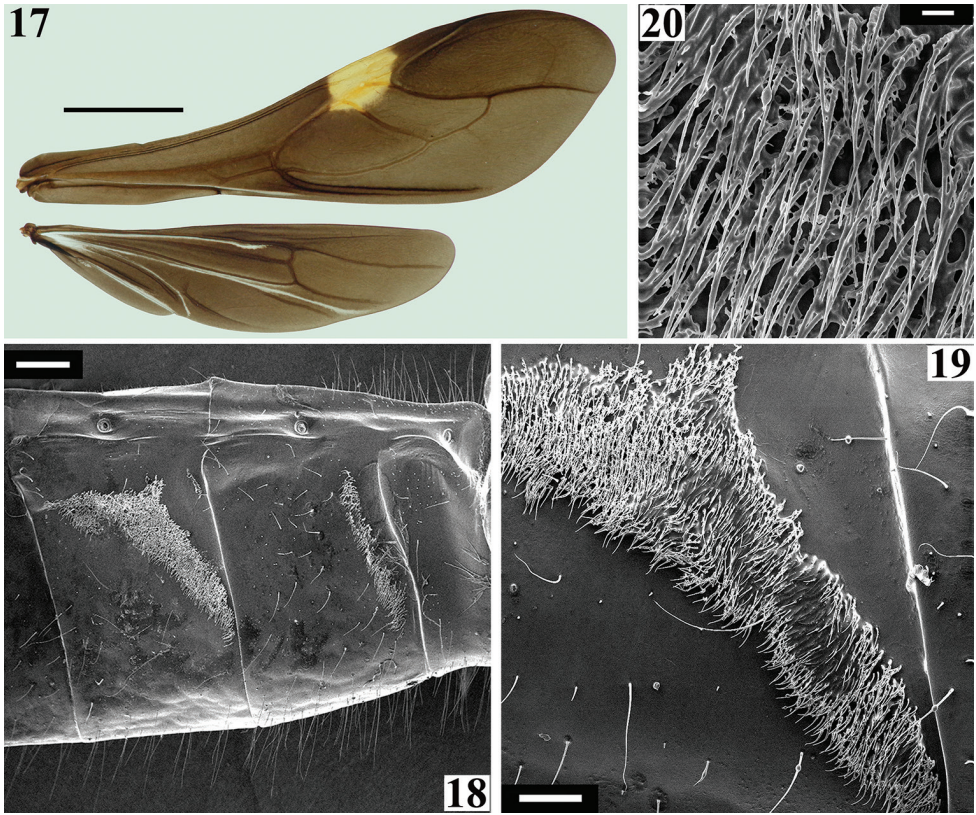
Figures 17–20. *Parahiranetis salgadoi* Gil-Santana, male. **17** hemelytron and hind wing **18** sternites II–IV, lateral view **19** patch of whitish, minute, thin, adpressed setae on midlateral portion of sternite IV, with few amount of wax-like substance on setae **20** upper portion of the same patch of minute setae on sternite IV under higher magnification. Scale bars: 3.0 mm (**17**); 0.5 mm (**18**); 0.2 mm (**19**); 0.02 mm (**20**).

are somewhat more numerous over costal and subcostal veins; membrane glabrous; venation of hemelytra and hind wing as in Fig. 17. Abdomen: elongate; spiracles rounded; sternites with integument shiny, covered with long, moderately thin, scattered, dark setae; sternite II with a somewhat elevated transverse area on basal half; fusiform or elongated patches of minute, short, adpressed, thin, whitish setae present on basal half of midlateral portions of sternites III and IV (Figs 18–19); these setae are frequently covered with a variable amount of white wax (Figs 19–20); when more abundant, wax forms flocky patches around and over the setae; when more scarce, wax just covers setae along their lengths (Fig. 20). In some specimens, all abdominal patches of white setae are extensively covered with wax-like substance, while in others, the setae are not covered with the wax or only some of the setae are covered: generally, those of superior part of patches are more extensively covered by wax (Fig. 19).

Male genitalia (Figs 21–41): pygophore blackish, suboval in ventral view, with an enlarged, somewhat arrow-shaped apex (medial process, mp), in which lateral margins
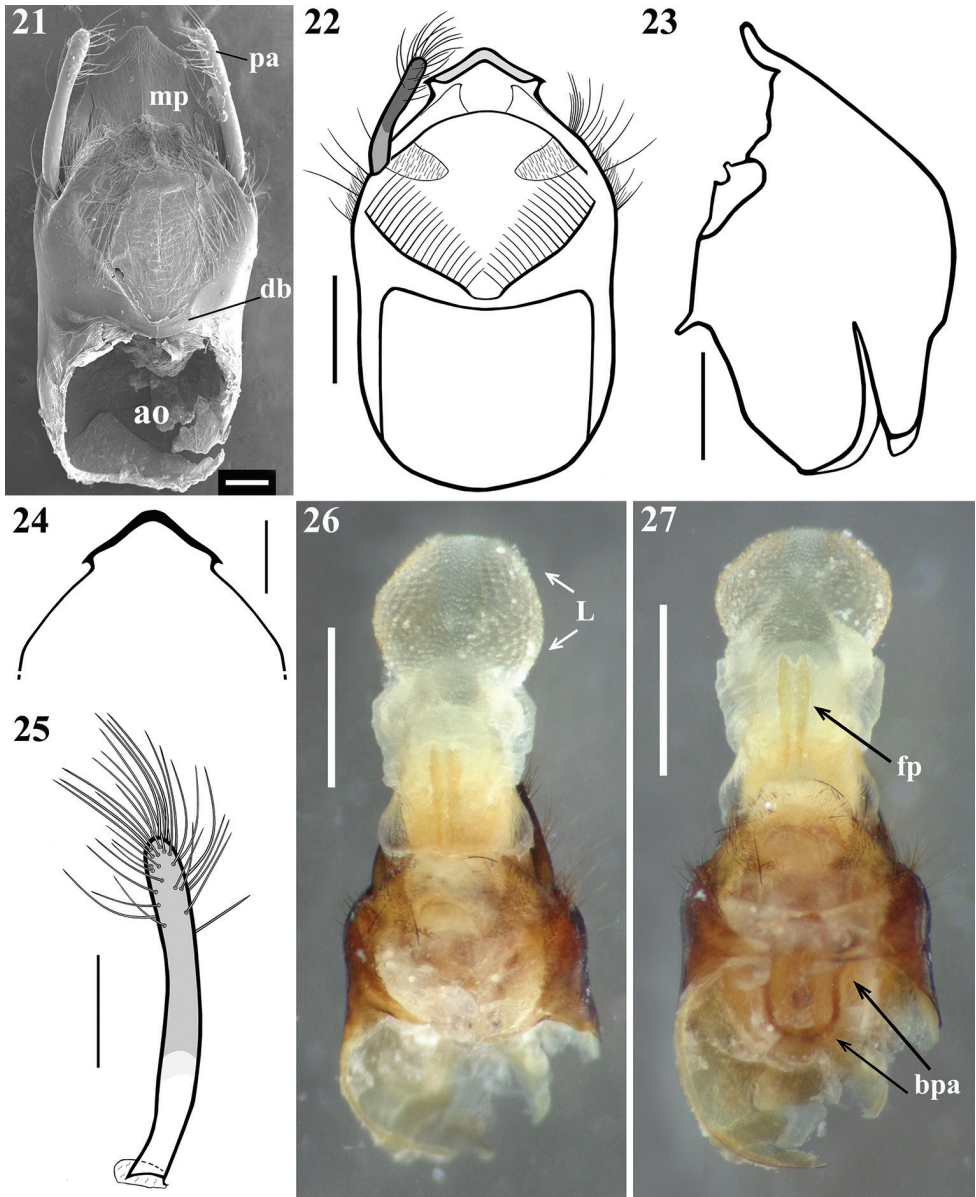
Figures 21–27. *Parahiranetis salgadoi* Gil-Santana, male genitalia. **21** dorsal view **22** pygophore and right paramere, dorsal view **23** pygophore without parameres, lateral view **24** shape of median process of pygophore, ventral view **25** left paramere **26–27** pygophore with endosoma completely inflated, dorsal view. (**ao**: anterior opening; **bpa**: basal plate arm; **db**: dorsal bridge; **fp**: pair of elongate, flat processes; **L**: globe-shaped lobe in distal third of endosoma; **mp**: medial process of pygophore; **pa**: paramere). Scale bars: 0.2 mm (**21**); 0.5 mm (**22–23**); 0.3 mm (**24–25**); 1.0 mm (**26–27**).
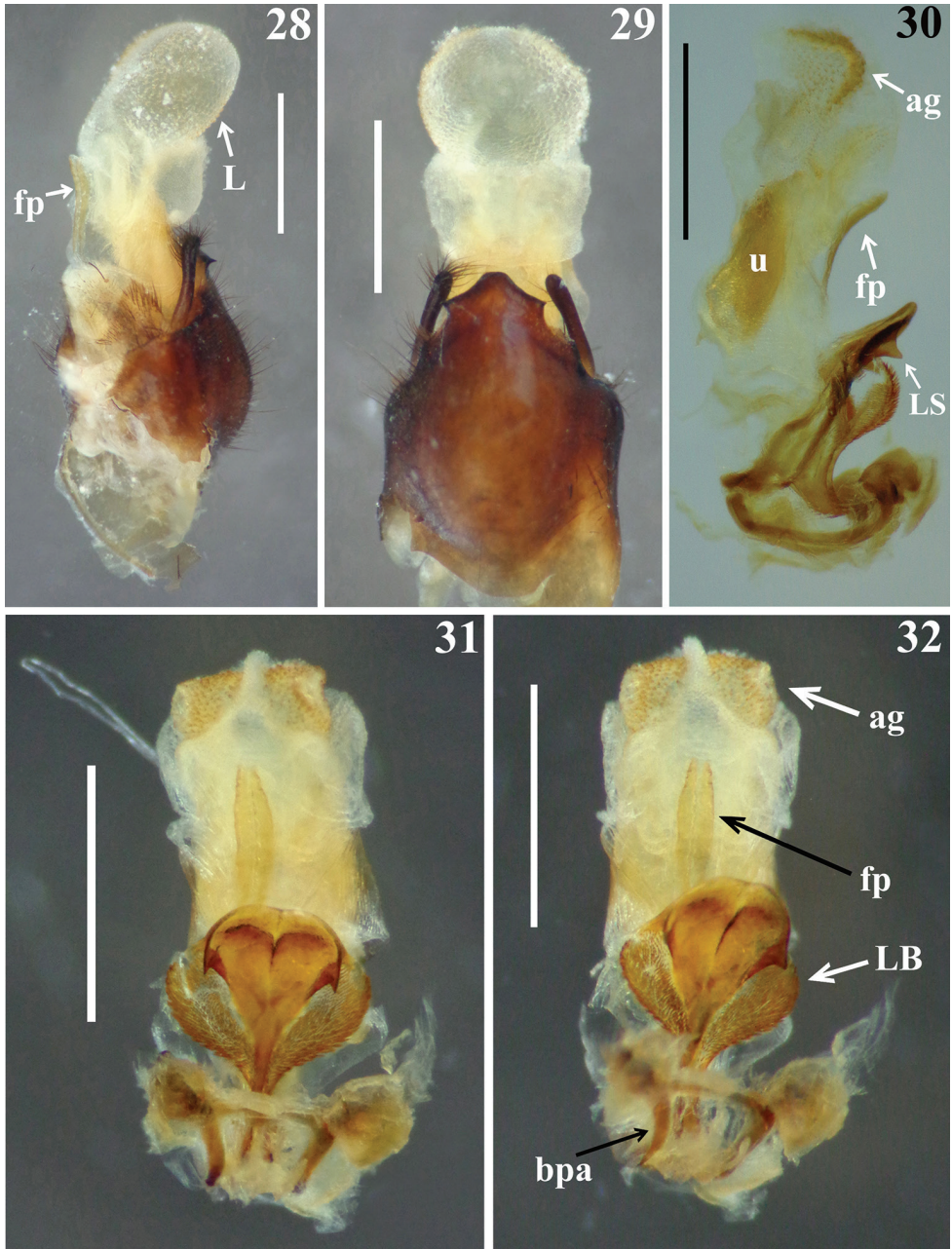
Figures 28–32. *Parahiranetis salgadoi* Gil-Santana, male genitalia. **28–29** pygophore with endosoma completely inflated **28** latero-dorsal view **29** ventral view **30–32** phallus **30** lateral view **31–32** dorsal view. (**ag**: apicolateral group of spiny processes of the endosoma; **bpa**: basal plate arm; **fp**: pair of elongate, flat processes; **L**: globe-shaped lobe in distal third of endosoma; **LB**: large lobe, middle third of the phallothecal plate; **LS**: lateral large spine of the phallothecal plate; **u**: U-shaped basal process). Scale bar: 1.0 mm.
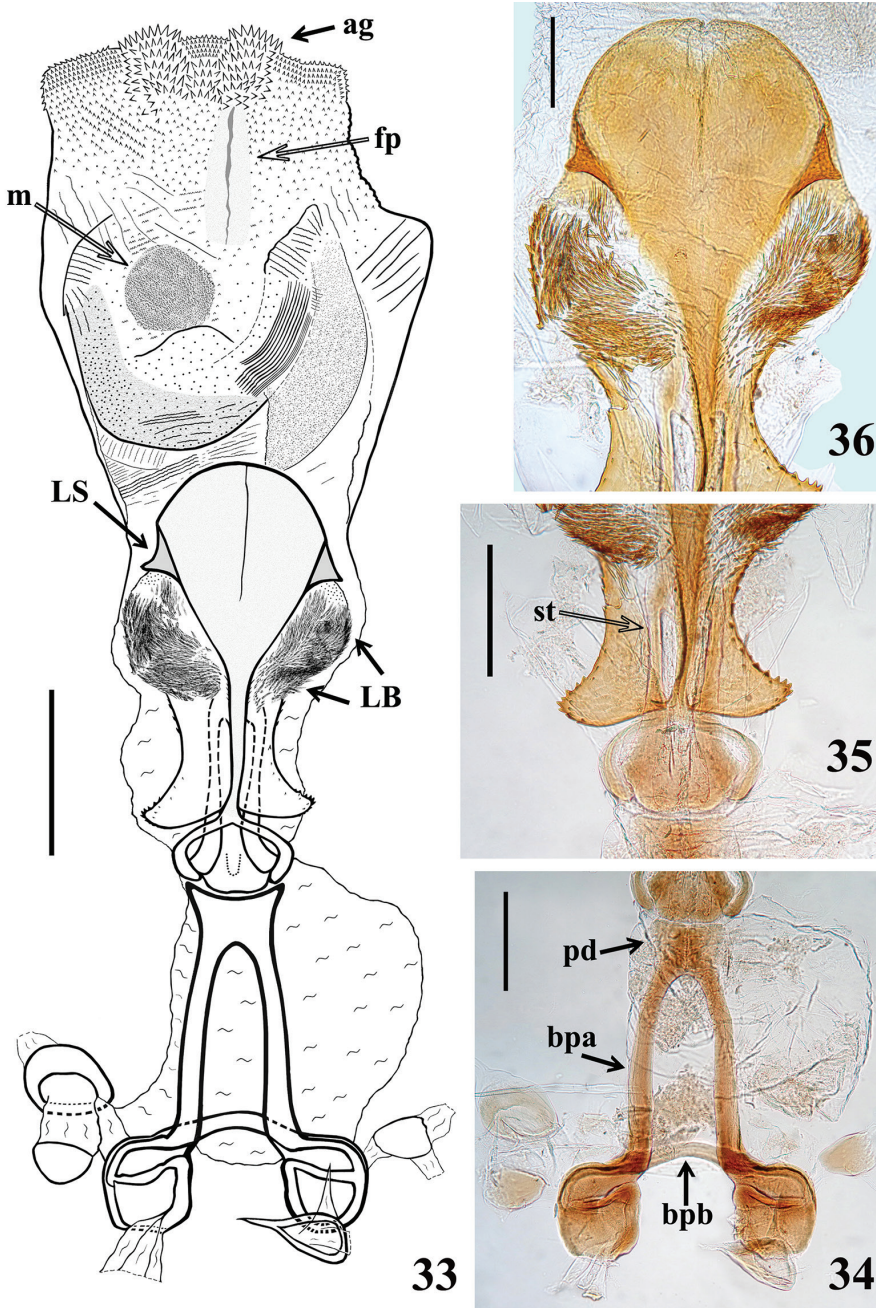
Figures 33–36. *Parahiranetis salgadoi* Gil-Santana, male genitalia, dorsal view. **33** phallus with expand-ed endosoma **34** articulatory apparatus **35–36** dorsal phallothecal plate and struts **35** basal portion **36** apical two-thirds. (**ag**: apicolateral group of spiny processes of the endosoma; **bpa**: basal plate arm; **bpb**: basal plate bridge; **fp**: pair of elongate, flat processes; **LB**: large lobe, middle third of the phallothecal plate; **LS**: lateral large spine of the phallothecal plate; **m**: median subspherical process; **pd**: pedicel; **st**: struts). Scale bars: 0.5 mm (**33**); 0.3 mm (**34–35**); 0.2 mm (**36**).
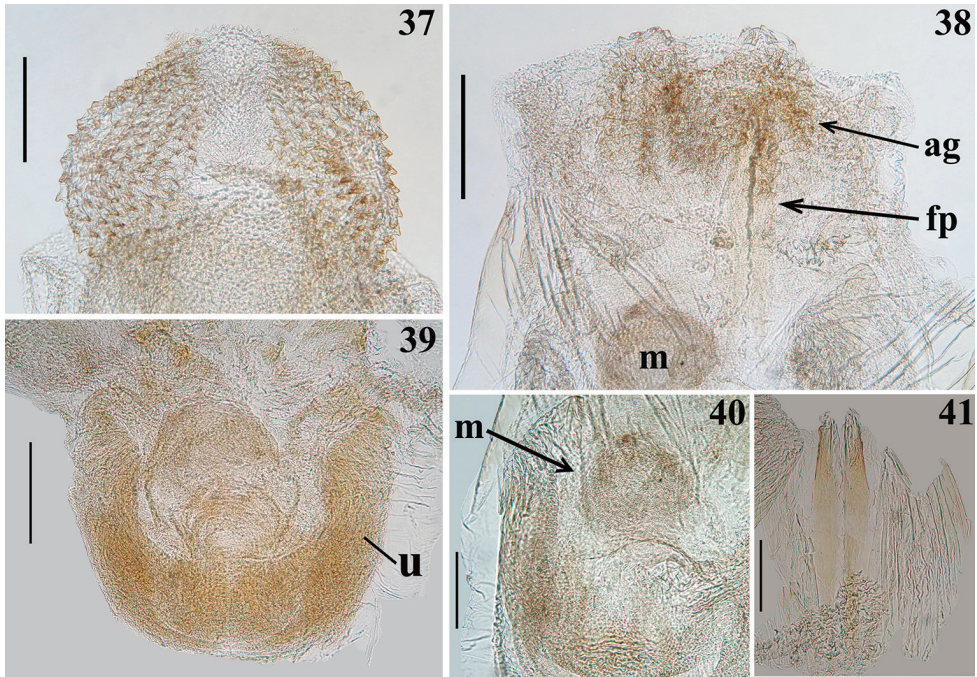
Figures 37–41. *Parahiranetis salgadoi* Gil-Santana, male genitalia, dorsal view. **37–40** endosoma portions and processes **37** globe-shaped lobe in distal third **38** distal portion **39** basal portion **40** midportion **41** a pair of elongate, flat processes. (**ag**: apicolateral group of spiny processes of the endosoma; **fp**: pair of elongate, flat processes; **m**: median subspherical process; **u**: U-shaped basal process). Scale bars: 0.3 mm (**37–39**); 0.2 mm (**40–41**).

are acutely pointed and the median portion is rounded (Figs 21–22, 24); between anterior and posterior genital openings, a very well sclerotized dorsal (transverse) bridge (db) with a conspicuous median rounded dorsal prominence (Figs 21–22); dorsolateral margin of pygophore (between the bridge and insertions of parameres) with numerous, long, erect setae (Figs 21–22); exposed surface of pygophore with long, thick and dark setae ventrally; these setae are somewhat more numerous on apicolateral portions. Parameres (pa) symmetrical (Fig. 21), rod-like in shape, somewhat curved (Fig. 25); apices rounded, clear at basal third, becoming darker in apical half (blackish); glabrous in basal two-thirds and with long, stout, dark setae in apical third (Figs 21–22, 25); those setae at apicomedial margins even longer (Fig. 25). Phallus elongated, even when not completely inflated (Figs 30–33); articulatory apparatus with long basal plate arms (bpa) (Figs 33–34); basal plate arms (bpa) and basal plate bridge (bpb) narrow and forming a subrectangular set, except in apical portion, where the arms are curved (Figs 33–34); pedicel (pd) moderately short, slightly expanded towards apex (Figs 33–34). Dorsal phallothecal plate weakly sclerotized (Figs 35–36); somewhat expanded laterally at basal third and with small acute spines on lateral margins (Fig. 35); middle third enlarged, with lateral large lobes (LB) covered with very numerous spiny processes

(Figs 31–33, 36); distal third together with central portion of basal two-thirds, forming a racket-shaped flat sclerite, with anterior margin largely rounded (Figs 33, 36); its distal third has also a pair of lateral large spines (LS) on its base and a thin median keel, which ends just before the apical margin (Figs 30–33, 36). Struts (st) with subparallel arms (Figs 33, 35–36). Endosoma wall smooth on basal half, becoming progressively more densely, minutely, spiny towards apex (Fig. 33); at distal third, endosoma forms a globe-shaped lobe (L), which is almost completely covered with numerous larger, spiny, somewhat sclerotized processes (Figs 26–29, 37); processes are absent from median portion, where the wall is only minutely spiny (Fig. 37); when the phallus is not completely inflated, larger spiny processes form two apicolateral groups of these processes (ag) (Figs 30–33, 38). The following endosomal processes were observed: 1 - a pair of elongate, parallel, flat, median and weakly sclerotized processes (fp), wrapped in smooth portion of endosoma wall (with fine longitudinal grooves) (Figs 26–28, 30–33, 38, 41); all of these lie dorsally to the other two basal processes described next (Fig. 28); 2 - a larger U-shaped basal process (u) formed by diffuse thickening (Figs 30, 39); 3 - a median subspherical process (m), situated between the lateral arms of the basal process and formed by a dense grouping of small thickenings (Figs 33, 38, 40).

Female. Figures 42–58. Similar to male in general. The recorded differences were: size (measurements presented in Tables 2 and 3; see comments below).

Coloration: yellowish rings on femora with the following relative values: on fore femora, the annulus is approximately 1/10 to 1/11 as long as fore femur and midpoint of annulus is about 8 to 12% distal from midpoint of fore femur; on mid femora, annulus is approximately 1/7 to 1/8 as long as mid femur and midpoint of annulus is about 8 to 10% distal from midpoint of mid femur, while on hind femora, the same relationships are about 1/7 to 1/11 and 8 to 9%, respectively. On abdominal sternites, generally reddish coloration extends to basolateral portion of sternite V (Figs 55–56).

Structure: Head: approximately 1.47 to 1.65 times as long as width across eyes (length measured excluding neck) in the type specimens; labial segment II (first apparent) slightly longer than segment III; antennal segment III somewhat thicker in basal portion (Figs 47–48), but much thinner as a whole than that in males, and becoming progressively thinner toward apex, without a clear separation between more or less thickened portions (Fig. 48); segment III is uniformly covered with pubescence formed by thin, pale setae (Fig. 51) (blackish, stiff, adpressed, very short setae that completely cover thicker portion in male are absent); segment III is approximately 1.1 to 1.3 times longer than segment I.

External genitalia (Figs 57–58): syntergite 9/10 (s) with very long, sparse, strong blackish setae; paired gonoplac (g) and posterior margin of first gonapophysis (fg) with strong shorter setae.

Comments. In the type specimens, the head and the body length to the tip of the hemelytra are slightly longer than those in the specimens from the state of São Paulo. The body length to the tip of the abdomen is also slightly longer in the holotype (Table 3). Moreover, all females are larger than males (Tables 1–3). The minimum body length in females (to tip of hemelytra/tip of abdomen: 21.5/17.5) is greater than the
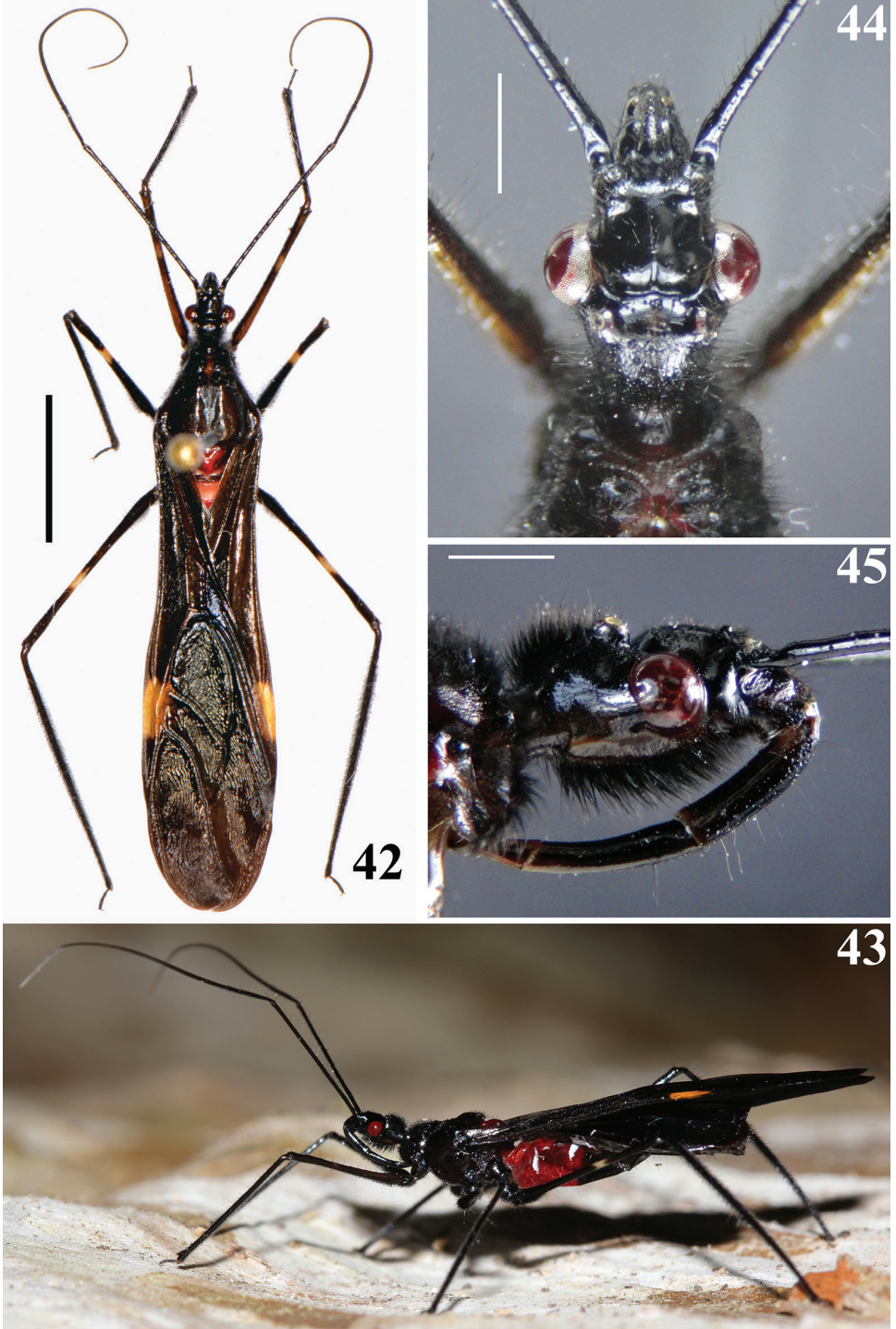
Figures 42–45. *Parahiranetis salgadoi* Gil-Santana, female. **42** dorsal view **43** live specimen, lateral view **44–45** head **44** dorsal view **45** lateral view. Scale bars: 5.0 mm (**42**); 1.0 mm (**44–45**).
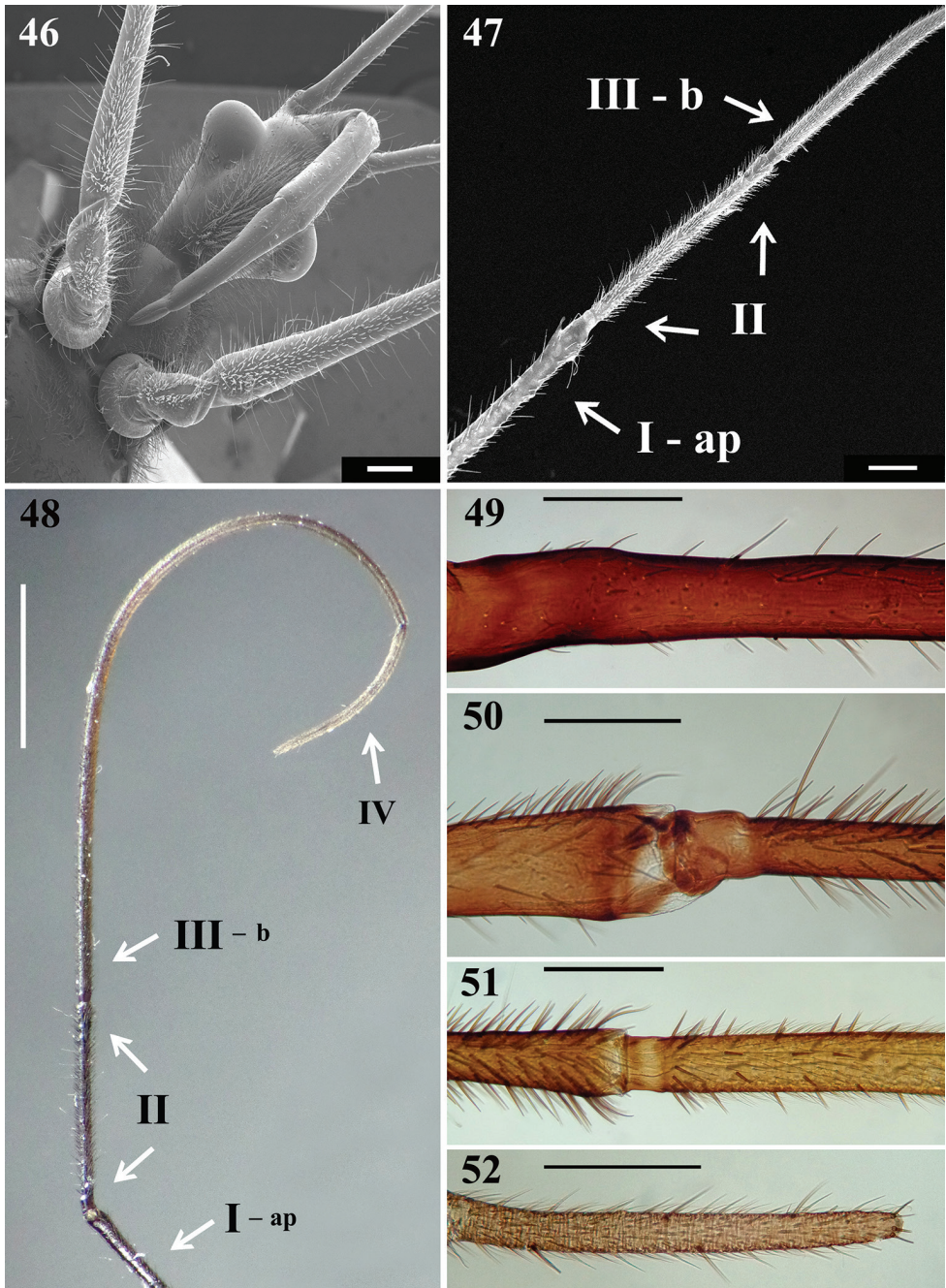
Figures 46–52. *Parahiranetis salgadoi* Gil-Santana, female. **46** head, fore coxae, fore trochanters and basal half of fore femora, ventral view **47–52** antenna **47** apex of segment I, segment II and basal portion of segment III **48** apex of segment I and segments II–IV. (**ap**: apex; **b**: basal portion) **49** basal portion of segment I **50** apex of segment I and basal portion of segment II **51** apex of segment II and basal portion of segment III **52** apex of segment IV. Scale bars: 0.5 mm (**46–47**); 2.0 mm (**48**); 0.3 mm (**49–52**).
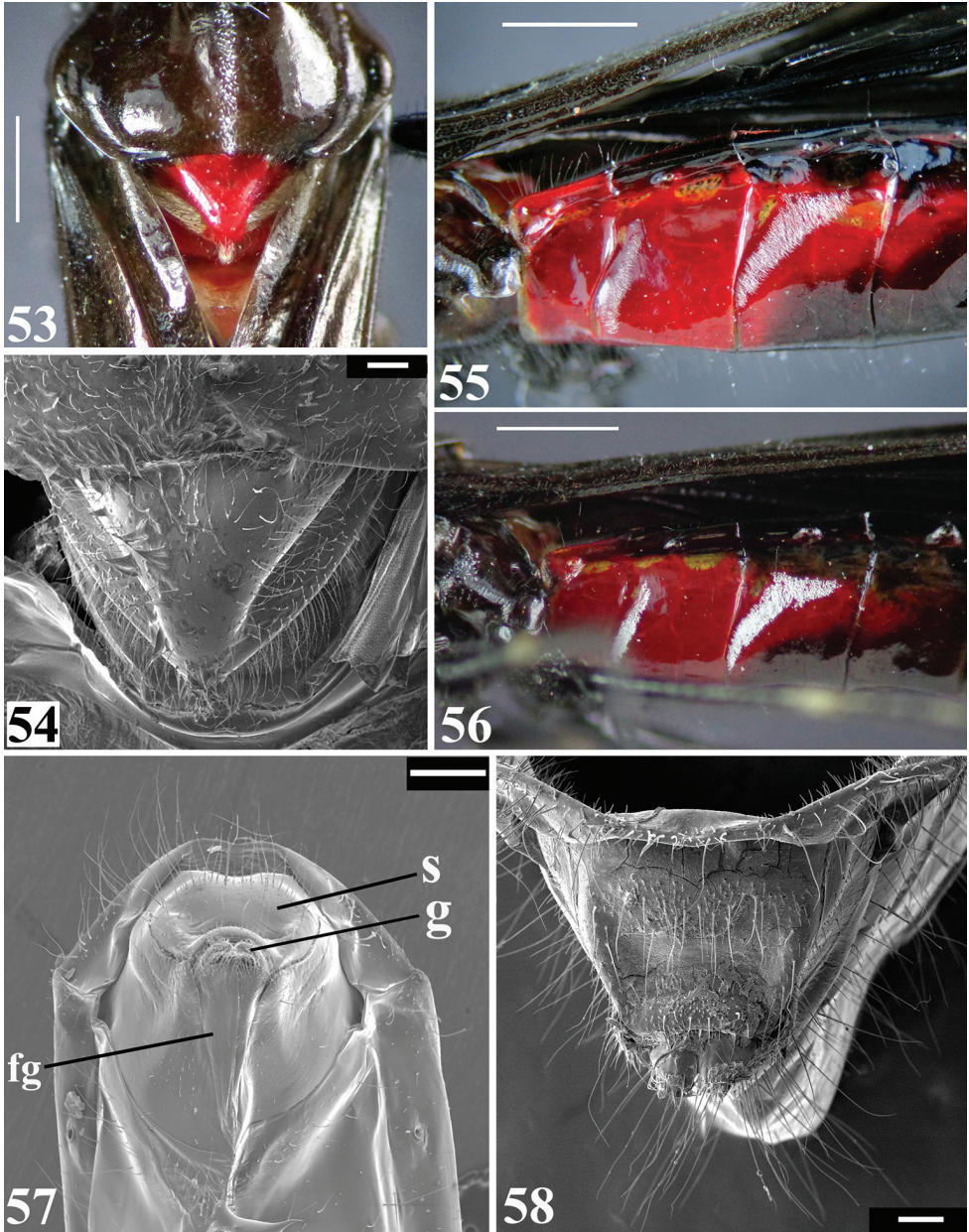
Figures 53–58. *Parahiranetis salgadoi* Gil-Santana, female. **53–54** dorsal view **53** posterior half of pronotum and scutellum **54** scutellum **55–56** abdominal segments II–IV, lateral view **55** patches of whitish, minute, thin, adpressed setae on midlateral portions of sternite III–IV without wax-like substance **56** the same with large amount of wax-like substance on setae **57–58** female genitalia **57** postero-ventral view (**fg**: first gonapophysis; **g**: gonoplac; **s**: syntergite 9/10) **58** posterior view. Scale bars: 1.0 mm (**53**); 0.2 mm (**54, 58**); 2.0 mm (**55–56**); 0.5 mm (**57**).

Table 2. Measurements (mm) of female specimens (N = 7) of *P. salgadoi* from São Paulo State.

Measurement	Mean	SD	Maximum	Minimum
Body length to tip of hemelytra	22.5	0.64	23.5	21.5
Body length to tip of abdomen	18.45	0.57	19.2	17.5
Head length (excluding neck)	2.6	0.07	2.7	2.5
Anteocular portion length	1.09	0.07	1.2	1.0
Postocular portion length	0.77	0.07	0.9	0.7
Head width across eyes	1.86	0.08	2.0	1.75
Interocular distance	0.98	0.02	1.0	0.95
Transverse width of right eye	0.42	0.04	0.5	0.38
Length of right eye	0.68	0.03	0.75	0.65
Antennal segment I length	6.6	0.18	6.9	6.4
Antennal segment II length	2.42	0.21	2.9	2.3
Ant. segment III length **(n = 4)**	8.02	0.25	8.3	7.7
Ant. segment IV length **(n = 4)**	2.11	0.19	2.3	1.9
Max. width ant. seg. III **(n = 6)**	0.15	0.01	0.17	0.14
Labial segment II length	1.51	0.03	1.6	1.5
Labial segment III length	1.59	0.03	1.65	1.55
Labial segment IV length	0.53	0.04	0.6	0.45
Ocellar tubercle width	1.04	0.07	1.2	1.0
Pronotum length	3.18	0.15	3.4	3.0
Pronotum maximum width	3.77	0.16	4.0	3.5
Scutellum length	1.14	0.11	1.25	1.0
Fore femur length	6.28	0.26	6.7	6.0
Fore tibia length	6.68	0.1	6.8	6.5
Fore tarsus length	0.75	0.0	0.75	0.75
Mid femur length	5.48	0.21	5.9	5.3
Mid tibia length	7.2	0.29	7.5	6.8
Mid tarsus length	0.77	0.02	0.8	0.75
Hind femur length	7.92	0.32	8.5	7.4
Hind tibia length	10.8	0.34	11.5	10.4
Hind tarsus length	0.81	0.03	0.85	0.75
Abdomen length	11.15	0.58	12.0	10.5
Abdomen maximum width	3.7	0.36	4.1	3.1

maximum body length in males (19.5/14.7). Most of the other measurements are proportionally greater in females, in accordance with their bigger size (Tables 1–3). One clear exception is the antennal segment III, which is longer in males (8.9 to 9.7 mm in length; n = 6) than in females (7.7 to 8.3 mm in length; n = 4). Also, the antennal segment III shows evident thickening, approximately in basal two-thirds in males (maximum width: 0.24–0.32 mm) (Figs 1, 5, 9, 11), but not in females (maximum

Figures 59–62. *Parahiranetis salgadoi* Gil-Santana, live specimens. **59–61** aggregates of adults and fifth instar nymphs on tree trunks **62** a fifth instar nymph.

Table 3. Selected measurements (mm) of female specimens of *P. salgadoi*.

Measurement	holotype	paratype	females from São Paulo State (maximum-minimum)
Body length to tip of hemelytra	24.5	24.2	23.5–21.5
Body length to tip of abdomen	19.5	19.1	19.2–17.5
Head length (excluding neck)	3.3	3.1	2.7–2.5
Head width across eyes	2.0	2.1	2.0–1.75
Interocular distance	1.1	1.0	1.0–0.95
Abdomen length	10.5	11.0	12–10.5
Abdomen maximum width	4.2	4.0	4.1–3.1

width: 0.14–0.17 mm) (Figs 42, 47–48, 51). This thickened region in males is completely covered by blackish, stiff, adpressed and very short setae (Figs 9–10, 12), which are absent in females (Fig. 51).

Distribution. Brazil, in states of Rio de Janeiro and São Paulo (Atlantic tropical moist forest and Atlantic semideciduous forest, respectively).

Observation of live specimens. Both nymphs and adults were observed in aggregates on tree trunks, where most individuals remained relatively motionless (Figs 59–63). The general coloration of nymphs is quite different from that of the adults. Nymphs have a general color pattern in which shades of gray and light brown predominate (Figs 59–60, 63). However, fifth-instar nymphs just before molting become reddish and progressively darker (Fig. 62).

Nymphs were not collected to allow them to reach the adult stage in the wild. Consequently, it is not possible to provide a formal description of them at this time.

Discussion

Examination of additional specimens, including males, allowed us to provide a more complete description of the adults of *Parahiranetis salgadoi*. Gil-Santana (2015), for example, had not recorded the sticky substance on some parts of the body and appendages or the white wax-like substance covering groups of setae on the thorax and abdomen (Figs 14–15, 19–20, 53–54, 56), as both were completely absent from the type specimens. Moreover, the sticky substance was present only on some specimens from São Paulo, while the wax-like substance was sometimes absent from portions where it was observed on other specimens (Figs 55–56). Both substances may be lost during manipulation of the individuals and, in the case of the wax-like substance, this may also include loss of the thin fragile setae associated with it (HRG-S pers. obs.). However, the patches of short adpressed setae on the midlateral portions of sternites III and IV were completely covered with wax in some specimens (Fig. 56), while others clearly had no wax and the setae were nonetheless well preserved (Fig. 55). This observation makes it clear that individual differences (at least regarding this trait) can
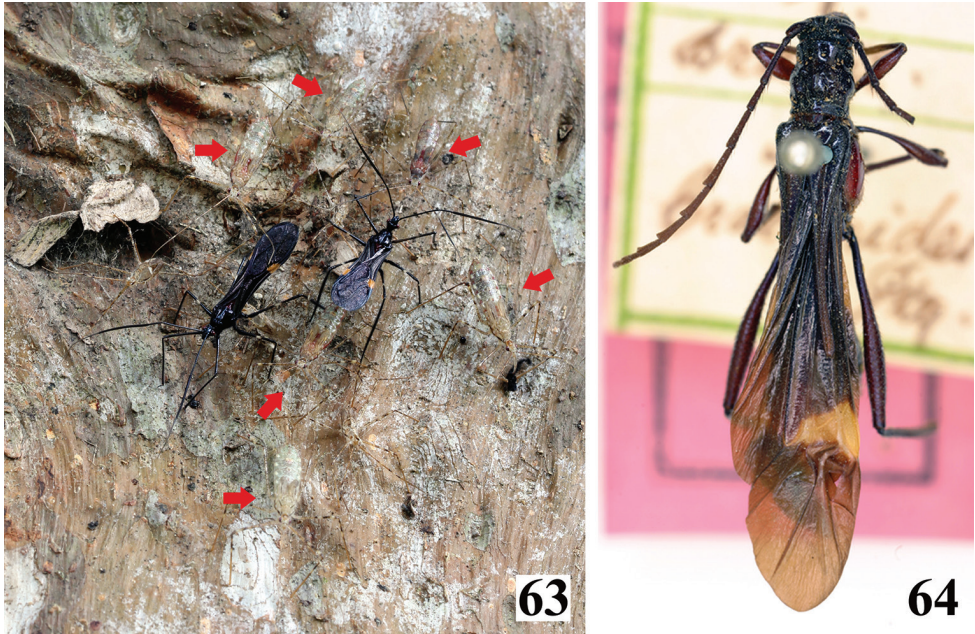
Figures 63–64. 63 *Parahiranetis salgadoi*, live specimens; two male adults and fifth instar nymphs on a tree trunk; red arrows point to nymphs **64** female holotype of *Isthmiade braconides* (Perty, 1832) (Coleoptera: Cerambycidae: Cerambycinae: Rhinotragini), deposited in the ZSM, Munich, Germany (courtesy of Steve Lingafelter).

be found even in the same population and at the same observation time, possibly associated to the age and/or behavioral state of each specimen prior collection. Thus, in the type specimens, both substances may have been inadvertently removed; or may have disappeared over time, taking into account the fact that these are old specimens; or alternatively, these specimens may never have had either substance. In any case, it is no longer possible to know the extent to which these substances were present when the specimens were alive.

The sticky, viscous substance that covers the integument of some species of Harpactorini, particularly their fore and mid legs, is produced by specialized epidermal glands. These species use it to catch their prey (Zhang and Weirauch 2013a). Using comparative phylogenetic methods, Zhang and Weirauch (2013b) showed that species of Harpactorini that use a 'sticky trap predation' strategy have evolved fore femora that are more slender and longer than those of "non-sticky" bugs. Among some other members of Harpactorini, sticky glands were recorded in species of two genera that are considered close to *Parahiranetis*: *Hiranetis braconiformis* (Burmeister, 1835) and *Graptocleptes* sp. (Zhang and Weirauch 2013a). Interestingly, in the phylogenies obtained by Zhang and Weirauch (2013b), species of the wasp-mimicking genera *Graptocleptes*, *Hiranetis*, *Myocoris*, *Neotropiconyttus* and *Xystonyttus* were nested in the same clade, among other clades that together make up the "sticky bug clade" within Harpactorini.

Body parts covered with patches of setae with whitish wax-like material have been registered in some Harpactorini species, such as *Cosmoclopius curacavensis* Cobben & Wygodzinsky, 1975 (Cobben and Wygodzinsky 1975), *Harpactor angulosus* (Lepeletier & Serville, 1825) (Pikart et al. 2014), various species of *Heza* Amyot & Serville, 1843 (Maldonado 1976) and *Sphedanolestes zhengi* Zhao, Ren, Wang & Cai, 2015 (Zhao et al. 2015). However, it is clear from the present study that both the sticky and the wax-like substance may be absent when specimens are examined and described, and thus the extent of their existence may remain unknown. The presence or absence of the sticky glands that produce the sticky substance has been shown to correlate with the phylogeny of Harpactorini and faster rates of evolution among "sticky bugs", in comparison with other reduviids (Zhang and Weirauch 2013b). Similarly, records of the presence or absence of a wax-like substance may turn out to be an additional feature of systematic or taxonomic importance, in the same way as suggested for the "extensive sericeous areas on the abdominal sterna" of *Heza ventralis* Stål, 1872 (Maldonado 1976). Therefore, future studies on Harpactorini should include careful handling of the specimens after collection, to avoid unintentional removal of these substances from their bodies. It is also recommended that this information should be included in the records and/or descriptions whenever present.

Differences in body size and in the structure and vesture of the third antennal segment were clear-cut enough to be considered as sexually dimorphic in *P. salgadoi*. Despite the small number of measurements obtained for the third antennal segments (because they were broken and lost in some specimens), adults can be sexed readily with the naked eye, by observing these two traits. Firstly, females were larger than males in almost all the morphological characteristics measured. Secondly, the third antennal segment was longer in males than in females, both in absolute and in relative terms (i.e. total length and the ratio between the third and first antennal segments, respectively). Moreover, in males, the third antennal segment was distinctly thickened, approximately in its basal two-thirds, with the thicker portion clearly separated in relation to the thinner, distal portion (Figs 1, 5, 9, 11–12). In females, it showed little or no thickening (Figs 42, 47–48, 51). Two of the sexual differences pointed out in *P. salgadoi* (i.e. females larger than males and the latter with third antennal segment thickened) are concordant with several observations in the literature (Champion 1899, Martin-Park et al. 2012, Gil-Santana et al. 2013, Gil-Santana 2016). Additionally, the thickened portion of the third antennal segment in males was completely covered by very short, stiff, adpressed, blackish setae (Figs 9–10, 12), which were absent in females (Fig. 51). Small differences in coloration were also recorded (see above); however, more specimens need to be examined in order to clarify whether such differences might be due to sexual dimorphism.

Some slight differences were also noted between the type specimens and the specimens from São Paulo. These are very probably due to intraspecific variation. However, measurements of the head and the ratio of head length to maximum width across the eyes are important for separating *Parahiranetis* from related genera, especially *Hiranetis* (Gil-Santana 2015, 2016). Gil-Santana (2015) measured the length of the head in-

cluding the neck and recorded that it was 1.6 to 1.8 times as long as width across the eyes (in the paratype and holotype, respectively). In the present study, in which head measurements excluded the neck, the head was recorded in the type specimens as being 1.47 to 1.65 times as long as width across the eyes (paratype/holotype). In parallel, this ratio was approximately 1.3 to 1.4 in the specimens from São Paulo. Therefore, the main diagnostic characteristics that separate *Hiranetis*, *Graptocleptes*, and *Parahiranetis* according to Spinola (1840a,b), Stål (1866, 1872), Maldonado and Lozada (1992), Gil-Santana et al. (2013), Gil-Santana (2015, 2016) and this work, are the following:

1) *Graptocleptes*: Head elongate, approximately 1.1 to 1.3 times as long as width across eyes, sparsely setose; legs thicker; fore femur shorter than head and pronotum together and of uniform thickness.
2) *Hiranetis*: Head gibbous, large, approximately as long as width across eyes, densely setose on ventral and post-ocular portions; legs elongated, slender; fore femur subequally longer than head and pronotum together, thicker basally.
3) *Parahiranetis*: Head elongate, approximately 1.3 times to 1.7 as long as width across eyes, densely setose on ventral and post-ocular portions; legs elongated, slender; fore femur subequally longer than head and pronotum together, thicker basally.

The male genitalia of *P. salgadoi* showed some similarities to those of *G. bicolor* (Gil-Santana et al. 2013) and *H. atra* (Gil-Santana 2016), such as: (i) parameres similar in shape and somewhat similar in vestiture; and (ii) presence of a pair of elongate, parallel, flat, weakly sclerotized endosomal processes. However, the latter were recorded with different locations and shapes in each of these species. Comparatively, they are somewhat more elongated, straighter and closer to each other in *P. salgadoi* (Figs 26–28, 31–33, 38, 41). The pygophores of all three species have a somewhat large medial process that is medially rounded at the apex, but in *G. bicolor* and *H. atra* it is subtriangular in shape, while in *P. salgadoi*, it is somewhat arrow-shaped, with the lateral margins acutely pointed (Figs 22, 24, 29). U-shaped and median subspherical endosomal processes that are very similar to those of *P. salgadoi* (Figs 33, 38–40) were recorded in *H. atra*. The distal third of the endosoma of *P. salgadoi*, except in the median portion, is almost completely covered by numerous larger spiny somewhat sclerotized processes (Fig. 37), while in the endosoma of *G. bicolor*, groups of larger similar spiny processes were also recorded. However, in the latter species, these processes were recorded as occurring mostly at the midportion, apically or subapically, and were more sclerotized and clearly triangularly shaped.

Moreover, the male genitalia of *P. salgadoi* differ from those of both of those species in some parts. Firstly, the basal plate arms of the articulatory apparatus are clearly longer in this species (Figs 33–34). Secondly, there is a very remarkable difference concerning the struts and especially the dorsal phallothecal plate. The latter has already been recorded as distinctive between *G. bicolor* and *H. atra*, but the differences are even more accentuated in *P. salgadoi*. The shape of the dorsal phallothecal plate and the portions of it (including the lateral large lobes) that are covered with very numerous

spiny processes in the middle third, along with the racket-shaped flat sclerite extending towards the apex with lateral large spines, are striking features and may be unique for this species (Figs 30–33, 35–36). Thus, in agreement with previous studies (Elkins 1954a, b, Hart 1975, 1986, 1987, Forero et al. 2008, Zhang et al. 2016), the features of the male genitalia of *P. salgadoi* that should especially be taken into consideration for comparative purposes are the shape of the medial process of the pygophore and the features of the phallothecal plate.

Historically, only the pattern of yellowish or straw-colored hemelytra with a median transverse black band has received attention in regards to the supposed mimicry between Harpactorini and species of hymenopteran Ichneumonidae and Braconidae (Champion 1899, Haviland 1931, Maldonado and Lozada 1992, Hogue 1993, Leathers and Sharkey 2003, Hespenheide 2010). However, some species that have similar patterns of blackish wings with yellowish 'pterostigmata' arise as possible candidates for mimetic complexes, including *P. salgadoi* (Gil-Santana 2015). These are the wasp-mimicking harpactorines *Graptocleptes bicolor*, *G. haematogaster* (Stål, 1860), and an undescribed species of *Hiranetis* as well as the ichneumon wasp *Pedinopelte gravenstii* (Guérin-Méneville, 1826) and the cerambycid beetle *Isthmiade braconides* (Perty, 1832) (Fig. 64). All of these have been recorded from southeastern Brazil, particularly in the states of Rio de Janeiro and/or São Paulo (harpactorines: Stål 1860, 1872, Gil-Santana et al. 2013, Gil-Santana 2015; ichneumon wasp: De Santis 1980; cerambycid beetle: Zikán and Zikán 1944, Zajciw 1972, Monné 1993, Monné and Bezark 2009).

Although there are records of color variation in some wasp-mimicking Harpactorini, at least in the species with the pattern of darkened or blackish hemelytra with yellowish pterostigmata, there is no variation in this pattern. The yellowish pterostigmata is always present (e.g. Gil-Santana et al. 2013, this study). Concerning this point, it is appropriate to correct an assertion by Gil-Santana et al. (2013). In the latter report, it was alleged that Stål (1872) would have "recorded variation of the coloration of the corium of hemelytra of *Graptocleptes bicolor*, describing it as either paler ("Var. b. - *pallidior*") or completely blackish ("bb. *Corio toto nigricante*")". This was a double misinterpretation of Stål's text. The statement "Var. b. - *pallidior*" did indeed refer to *G. bicolor*, but it was in relation to a "variety" with paler general coloration, and this did not necessarily relate to its hemelytra. Regarding the second assertion, an accurate reading of Stål's paper makes it clear that "*Corio toto nigricante*" was considered to be a characteristic of another species: *Graptocleptes sanguineiventris* Stål, 1862. Moreover, just above this, Stål (1872) included the previous alternative "b.", through which the characteristic of "*Corio apice vel prope apicem pallescente vel croceo*" was attributed to another species (*G. gastricus* (Stål, 1860), *G. haematogaster* and *G. bicolor*). This is a clear description of the pale to yellowish spot on the distal portion of the corium of the hemelytra in all these three species. Therefore, the alternative "bb." (corium completely blackish) was clearly stated as opposite to this latter and was diagnostic of another species (*G. sanguineiventris*).

In contrast to the adults, nymphs of *P. salgadoi* were quite inconspicuous on the tree trunks where they naturally occurred (Figs 59–63). Their cryptic coloration probably has a protective function, which is present to some extent in almost every family

of Heteroptera (Schuh and Slater 1995). Ecological studies might improve the current understanding of the contrasting strategies adopted by different life stages in *P. salgadoi*. Additionally, as emphasized by Gil-Santana (2015), it is necessary to elucidate which species or groups of insects sharing the same color pattern as in *P. salgadoi* (i.e. blackish to reddish coloration with yellowish 'pterostigmata' on wings and/or yellowish markings on legs) are involved in possible mimicry complexes.

Acknowledgments

References

Amyot CJB, Serville A (1843) Histoire Naturelle des Insectes. Hémiptères. Librairie Encyclopedique de Roret, Paris, 675 pp.

Bergroth E (1913) A new Neotropical genus of Reduviidae. Annales de la Société entomologique de Belgique 57: 240–242. https://doi.org/10.5962/bhl.part.4593

Burmeister H (1835) Handbuch der Entomologie. Zweiter Band. Theodor Christian Friedrich Enslin, Berlin, 400 pp.

Burmeister H (1838) Some account of the genus *Myocoris*, of the family Reduvini. Transactions of the Entomological Society of London 2: 102–107. https://doi.org/10.1111/j.1365-2311.1836.tb00303.x

Champion GC (1899) Insecta Rhynchota. Hemiptera-Heteroptera, Vol II. In: Godman FD, Salvin O (Eds) Biologia Centrali Americana.Taylor and Francis, London, 193–304.

Cobben RH, Wygodzinsky P (1975) The Heteroptera of the Netherlands Antilles – IX. Reduviidae (Assassin Bugs). Studies on the Fauna of Curaçao and other Caribbean Islands 48: 1–62.

Davis NT (1969) Contribution to the morphology and phylogeny of the Reduvioidea. Part IV. The Harpactoroid Complex. Annals of the Entomological Society of America 62: 74–94.

De Santis L (1980) Catalogo de los Himenopteros Brasileños de la serie parasítica incluyendo Bethyloidea. Curitiba, Editora da Universidade Federal do Paraná, 395 pp.

Elkins JC (1954a) A new American Harpactorine genus (Hemiptera, Reduviidae). Texas Reports on Biology and Medicine 12: 39–48.

Elkins JC (1954b) A synopsis of *Atrachelus* (Hemiptera, Reduviidae). Proceedings of the Entomological Society of Washington 56: 97–120.

Elkins JC (1969) A new genus of hemipteran wasp mimics (Reduviidae, Harpactorinae). Journal of the Kansas Entomological Society 42: 456–461.

Fabricius JC (1803) Systema Rhyngotorum secundum ordines, genera, species, adjectis synonymis, locis, observationibus, descriptionibus. Carolum Reichard, Brunsvigae, 314 pp. https://doi.org/10.5962/bhl.title.11644

Forero D (2011) Classification of Harpactorinae, assassin bugs Hemiptera: Heteroptera: Reduviidae. Boletín del Museo Entomológico Francisco Luís Gallego 1: 9–24.

Forero D (2012) *Pronozelus*, a new Neotropical harpactorine genus and species from Colombia (Hemiptera: Heteroptera: Reduviidae: Harpactorinae). Entomologica Americana 118: 278–284. https://doi.org/10.1664/12-RA-021.1

Forero D, Giraldo-Echeverry N (2015) First record of the assassin bug genus *Coilopus* Elkins, 1969 (Hemiptera: Heteroptera: Reduviidae) from Colombia. CheckList 11: 1364. https://doi.org/10.15560/11.3.1634

Forero D, Gil-Santana HR, Doesburg PH van (2008) Redescription of the Neotropical genus *Aristathlus* (Heteroptera, Reduviidae, Harpactorinae). In: Grozeva S, Simov N (Eds) Advances in Heteroptera research: festschrift in honor of 80th anniversary of Michail Josifov. Pensoft, Sofia-Moscow, 85–103.

Guérin-Méneville FE (1826) Zoologie Atlas pt. 3. In: Duperrey MLI (Ed.) Voyage autour du monde: exécuté par ordre du roi, sur la corvette de Sa Majesté, la Coquille, pendant les années 1822, 1823, 1824, et 1825. Arthus Bertrand, Paris, 16 pls. https://doi.org/10.5962/bhl.title.57936

Gil-Santana HR (2008) New records, and nomenclatural and biological notes on Reduviidae (Hemiptera: Heteroptera) from Bolivia and Brazil. Zootaxa 1785: 43–53.

Gil-Santana HR (2015) *Parahiranetis salgadoi*, a new genus and species of Harpactorini (Hemiptera: Heteroptera: Reduviidae), with a key to Neotropical wasp-mimicking harpactorine genera. Acta Entomologica Musei Nationalis Pragae 55: 29–38.

Gil-Santana HR (2016) First description of the male of *Hiranetis atra* Stål and new country records, with taxonomic notes on other species of *Hiranetis* Spinola (Hemiptera, Heteroptera, Reduviidae, Harpactorinae). ZooKeys 605: 91–111. https://doi.org/10.3897/zookeys.605.8797

Gil-Santana HR, Davranoglou L-R, Neves JA (2013) A new synonym of *Graptocleptes bicolor* (Burmeister), with taxonomical notes (Hemiptera: Heteroptera: Reduviidae: Harpactorini). Zootaxa 3700: 348–360. https://doi.org/10.11646/zootaxa.3700.3.2

Gil-Santana HR, Forero D, Weirauch C (2015) Assassin bugs (Reduviidae excluding Triatominae). In: Panizzi AR, Grazia J (Eds) True bugs (Heteroptera) of the Neotropics, Entomology in Focus 2. Springer Science+Business Media, Dordrecht, 307–351. https://doi.org/10.1007/978-94-017-9861-7_12

Hart ER (1975) A new species of *Ischnoclopius* Stål, with notes on the systematic position of the genus (Hemiptera: Reduviidae). Proceedings of the Entomological Society of Washington 94: 162–165.

Hart ER (1986) Genus *Zelus* Fabricius in the United States, Canada, and Northern Mexico (Hemiptera: Reduviidae). Annals of the Entomological Society of America 77: 419–425. https://doi.org/10.1093/aesa/79.3.535

Hart ER (1987) The genus *Zelus* Fabricius in the West Indies (Hemiptera: Reduviidae). Annals of the Entomological Society of America 80: 293–305. https://doi.org/10.1093/aesa/80.2.293

Haviland MD (Mrs. HH Brindley) (1931) The Reduviidae of Kartabo, Bartica District, British Guiana. Zoologica 7: 129–154.

Hespenheide HA (2010) New *Agrilus* Curtis (Coleoptera: Buprestidae) from México and Costa Rica mimicking parasitic wasps. Zootaxa 2545: 39–46.

Hogue CL (1993) Latin American Insects and Entomology. University of California Press, Los Angeles, 536 pp.

Leathers JW, Sharkey MJ (2003) Taxonomy and life history of Costa Rican *Alabagrus* (Hymenoptera: Braconidae), with a key to World species. Contributions in Science 497: 1–78.

Lepeletier ALM, Serville JGA (1825) Hemiptera Heteroptera. In: Olivier GA (Ed.) Dictionnaire des Insectes. 10. Encyclopédie Méthodique, Paris, 270–273.

Maldonado CJ (1976) The genus *Heza* (Hemiptera: Reduviidae). Journal of Agriculture of University of Puerto Rico 60: 403–433.

Maldonado CJ, Lozada R PW (1992) Key to the group of Neotropical Wasp-mimetic Harpactorine genera and the description of a new species (Hemiptera: Reduviidae). Proceedings of the Entomological Society of Washington 94: 162–165.

Martin-Park A, Delfín-González H, Coscarón MC (2012) Revision of genus *Repipta* Stål 1859 (Hemiptera: Heteroptera: Reduviidae: Harpactorinae) with new species and distribution data. Zootaxa 3501: 1–54.

McPherson JE, Ahmad I (2011) *Parasinea*, a new genus of assassin bug, with description of a new species from Colombia (Hemiptera: Heteroptera: Reduviidae). Annals of the Entomological Society of America 104: 1285–1291. https://doi.org/10.1603/AN11128

Monné MA (1993) Catalogue of the Cerambycidae (Coleoptera) of the western hemisphere. Part VII. São Paulo, Sociedade Brasileira de Entomologia, 81 pp.

Monné MA, Bezark LG (2009) Checklist of the Cerambycidae or longhorned wood-boring beetles of the Western Hemisphere. Rancho Dominguez, BioQuip Publications, 460 pp.

Perty JAM (1832) Delectus animalium articulatorum: quae in itinere per Brasiliam, annis MDCCXVII-MDCCCXX jussu et auspiciis Maximiliani Josephi I, Bavariae Regis Augustissimi. Impensis Editori, Monachii, 224 pp. https://doi.org/10.5962/bhl.title.102991

Pikart TG, Souza GK, Ribeiro RC, Zanuncio JC, Serrão JE (2014) Epidermis associated with wax secretion in the *Harpactor angulosus* (Hemiptera: Reduviidae). Annals of the Entomological Society of America 107: 227–233. https://doi.org/10.1603/AN13003

Rédei D, Tsai J-F (2011) The assassin bug subfamilies Centrocnemidinae and Holoptilinae in Taiwan (Hemiptera: Heteroptera: Reduviidae). Acta Entomologica Museu Nationalis Pragae 51: 411–442.

Rosa JA, Mendonça VJ, Gardim S, Carvalho DB, Oliveira J, Nascimento JD, Pinotti H, Pinto MC, Cilense, M, Galvão C, Barata JMS (2014) Study of the external female genitalia of 14 *Rhodnius* species (Hemiptera, Reduviidae, Triatominae) using scanning electron microscopy. Parasites & Vectors 7: 17. https://doi.org/10.1186/1756-3305-7-17

Rosa JA, Mendonça VJ, Rocha CS, Gardim S, Cilense M (2010) Characterization of the external female genitalia of six species of Triatominae (Hemiptera, Reduviidade) by scanning

electron microscopy. Memórias do Instituto Oswaldo Cruz 105: 286–292. https://doi.org/10.1590/S0074-02762010000300007

Schuh RT, Slater JA (1995) True Bugs of the World (Hemiptera: Heteroptera). Classification and natural history. Cornell University Press, Ithaca, 336 pp.

Spinola M (1840a) [1837] Essai sur les genres d'insectes appartenants à l'ordre des Hémiptères, Lin. ou Rhyngotes, Fab. et à la section des Hétéroptères, Dufour. Yves Gravier, Gènes, 383 pp. https://doi.org/10.5962/bhl.title.65481

Spinola M (1840b) Essai sur les Insectes Hémiptères Rhyngotes ou Hétéroptères. Chez J.-B. Baillière, Paris, 383 pp. https://doi.org/10.5962/bhl.title.48511

Stål C (1860) Bidrag till Rio de Janeiro-Traktens Hemipter-Fauna. Kongliga Svenska Vetenskaps-Akademiens Handlingar 2: 1–84.

Stål C (1862) Hemiptera mexicana enumeravit speciesque novas descripsit. Stettiner Entomologische Zeitung 23: 437–462.

Stål C (1866) Bidrag till Reduviidernas kännedom. Öfversigt af Kongliga Vetenskaps-Akademiens Förhandlingar 23: 235–302.

Stål C (1868) Hemiptera Fabriciana. Kongliga Svenska Vetenskaps-Akademiens Handlingar 7: 93–131.

Stål C (1872) Enumeratio Reduviinorum Americae – Enumeratio Hemipterorum. Kongliga Svenska Vetenskaps-Akademiens Handlingar 10: 66–128.

Swanson DR (2012) A new synonym in the Harpactorinae of the New World (Heteroptera: Reduviidae). Proceedings of the Entomological Society of Washington 114: 250–254. https://doi.org/10.4289/0013-8797.114.2.250

Zajciw D (1972) Revisão das espécies sul-americanas do gênero *Isthmiade* Thomson, 1864 (Coleoptera, Cerambycidae, Rhinotragini). Revista Brasileira de Biologia 32: 573–583.

Zhang G, Hart ER, Weirauch C (2016) A taxonomic monograph of the assassin bug genus *Zelus* Fabricius (Hemiptera: Reduviidae): 71 species based on 10,000 specimens. https://doi.org/10.3897/BDJ.4.e8150

Zhang G, Weirauch C (2013a) Sticky predators: a comparative study of sticky glands in harpactorine assassin bugs (Insecta: Hemiptera: Reduviidae). Acta Zoologica 94: 1–10. https://doi.org/10.1111/j.1463-6395.2011.00522.x

Zhang G, Weirauch C (2013b) Molecular phylogeny of Harpactorini (Insecta: Reduviidae): correlation of novel predation strategy with accelerated evolution of predatory leg morphology. Cladistics 30(4): 339–351. https://doi.org/10.1111/cla.12049

Zhao P, Ren S, Wang B, Cai W (2015) A new species of the genus *Sphedanolestes* Stål 1866 (Hemiptera: Reduviidae: Harpactorinae) from China, with a key to Chinese species. Zootaxa 3985: 591–599. https://doi.org/10.11646/zootaxa.3985.4.8

Zikán JF, Zikán W (1944) A inseto-fauna do Itatiaia e da Mantiqueira. Boletim do Ministério da Agricultura 33: 1–5.

RESEARCH ARTICLE

Delfinoia, a new South American aphid genus (Hemiptera, Aphididae, Macrosiphini) on *Cayaponia* (Cucurbitaceae)

Juan M. Nieto Nafría[1], M. Pilar Mier Durante[1], Sara I. López Ciruelos[1]

I *Departamento de Biodiversidad y Gestión Ambiental; Universidad de León; 24071 Leon*

Corresponding author: *Juan M. Nieto Nafría* (jmnien@unileon.es)

Citation: Nieto Nafría JM, Mier Durante MP, López Ciruelos SI (2017) *Delfinoia*, a new South American aphid genus (Hemiptera, Aphididae, Macrosiphini) on *Cayaponia* (Cucurbitaceae). ZooKeys 671: 49–60. https://doi.org/10.3897/zookeys.671.12247

Abstract

The genus *Delfinoia* Nieto Nafría & Mier Durante **gen. n.** is established, and *Utamphorophora peruviana* (Essig), originally *Amphorophora peruviana* and currently *Delfinoia peruviana* **comb. n.**, is designated species type of the genus. The synonymy between this species and *Wahlgreniella australis* Delfino **syn. n.** is established. Apterous and alate viviparous females of *D. peruviana* are redescribed; the male is also described. The species is currently known from Peru and Argentina; a plant of the genus *Cayaponia* (Cucurbitaceae) is the only identified host.

Keywords

Introduction

Utamphorophora peruviana (Essig, 1953) and *Wahlgreniella australis* Delfino, 1981 are two South American macrosiphine aphids (Hemiptera, Aphididae, Macrosiphini) that have never been recorded after their respective descriptions.

Utamphorophora peruviana was described by Essig (1953) as *Amphorophora peruviana* from three alate and four apterous viviparous females, although he wrote three alatae and five apterae, which were "obtained by beating onto a canvas sheet" in Rio Pampas (Peru). This capture procedure allows us to speculate whether the host plant was a tree, or perhaps a shrub, but it also could be a vine climbing on a tree. The species was subsequently transferred to *Utamphorophora* Knowlton, 1946 by Eastop (in Remaudière and Remaudière 1997) without any explanation. Favret (2016) maintains this taxonomic position, which is nevertheless controversial because the ultimate rostral segment of the viviparous females of this species carries many accessory setae, as Essig (1953) illustrated (Fig. 1), while it has only two accessory setae in the viviparous females of the other currently known *Utamphorophora* species. The species is not included in the identification keys by Blackman and Eastop (2016) because its host plant was unknown.

Wahlgreniella australis was described (Delfino, 1981) from 11 alate and 16 apterous viviparous females collected from *Cayaponia* sp. in Cordoba (Argentina). *Cayaponia* (Cucurbitaceae) includes nearly 60 species, which characteristically are vine plants, and are spread over diverse territories of America from Oklahoma (USA) to Uruguay; several species have been recorded from Argentina, and three from Cordoba province, (Duchen and Renner 2010; Pozner 2016). The novelty of the aphid species and implicitly its generic adscription had been endorsed by D. Hille Ris Lambers (see Delfino 1981: 185). The species was maintained in *Wahlgreniella* Hille Ris Lambers, 1949 by Remaudière and Remaudière (1997), Blackman and Eastop (2016) and Favret (2016). Nevertheless this generic adscription is also debatable because the species exhibits some morphological characteristics that are different to those in other *Wahlgreniella* species; for example the triangular (rather than digitiform) cauda and the relatively weakly developed frontolateral tubercles. In addition all other *Wahlgreniella* species are North American or European in origin, and their host plants are species of *Rosa* and of Ericaceae in migrant species, or species of either *Rosa* or Ericaceae in monoecious species (Blackman and Eastop, 2016).

Comparing the descriptions of the two species, and Essig's drawings of *U. peruviana* (Fig. 1) with the prepared specimens of *W. australis* conserved in the collection of the *Muséum national d'Histoire naturelle* in Paris (France) (Fig. 2C, D), some similarities between them appear: shape of frons (divergent frontolateral tubercles present), length of antennal segment VI terminal process (near six times antennal segment VI base), shape of siphunculi (swollen, with long pedunculate proximal portion), cuticular ornamentation of siphunculi (absent in swollen portion), shape of cauda (triangular), setae of penultimate and ultimate rostral segments (abundant), secondary sensoria (only present on antennal segment III of alate viviparous females), and wing veins (cubitals dusky bordered).

The aim of this work is to contribute to knowledge of South American native aphid species by (1) increasing the known data of *Utamphorophora peruviana* from the re-examination of its types, (2) increasing the known data for viviparous females of *Wahlgreniella australis* and describing its male, and (3) reassessing the taxonomic position of these two nominal species.
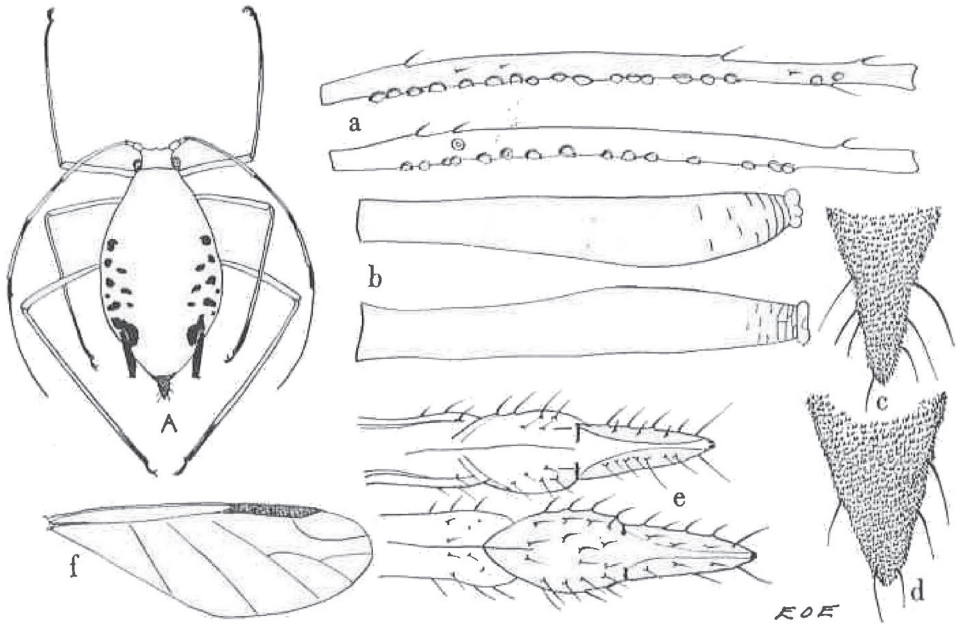
Figure 51. Peruvian aphid, *Amphorophora peruviana* Essig, new species. A, aptera showing color pattern; a, antennal segment III of alate above and aptera below; b, cornicles; c, cauda of alate; d, cauda of aptera; e, rostrum upper and lower surfaces; f, wing.

Figure 1. Illustration by Essig ("E O E"), with its legend, of the description of *Amphorophora peruviana*, on page 133 of his article (Essig, 1953). (Note: contrary to the legend, the antennal segment III attributed to an apterous viviparous female must be from an alate female, as Essig described the aptera (on page 135) as being without secondary sensoria).

Materials and methods

Studied specimens of *Utamphorophora peruviana* (Essig): PERU: Rio Pampas (PERU) [possibly near Ayacucho, from the data base of the Essig Museum, University of California in Berkeley], March 8, 1951, beating [onto a canvas sheet], A. E. Michelbacher *leg.*; E. O. Essig *det.* (V-1951); three alate viviparous females and four apterous viviparous females; one alata, the holotype, in the California Academy of Science Entomological collection; others specimens, paratypes, in the Essig Museum of Entomology collection, University of California Berkeley.

Studied specimens of *Wahlgreniella australis* Delfino: (1) ARGENTINA, Cordoba [province], Cordoba [city], 16 May 1982, on *Cayaponia* sp., Delfino *leg.* & *det.*; 15 apterous viviparous females, six alate viviparous females and one male (winged); (2) ARGENTINA, Cordoba [province], Cordoba [city], barrio Cerro de las Rosas, 1 March1985, on an unidentified species of Brassicaceae, Bahamondes *leg.*, Remaudière *det.*; 11 apterous and three alate viviparous females. These are all located in the Muséum national d'Histoire naturelle (Paris, France) and Universidad de León aphidological collections.

Measurements were taken according to Nieto Nafría and Mier Durante (1998) with an ocular micrometer mounted on a light-field microscope. Microphotographs were taken with a Nikon set: SMZ1500 stereoscopic microscope with oblique coherent light, DXM1200F digital camera, and NIS-Elements F version 3.22 software (for Fig. 2), and with a smartphone through the eyepiece of a microscope Olympus CX41 (for Fig. 4). Drawings (Fig. 3) were made with the help of a camera lucida attached to the microscope.

Results and discussions

The qualitative features of the studied viviparous females of *U. peruviana* (Essig) and *W. australis* Delfino are identical (Fig. 2) and the metric and meristic features are very similar (Table 1). Consequently, we propose that *Wahlgreniella australis* Delfino, 1981 syn. n. is a junior synonym of *Utamphorophora peruviana* (Essig, 1953).

Additionally several qualitative features, particularly the absence of cilia in the relatively thick edge of the primary sensoria, allow us to separate this species from species in other genera of Macrosiphini with similar characteristics, establishing a new genus, which is named *Delfinoia*.

Delfinoia Nieto Nafría & Mier Durante, gen. n.
http://zoobank.org/94ECE792-62B4-4CBD-BAB4-8DB36BEDB5C0
Figs 2, 3, 4

Diagnosis. Aphid genus belongig to tribe Macrosiphini (Aphididae, Aphidinae) with primary sensoria on antennal segments V and VI with thick and non-ciliated edge (Fig. 4).

Description. Macrosiphine aphid with (1) primary sensoria with thick and non-ciliated edge (Fig. 4), in addition to presence of (2) moderately divergent and smooth frontolateral tubercles and a small frontomedial tubercle and small frontal sinus in apterous viviparous females (Figs 2, 3A), (3) long antenna with long antennal segment VI terminal process (Fig. 2), (4) long and moderately swollen siphunculi (Figs 2, 3E), and also (5) secondary sensoria on antennae absent in apterous viviparous females and present on segment III in alate viviparous females (Figs 2, 3G), (6) penultimate and ultimate rostral segments provided with many robust, long and pointed setae (Fig. 3C), (7) first segments of tarsi with three setae, (8) dorsum scarcely sclerotized, mainly unpigmented in wingless forms and with marginal and intersegmental sclerites in winged forms (Fig. 2), (9) rugose and pale spiracular sclerites and circular or subcircular spiracular apertures (Fig. 3D), (10) truncated and short setae on most part of body dorsum and appendages (Fig. 3B), (11) siphunculi tenuously ornamented in the proximal part, smooth on remaining length, and provided with few and not always complete lines under the flange (Figs 2, 3E), (12) triangular and relatively short cauda (Table 1, Figs 2, 3F), and (13) dusky bordered forewing cubital veins in winged forms (Fig. 2).

Type species. *Amphorophora peruviana* Essig, 1953.

Table 1. Metric and meristic features of viviparous females of *Utamphorophora peruviana* (Essig), and viviparous females and males of *Wahlgreniella australis* Delfino (all of them now under the name *Delfinoia peruviana*). The measurements are lengths, except where indicated that they are a width or diameter. Values in brackets are data from Delfino's description of *W. australis*. Values in bold are new minima or maxima for each character in apterous or alate females based on our data. Abbreviations: AL, alate viviparous females; AP, apterous viviparous females; M, males; n, number of measured specimens; Abd., abdominal segment; AntIII, AntIV, AntV, AntVIb, AntVIpt, antennal segments, b and pt respectively being base and processus terminalis of sixth segment; *D*, subarticular width of AntIII; seg., segment; *SPW* and *SSW*, respectively minimal width of proximal pedunculate portion and maximal width of swollen portion of siphunculus.

	U. peruviana AP types (n=4)	*W. australis* AP new data (n=18) & [orig.descr.]	*U. peruviana* AL types (n=3)	*W. australis* AL new data (n=8) & [orig.descr.]	M n=1
Body [mm]	2.800–**3.575**	**2.150**–3.150	2.600–**3.125**	**2.350**–3.025	2.200
Antenna [mm]	3.875–**4.050**	**2.875**–4.050	3.600–**4.175**	**3.200**–3.875	3.513–3.675
Antenna / body [times]	**1.12**–1.42	1.18–**1.48**	1.31–1.39	**1.28**–1.48	1.60–1.67
AntIII [mm]	0.64–**0.90**	**0.58**–0.79	0.71–**0.88**	**0.63**–0.72	0.66–0.67
AntIV [mm]	**0.45**–0.78	0.50–**0.80**	0.65–**0.80**	**0.53**–0.69	0.60–0.62
AntV [mm]	**0.38**–0.71	0.51–**0.77**	0.59–**0.75**	**0.56**–0.69	0.60–0.61
AntVIb [mm]	**0.10**–0.20	0.16–**0.20**	**0.17**–0.19	**0.17**–0.20	0.16–0.17
AntVIpt [mm]	1.03–1.24	**1.01**–1.27	1.18–1.32	**1.11**–1.33	1.13–1.25
AntVIpt / AntIII [times]	**1.3**–1.4	1.5–**1.8**	**1.5**–1.7	1.7–**1.9**	1.7–1.9
AntVIpt / AntVIb [times]	**5.4**–6.9	5.5–**7.1** [~ 6.0]	6.6–7.1	**6.4**–7.2 [5.8–7.2]	6.6–7.8
Femur of hind legs [mm]	0.97–**1.38**	**0.87**–1.23	1.05–**1.20**	**0.88**–1.10	0.37–0.38
Tibia of hind legs [mm]	1.85–**2.50**	**1.70**–2.25	2.05–**2.38**	**1.85**–2.27	0.73–0.74
Ultimate rostral seg. [mm]	0.16–**0.18**	**0.15**–0.18 [0.16]	0.16–**0.17**	**0.15**–0.17	0.15
Ultimate rostral segment / its basal width [times]	2.2	**2.1**–2.6		2.6–2.8	
Ultimate rostral seg. / AntVIb [times]	0.9–**1.6**	**0.8**–1.1	0.9–**1.0**	**0.8**–0.9	0.9
Ultimate rostral seg / 2nd seg. hind tarsi [times]	1.2–**1.4**	**1.1**–1.4 [1.3]	1.2–1.4	1.3–**1.5** [**1.2**–1.3]	1.4
2nd seg. hind tarsi [mm]	**0.11**–0.15	0.12–0.14	0.12–**0.14**	**0.11**–0.13	0.11
Siphunculus [mm]	0.48–0.61	**0.44**–0.65	0.44–0.53	**0.41**–0.54	0.39
SPW [mm]	0.05–**0.07**	**0.04**–0.07	0.04–0.5	0.04–0.05	0.04
SSW [mm]	0.07–**0.11**	**0.06**–0.10	**0.07**–0.08	**0.07**–0.09	0.06
Siphunculus / body [mm]	**0.17**–0.21	0.19–**0.23**	**0.16**–0.18	0.17–**0.20**	0.18
Siphunculus / AntIII [times]	**0.7**–0.8	**0.7**–0.9	**0.6**–0.7	**0.6**–0.8	0.6
Siphunculus / *SPW* [times]	**8.1**–9.7	8.5–**11.2**	**9.0**–11.0	9.2–**13.5**	11.3
Siphunculus / *SSW* [times]	**5.1**–6.9	5.6–**7.9**	6.0–6.6	**5.0**–7.2	6.6
SSW / *SPW* [times]	1.3–**1.8**	**1.2**–1.8	1.4–1.8	**1.4**–2.1	1.7
Cauda [mm]	0.24–0.30	**0.20**–0.31	0.21–**0.25**	**0.19**–0.25	0.15
Cauda / siphunculus [times]	0.5	**0.4**–0.5 [0.5]	0.5	**0.4**–0.5 [0.4–0.5]	0.4
Cauda / its basal width [times]	**1.3**–1.4	**1.3**–1.8	**1.2**–1.3	**1.2**–1.4	1
Secondary sensoria on…					
… AntIII [quantity]	0	0 [0]	14–**19**	**4**–19 [6–17]	58–61

	U. peruviana AP types (n=4)	*W. australis* AP new data (n=18) & [orig.descr.]	*U. peruviana* AL types (n=3)	*W. australis* AL new data (n=8) & [orig.descr.]	**M** n=1
… AntIV [quantity]	0	0 [0]	0 [0]	0 [0]	15–33
… AntV [quantity]	0	0 [0]	0 [0]	0 [0]	7–12
Setae on…					
… head, dorsal med. [μm]	25–**30**	**17–30**	**16**–25	17–**28**	23
… head, dorsal med. / *D* [times]	0.7	**0.5–1.2**	**0.4**–0.7	0.5–**0.8**	0.7
… AntIII [μm]	15–**18**	**10–18**	15–18	**10–20**	18
… AntIII / *D* [times]	0.4–0.5	**0.3–0.6**	0.4–0.5	**0.3–0.6**	0.5
… penultimate rostral seg. [quantity]	20–**29**	**18**–24	20–**23**	**16**–19	18
… ultimate rostral seg., accessory [quantity]	7–11	**7–12** [9]	10–11	**9–14** [9]	11
… ultimate rostral seg., accessory [μm]	35–**48**	**25–3**5	**28**–35	30–**40**	
… hind femur, dorsal [μm]	**10–20**	**10–13**	**17–25**	17–23	
… hind femur, dorsal / *D* [times]	**0.3**–0.5	**0.3–0.6**	0.6–**0.8**	**0.5**–0.7	
… hind tibia, dorsal medial [μm]	22–**25**	**15–23**	20–**23**	**15**–20	
… hind tibia, dorsal medial / *D* [times]	**0.5**–0.7	**0.5–1.0**	0.6–**0.7**	**0.5–0.7**	
… Abd.2-Abd.5, spinal per segment [quantity]	10–12	**6–15**	10–14	**9–15**	
… Abd.2-Abd.5, spinal [μm]	10–14	**8–20**	**10**	10–**18**	13
… Abd.2-Abd.5, spinal / *D* [times]	0.3–0.4	**0.2–0.6**	**0.3**	**0.3–0.5**	0.4
… Abd.2-Abd.5, ventral [μm]	**20–35**	25–**38**	**23–35**	25–35	20
… Abd.2-Abd.5, ventral / *D* [times]	**0.5**–1.0	0.8–**1.7**	**0.7–1.1**	0.8–**1.1**	0.6
… Abd.8 [quantity]	5–**8**	**4–8** [6]	6–**8**	**4–8** [5–7]	4
… Abd.8 [μm]	**25–53**	30–40	30–38	**27–35**	48
… Abd.8 / *D* [times]	**0.7**–1.5	0.9–**1.7**	**0.9**–1.0	**0.8–1.1**	1.5
… genital plate, discal [quantity]	**2–5**	**2–5**	2–3	**2–4**	///
… genital plate, posterior [quantity]	**12–16**	16–**24**	**14–15**	17–**24**	///
… cauda [quantity]	**7**	**3–6** [5]		4–7 [5]	5

Taxonomic discussion. Ten genera and one subgenus of Macrosiphini known in the Americas have more or less developed and divergent or parallel frontolateral tubercles, long antennae and elongate swollen siphunculi (characters 2, 3 and 4); they are *Amphorophora* Buckton, 1876, *Delphiniobium* Mordvilko, 1914, *Gibbomyzus* Nieto Nafría, Pérez Hidalgo, Martínez-Torres & Villalobos Muller, 2013, *Glabromyzus* Richards, 1960, *Hyperomyzus* Börner, 1933, *Illinoia* Wilson, 1910, *Rhopalomyzus* Mordvilko, 1921 and *Ucrimyzus* Mier Durante & Pérez Hidalgo, 2013, *Utamphorophora* and *Wahlgreniella*, and the subgenus *Picturaphis* Blanchard, 1922 which is currently included in genus *Microparsus* Patch, 1909.

Feature 1 is the most distinctive character of the new genus, and is very exceptional in Macrosiphini, and features 5 to 13 in combination help to separate the new genus from any of the above mentioned genera, although they are present in some of them.

The novelty of the genus could be assured with complete certainty by the analysis of some genetic marker, which cannot be carried out at present because all the known material of the species is mounted on microscopic slides.

Etymology. The name *Delfinoia* is in honour of Dr. Miguel Ángel Delfino (retired professor of entomology, University of Cordoba (Argentina), aphidologist and good friend for decades), who was the author of *W. australis*.

Delfinoia peruviana (Essig, 1953), comb. n.

Figs 2A, C, 3, 4

Amphorophora peruviana Essig: Essig, 1953; Proceedings of the California Academy of Sciences, Fourth Series, 28 (3): 133 & 135.
Wahlgreniella australis Delfino: Delfino, 1981; Revista de la Sociedad Entomológica Argentina, 40 (1-4): 183–186; **syn. n.**
Utamphorophora peruviana (Essig, 1953): Eastop, 1997; in Remaudière (G.) & Remaudière (M.), Catalogue des Aphididae du monde / Catalogue of the World's Aphididae (Homoptera Aphidoidea): page 158.

Description. Apterous viviparous females (redescription, from 30 studied specimens [see "Materials and methods"] and original descriptions of both nominal species).

Colour unknown when alive, possibly green or light green, and perhaps, from Essig's drawing, with two small dark spots on each side of several abdominal segments, brown cauda and dark brown or blackish brown siphunculi. When mounted variably light yellow, with head, including antennae and rostrum, legs, siphunculi, anal plate and cauda more or less pigmented (see below). Quantitative characters are in Table 1. *Head*. Brownish yellow. Frons sinuated, with broadly divergent and moderately developed frontolateral tubercles and low frontomedial tubercle. Dorsum smooth and ventrum with stretch marks. Setae of first and second dorsal row (each with two setae) and internal setae of third dorsal row (with four setae) similar in length to each other; external setae of third row approximately half as long as the other six. These eight dorsocephalic setae, the frontolateral apical setae and the three ventrolateral setae on each side (near the margins of the antennal alveoli) have truncate apices; other ventral setae, including those on clypeus and on mandibular and maxillar laminae, are pointed. Antennal segment I slightly pigmented and mostly smooth, with its inner side somewhat darker and gently scabrous; segment II also slightly pigmented, dorsally smooth and ventrally scabrous. Antennal segment III also pale, with a smoky apical ring, and tenuous cuticular ornamentation, which is more marked on the ventral face of its 1/5 proximal portion. Its subarticular constriction is less marked than in some other aphids; possibly the antennal flagellum has reduced mobility with respect to the pedicel as a result of this structural feature. Antennal segment IV softly imbricated and mostly pale, with smoky small proximal ring and distal portion; segment V similar to segment IV but more intensely imbricated and with a longer and more pigmented
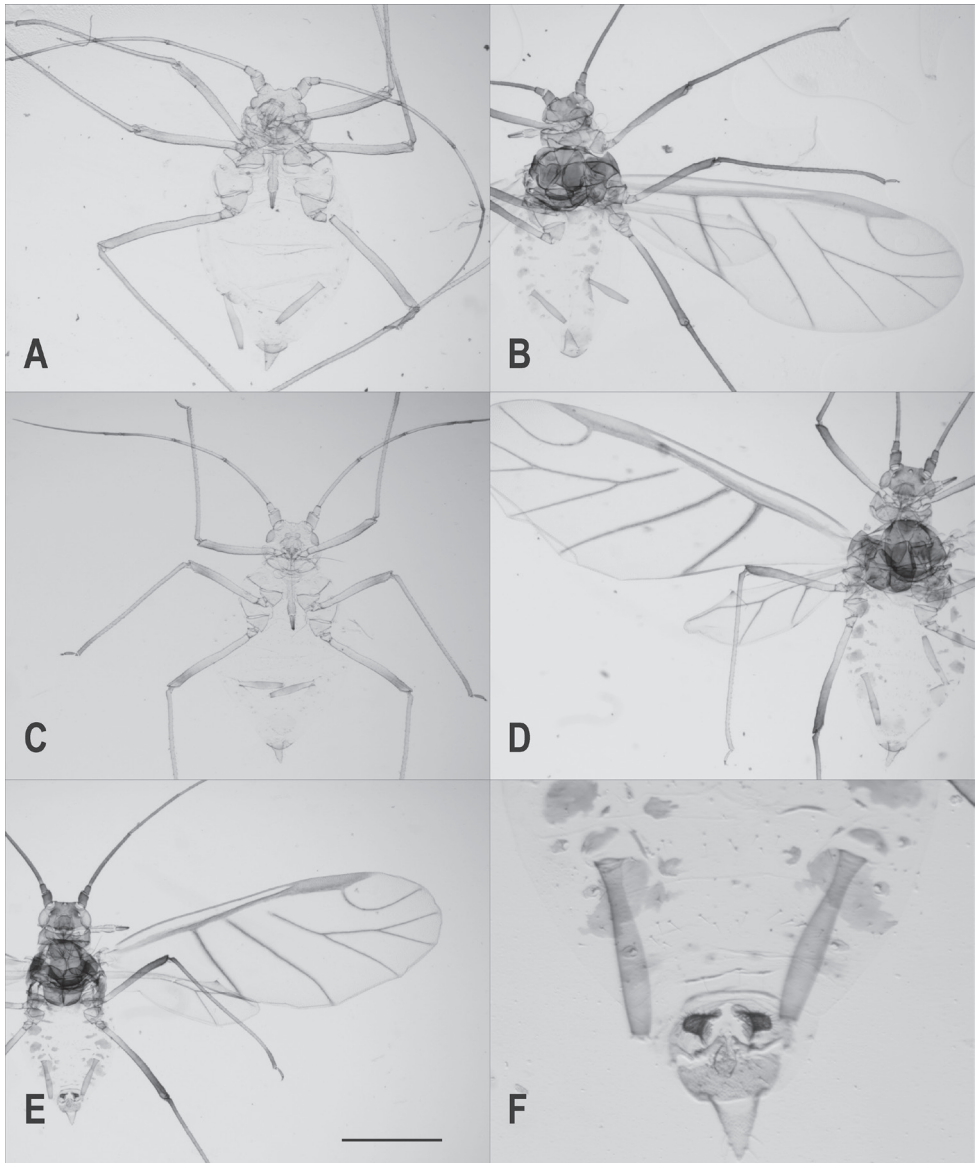
Figure 2. *Delfinoia peruviana* (Essig). **A–B** specimens from Peru, previously labelled *Utamphorophora peruviana* (Essig) **C–F** specimens from Argentina, previously labelled *Wahlgreniella australis* Delfino **A, C** apterous viviparous females **B, D** alate viviparous females **E–F** male. Scale bar: **A–D** 1 mm; **E, F** 0.21 mm.

distal portion. Antennal segment VI brown and imbricated. Several setae on segment VI are pointed and longer than other antennal setae, which are similar in shape and size to dorsocephalic ones. Secondary sensoria absent. Primary sensoria on antennal segments V and VI with thick, sclerotic and non-ciliate margins. Satellite sensoria
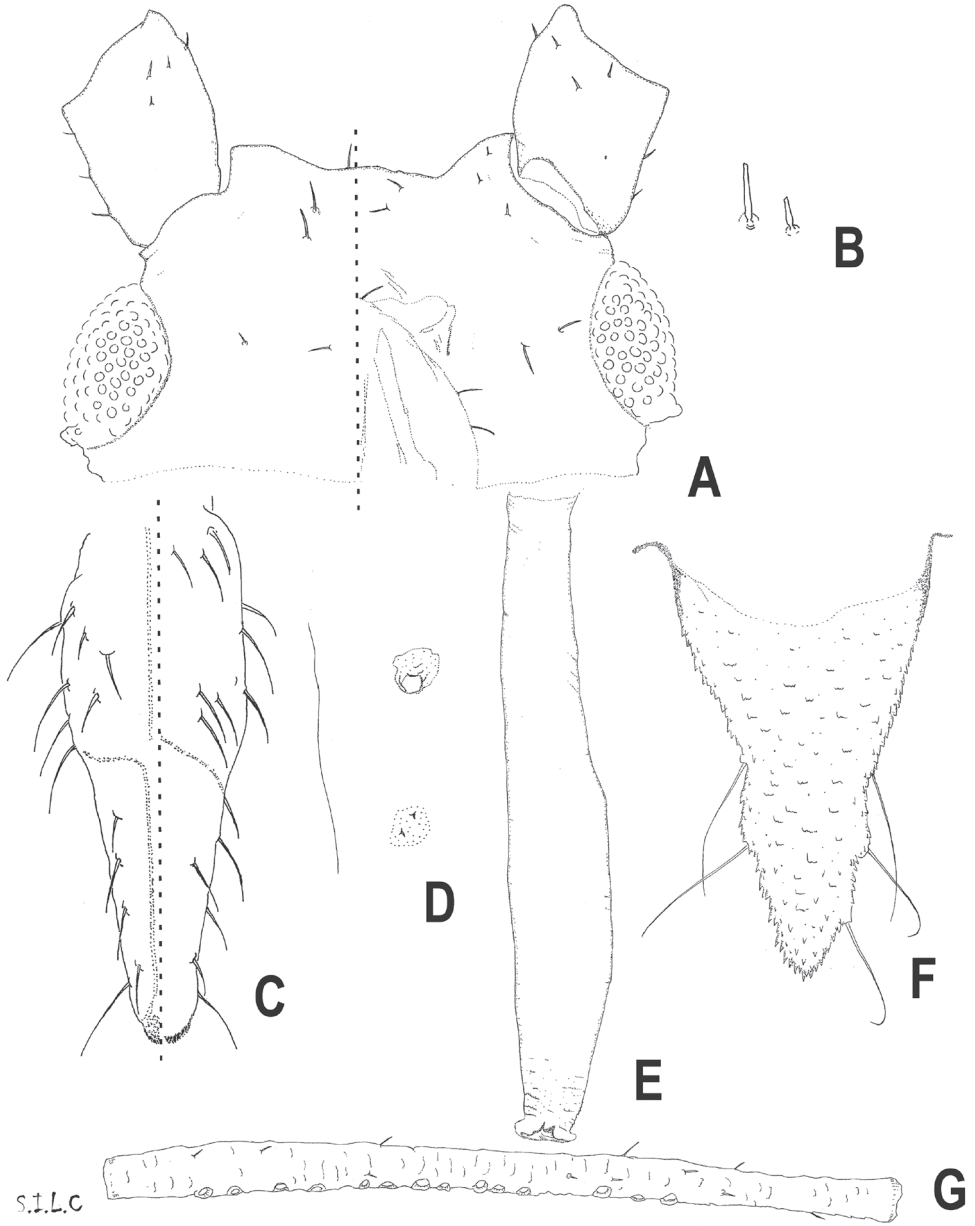
Figure 3. *Delfinoia peruviana* (Essig). **A–F** apterous viviparous females **G** alate viviparous female **A** frontal edge **B** dorsocephalic setae, third row, the shorter is the external one **C** pre-ultimate and ultimate rostral segments **D** spiracular abdominal plate and aperture **E** siphunculus **F** cauda **G** antennal segment III.

grouped ventrad to the primary sensorium. Rostrum extends back to slightly beyond hind coxae. Penultimate and ultimate rostral segments similar in length and colour (light brown) and bearing many robust, rigid and pointed setae. ***Thorax.*** Paler than

Figure 4. *Delfinoia peruviana* (Essig) apterous viviparous female. Antennal segments V and VI, in part, showing primary and satellite (on VI) sensoria.

head and generally devoid of marked cuticular ornamentation. Spiracular sclerites rugose and unpigmented, spiracular apertures circular or subcircular. Marginal papillae on prothorax if present are small, flat and unpigmented. Both dorsal and ventral setae similar in shape and size to those on anterior abdominal segments. Tarsi and apex of tibiae pale brown, rest of legs brownish yellow. Setae on femora and most of those on tibiae short and with truncate apices; setae on coxae (which are longer than others), trochanters and tarsi pointed, as also are dorsoapical tibial setae. First segments of tarsi with three setae. ***Abdomen***. In general paler than head. Spiracular sclerites and apertures similar to those on thorax. Intersegmental sclerites inconspicuous. Small presiphuncular sclerites small, postsiphuncular sclerites relatively wide, and a narrow transverse stripe on segment VIII; all of these sclerites spinuled and pale yellow. Dorsal setae short and with truncate apices, except those on abdominal segment VIII, which are pointed. Ventral setae pointed. One specimen (paratype) has one marginal tubercle on abdominal segment IV, small and pale. Siphunculi light brown, swollen over distal half of length, smooth or nearly smooth for most of length, and with three or four complete or incomplete circular lines below the flange, which is protruding and relatively thick. Genital plate very pale; anal plate with similar pigmentation to cauda, which is triangular with blunt apex. Setae on these plates and cauda pointed.

Alate viviparous females (redescription, from 12 studied specimens [see "Materials and methods" section] and from original descriptions of both nominal species). Fig. 2B, D.

Colour unknown when alive, possibly with dark brown or black head and thorax, including antennae and legs, and green abdomen with dark brown lateral spots, cauda and siphunculi. Quantitative characters are in Table 1; qualitative characters like those of apterae are not mentioned. ***Head***. Brown with darker areola around each ocellus. Dorsum with tenuous ornamentation. Frontolateral tubercles very low and frontomedial tubercle inconspicuous. Antennae homogeneously brown. Antennal segment III with secondary sensoria, which are similar in shape to the primary ones and variable in size, more-or-less aligned over almost the entire length. ***Thorax***. Legs brown, with paler coxae, trochanters and proximal part of femora. Fore wings with veins well-marked and the cubital veins dark-bordered; hind wings veins also well-marked but not bor-

dered. **Abdomen**. Pale in general. Sclerites variably pigmented, sometimes as pale as the rest of the abdominal cuticle. Intersegmental sclerites smooth. Marginal sclerites on segments I - VII spinuled, the postsiphuncular sclerites being wider than the others. Setiferous spinal and pleural sclerites present on segment VIII and sometimes on segments VI and VII, all of them spinuled and usually pale or very pale. One specimen (holotype) has four small, ill-defined and pale marginal tubercles on abdominal segments II, III (on both sides) and IV; another specimen (paratype) also has similar tubercles on one side of abdominal segments III and IV.

Males (from one specimen, see "Materials and methods" section). Fig. 2E–F. Winged; similar to alate viviparous females in general aspect, pattern of sclerotisation, extent of pigmentation and cuticular ornamentation. Colour when alive unknown. Secondary sensoria present on antennal segments III, IV and V. Hind wings have a single oblique vein, which could well be an anomaly, although the presence of an identical anomaly in both wings is strange. Two small pale abdominal marginal tubercles present. Parameres broad, curved back, very dark brown and provided with many, rigid, pointed and relatively long hairs. Quantitative characters are in Table 1.

Biology. It is certain that *Delfinoia peruviana* feeds on plants of one or more species of *Cayaponia* in Argentina, and perhaps also in Peru (see "Introduction"). The species has been also caught on a cruciferous plant in Cordoba (Argentina). The collector of those specimens, L. Bahamondes, was an experienced (but now deceased) entomologist and a connoisseur of Argentinean flora, so one can be certain that the specimens were collected on a plant of family Brassicaceae, but it is also conceivable that the specimens collected had fallen from some vine of the genus *Cayaponia*.

Distribution. The species is currently known in two localities (one in Peru and the other in Argentina) that are 2,200 kilometers distant from each other. Possibly the species can be found in much of northern Argentina, southern Peru and also in eastern Bolivia and southwestern Brazil.

Acknowledgments

References

Blackman RL, Eastop VF (2016) Aphids on World's plants. An online identification and informative guide. http://www.aphidsonworldsplants.info [accessed January 2017]

Delfino MA (1981) Una nueva especie del género *Wahlgreniella* Hille Ris Lambers, 1949 (Homoptera: Aphididae). Revista de la Sociedad Entomológica Argentina 40(1–4): 183–186.

Duchen P, Renner SS (2010) The evolution of *Cayaponia* (Cucurbitaceae): Repeated shifts from bat to bee pollinitation and long-distance dispersal to Africa 2–5 million years ago. American Journal of Botany 97(7): 1129–1141. https://doi.org/10.3732/ajb.0900385

Essig EO (1953) Some new and noteworthy Aphididae from Western and Sourthern South America. Proceedings of the Californian Academia of Sciences, Fourth Series 28(3): 59–164

Favret C (2016) Aphid Species File. Version 5.0/5.0. http://aphid.speciesfile.org [accessed January 2017]

Nieto Nafría JM, Mier Durante MP (1998) Hemiptera Aphididae I. In: Ramos MA et al. (Eds) Fauna Ibérica (Vol. 11). Museo Nacional de Ciencias Naturales (CSIC), Madrid, 424 pp.

Pozner R (2016) Cucurbitaceae. In: Antón AM, Zuloaga FO (Eds) Flora Argentina. http://www.floraargentina.edu.ar [accessed December 2016]

Remaudière G, Remaudière M (1997) Catalogue des Aphididae du monde [Catalogue of World's Aphididae] – Homoptera Aphidoidea. INRA Editions, Paris, 474 pp.

RESEARCH ARTICLE

A new cryptic species and review of the east-Andean leaf chafer genus *Mesomerodon* Ohaus, 1905 (Coleoptera, Scarabaeidae, Rutelinae)

Matthias Seidel[1,2,3], Mary L. Jameson[4], Rachel L. Stone[4]

1 *Department of Zoology, Faculty of Science, Charles University, Viničná 7, Praha 2, Czech Republic, CZ-12383* **2** *Department of Entomology, National Museum, Cirkusová 1740, Praha 9, Czech Republic, CZ-19300* **3** *Zentralmagazin Naturwissenschaftlicher Sammlungen, Martin-Luther-Universität Halle-Wittenberg, Domplatz 4, Halle (Saale), Germany, D-06108* **4** *Department of Biological Sciences, Wichita State University 1845 Fairmount, Box 26, Wichita, KS, USA 67260-0026*

Corresponding author: *Matthias Seidel* (seidelma@natur.cuni.cz)

Abstract

The Neotropical scarab beetle genus *Mesomerodon* Ohaus (Scarabaeidae: Rutelinae: Rutelini) is distributed in the western (lowland) Amazonian region from Colombia to Bolivia. Based on our research, the genus includes three species including a new cryptic species from Ecuador. We use niche modeling to predict potential suitable habitat and identify environmental factors associated with the distribution of *Mesomerodon* species. We characterize the genus, provide a key to species, diagnose each species, describe a new species, provide spatial and temporal distributions, and discuss distributions of the species in relation to Amazonian landscape biodiversity.

Resumen

El género neotropical de escarabajos *Mesomerodon* Ohaus (Scarabaeidae: Rutelinae: Rutelini) se distribuye en las zonas bajas del oeste de la Amazonía, de Colombia a Bolivia. Con base en nuestro estudio, este género se compone por tres especies, incluyendo una nueva especie críptica de Ecuador. Utilizamos el modelado de nicho para predecir el hábitat adecuado potencial e identificar los factores ambientales asociados con la distribución de las especies de *Mesomerodon*. Aquí caracterizamos al género, proporcionamos una clave dicotómica para las especies, diagnosticamos cada especie, describimos una nueva especie, proveemos información sobre la distribución espacial y temporal de las especies y discutimos la distribución de las especies en relación a la biodiversidad de paisajes de la Amazonía.

Introduction

The South American genus *Mesomerodon* Ohaus (Figs 1–8) is a member of the pelidnotine leaf chafer scarabs, a polyphyletic assemblage of beetles which are in need of comprehensive revision (Moore et al. 2017). Members of the genus *Mesomerodon* are ovate, 17–25 mm in length, and cream-colored when alive (Figs 7–8). After death the color fades to testaceous or yellowish with weak metallic reflections. The genus is sexually dimorphic: males possess elongated, spinose elytral apices as well as an acute process on the posterior margin of the mesofemur (both lacking in females). The unusual form of the spinose elytral apex is a character state that is shared with males of the Neotropical leaf chafer *Hoplopelidnota metallica* (Laporte, 1840). Sister group relationships have not been addressed, host plant information is lacking, and larvae are undescribed. Members of this distinctive but poorly known group are distributed in lowland Amazonian regions (ca. 150–760 m elevation) from Colombia to Bolivia and are collected at light at night. In overall body form, the genus *Mesomerodon* resembles some species of *Pelidnota* MacLeay, 1819 (with which it is closely allied).

Ohaus (1905) established the genus *Mesomerodon* Ohaus and included in it one species with 'peculiar sexual characteristics' from Peru. Nearly 100 years after Ohaus' (1905) description of the genus, Soula (2008) described a second species, *Mesomerodon gilletti* from Ecuador. In an overview of pelidnotine leaf chafers (Moore et al. 2017), the distribution of the genus was expanded to include Colombia and Bolivia. The distributional data provided for the genus *Mesomerodon* (Moore et al. 2017) were derived from the data in this study and are therefore given for the first time with specimen associations.

Species in the genus *Mesomerodon* possess many external similarities in form, but the male genitalia are sufficiently different as to warrant species status for three, distinct operational taxonomic units that we treat as species. Soula (2008) recognized *M. gilletti* as distinct from *M. spinipenne* based entirely on the form of the male genitalia (Fig. 23 versus Fig. 24). Cryptic species such as these are difficult or sometimes impossible to distinguish morphologically, and they are often incorrectly classified as a single taxon (Beheregaray and Caccone 2007, Bickford et al. 2007). Our synthesis of information on this group of beetles, which is based on 302 specimens and morphological data, led to the unveiling of an additional cryptic species in the genus.

We provide a synthesis of the biodiversity of the genus, including descriptions, key to species, diagnoses, and images. As a result of our research, the genus *Mesomerodon* includes three species, all of which are distributed in the western (lowand) Amazonia, including a new unexpected and cryptic species.

Material and methods

Characters. Morphological characters formed the basis of this work. The broadest range of potentially phylogenetically informative morphological characters was used for morphological analyses and comparisons. Morphological terminology is based primarily on Jameson (1998), however we use the term venter instead of sternum and antennomeres instead of antennal segments. Antennomeres are defined as the pedicel plus flagellum (or flagellum and club). Consistent with use of venter, the term mesometasternum is replaced with mesometaventrum and the term sternite is replaced with ventrite. For measurements, we used an ocular micrometer. Body measurements, puncture density, puncture size, and density of setae are based on the following standards. Body length was measured from the apex of the clypeus to the apex of the pygidium. Body width was measured at the widest width of the elytra. Puncture density was considered 'dense' if punctures were nearly confluent to less than two puncture diameters apart, 'moderately dense' if punctures were from two to six puncture diameters apart, and 'sparse' if punctures were separated by more than six puncture diameters. Puncture size was defined as 'small' if punctures were 0.02 mm in diameter or smaller; 'moderate' if 0.02–0.07 mm, 'moderately large' if 0.07–0.12 mm, and 'large' if 0.12 mm or larger. Setae density was defined as 'dense' if the surface was not visible through the setae, 'moderately dense' if the surface was visible but with many setae, and 'sparse' if there were few setae. It should be noted that setae are subject to wear and may be abraded away. Elytral striae are defined as the striae located between the elytral suture and the elytral humerus. The interocular width measures the number of transverse eye diameters that span the width on the frons between the eyes. This was measured by placing the ocular micrometer in a position such that it intersects the frons and eyes (dorsal view), focusing on the surface of the frons, and then measuring the width of the frons and width of the eyes without adjusting the focus. Sclerotized portions of the male genitalia are used for diagnosis and identification. This includes the parameres, phallobase (or "basal piece" [d'Hotman and Scholtz 1990]), and the ventral sclerite of the phallobase (e.g., Fig. 22). Mouthparts, wings, and genitalia were examined and card-mounted beneath the specimen.

Characters and specimens were observed with 6–48× magnification and fiber-optic illumination. Digital images of specimens and structures were captured using the Leica Application Suite V3.8. Images were edited in Adobe Photoshop CS2 (background removed, contrast manipulated).

Species concept. Species are characterized by combinations of characters including the form the male protarsomeres and form of the male parameres in caudal and lateral views, and form of the ventral sclerite of the phallobase. Identification of female specimens required associated males from the same collecting event (place and date). We use the phylogenetic species concept (Wheeler and Platnick 2000) in this work: "A species is the smallest aggregation of (sexual) populations or (asexual) lineages diagnosable by a unique combination of character states."

Locality data. Locality data for all specimens examined as part of this study were translated into decimal latitude and longitude using GoogleEarth (http://www.google.com/earth/index.html) and provided (Suppl. material 1). If latitude and longitude data were not included in label data or were too vague to be informative, then we searched for GPS data in GoogleEarth and GoogleMaps. Maps were generated by entering the coordinates into an Excel sheet. These files were subsequently used to construct distribution maps using an R script which plots the distribution points on an elevational map constructed using Global Land One-kilometer Base Elevation (GLOBE) data (Hastings et al. 1999). For species accounts, locality data are recorded for country, department and province (Bolivia), region and province (Peru), department (Colombia), or province (Ecuador). Additional locality data are provided (Suppl. material 1).

Distribution modelling. To model the potential distribution and to identify environmental factors associated with *Mesomerodon* species, we used the maximum entropy algorithm (MaxEnt; Phillips et al. 2006, Elith et al. 2011) for the species distribution modeling and followed the workflow of Fikáček et al. (2014). For occurrence data, we summarized all available records for all species of *Mesomerodon*. We ran three independent analyses: a genus-level distribution analysis that included data for all species and unidentified specimens, an analysis of the distribution of *Mesomerodon spinipenne,* and a combined analysis of the Ecuadorian and Colombian species (*M. gilletti* + *M. barclayi* sp. n.). A separate analysis for either *M. gilletti* or *M. barclayi* sp. n. was not conducted due to the few number of data points per species. Because two species occur in sympatry and in similar climatic conditions (*M. gilletti* and *M. barclayi* sp. n.), we concluded that the combined species analysis is justified. Furthermore, a combined analysis of the latter two species made it possible to include data points with unassociated species (female specimens which could not be identified). We employed the high-resolution climate data available in the Worldclim database (Hijmans et al. 2005) containing 19 layers of climatic variables. Analyses were performed in R (MaxEnt command in Dismo package). After mapping the ecological niche of the genus and/or species, prediction values were converted into binary values (presence and absence) using the threshold for maximum training sensitivity and specificity provided by the outputs of the resulting models (Figs 19–21).

Type specimens. Friedrich Ohaus provided a legacy for understanding the biodiversity of Rutelinae with over 170 published papers and research collections (for biography see Smith 2003). Perhaps due to concern with destruction of museums during World War II, Ohaus often labeled specimens as types long after publication (e.g., Kuijten 1988, 1992; Jameson 1990, 1998; Smith 2003). These erroneous type specimens can be recognized because label data are incongruous with data in the original description. As part of this research, we found 10 specimens that were labeled as type specimens. Six of these specimens do not belong to the syntype series of *M. spinipenne* (Suppl. material 1): one specimen from ZMHB, four specimens from ZSM, one specimen from NHMB. To reduce future confusion, these were labeled "NOT a type specimen of *Mesomerodon spinipenne*, Ohaus, 1905, des. Seidel 2016" (see "Remarks" for *M. spinipenne*").

Collections (Suppl. material 1). This research is based on 302 specimens in 25 collections. The material examined in the present study is housed in the following collections and was provided by the curators and/or collections managers:

AMNH	American Museum of Natural History, New York, USA (Lee Herman)
BMNH	The Natural History Museum, London, United Kingdom (Max Barclay, Beulah Garner)
CCECL	Musée des Confluences, Lyon, France (Cédric Audibert)
CMNC	Canadian Museum of Nature Collection, Ottawa, Canada (Andrew Smith, François Génier)
DBPC	Denis Bouchard Personal Collection, Autouillet, France
DCCC	David Carlson Personal Collection, Fair Oaks, California, USA
DJCC	Daniel Curoe Personal Collection, Palo Alto, California, USA
FMNH	Field Museum of Natural History, Chicago, Illinois, USA (Alfred Newton, Crystal Maier)
FSCA	Florida State Collection of Arthropods, Gainesville, Florida, USA (Paul Skelley)
IRSNB	Institute Royal des Sciences Naturelles de Belgique, Brussels (Alain Drumont, Pol Limbourg)
JWPC	Jim Wappes Personal Collection, San Antonio, Texas, USA
LACM	Los Angeles County Museum of Natural History, Los Angeles, California, USA (Brian Brown, Weiping Xie)
MLJC	Mary Liz Jameson Personal Collection, Wichita, Kansas, USA
MNHN	Muséum National d'Histoire Naturelle, Paris, France (Olivier Montreuil)
MSPC	Matthias Seidel Personal Collection, Prague, Czech Republic
NHMB	Naturhistorisches Museum, Basel, Switzerland (Daniel H. Burckhardt)
NMPC	Department of Entomology, National Museum (Natural History), Prague, Czech Republic (Jiří Hájek)
QCAZ	Catholic Zoology Museum, Pontificia Universidad Catolica del Ecuador, Quito, Ecuador (Giovanni Onore)
SLCC	Stephane LeTirant Collection, Montreal, Canada
SMNS	Staatliches Museum für Naturkunde, Stuttgart, Germany (W. Schawaller)
UASC	Museo de Historia Natural Noel Kempff Mercado, Santa Cruz de la Sierra, Bolivia (Julieta Ledezma Arias)
UNSM	University of Nebraska State Museum, Lincoln, Nebraska, USA (Brett Ratcliffe, M. J. Paulsen)
USNM	U.S. National Museum, Washington, D.C. (currently housed at the University of Nebraska State Museum for off-site enhancement) (Floyd Shockley and Dave Furth)
ZMHB	Museum für Naturkunde, Leibniz-Institut für Evolutions-und Biodiversitätsforschung an der Humboldt-Universität, Berlin, Germany (Joachim Willers, Johannes Frisch)
ZSM	Zoologische Staatssammlung des Bayerischen Staates, Munich, Germany (Michael Balke)

Taxonomy

Genus *Mesomerodon* Ohaus, 1905
Figs 1–27

Mesomerodon Ohaus, 1905: 319. Type species *M. spinipenne* Ohaus, 1905: 320–321
    (by monotypy).

Description. Length from apex of clypeus to apex of pygidium 17.0–20.0 mm (♂)
and 19.0–24.0 mm (♀); width at mid-elytra 10.0–12.0 mm (♂) and 11.0–14.0
mm (♀). Color: Dorsal surface tan to ochre (cream or whitish when alive) with or
without weak green reflections, ventral surface castaneous with weak metallic green or
red reflections; specimens tend to darken with age. Form (Figs 1–8): Elongate oval,
widest at mid-elytra, pygidium exposed beyond apices of elytra; apices rounded with
one short spine or tubercle near apex (males) or swelling (females). Head: Disc of
frons and clypeus in lateral view flat, clypeus with margins and apex weakly reflexed;
length of clypeus to frons (ratio) 0.5–0.6 : 1.0. Frons and clypeus moderately densely
punctate, punctures small to moderate in size. Frontoclypeal suture weakly impressed,
incomplete at middle. Eye canthus flattened, not weakly cariniform. Interocular width
2.5–3.8 transverse eye diameters. Clypeus rounded, with apex and lateral margin
weakly reflexed, lacking bead; frontal view flat with short tawny setae, length (at
middle) about 1/10 length of frons, disc moderately densely punctate, lacking setae.
Mandible (Fig. 9) broadly rounded externally with 2 interior, acute teeth; molar region
broad; mandibular apex always exposed. Labrum (Fig. 11) with apex emarginate
medially, surface moderately densely punctate, punctures moderate in size, setose
(setae moderately long and thick, tawny). Maxilla (Fig. 10) with 6 teeth; galea not
fused, with moderately long setae. Mentum (Fig. 12) subrectangular in shape, broadest
at middle, apex emarginated. Antenna with 10 antennomeres and 3-segmented club;
club subequal in length to antennomeres 2–7 combined. Pronotum: Widest at base,
apical angles acute, basal angles obtuse. Dorsal surface moderately densely punctate;
punctures small and moderate in size. Bead complete anteriorly, laterally, and basally;
setose basolaterally (setae moderately long, tawny or white). Scutellum: Parabolic,
wider than long; base declivous at elytral base; dorsal surface as in pronotum. Wing
(Fig. 14): Dense, thick setae present anterior to RA_{3+4} to apex; ScA with dense, thick
setae near fold and with weak precostal pegs from near fold to base; AA_{1+2} shorter than
AA_{3+4}. Elytra: Surface punctate with weakly impressed striae; finely, densely rugose
at apex. Punctures sparse to moderately dense, small to moderate in size, lacking
setae. Sutural stria indicated by a row of punctures from base of scutellum to apex.
Epipleuron from base to metacoxa with shelf and associated setae; beaded. Apex of
elytra (Fig. 17) weakly rounded; elytral callus with well-defined tubercle or spine;
sutural apex spiniform. Elytral sutural length about 10 times length of scutellum.
Propygidium: Hidden beneath elytra. Pygidium: Subtriangular, about twice as wide as
long at middle; finely, densely rugopunctate. Margins beaded with sparse, moderately

long setae; setae tawny. Apex rounded. Venter (Figs 2–3): Prosternal process elongate-oval, projecting anteroventrally at about 35° with respect to ventral plane; apex produced to level of protrochanter, rounded; surface posteriorly protuberant in basal 1/4, with setaceous punctures; setae long, dense, tawny. Mesometaventral process produced anteriorly to prosternal process; apex acuminate, rounded; ventral surface weakly recurved toward apex in lateral view, lacking setae apically, with moderately dense setae basally (setae moderately dense, moderately long, tawny). Abdominal ventrites 1–4 subequal in length in male and female, ventrite 5 about 1.5–2 times the length of ventrite 4, ventrite 6 subequal in length to ventrite 4 (male) or 1.3 times length of ventrite 4 (female). Abdominal ventrites 1–4 subequal in length in male and female, ventrite 5 about 1.5–2 times the length of ventrite 4, ventrite 6 subequal in length to ventrite 4 (male) or 1.3 times length of ventrite 4 (female). Last ventrite with widest width to median length in males about 5.5:1 and in females about 4.3:1; surface smooth (male) or rugose (female). Last ventrite (male) subequal in length to ventrite 5, quadrate at subapex, subapical corners not produced, surface moderately densely punctate; region from subapex to apex less sclerotized, surface smooth. Last ventrite (female) subequal to ventrite 4, apex trapezoidal, surface rugose. In lateral view, male ventrites flat, female ventrites weakly convex. Legs: Protibia with 3 external teeth subequally separated in apical half; spur present, subapical; inner base lacking protibial notch. Protarsomere 5 of male a little longer than tarsomeres 1–4 and with well-defined ventromedial emargination (Fig. 15). Modified foreclaw of male 1.5–2 times width of unmodified claw, inner subapical tooth present, small. Foreclaws of female simple, internal claw as wide as outer claw. Unguitractor plate laterally flattened, weakly exposed beyond tarsomere 5; apex with 2 short setae. Protarsomere 2 (male) with or without striated region at ventral apex; lacking in female. Mesofemur with acute process projecting posteriorly on posterior margin (male) (Fig. 16). Mesotibia with sides subparallel, apex weakly divergent or parallel; external edge with 2 weak carinae (female), less pronounced in male; inner apex with 2 spurs; apex with 12–15 spinulae. Meso- and metatarsomere 4 apicomedially with 1 outer spinose seta and 1 inner stout spinose seta (male and female). Meso- and metatarsomere 5 with weak, triangular interomedial tooth or swelling. Outer claw of meso- and metatarsal claws slightly longer than inner claw; outer mesotarsal claw twice as wide as inner claw in males, subequal in width in females; metatarsal claws subequal in width; claws simple. Metatibia with sides subparallel, weakly divergent towards apex; external edge with 1–2 weak carinae (slightly more robust in female); inner apex with 2 spurs; inner apex with 14–26 short, stout spinulae. Metacoxal corner (female) weakly produced or square. Spiculum gastrale (Fig. 13): Weakly Y-shaped (arms ~30 degree angle), lacking associated sclerites and setae. Male genitalia (Figs 22–24): Parameres less than twice length of phallobase. Parameres fused dorsoventrally (not laterally), asymmetrical; diagnostic, species specific (Figs 22a, 23a, 24a). Ventral sclerite of phallobase asymmetrical or symmetrical, elongate (produced to apex of phallobase), apex subquadrate; diagnostic, species specific (Figs 22c, 23c, 24c). Female genitalia: Gonocoxites subtriangular to subquadrate with sparse setae; not diagnostic for species.

Natural history. Biology for species in the genus is not known. Adults likely feed on plant foliage, but no host has been recorded. Because adults are attracted to lights at night, it is likely that feeding occurs at night. Larvae are not described, but likely feed on compost and/or roots.

Etymology. From the Greek, "*mesos*" meaning middle or in the middle, "*mero*" meaning femur, and "*odon*" meaning tooth. The name refers to the spinose process on the posterior margin of the mesofemur in males, a synapomorphy for species in the genus. The gender is neuter.

Composition and distribution (Fig. 18). Three species distributed on western (lowland) Amazonia from Colombia, Ecuador, Peru, and Bolivia. An erroneous record from Brazil (Ohaus 1905) was repeatedly cited by subsequent authors (Blackwelder 1944, Ohaus 1934, 1952, Machatschke 1972, Krajcik 2008, Soula 2008, Moore et al. 2017) (see *Mesomerodon spinipenne* type material). We record the genus from elevations between 150 to 762 m. A record of the genus occurring at 2800 m (Paucar-Cabrera 2005) is beyond the limits of the genus, and we consider it erroneous. A locality record of *M. gilletti* from Loja (Ecuador) (Fig. 18 [indicated with question mark]) waits for confirmation through future collecting since a short series of specimens supposedly collected from Loja province (west side of the Andes) seems to be out of the altitudinal and longitudinal reach of the genus. The ranges of two species of *Mesomerodon* overlap in aseasonal Ecuador in a region known for the highest levels of mammal and plant species diversity (Hoorn et al. 2010). Rutelinae biodiversity in Ecuador is the highest recorded in South America, with 53 genera and 298 species (Paucar-Cabrera 2005). Of these, 92 species of Rutelinae (or 36%) are endemic to the country (Paucar-Cabrera 2005). The distribution of the genus is restricted to low elevations alongside the Andes without extending eastward into the Brazilian Amazon. *Mesomerodon* exhibits a distributional gap between *M. spinipenne* and the Ecuadorian species in northern Peru.

Niche modeling. Within the Andean corridor, the genus level distribution model is congruent with the specimen-based distribution (Fig. 19 vs. Fig. 18). Therefore, the apparent distributional gap between *Mesomerodon spinipenne* and the Ecuadorian species in northern Peru is unlikely a result of a lack of sampling. The distribution model of the Ecuadorian species (Fig. 20) suggests that either *M. barclayi* sp. n. or *M. gilletti* extend into northern Peru. The distribution model for *M. spinipenne* (Fig. 21) shows a continuous distribution in central and southern Peru with a disconnected population in Bolivia (also corroborated with the specimen-based distribution). Specimen-level data do not corroborate the occurrence of *M. spinipenne* in western Brazil, northern Colombia, or Venezuela. Collecting may reveal occurrence of the taxon in western Brazil, but we consider it unlikely that the taxon occurs in Colombia or Venezuela because these countries have been well collected.

Diagnosis. Species in the genus *Mesomerodon* are distinguished from other pelidnotine leaf chafers based on the acute, spiniform processes on the apical callus of the elytra in males (Fig. 17; shared with *Hoplopelidnota*) and an acute process on the posterior margin of the mesofemur in males (Fig. 16; autapomorphic for the genus). The

ovate body form, size, and color are similar to some species of *Pelidnota* (*Pelidnota*) (e.g., *Pelidnota lucida* Burmeister, 1844), but the form of the mandible clearly separates the two genera (*Mesomerodon* species possess a rounded mandibular apex [Fig. 9] whereas *Pelidnota* species possess a bidentate, reflexed mandibular apex). Additional characters that assist with diagnosis of *Mesomerodon* include: external edge of protibia with three teeth; pronotum with bead complete anteriorly, laterally and basally; mesoventrite produced beyond mesometaventral suture (Fig. 3); and male genitalia with highly sclerotized ventral sclerite of the phallobase (Figs 22c, 23c, 24c). See Moore et al. (2017) for a key to genera of pelidnotine scarabs.

Key to *Mesomerodon* species

1   Mesofemur without process projecting posteriorly on posterior margin (♀) **2**
–   Mesofemur with acute process projecting posteriorly on posterior margin (Fig. 16) (♂) **3**
2   Distributed in Bolivia and Peru (Fig. 18) ....***M. spinipenne*** (♀) **Ohaus**
–   Distributed in Ecuador and Colombia (Fig. 18)..
        .....***M. gilletti*** (♀) **Soula** or ***M. barclayi*** (♀) **Seidel, Jameson, & Stone, sp. n.**
3   Protarsomere 2 ventrally with striate region at apex (Fig. 27) ....
        ....***M. spinipenne*** (♂) **Ohaus**
–   Protarsomere 2 ventrally lacking striate region at apex (Figs 25–26)............**4**
4   In lateral view, parameres curved posteriorly (Fig. 23b) .....***M. gilletti*** (♂) **Soula**
–   In lateral view, parameres sinuate (Fig. 22b)...
        ....***M. barclayi*** (♂) **Seidel, Jameson, & Stone, sp. n.**

Clave para las especies de *Mesomerodon*

1   Mesofémur sin proceso proyectándose posteriormente en el margen posterior **2**
–   Mesofémur con un proceso agudo proyectado posteriormente en el margen posterior (Fig. 16) **3**
2   Distribuido en Bolivia y Perú (Fig. 18) ....***M. spinipenne*** (♀) **Ohaus**
–   Distribuido en Ecuador y Colombia (Fig. 18)..
        ....***M. gilletti*** (♀) **Soula** o ***M. barclayi*** (♀) **Seidel, Jameson, & Stone, sp. n.**
3   Protarsómero 2 ventralmente con una zona estriada en el ápice (Fig. 27) ......
        ....***M. spinipenne*** (♂) **Ohaus**
–   Protarsómero 2 ventralmente sin una zona estriada en el ápice (Fig. 25–26).... **4**
4   En vista lateral, parámeros curvados posteriormente (Fig. 23b) ....
        ....***M. gilletti*** (♂) **Soula**
–   En vista lateral, parámeros sinuados (Fig. 22b)...
        ....***M. barclayi*** (♂) **Seidel, Jameson, & Stone, sp. n.**

Mesomerodon barclayi Seidel, Jameson, & Stone, sp. n.

http://zoobank.org/4B70B243-1A6A-445D-9C33-5E859DE8B086

Figs 1–3, 8, 15, 18, 22, 25

Type material. Holotype male and 19 paratypes (10 males, 9 females). Holotype male at ZMHB with label data: a) "Rutelide, Pacayacu, 23.8.37" (handwritten), b) "Mesomerodon spinipenne Ohs., MNHUB Berlin" (typeset), c) male genitalia card mounted, d) our red holotype label. Paratype female at MSPC with label data: a) "Ecuador, Pacayacu, 3.X.37, Dr. Schultze – Rhonhof S.G." (typeset and handwritten), b) "Pacayacu 3.10.37" (handwritten), c) "loan from Zool.Mus. Berlin" (typeset), d) "Mesomerodon spinipenne Ohs., MNHUB Berlin" (typeset), e) our yellow paratype label. Paratype male at ZMHB with label data: a) "O.ECUADOR, Sarayacu Feyer" (typeset), b) "Mesomerodon spinipenne, Cotype ♂ Ohs." (handwritten on red label), c) "kein typus" (handwritten), d) male genitalia card mounted e) our yellow paratype label. Paratype female at ZMHB with label data: a) "O.ECUADOR, Sarayacu Feyer" (typeset), b) "Mesomerodon spinipenne, Cotype ♀ Ohs." (handwritten on red label), c) "kein Typus" (handwritten), d) our yellow paratype label. Paratype male at ZMHB with label data: a) "O.ECUADOR, Sarayacu Feyer" (typeset), b) "88882" (typeset), c) "♂" (typeset on black bordered label), d) "Mesomerodon spinipenne Ohs., MNHUB Berlin" (typeset), e) male genitalia card mounted, f) our yellow paratype label. Paratype female at ZMHB with label data: a) "Rutelide u. Cyclocephala, Pacayacu 24.9.37" (handwritten), b) "Mesomerodon spinipenne Ohs., MNHUB Berlin" (typeset), c) our yellow paratype label. Paratype female at ZMHB with label data: a) "O. Ecuador, Puyo, A. Schulze" (typeset), b) "Ohaus determ., Mesomerodon spinipenne ♀ Ohs." (typeset and handwritten), c) our yellow paratype label. Paratype female at ZMHB with label data: a) "O. Ecuador, Puyo, A. Schulze" (typeset), b) "Mesomerodon spinipenne Ohs." (handwritten), c) "♀" (typeset), d) our yellow paratype label. Paratype male at CCECL with label data: a) ECUADOR (Orellana), Payamino Research Station, 0°29'967"S, 77°17'083"W, 300m Tropical Rainforest, At M.V. light at night, 30.vii–12 viii.2007" (typeset), b) male genitalia card mounted, c) our yellow paratype label. Paratype male at MSPC with label data: a) ECUADOR (Orellana), Payamino Research Station, 0°29'967"S, 77°17'083"W, 300m Tropical Rainforest, At M.V. light at night, 30.vii -12 viii.2007" (typeset), b) "coll. CPDT Gillett, BMNH(E) 2007-65" (typeset), c) "DNA extract No: Meso1, deposited at MSPC" (handwritten), d) male genitalia card mounted, e) "Matthias Seidel Collection 2016", f) our yellow paratype label. Paratypes (2 males) at BMNH with label data: a) ECUADOR (Orellana), Payamino Research Station, 0°29'967"S, 77°17'083"W, 300m Tropical Rainforest, At M.V. light at night, 30.vii -12 viii.2007" (typeset), b) "coll. CPDT Gillett, BMNH(E) 2007-65" (typeset), c) "DNA extract No: Meso2, deposited at MSPC; no PCR amplification" (handwritten), d) male genitalia card mounted, e) our yellow paratype label. Paratype male at SLCC with label data: a) "PARAGUAY: Alto Parana, 1.XI.1990" (typeset), b) "Collection S. Le Tirant" (typeset), c) "supposedly mislabeled locality, des. Seidel 2016" (typeset), d) "MESOMERODON SPINIPENNE OHAUS, det. M.E. Jameson 2003" (typeset and handwritten), d) male genitalia card mounted, e) our yellow paratype
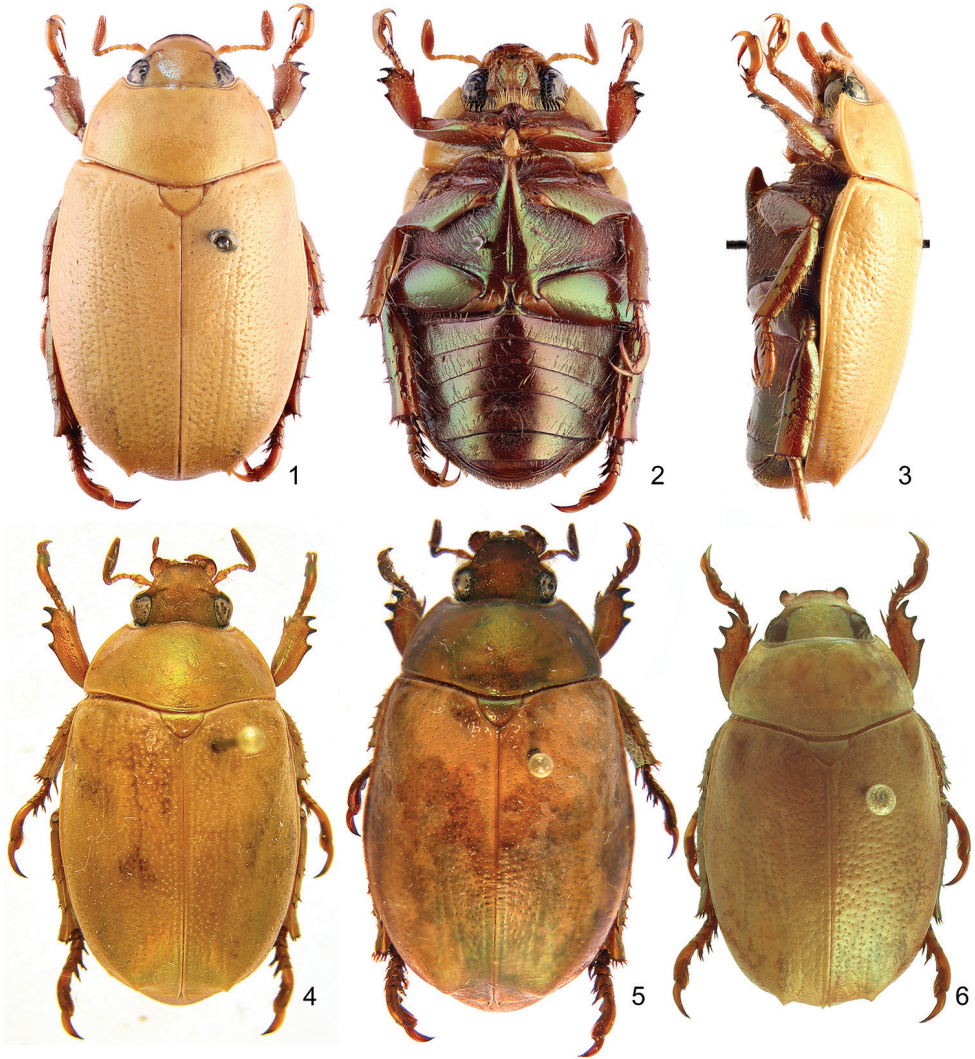
Figures 1–6. Dorsal and lateral habitus of *Mesomerodon* species. **1–3** *M. barclayi* sp. n., male holotype, dorsal, ventral, and lateral view **4–5** *M. gilletti* Soula holotype male specimen and female allotype specimen **6** *M. spinipenne* Ohaus male non-type specimen

label. Paratype male at IRSNB with label data: a) "ECUADOR (Orellana), Payamino Territory, 300m Tropical Rainforest, July 2007" (typeset), b) "DNA extract: Rut105, det. M.Seidel 2016" (typeset and handwritten), c) male genitalia card mounted, d) our yellow paratype label. Paratype male at ZSM with label data: a) "O.Ecuador, Puyo, A. Schulze, 6.V.35" (typeset and handwritten), b) "Mesomerodon spinipenne Ohs." (handwritten), c) "Staatssammlung München, 1975, Erwerb Coll. Machatschke", d) male genitalia card mounted, e) our yellow paratype label. Paratype female at NMPC with label data: a) "O.Ecuador, Puyo, A. Schulze, 6.V.35" (typeset and handwritten), b) "Ohaus determ.,

Mesomerodon spinipenne ♀ Ohs." (typeset and handwritten), c) "Staatssammlung München, 1975, Erwerb Coll. Machatschke", d) our yellow paratype label. Paratype female at ZSM with label data: a) "O.Ecuador, Sarayacu Feyer" (typeset), b) "Paratypus, Mesomerodon spinipenne Cotype ♀ Ohs." (typeset and handwritten), c) "Staatssammlung München, 1975, Erwerb Coll. Machatschke", d) "NOT a type specimen of *Mesomerodon spinipenne*, Ohaus, 1905, des. Seidel 2016" (typeset), e) our yellow paratype label. Paratype male at FMNH with label data: a) "ECUADOR: Pastaza; 300m confluence R. Macuma & R. Morona VII:17:1971, leg. B. Malkin" (typeset), b) "at light" (typeset), c) "on sand river bank" (typeset), d) male genitalia card mounted, f) our yellow paratype label. Paratype female at FMNH with label data: a) "ECUADOR: Pastaza; 300m confluence R. Macuma & R. Morona VII:17:1971, leg. B. Malkin" (typeset), b) "at light" (typeset), c) "on sand river bank" (typeset), d) "Mesomerodon spp??? DET. A.R.Hardy 1980" (typeset and handwritten), f) our yellow paratype label. Paratype female at FMNH with label data: a) "ECUADOR: Pastaza; 300m confluence R. Macuma & R. Morona VII:17:1971, leg. B. Malkin" (typeset), b) our yellow paratype label.

Description (based on 11 males and 9 females). The holotype does not differ significantly from the generic description and suffices for the description of this cryptic species (see "Remarks"). Descriptive details specific to the holotype specimen are indicated. Length from apex of clypeus to apex of pygidium 18–22 mm (♂) (holotype: 19 mm) and 22–25 mm (♀); width at mid-elytra 11–12 mm (♂) (holotype: 11 mm) and 12–15 mm (♀). Color: Cream colored (holotype), tan, or ochre; ventral surface castaneous with weak metallic green reflections. Form: Elytral apices with one short spine (holotype) or swelling (females). Legs: Protarsomere 2 of male ventrally lacking well-defined striae at ventral apex (Fig. 25). Male genitalia (Fig. 22a–c): Parameres with elongate, narrow projection (=stem) and with longitudinal, impressed fissure (Fig. 22a); stem gradually and weakly broadened toward apex, subapex lacking paired, spinose projections; ventral sclerite of phallobase with surface concave, apex quadrate (Fig. 22c); lateral view diagnostic (Fig. 22b).

Diagnosis. Males of *Mesomerodon barclayi* sp. n. are differentiated from other *Mesomerodon* species by the following combination of characters: Protarsomere 2 ventrally lacking a striated region at the ventral apex (striated in *M. spinipenne*; apical region lacking striae in *M. gilletti* [Figs 25–27]) and form of the male genitalia (Fig. 22 versus Fig. 24 in *M. spinipenne* and Fig. 23 in *M. gilletti*). Females can only be confidently determined when associated to male specimens from the same collecting event.

Etymology. It is our honor to dedicate this species to Max Barclay (Curator, Coleoptera, Department of Entomology), who invited the first and second authors to the 1st Scarab Symposium at the BMNH in 2014 where cooperation on this work was initiated. Max Barclay has led the way in making biodiversity science more accessible to scientists and citizens alike.

Distribution (Fig. 18). Known from western (lowland) Amazonia areas in Ecuador and occurring in apparent sympatry with *M. gilletti*. Ohaus (1934, 1952) recorded *M. spinipenne* from Sarayacu, Ecuador. We recovered these specimens in ZMHB and ZSM and identified them as belonging to *M. barclayi* sp. n.

Figures 7–8. Live specimens showing cream coloration of *Mesomerodon* species. **7** *M. spinipenne* from Manú National Park, Madre de Dios, Peru [image courtesy of Rich C. Hoyer] **8** *M. barclayi* sp. n. from Payamino Research Station, Orellana, Ecuador [image courtesy of Conrad Gillett].

Locality data (Suppl. material 1). 20 specimens from 9 collections.

ECUADOR: Morona-Santiago, Orellana, Pastaza

Temporal data. Based on label data, this species is known to be active in the months of February, August, and November.

Natural history. Based on label data, adult *M. barclayi* sp. n. is usually collected at light, thus suggesting activity and feeding at night. Individuals probably occur throughout the year. Immature stages are unknown. Specimens have been recorded at an elevation of 300 m.

Remarks. As with other cryptic species, the overall body form of *M. barclayi* sp. n. is similar to other species in the genus. The form of the male genitalia (Fig. 22 versus Figs 23–24) however, is sufficient for identification of *M. barclayi* sp. n. When developing our species hypotheses, we examined this morphotype in terms of phenotypic, elevational, and seasonal variation within *M. spinipenne* or *M. gilletti*, but the consistency in the form of the male genitalia led us to conclude that it is a justified species. Apparent sympatry (in location and phenology) with *M. gilletti* also led us to carefully examine this species pair. Again, we found that consistency in the male genitalia form was sufficient for diagnosis of both species. Females of *M. barclayi* sp. n. cannot be identified unless associated with males from the same collecting event.

Mesomerodon gilletti **Soula, 2008**
Figs 4–5, 8–13, 16–18, 23, 26

Mesomerodon gilletti Soula, 2008: 21 (original combination)

Type material. Holotype male, allotype female, and eight paratypes (four male, four females. Holotype male at CCECL with label data: a) "Tena (E), 9/91, (750m)" (handwritten), b) male genitalia card mounted c) "Holotype, 2007, Mesomerodon gilletti S.,

Soula" (typeset and handwritten on red label). Allotype female at CCECL with label data: a) "Tena (E), 9/91, (750m)" (handwritten), b) "Allotype, 2007, Mesomerodon gilletti S., Soula" (typeset and handwritten on red label). Paratype male at CCECL with label data: a) "Tena (E), 9/91, (750m)" (handwritten), b) male genitalia card mounted, c) "Paratype, 2007, Mesomerodon gilletti S., Soula" (typeset and handwritten on red label). Paratypes (2 females) at CCECL with label data: a) "Tena (E), 9/91, (750m)" (handwritten), b) "Paratype, 2007, Mesomerodon gilletti S., Soula" (typeset and handwritten on red label). Paratypes (2 males) at CCECL with label data: a) "Misahuali (E.), 5/91" or "Misahuali (Eq.), 5/91" (handwritten), b) male genitalia card mounted, c) "Paratype, 2007, Mesomerodon gilletti S., Soula" (typeset and handwritten on red label). Paratype male at CCECL with label data: a) "EQUATEUR: Prov. NAPO, MISAHUALLI ile ANACONDA, Alt. 350 m.; 17–22.9.1990, Leg. Joss" (typeset), b) male genitalia card mounted, c) "Paratype, 2007, Mesomerodon gilletti S., Soula" (typeset and handwritten on red label). Paratypes (2 females) at CCECL with label data: a) "Misahuali (E.), 5/91" (handwritten), b) "Paratype, 2007, Mesomerodon gilletti S., Soula" (typeset and handwritten on red label).

Description (based on 50 males and 19 females). Length from apex of clypeus to apex of pygidium 18.0–20.0 mm (♂) and 21.0–24.0 mm (♀); width at mid-elytra 10.0–11.0 mm (♂) and 12.0–14.0 mm (♀). Legs: Protarsomere 2 of male lacking well-defined striae at ventral apex (Fig. 26). Male genitalia (Figs 23): Parameres with elongate, narrow projection (=stem) and with nearly obsolete impressed longitudinal fissure (Fig. 23a); stem broad, not narrowed toward apex, subapex lacking paired, spinose projections; ventral sclerite of phallobase with surface concave, apex quadrate (Fig. 23c); lateral view diagnostic (Fig. 23b).

Diagnosis. *Mesomerodon gilletti* males are differentiated from other *Mesomerodon* species by the following combination of characters: Protarsomere 2 of male ventrally with striated region poorly defined or lacking at apex (striated in *M. spinipenne*; lacking in *M. barclayi* sp. n.; [Figs 25–27]) and parameres, and ventral sclerite of phallobase (Fig. 23 versus Fig. 24 in *M. spinipenne* and Fig. 22 in *M. barclayi* sp. n.). *Mesomerodon gilletti* females can only be confidently determined when associated with male specimens from the same collecting event.

Distribution (Fig. 18). Known from western (lowland) Amazonia in Ecuador and Colombia (new country record). The species occurs in apparent sympatry with *M. barclayi* sp. n. A record of '*Mesomerodon* species 1' from Napo Province in Paucar-Cabrera (2005) probably represents a record of *Mesomerodon gilletti*. Records of *Mesomerodon* from Ecuador (Blackwelder 1944, Ohaus 1918, 1934, 1952, Machatschke 1972, Moore et al. 2017, Paucar-Cabrera 2005) are records for either *M. gilletti* or *M. barclayi* sp. n.

Locality data (Suppl. material 1). 69 specimens from 12 collections.
COLOMBIA: Putumayo
ECUADOR: Napo, Orellana, Sucumbíos

Temporal data. Based on label data, this species is known to be active in the months of February, May, June, August, September, October, and November.
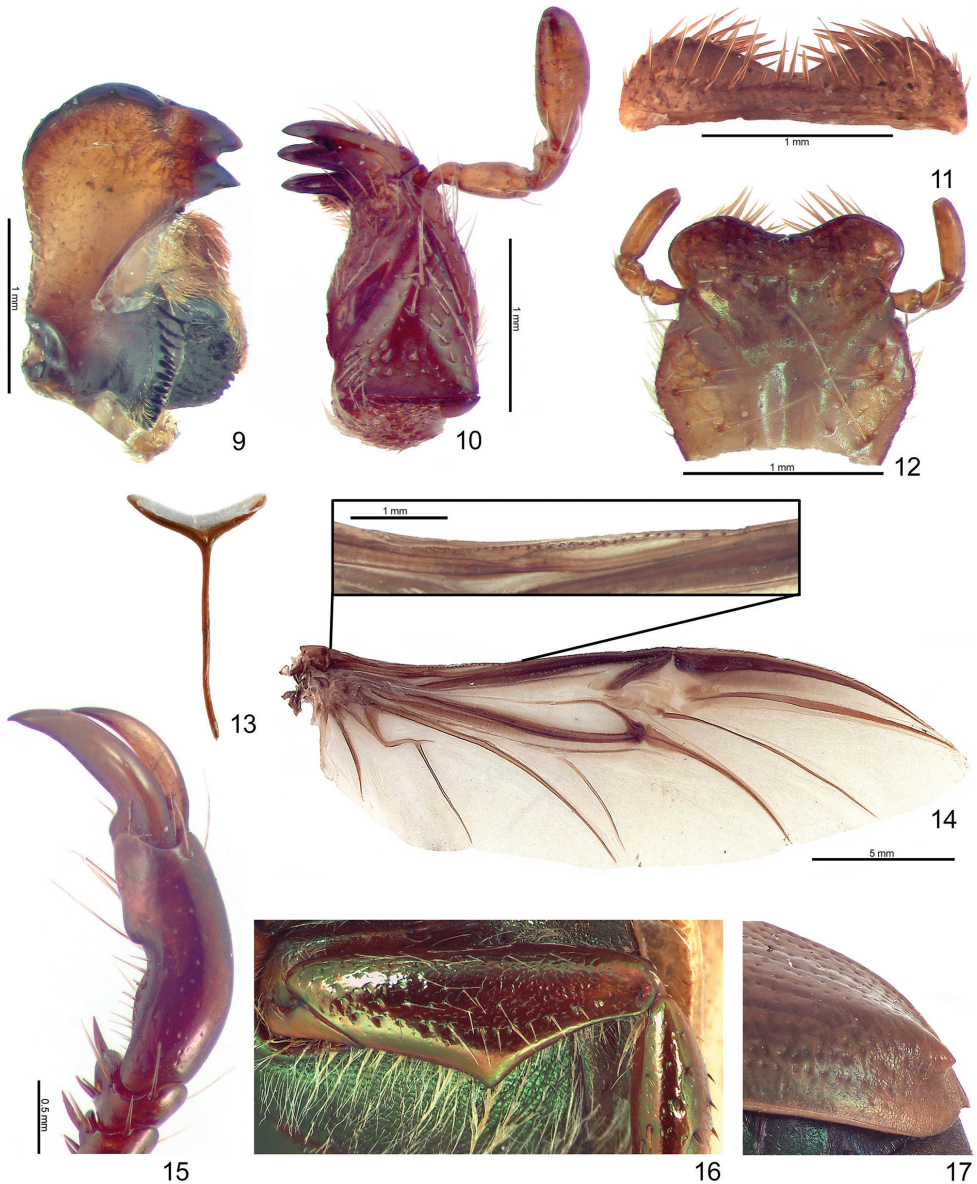
Figures 9–17. Generic characters for *Mesomerodon*. **9** Left mandible of *M. gilletti*, dorsal view (broadly rounded externally with 2 interior, acute teeth; molar region broad) **10** Maxilla of *M. gilletti*, ventral view (with 6 teeth; galea not fused) **11** Labrum, dorsal view, of *M. gilletti* (apex emarginate medially) **12** Mentum, ventral view, of *M. gilletti* (subrectangular in shape, broadest at middle, apex emarginated) **13** Spiculum gastrale of *M. gilletti* **14** Wing of *M. spinipenne* showing venation and inset showing dense, thick setae associated with ScA and setose region anterior to RA_{3+4} **15** Protarsomere 5 of *M. barclayi* sp. n., male, showing well defined, ventromedial emargination **16** Mesofemur of *M. gilletti* male, ventral view, showing acute process projecting posteriorly on posterior margin **17** Elytral apex of *M. gilletti*, lateral view, showing spiniform callus

Natural history. Based on label data, adult *M. gilletti* are found associated with lights at night. Immature stages are unknown.

Remarks. Soula (2008) named this species based on twelve specimens, dedicating the species to Conrad Gillett (then at the BMNH) who provided specimens for Soula's study. In overall appearance, *M. gilletti* was not discernable from *M. spinipenne* except for the "parameres that are different enough to justify the status of the species in its own right" (Soula 2008).

Mesomerodon spinipenne Ohaus, 1905
Figs 6–7, 14, 18, 24, 27

Mesomerodon spinipenne Ohaus, 1905: 320–321 (original combination).

Type material. Lectotype male (designated by Soula 2008) and three paralectotypes (1 male, 2 females). Lectotype male at ZMHB with label data: a) "bei Pozuzu, Eckardt S." and "O. Peru, Chuchurras" (handwritten on verse and obverse), b) "Mesomerodon spinipenne, Type ♂ Ohs." (handwritten on red label), c) "SYNTYPUS, Mesomerodon spinipenne Ohaus, 1905, labelled by MNHUB 2007" (typeset on red label), d) male genitalia card mounted, e) "Lectotype Mesomerodon spinipenne Oh., 2007 Soula" (typeset and handwritten on red label). Paralectotype female at ZMHB with label data: a) "60." (handwritten, one egg mounted), b) "BRAZIL R.Purus" (typeset), c) "Mesomerodon spinipenne ♀, Cotype Ohs." (handwritten on red label), d) "SYNTYPUS, Mesomerodon spinipenne Ohaus, 1905, labelled by MNHUB 2007" (typeset), e) "Paralectotype 2007, Mesomerodon spinipenne Oh. Soula det." (typeset and handwritten on red label). Paralectotype female at ZMHB with label data: a) "Chuchuras, Amazonas" (handwritten), b) "Mesomerodon spinipenne, Cotype ♀ Ohs." (handwritten on red label), c) "SYNTYPUS, Mesomerodon spinipenne Ohaus, 1905, labelled by MNHUB 2007" (typeset on red label), d) "Paralectotype 2007, Mesomerodon spinipenne S., Soula det." (typeset and handwritten on red label). Paralectotype male deposited at BMNH with label data: a) "Chuchurras Peru" (handwritten), b) "Ohaus determ., Mesomerodon spinipenne Ohs." (typeset and handwritten), c) "Peru 1907•27" (handwritten), d) "Co-type" (typeset on round yellow label), d) "♂" (typeset), e) "Cotypus!" (typeset on red label), f) male genitalia card mounted, g) "Paralectotype, Mesomerodon spinipenne, Ohaus, 1905, M Seidel des. 2016" (typeset on red label).

Ohaus (1905: 321) stated that the type series included at least one male and at least one female (but likely at least two females based on the length/width range that Ohaus provided) from "Peru Chuchuras (Eckhard); Amazonas, Rio Purus." We found one additional male syntype at the BMNH that fits the measurements provided by Ohaus (1905), and we labeled it as a paralectotype. It is possible that additional paralectotypes may be found in collections.
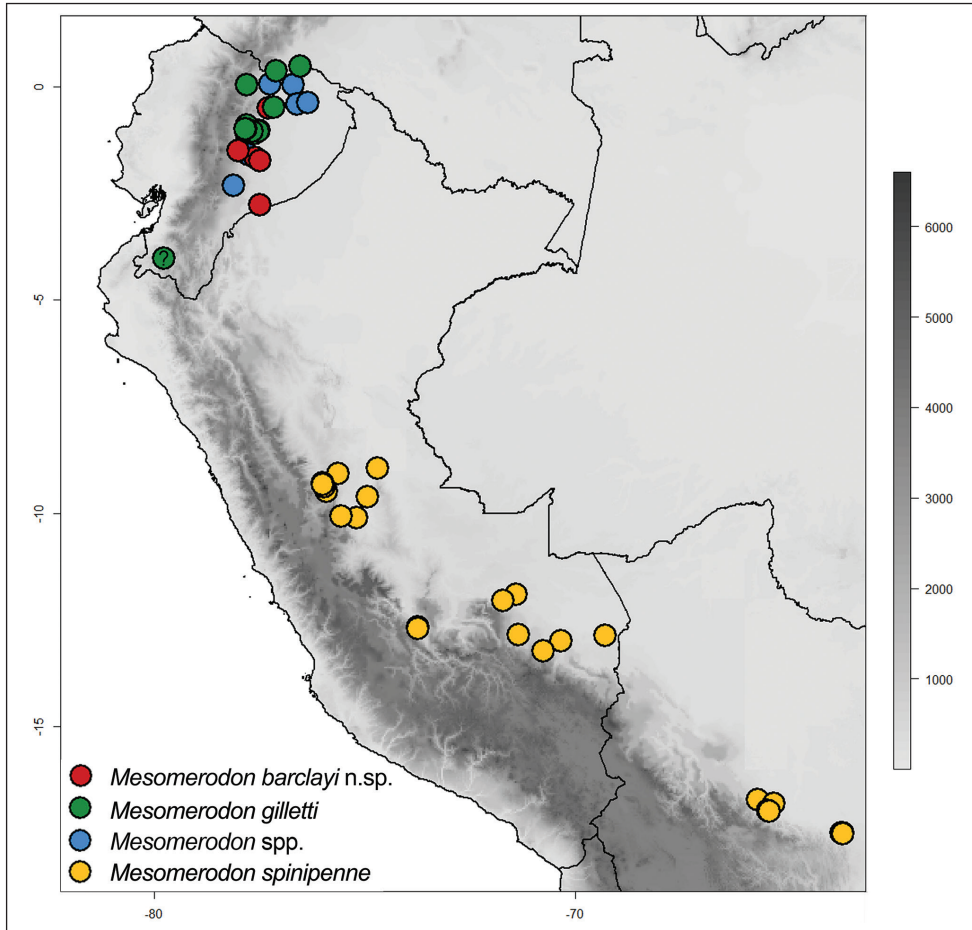
Figure 18. Distribution of *Mesomerodon* species in South America. Refer to Suppl. material 1 for associated data.

Description (based on 52 males and 161 females). Length from apex of clypeus to apex of pygidium 17.0–20.0 mm (♂) and 19.0–24.0 mm (♀); width at mid-elytra 10.0–12.0 mm (♂) and 11.0–14.0 mm (♀). Legs: Protarsomere 2 (♂) with well-defined striae at ventral apex (Fig. 27). Male genitalia (Fig. 24): Parameres with elongate, narrow projection (=stem) and with longitudinal, impressed fissure (Fig. 24a); stem broadened abruptly at apex, subapex with paired, spinose projections (almost appearing broken); ventral sclerite of phallobase with surface concave, apex quadrate (Fig. 24c); lateral view diagnostic (Fig. 24b).

Diagnosis. *Mesomerodon spinipenne* males are differentiated from other *Mesomerodon* species by the following combination of characters: Protarsomere 2 with well-defined striae at ventral apex (Fig. 27) (lacking striae in *M. gilletti* and *M. barclayi* sp. n.; Figs 25–26) and form of the parameres, and form of the ventral
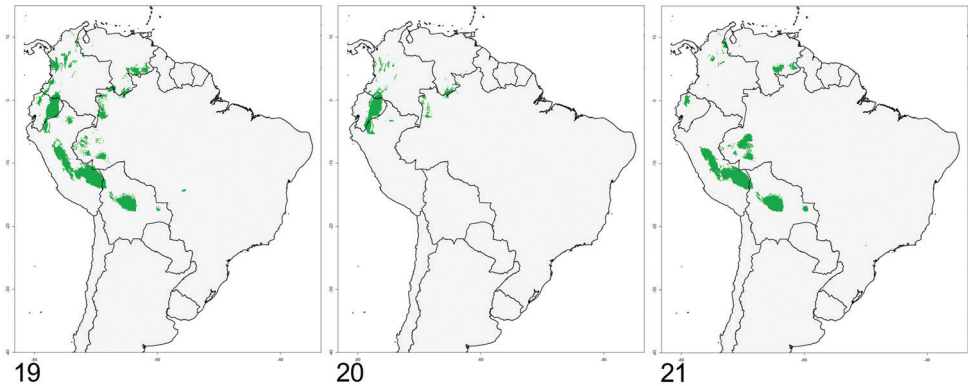
Figure 19–21. Distributional model for *Mesomerodon* species in South America. **19** all *Mesomerodon* species **20** *M. barclayi* sp. n., *M. gilletti* and unassociated females **21** *M. spinipenne*. Refer to Appendix 1 for associated data

sclerite of the phallobase (Fig. 24 versus Fig. 23 in *M. gilletti* and Fig. 22 in *M. barclayi* sp. n.). Females can only be confidently determined when associated with male specimens from the same collecting event. Females occurring in Bolivia and Peru are most likely conspecific with *M. spinipenne* (Figs 6–7).

Distribution (Fig. 18). *Mesomerodon spinipenne* is the most broadly distributed species in the genus, and it occurs from central Peru to central Bolivia in the western (lowland) Amazonia (from 230 to 762 m elevation). The species has been recorded from Brazil, "Rio Purus" (Blackwelder 1944, Ohaus 1905, 1934, 1952, Machatschke 1972, Krajcik 2008, Soula 2008, Moore et al. 2017), but in our view this is an erroneous record. The record is based on a paralectotype female collected at the Rio Purus that rises in the Uyacali Region in Peru and flows into Brazil and which could, therefore, have been collected either in Peru or Brazil. Based on our examination of 213 specimens, we think that this specimen represents a Peruvian locality. Records of the species from Ecuador (Blackwelder 1944, Ohaus 1918, 1934, 1952, Machatschke 1972, Moore et al. 2017, Paucar-Cabrera 2005) are incorrect. These are records for either *M. gilletti* or *M. barclayi* sp. n.

Locality data (Suppl. material 1). 213 specimens from 18 collections.

BOLIVIA: Cochabamba (Chapare), Huánuco (Blackwelder 1944, Ohaus 1905, 1918, 1934, 1952, Machatschke 1972, Soula 2008, Ratcliffe et al. 2015), Junín (Blackwelder 1944, Ohaus 1905, 1918, 1934, 1952, Machatschke 1972, Soula 2008, Ratcliffe et al. 2015), Pasco (Blackwelder 1944, Ohaus 1905, 1918, 1934, 1952, Machatschke 1972, Soula 2008, Ratcliffe et al. 2015), Santa Cruz (Ichilo, Sara)

PERU: Ayacucho (La Mar), Cusco (Quispicanchi), Huánuco (Leoncio Prado, Puerto Inca), Madre De Dios (Manú, Tambopata), Pasco (Oxapampa), Ucayali (Padre Abad), Santa Cruz (Blackwelder 1944, Ohaus 1918, 1934, 1952, Gutiérrez 1951, Machatschke 1972, Moore et al. 2017).
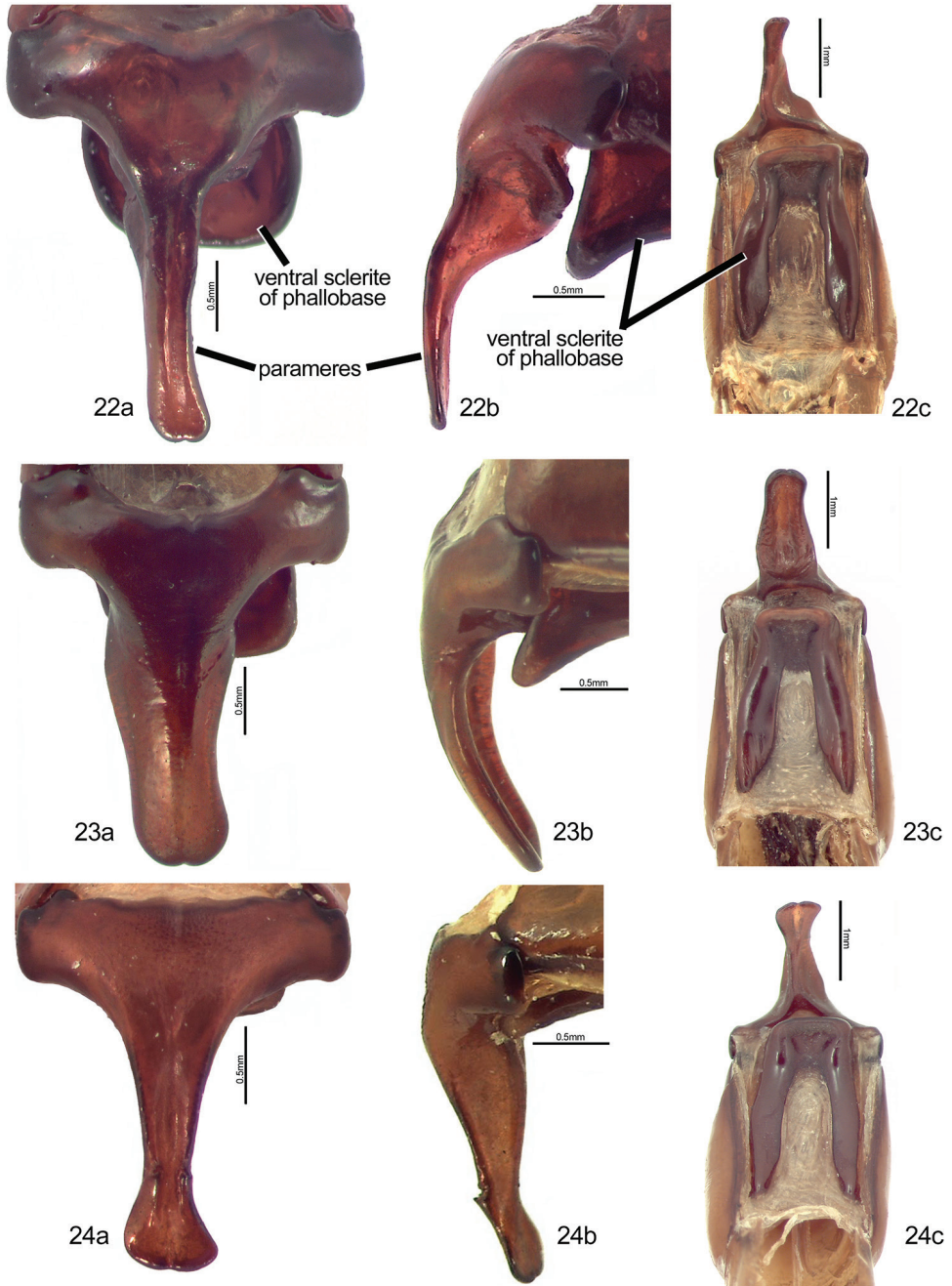
Figures 22–24. Form of the male genitalia (dorsal [**a**], lateral [**b**], ventral [**c**] views) in *Mesomerodon* species. **22** *M. barclayi* sp. n. **23** *M. gilletti* **24** *M. spinipenne*
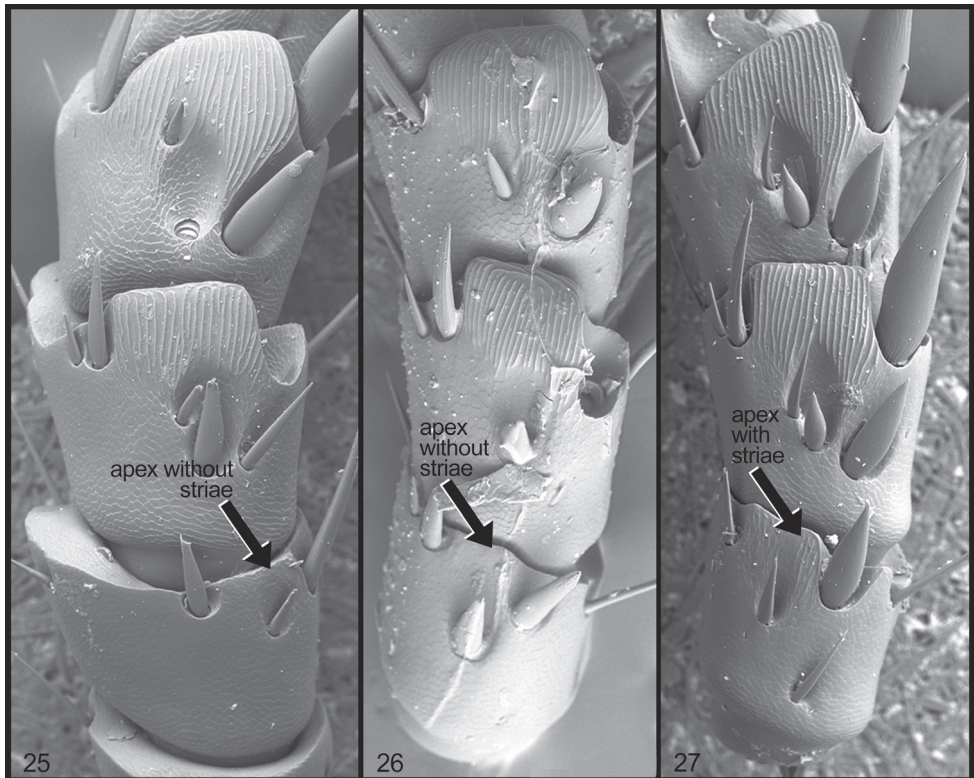
Figures 25–27. Form of protarsomeres 2 to 4, ventral view, in *Mesomerodon* species. **25** *M. barclayi* sp. n., showing protarsomere 2 without stiate region at apex **26** *M. gilletti* showing protarsomere 2 without striate region at apex **27** *M. spinipenne* showing protarsomere 2 with striate region apically.

Temporal data. Based on label data, this species is known to be active in all months except January and February.

Natural history. Based on label data, adult *M. spinipenne* are active at night and can be collected at lights. Immature stages are unknown.

Remarks. Based on body measurements provided by Ohaus (1905), we conclude that he had a minimum of 3 specimens: 1 male (length 18.5mm, width 10.5mm) and 2 females (length 22–23.5mm, width 12.5–13.5mm) from two localities (Chuchuras and Rio Purus). The lectotype specimen at ZMHB was designated by Soula (2008), and it is a male specimen labeled by Ohaus as "type" ("Mesomerodon spinipenne, Type ♂ Ohs.") and with the locality label "bei Pozuzu, Eckardt S." and "O. Peru, Chuchurras". As part of this research, we found and labeled specimens that were invalidly labeled as type specimens and that do not belong to the type series (see "Type Specimens").

It is possible that the specific epithet, "*spinipenne*", refers to the apex of the elytra in the male which possess an apical spine or tubercle. The Latin root "*spini*" refers to spine or thorn, and the Latin root "*penna*" refers to wing. This character state is not unique to *M. spinipenne*; instead, it is a synapomorphy for all species in the genus.

Discussion

The genus *Mesomerodon* is composed of three very similar species, two of which that have evaded discovery since the description of the genus by Ohaus (1905). We discovered specimens of our new species, *M. barclayi* sp. n. in collections that were studied by Ohaus and Soula, both experts who were not able to detect this cryptic species based on external features. Stasis in external morphology, in combination with the apparent sympatry of two *Mesomerodon* species in Ecuador, corroborate two hypotheses for generation of cryptic species: nonvisual mating signals and ecological specialization in similar niches (Bickford et al. 2007). Sympatric distribution and external similarity of *M. barclayi* sp. n. and *M. gilletti* suggest that sexual selection might be a driver for diversification in the genus. Only aedeagal characters differ between species, thus sexual selection by female choice may drive the evolution of male genitalia (Eberhard 1985), and this could be accompanied with differences in mating pheromones or mating calls (Bickford et al. 2007). It is possible that specialization in food plants or other life history-dependent factors may drive diversification. Studies of presumed dietary generalists in narrow ecological regions have revealed cryptic beetle and butterfly species complexes with dietary specializations (Blair et al. 2005, Hebert et al. 2004).

Co-distributed cryptic species complexes may be a function of the western (lowland) Amazonian region with its aseasonal climate, humid forest, and heterogeneous vegetation. The distribution of two species of *Mesomerodon* in Ecuador coincides with highest global diversity of passerine birds and anurans (InfoNatura 2007) as well as the region for highest wood biomass productivity (Hoorn and Wesselingh 2010). The Ecuadorian Amazonian region descends from the foothills to elevations of 200–400 m and receives approximately 282 cm of precipitation annually (Dangles et al. 2009). The absence of a prolonged dry season, varied topography, and warm temperatures make the region a hotspot for biodiversity (Myers et al. 2000). In this region, small differences in elevation and vegetational cover create refuges (Dangles et al. 2009) that may allow for ecological niche diversification, especially for herbivorous species such as those in the genus *Mesomerodon*.

Future studies associated with these cryptic species are needed to examine divergence, population structure, and sister group relationships of the genus. Molecular data will allow association of males and females for each species. Focused fieldwork could determine distributional limits and yield ecological data which will assist in understanding the origin and cause of sympatry.

Acknowledgments

References

Beheregaray LB, Caccone A (2007) Cryptic biodiversity in a changing world. Journal of Biology 6(4): 9–14. https://doi.org/10.1186/jbiol60

Bickford D, Lohman DJ, Sodhi NS, Ng PK, Meier R, Winker K, Ingram KK, Das I (2007) Cryptic species as a window on diversity and conservation. Trends in Ecology & Evolution 22(3):148–55. https://doi.org/10.1016/j.tree.2006.11.004

Blackwelder RE (1944) Checklist of the Coleopterous Insects of Mexico, Central America, the West Indies, and South America. United States National Museum Bulletin 185: 189–265.

Blair CP, Abrahamson WG, Jackman JA, Tyrrell L (2005) Cryptic speciation and host-race formation in a purportedly generalist tumbling flower beetle. Evolution 59(2): 304–316. https://doi.org/10.1111/j.0014-3820.2005.tb00991.x

Dangles O, Barragán Á, Cárdenas RE, Onore G, Keil C (2009) Entomology in Ecuador: Recent developments and future challenges. Annals de la Société Entomologique de France (NS) 45(4): 424–436. https://doi.org/10.1080/00379271.2009.10697627

D'Hotman D, Scholtz CH (1990) Phylogenetic significance of the structure of the external male genitalia in the Scarabaeoidea (Coleoptera). Entomology Memoir-Republic of South Africa, Department of Agricultural Development (77): 1–56.

Eberhard WG (1985) Sexual Selection and Animal Genitalia. Harvard University Press Cambridge, Massachusetts. https://doi.org/10.4159/harvard.9780674330702

Elith J, Phillips SJ, Hastie T, Dudík M, Chee YE, Yates CJ (2011) A statistical explanation of MaxEnt for ecologists. Diversity and Distributions 17(1): 43–57. https://doi.org/10.1111/j.1472-4642.2010.00725.x

Fikáček M, Vondráček D (2014) A review of *Pseudorygmodus* (Coleoptera: Hydrophilidae), with notes on the classification of the Anacaenini and on distribution of genera endemic to southern South America. Acta Entomologica Musei Nationalis Pragae 54(2): 479–514.

Gutiérrez AR (1951) Notas sobre Scarabaeidae neotrópicos II (Coleopt. Lamellic.). Anales de la Sociedad Científica Argentina 151: 106–125.

Hastings DA, Dunbar PK, Elphingstone GM, Bootz M, Murakami H, Maruyama H, Masaharu H, Holland P, Payne J, Bryant NA, Logan TL, Muller J-P, Schreier G, MacDonald JS (1999) The Global Land One-kilometer Base Elevation (GLOBE) Digital Elevation Model, Version 1.0. National Oceanic and Atmospheric Administration, National Geophysical Data Center, Boulder, Colorado. http://www.ngdc.noaa.gov/mgg/topo/globe.html [accessed Nov. 2016]

Hebert PD, Penton EH, Burns JM, Janzen DH, Hallwachs W (2004) Ten species in one: DNA barcoding reveals cryptic species in the neotropical skipper butterfly *Astraptes fulgerator*. Proceedings of the National Academy of Sciences of the United States of America 101(41): 14812–14817. https://doi.org/10.1073/pnas.0406166101

Hijmans RJ, Cameron SE, Parra JL, Jones PG, Jarvis A (2005) Very high resolution interpolated climate surfaces for global land areas. International Journal of Climatology 25(15): 1965–1978. https://doi.org/10.1002/joc.1276

Hoorn C, Wesselingh F (2011) Amazonia, Landscape and Species Evolution: A Look Into the Past. Wiley-Blackwell, 464 pp.

Hoorn C, Wesselingh FP, Ter Steege H, Bermudez MA, Mora A, Sevink J, Jaramillo C, Riff D, Negri FR, Hooghiemstra H, Lundberg J, Stadler T, Särkinen T, Antonelli A (2010) Amazonia through time: Andean uplift, climate change, landscape evolution, and biodiversity. Science 330(6006): 927–931. https://doi.org/10.1126/science.1194585

InfoNatura (2007) InfoNatura: Animals and Ecosystems of Latin America, Version 5.0 NatureServe, Arlington, Virginia. http://infonatura.natureserve.org [accessed: Nov. 2016]

Jameson ML (1990) Revision, phylogeny and biogeography of the genera *Parabyrsopolis* Ohaus and *Viridimicus*, new genus (Coleoptera: Scarabaeidae: Rutelinae). The Coleopterists Bulletin 44: 377–422.

Jameson ML (1998) Phylogenetic analysis of the subtribe Rutelina and revision of the *Rutela* generic groups (Coleoptera: Scarabaeidae: Rutelinae: Rutelini). Bulletin of the University of Nebraska State Museum 14: 1–184. [Dated 1997].

Krajcik M (2008) Animma. X. Supplement 4. Checklist of the Scarabaeoidea of the World. 2. Rutelinae (Coleoptera: Scarabaeidae: Rutelinae). Second Edition. Plzen, 142 pp.

Kuijten PJ (1988) *Rutelarcha*, *Lutera* and *Cyphelytra*: notes on taxonomy and nomenclature, diagnoses, and keys (Coleoptera: Rutelinae, Rutelini). Zoologische Mededelingen, Leiden 62: 75–90.

Kuijten PJ (1992) A revision of the genus *Parastasia* in the Indo-Australian region (Coleoptera: Scarabaeidae: Rutelinae). Zoologische Verhandelingen, Leiden 275: 1–207.

Machatschke JW (1972) Scarabaeoidea: Melolonthidae, Rutelinae. Coleopterorum Catalogus Supplementa 66: 1–361.

Moore MR, Jameson ML, Garner BH, Audibert C, Smith ABT, Seidel M (2017) Synopsis of the pelidnotine scarabs (Coleoptera: Scarabaeidae: Rutelinae: Rutelini) and annotated catalog of the species and subspecies. ZooKeys 666: 1–349. https://doi.org/10.3897/zookeys.666.9191

Myers N, Mittermeier RA, Mittermeier CG, Da Fonseca GA, Kent J (2000) Biodiversity hotspots for conservation priorities. Nature 403(6772): 853–8. https://doi.org/10.1038/35002501

Ohaus F (1905) Beiträge zur Kenntniss der amerikanischen Ruteliden. Stettiner Entomologische Zeitung 66: 283–329.

Ohaus F (1918) Scarabaeidae: Euchirinae, Phaenomerinae, Rutelinae. Coleopterorum Catalogus 20: 1–241.

Ohaus F (1934) Coleoptera lamellicornia, Fam. Scarabaeidae, Subfam. Rutelinae. T.1: Tribus Rutelini. Genera Insectorum Fasc. 199A: 1–172.

Ohaus F (1952) Rutelinae (Col. Scarab.). In: Titschack E (Ed.) Beiträge zur Fauna Perus. Gustav Fischer, Jena, 1–10.

Paucar-Cabrera A (2005) A catalog and distributional analysis of the Rutelinae (Coleoptera: Scarabaeidae) of Ecuador. Zootaxa 948:1–92. https://doi.org/10.11646/zootaxa.948.1.1

Phillips SJ, Anderson RP, Schapire RE (2006) Maximum entropy modeling of species geographic distributions. Ecological modelling 190(3): 231–259. https://doi.org/10.1016/j.ecolmodel.2005.03.026

Ratcliffe BC, Jameson ML, Figueroa L, Cave RD, Paulsen MJ, Cano EB, Beza-Beza C, Jimenez-Ferbans L, Reyes-Castillo P (2015) Beetles (Coleoptera) of Peru: a Survey of the Families. Scarabaeoidea. Journal of the Kansas Entomological Society 88: 186–207. https://doi.org/10.2317/kent-88-02-186-207.1

Smith ABT (2003) A monographic revision of the genus *Platycoelia* Dejean (Coleoptera: Scarabaeidae: Rutelinae: Anoplognathini). Bulletin of the University of Nebraska State Museum 15: 1–202.

Soula M (2008) Les coléoptères du nouveau monde. Volume 2: Rutelini 2. Révision des Pelidnotina 2. Révision des genres: *Parhoplognathus*, *Chipita* n. gen., *Heteropelidnota*, *Homothermon*, *Hoplopelidnota*, *Mesomerodon*, *Mecopelidnota*, *Patatra* n. gen. (Coleoptera: Scarabaeidae, Rutelinae, Rutelini). Besoiro: Supplément au Bulletin de liaison de l'Association Entomologique pour la Connaissance de la Faune Tropicale. AECFT, Saintry, 40 pp.

Wheeler QD, Platnick NI (2000) The phylogenetic species concept (*sensu* Wheeler and Platnick). In: Wheeler QD, Meier R (Eds) Species Concepts and Phylogenetic Theory: A Debate. Columbia University Press, New York.

Supplementary material 1

Distribution data for *Mesomerodon* species (Coleoptera, Scarabaeidae, Rutelinae)
Authors: Matthias Seidel, Mary L. Jameson, Rachel L. Stone
Data type: occurrence data
Explanation note: Specimen level data used for niche model, phenology, and overall distribution.
Copyright notice: This dataset is made available under the Open Database License (http://opendatacommons.org/licenses/odbl/1.0/). The Open Database License (ODbL) is a license agreement intended to allow users to freely share, modify, and use this Dataset while maintaining this same freedom for others, provided that the original source and author(s) are credited.

RESEARCH ARTICLE

A peer-reviewed open-access journal

ZooKeys

Launched to accelerate biodiversity research

The genus *Scaptodrosophila* Duda part I: the *brunnea* species group from the Oriental Region, with morphological and molecular evidence (Diptera, Drosophilidae)

Yi-Qin Liu[1], Qing-Song Gao[1], Hong-Wei Chen[1]

I *Department of Entomology, South China Agricultural University, Tianhe, Guangzhou, 510642, China*

Corresponding author: *Hong-Wei Chen* (hongweic@scau.edu.cn)

Citation: Liu Y-Q, Gao Q-S, Chen H-W (2017) The genus *Scaptodrosophila* Duda part I: the *brunnea* species group from the Oriental Region, with morphological and molecular evidence (Diptera, Drosophilidae). ZooKeys 671: 87–118. https://doi.org/10.3897/zookeys.671.11275

Abstract

Seven new species of the *Scaptodrosophila brunnea* species group are described from east Asia: *S. maculata* **sp. n.**, *S. melanogaster* **sp. n.**, *S. nigricostata* **sp. n.**, *S. nigripecta* **sp. n.**, *S. obscurata* **sp. n.**, *S. protenipenis* **sp. n.** and *S. rhina* **sp. n.** Three known species, *S. parabrunnea* (Tsacas & Chassagnard), *S. pressobrunnea* (Tsacas & Chassagnard) and *S. scutellimargo* (Duda) are redescribed. A key to all the examined species in the *brunnea* group is provided. Species delimitations have been improved by integrating the DNA sequences with morphological information. The intra- and interspecific pairwise p-distances (proportional distance) are summarized. Some nucleotide sites with fixed status in the alignment of the *COI* sequences (664 nucleotide sites in length) are used as "pure" molecular diagnostic characters to delineate species in the *brunnea* group.

Keywords

China, DNA barcoding, integrated taxonomy, *Scaptodrosophila brunnea* species group

Introduction

To date, a total of 280 species (Bächli 2016) has been described in the genus *Scaptodrosophila* Duda, 1923 from around the world: four species from the Nearctic region, two species from the Neotropical region, ten species from the Palearctic region, 32 species from the Afrotropical region, 79 species from the Oriental region and 167 species from the Australasian region (Brake and Bächli 2008; Bächli 2016). So far, 12 species groups (Bächli 2016) have been established in *Scaptodrosophila*: the *albifrontata* group (Wheeler and Takada 1966), the *aterrima* group (Tsacas et al. 1988), the *barkeri* group (Bock and Parsons (1978), the *brunnea* group (Tsacas and Chassagnard 1976), the *brunneipennis* group (Bock and Parsons 1978), the *bryani* group (Throckmorton 1962), the *coracina* group (Mather 1955), the *inornata* group (Parsons and Bock 1978), the *latifasciaeformis* group (Burla 1954), the *rufifrons* group (Papp et al. 1999), the *saba* group (Burla 1954) and the *victoria* group (Wheeler 1949).

The *brunnea* group includes eleven known species (Bächli 2016), and was divided into two subgroups by Tsacasand and Chassagnard (1976): the *brunnea* subgroup including five species, all from Oriental region (scutellum yellow at tip): *S. brunnea* de Meijere, 1911, *S. parabrunnea* (Tsacas & Chassagnard, 1976), *S. pressobrunnea* (Tsacas & Chassagnard, 1976), *S. scutellimargo* (Duda, 1924), *S. kyushuensis* (Tsacas & Chassagnard, 1976); the *eoundo* subgroup including two species from Afrotropical region (scutellum pale at tip): *S. eoundo* (Tsacas & Chassagnard, 1976), *S. medleri* (Tsacas & Chassagnard, 1976). However, these two subgroups have not been mentioned since for the following species: *S. cultello* (Bock, 1982), *S. koraputae* (Gupta & Panigrahy, 1982), *S. paracultello* (Bock, 1982), and *S. variata* (Bock, 1982) which were added to the *brunnea* group in 1982. Due to the limited materials, the subgroup will not be discussed in this paper. The diagnosis of the *brunnea* group was revised by Bock (1982) as following: arista exceptionally large, fan-like, with curved rays; carina large; rather large species; prescutellar bristles weak.

In the present study, seven new species from East Asian are described, and three known species are redescribed. DNA barcoding was conducted to evaluate morphological delimitation for the *brunnea* group, and for this, a total of 44 *COI* (mitochondrial cytochrome c oxidase I) gene sequences of the above-mentioned ten species mentioned above are determined (Table 1).

Materials and methods

Specimens

The *brunnea* group flies were collected by net sweeping from tussocks and tree trunks near streams in forests. All the examined specimens were preserved in 75% ethanol. In the species descriptions, an asterisk * denotes a new record.

Table 1. Specimens of the *brunnea* group used for DNA barcoding.

Species	Sex	BOLD Process ID	GenBank accession number	Collection site
S. parabrunnea	♂	BDORS034-15	KR070839	Menglun, Mengla, Yunnan, China
S. pressobunnea –1	♂	BDORS013-15	KR070841	Nonggang, Chongzuo, Guangxi, China
S. pressobunnea –2	♀	BDORS012-15	KR070840	Nonggang, Chongzuo, Guangxi, China
S. scutellimargo –1	♂	BDORS001-15	KR070847	Jianfengling, Ledong, Hainan, China
S. scutellimargo –2	♂	BDORS002-15	KR070854	Iriomote Is., Okinawa, Japan
S. scutellimargo –3	♀	BDORS003-15	KR070853	Longdong, Guangzhou, Guangdong, China
S. scutellimargo –4	♂	BDORS004-15	KR070852	Liuxihe, Conghua, Guangdong, China
S. scutellimargo –5	♂	BDORS005-15	KR070851	Wangtianshu, Mengla, Yunnan, China
S. scutellimargo –6	♂	BDORS006-15	KR070850	Wangtianshu, Mengla, Yunnan, China
S. scutellimargo –7	♂	BDORS008-15	KR070848	Wangtianshu, Mengla, Yunnan, China
S. scutellimargo –8	♂	BDORS007-15	KR070849	Menglun, Mengla, Yunnan, China
S. scutellimargo –9	♀	BDORM026-17	KY610504	Jianfengling, Ledong, Hainan, China
S. maculata sp. n. –1	♂	BDORS030-15	KR070820	Menglun, Mengla, Yunnan, China
S. maculata sp. n. –2	♂	BDORS031-15	KR070819	Menglun, Mengla, Yunnan, China
S. maculata sp. n. –3	♂	BDORS033-15	KR070821	Wangtianshu, Mengla, Yunnan, China
S. maculata sp. n. –4	♂	BDORS032-15	KR070818	Wangtianshu, Mengla, Yunnan, China
S. maculata sp. n. –5	♀	BDORM027-17	KY610505	Menglun, Mengla, Yunnan, China
S. maculata sp. n. –6	♀	BDORM028-17	KY610506	Wangtianshu, Mengla, Yunnan, China
S. melanogaster sp. n. –1	♂	BDORS020-15	KR070823	Baihualing, Baoshan, Yunnan, China
S. melanogaster sp. n. –2	♂	BDORS018-15	KR070824	Baihualing, Baoshan, Yunnan, China
S. melanogaster sp. n. –3	♂	BDORS017-15	KR070825	Hesong, Menghai, Yunnan, China
S. melanogaster sp. n. –4	♂	BDORS019-15	KR070822	Hesong, Menghai, Yunnan, China
S. melanogaster sp. n. –5	♂	BDORS021-15	KR070826	Menglun, Mengla, Yunnan, China
S. melanogaster sp. n. –6	♀	BDORM029-17	KY610507	Hesong, Menghai, Yunnan, China
S. nigricostata sp. n. –1	♂	BDORS022-15	KR070829	Baihualing, Baoshan, Yunnan, China
S. nigricostata sp. n. –2	♂	BDORS023-15	KR070827	Baihualing, Baoshan, Yunnan, China
S. nigricostata sp. n. –3	♂	BDORS024-15	KR070828	Wangtianshu, Mengla, Yunnan, China
S. nigricostata sp. n. –4	♀	BDORM030-17	KY610508	Baihualing, Baoshan, Yunnan, China
S. nigripecta sp. n. –1	♂	BDORS027-15	KR070831	Wangtianshu, Mengla, Yunnan, China
S. nigripecta sp. n. –2	♂	BDORS028-15	KR070832	Wangtianshu, Mengla, Yunnan, China
S. nigripecta sp. n. –3	♂	BDORS029-15	KR070830	Wangtianshu, Mengla, Yunnan, China
S. obscurata sp. n. –1	♂	BDORS035-15	KR070838	Wangtianshu, Mengla, Yunnan, China
S. obscurata sp. n. –2	♂	BDORS039-15	KR070834	Wangtianshu, Mengla, Yunnan, China
S. obscurata sp. n. –3	♂	BDORS037-15	KR070836	Menglun, Mengla, Yunnan, China
S. obscurata sp. n. –4	♀	BDORS038-15	KR070835	Menglun, Mengla, Yunnan, China
S. obscurata sp. n. –5	♂	BDORS036-15	KR070837	Menglun, Mengla, Yunnan, China
S. obscurata sp. n. –6	♂	BDORS040-15	KR070833	Hesong, Menghai, Yunnan, China
S. protenipenis sp. n. –1	♂	BDORS014-15	KR070843	Baihualing, Baoshan, Yunnan, China
S. protenipenis sp. n. –2	♂	BDORS016-15	KR070844	Hesong, Menghai, Yunnan, China
S. protenipenis sp. n. –3	♂	BDORS015-15	KR070842	Hesong, Menghai, Yunnan, China
S. protenipenis sp. n. –4	♀	BDORM031-17	KY610509	Hesong, Menghai, Yunnan, China
S. rhina sp. n. –1	♂	BDORS025-15	KR070845	Menglun, Mengla, Yunnan, China
S. rhina sp. n. –2	♂	BDORS026-15	KR070846	Baihualing, Baoshan, Yunnan, China
S. rhina sp. n. –3	♀	BDORM032-17	KY610510	Menglun, Mengla, Yunnan, China

Species identification

The specimens were first identified as of the *brunnea* group in light of morphology referring to Bock (1982) diagnosis of it. Then, they were examined for morphometric characters and detailed structures of terminalia, and sorted into putative species. For each of these putative species, representative specimens suitable for DNA sequencing were selected, considering also the numbers, geographical origins, and genders of available specimens. For each of the selected specimens, the total DNA was extracted from the abdominal tissue of samples after the dissection of the genitalia, using the TIAN-GEN™ DNA extraction kit following the recommended protocol. The PCR/sequencing primer pair was either that designed by He et al. (2009, 5'- CGCCT AAACT TCAGC CACTT -3'), or that by Folmer et al. (1994, 5'- GGTCAA CAAAT CATAA AGATA TTGG -3', 5'-TAAAC TTCAG GGTGA CCAAA AAATC A-3'). The *COI* fragments were amplified using the cycle protocol as in Zhao et al. (2009).

All sequences generated determined in this study were submitted to BOLD (The Barcode of Life Data system) and GenBank (Table 1). A total of 44 *COI* sequences of the *brunnea* group were examined and aligned in MEGA 7.0 (Kumar et al. 2016). Then the inter- and intraspecific genetic distances were calculated for the species of the *brunnea* group using the p-distance model in MEGA 7.0. A NJ (Neighbor-joining) tree was constructed in MEGA 7.0 with p-distances.

In addition, we also conducted a character-based species delimitation. In the sequence alignment, sites being fixed within the focal species but differing from the remaining species were manually selected as diagnostic sites (i.e. "pure" diagnostics; Sarkar et al. 2002, Desalle et al. 2005) for each species. In this analysis, *S. latifasciaeformis* Duda, 1940 (GenBank accession number: GU597448) and *S. dorsocentralis* Okada, 1965 (GU597447), *S. puncticeps* Okada, 1956 (KJ841770, KJ841771) were used as the outgroups.

Description of species

A Mshot Camera was used to microphotograph all the photographs, illustrations and line drawings were processed with the software Adobe Photoshop 7.0 and Easy Paint Tool SAI Ver.1.0.0. Zhang and Toda (1992) and Chen and Toda (2001) are followed for the definitions of measurements, indices and abbreviations.

The type specimens were deposited in Department of Entomology, South China Agricultural University, Guangzhou, China (**SCAU**).

Results

The alignment of the 44 *COI* sequences spanned 664 nucleotide sites in length, with 202 variable sites, among which 177 were parsimony informative. The inter- and intraspecific p-distances between species of the *brunnea* group are given in Table 2. In most cases, the

Table 2. Summary of intra- and interspecific genetic distances in the *brunnea* group.

Species	N	Intraspecific genetic distances	Interspecific genetic distances
		Min. / Max. / Mean ± SD	Min./ Max./ Mean ± SD
S. parabrunnea	1	NA	0.033/ 0.130/ 0.106 ± 0.031
S. pressobunnea	2	NA	0.053/ 0.125/ 0.103 ± 0.026
S. scutellimargo	9	0.002/ 0.024/ 0.009 ± 0.006	0.053/ 0.123/ 0.100 ± 0.014
S. maculata sp. n.	6	0.000/ 0.005/ 0.002 ± 0.002	0.033/ 0.125/ 0.107 ± 0.015
S. melanogaster sp. n.	6	0.000/ 0.027/ 0.017 ± 0.009	0.048/ 0.130/ 0.104 ± 0.019
S. nigricostata sp. n.	4	0.002/ 0.008/ 0.005 ± 0.002	0.087/ 0.123/ 0.103 ± 0.008
S. nigripecta sp. n.	3	0.003/ 0.008/ 0.005 ± 0.002	0.083/ 0.123/ 0.103 ± 0.009
S. obscurata sp. n.	6	0.000/ 0.009/ 0.005 ± 0.003	0.087/ 0.123/ 0.108 ± 0.010
S. protenipenis sp. n.	4	0.000/ 0.003/ 0.002 ± 0.001	0.048/ 0.128/ 0.100 ± 0.020
S. rhina sp. n.	3	0.000/ 0.003/ 0.002 ± 0.002	0.083/ 0.117/ 0.103 ± 0.013

N – the numbers of *COI* sequences involved in distance calculation; **Min.** – minimum; **Max.** – maximum; **SD** – standard deviation; **NA** – no applicable.

intraspecific p-distances in the *brunnea* group were less than 1%, while the largest intraspecific p-distance in the *brunnea* group was found in *S. melanogaster* sp. n. (= 2.7%). The interspecific p-distance ranged from 3.3% to 13.0%, while the smallest interspecific one was found between *S. maculata* sp. n. and *S. parabrunnea* sp. n.

The NJ tree was shown in Fig. 1. In this tree, each morphologically recognized species was strongly supported [bootstraps percentage (BP) = 99 or 100, apart from *S. parabrunnea* with single specimen), and they formed a monophyletic group with respect to the outgroups (BP = 56). Fig. 2 shows nucleotides at the sites where "pure" diagnostics for any species of the *brunnea* group in this study. Except *S. maculata* sp. n., at least one diagnostic site was recognized for each species. For example, the site 124 is diagnostic for *S. rhina* sp. n.: this site has a fixed nucleotide status of C (Cytosine) in this species, but T (Thymidine) in the other species.

Taxonomy

Scaptodrosophila brunnea species group

Drosophila brunnea species group Tsacas & Chassagnard, 1976: 96; Bock, 1982: 72.

Diagnosis (modified from Bock 1982). Arista exceptionally large, fan-like, with 4 (mostly) to 5 (occasionally) long, curved dorsal branches and 3 long, straight ventral branches in addition to terminal bifurcation (Figs 3–7A, E); facial carina large and prominent, as 2/5 length as face (Figs 3–7A, E).

Description. Male and female: *Head* (Figs 3–7A, E): eyes red to brownish red. Ocellar triangle yellowish brown to brown, mostly with 3 pairs of setae above ocellar setae. Frons nearly 1/3 width of head, with a few minute setulae medially. Anterior
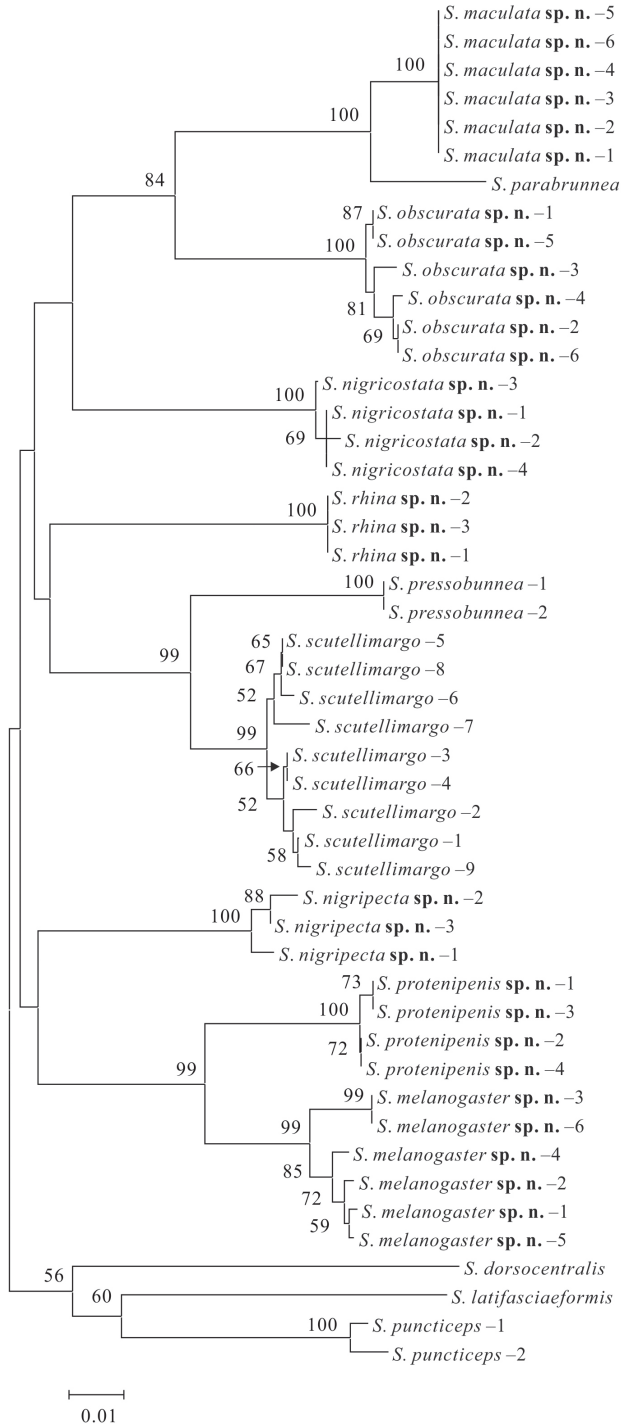
Figure 1. Neighbor-joining (NJ) tree of the *brunnea* group. The numbers around the nodes are bootstrap percentages (BP). BP values lower than 50 are not shown.

```
                           1 1 1 1 1 2 2 2 2 2 3 3 3 3 4 4 4 4 4 4 4 4 4 4 4 5 5 5 5 5 5 5 6 6
                       2 3 5 6 6 7 7 0 1 2 2 9 0 2 3 4 5 7 0 4 5 8 0 0 2 3 3 4 4 4 5 5 6 7 9 9 1 1 3 5 5 6 6 8 3 5
                       2 7 2 4 7 0 3 6 0 1 4 9 2 4 8 7 0 4 2 0 8 2 3 4 4 3 9 2 6 8 1 4 6 2 1 6 4 7 5 4 7 0 5 6 4 2
S. parabrunnea         A T T T A T A A A T T T A T T T A T A T T A T T T T T T A T A A A C T G A A T A C A T A T A
S. pressobunnea −1     . . C G . . G C T . . C G . A . . . T C . T . . A A C C T . . T . T . . A . A . . . C .
S. pressobunnea −2     . . C G . . G C T . . C G . A . . . T C . T . . A A C C T . . T . T . . A . A . . . C .
S. scutellimargo −1    . . . . . . C . T . . . . T . A . . . C . T . . A A . A T . . T . T . T . . . A . . . .
S. scutellimargo −2    . . . . . . C . T . . . . T . A . . . C . T . . A A . A T . . T . T . T . . . A . . . .
S. scutellimargo −3    . . . . . . C . T . . . . T . A . . . T . T . . A A . A T . . T . T . T . . . A . . . .
S. scutellimargo −4    . . . . . . C . T . . . . T . A . . . T . T . . A A . A T . . T . T . T . . . A . . . .
S. scutellimargo −5    . . . . . . C . T . . . . T . A . . . T . T . . A A . A T . . T . T . T . . . A . . . .
S. scutellimargo −6    . . . . . . C . T . . . . T . A . . . T . T . . A A . A T . . T . T . T . . . A . . . .
S. scutellimargo −7    . . . . . . C . T . . . . T . A . . . T . T . . A A . A T . . T . T . T . . . A . . . .
S. scutellimargo −8    . . . . . . C . T . . . . T . A . . . T . T . . A A . A T . . T . T . T . . . A . . . .
S. scutellimargo −9    . . . . . . C . T . . . . T . A . . . C . T . . A A . A T . . T . T . T . . . A . . . .
S. maculata sp. n. −1  . . . . . . . . . . . . C . . . . . . T . . . . . . . . . . . . T C A . A . . . T . . . . .
S. maculata sp. n. −2  . . . . . . . . . . . . C . . . . . . T . . . . . . . . . . . . T C A . A . . . T . . . . .
S. maculata sp. n. −3  . . . . . . . . . . . . C . . . . . . T . . . . . . . . . . . . T C A . A . . . T . . . . .
S. maculata sp. n. −4  . . . . . . . . . . . . C . . . . . . T . . . . . . . . . . . . T C A . A . . . T . . . . .
S. maculata sp. n. −5  . . . . . . . . . . . . C . . . . . . T . . . . . . . . . . . . T C A . A . . . T . . . . .
S. maculata sp. n. −6  . . . . . . . . . . . . C . . . . . . T . . . . . . . . . . . . T C A . A . . . T . . . . .
S. melanogaster sp. n. −1  T . . . T . . T G . . . T . A . G . T . . C . A A . T . . . . T . A . A . . C . T T C G . .
S. melanogaster sp. n. −2  T . . . T . . T G . . . T C A . G . T . . T . A A . T . . . . T . A . A . . C . T T C G . .
S. melanogaster sp. n. −3  T . . . T . . T G . . . T C A . G . T . . T . A G . T . . . . T . A . A . . . . T T C G . .
S. melanogaster sp. n. −4  T . . . T . . T G . . . T . A . G . T . . T . A A . T . . . . T . A . A . . C . T T C G . .
S. melanogaster sp. n. −5  T . . . T . . T G . . . T . A . G . T . . T . A A . T . . . . T . A . A . . C . T T C G . .
S. melanogaster sp. n. −6  T . . . T . . T G . . . T C A . G . T . . T . A G . T . . . . T . A . A . . . . T T C G . .
S. nigricostata sp. n. −1  . . . G . . . T . A . . . A A . . . T . . C . . . C . A T . . G . T . T . . A . T T . T . G
S. nigricostata sp. n. −2  . . . G . . . T . A . . . A A . . . T . . C . . . C . A T . . G . T . T . . A . T T . T . G
S. nigricostata sp. n. −3  . . . G . . . T . A . . . A A . . . T . . C . . . C . A T . . G . T . T . . A . T T . T . G
S. nigricostata sp. n. −4  . . . G . . . T . A . . . A A . . . T . . C . . . C . A T . . G . T . T . . A . T T . T . G
S. nigripecta sp. n. −1    . A A . . . . A . T . . C . . G . . C . . A A . T . . . T C A . A . T C . . .
S. nigripecta sp. n. −2    . A A . . . . A . T . . C . . G . . C . . A A . T . G . T C A . A . T C . . .
S. nigripecta sp. n. −3    . A A . . . . A . T . . C . . G . . C . . A A . T . . . T C A . A . T C . . .
S. obscurata sp. n. −1     G . . A G . . C . . . . A . . . C T . A C . . . . . . A A T . . T . . . .
S. obscurata sp. n. −2     G . . A G . . C . . . . A . . . C T . A C . . . . . . A A T . . T . . . .
S. obscurata sp. n. −3     G . . A G . . C . . . . A . . . C T . A C . . . . . . A A T . . T . . . T
S. obscurata sp. n. −4     G . . A G . . C . . . . A . . . C T . A C . . . . . . A A T . . T . . . .
S. obscurata sp. n. −5     G . . A G . . C . . . . A . . . C T . A C . . . . . . A A T . . T . . . .
S. obscurata sp. n. −6     G . . A G . . C . . . . A . . . C T . A C . . . . . . A A T . . T . . . .
S. protenipenis sp. n. −1  T C . C T . . T . C . . T C G . . . T . . C C . G A . C . . . T . A . . G T T . .
S. protenipenis sp. n. −2  T C . C T . . T . C . . T C G . . . T . . C C . G A . C . . . T . A . . G T T . .
S. protenipenis sp. n. −3  T C . C T . . T . C . . T C G . . . T . . C C . G A . C . . . T . A . . G T T . .
S. protenipenis sp. n. −4  T C . C T . . T . C . . T C G . . . T . . C C . G A . C . . . T . A . . G T T . .
S. rhina sp. n. −1         . . . A . . . A C . T . A . . T . . C . C A A . A T C T T T . A T G G . T T . T . .
S. rhina sp. n. −2         . . . A . . . A C . T . A . . T . . C . C A A . A T C T T T . A T G G . T T . T . .
S. rhina sp. n. −3         . . . A . . . A C . T . A . . T . . C . C A A . A T C T T T . A T G G . T T . T . .
S. latifasciaeformis       - - - - - - - - . . . A . . T . T . . . . . . . . A A A . . . . T T . . . .
S. dorsocentralis          - - - - - - - - . . . . . . . . . T A . A A . A . . A A A . . A . A T . T . T
S. puncticeps −1           . . . . . . . . T A . T C A . T . . T A . A . . A . . T A A . . A . T . . . . -
S. puncticeps −2           . . . . . . . . T A . T C A . T . . T A . A . . A . . T A A . . A . T . . . . -
```

Figure 2. Diagnostic nucleotide sites in the alignment of *COI* sequences of the *brunnea* group. Numbers at the top show the positions of the sites in the *COI* alignment (660 bp in length). Shaded sites are diagnostic for each species. Hyphens (-) indicate missing data.

reclinate orbital setae usually outside and close to proclinate orbital setae; posterior reclinate orbital seta larger than others. Face usually yellowish brown to brown. Clypeus mostly yellowish brown to brown. Palpus usually yellowish brown. Vibrissa prominent; subvibrissal setae small. Gena and postgena narrow.

Thorax (Figs 3–7B, C, F, G): mesonotum yellowish brown to brown, usually with longitudinal stripe(s). Postpronotal lobe mostly yellowish, with 2–3 long setae and a few of shorter setae. Acrostichal setulae mostly in ca. 8–10 irregular rows. Prescutellar setae usually weak. Pleura mostly brown to dark brown. One small proepisternal seta. Katepisternal with three large setae and some small medially. Scutellum yellowish

brown to brown, dark around basal scutellar setae, paler at tip. Wing hyaline, sometimes infuscate. Basal medial-cubital crossvein absent. R_{4+5} nearly parallel with M_1 distally. Halter mostly white. Legs mostly yellowish brown.

Abdomen (Figs 3–7D, H): tergites yellow to yellowish brown anteromedially, with dark brown caudal bands.

Male terminalia (Figs 8–17A–D): epandrium usually pubescent, with several setae around anteroventral corner to posterior margin. Surstylus with several peg-like prensisetae apically, several setae on outer and inner surfaces. Cercus separated from epandrium, pubescent and setigerous. Hypandrium pale brown, usually with paramedian setae. Paramere with several sensilla. Gonopods fused with each other, broadened to hood-shaped. Aedeagus bilobed subbasally.

Female terminalia (Figs 9–13, 15–17E): oviscapt valve long, mostly yellowish brown, usually with one subapical trichoid ovisensillum and approximately 16, 12, 5 peg-like ovisensilla per side on ventral, dorsal and apical margins, respectively.

In the following individual species descriptions, only characters that depart from the above universal characters are provided for brevity.

Scaptodrosophila parabrunnea (Tsacas & Chassagnard, 1976)
Figs 3A–D, 8

Drosophila parabrunnea Tsacas & Chassagnard, 1976: 92.

Specimen examined. CHINA: 1♂ (SCAU, No. 128342), Menglun, Mengla, Yunnan, 21°55'N, 101°16'E, alt. 570 m, 3–4.xi.2001, JJ Gao.

Diagnosis. This species is very similar to *S. maculata* sp. n. in the patterns of abdominal tergites (Fig. 3B) and aedeagus curved dorsally in lateral view (Fig. 8D), but it can be distinguished from the latter by having the paramere apically round in lateral view (Fig. 8D); gonopods dorsally expanded in lateral view (Fig. 8D); see under that species.

Description. Male and female: *Head* (Fig. 3A): frons yellowish to brown. Pedicel brownish; first flagellomere yellowish brown. Facial carina brown, short, as 1/3 length as face.

Thorax (Fig. 3B, C): mesonotum yellowish brown, with a brown longitudinal stripe medially. Acrostichal setulae in ca. 8–10 irregular rows. Scutellum yellow, dark brown near basal scutellar setae, pale at tip. Pleura brownish.

Abdomen (Fig. 3D): tergites II to V yellow, with dark brown caudal bands, the caudal bands on tergites II and III narrowed medially; tergite VI entirely dark brown.

Male terminalia (Fig. 8): epandrium with ca. 16 setae near posterior and ventral margins per side. Surstylus with 6–7 peg-like prensisetae. Hypandrium with a pair of paramedian setae and pubescence basomedially. Paramere with ten sensilla medially. Aedeagus lacking pubescence.
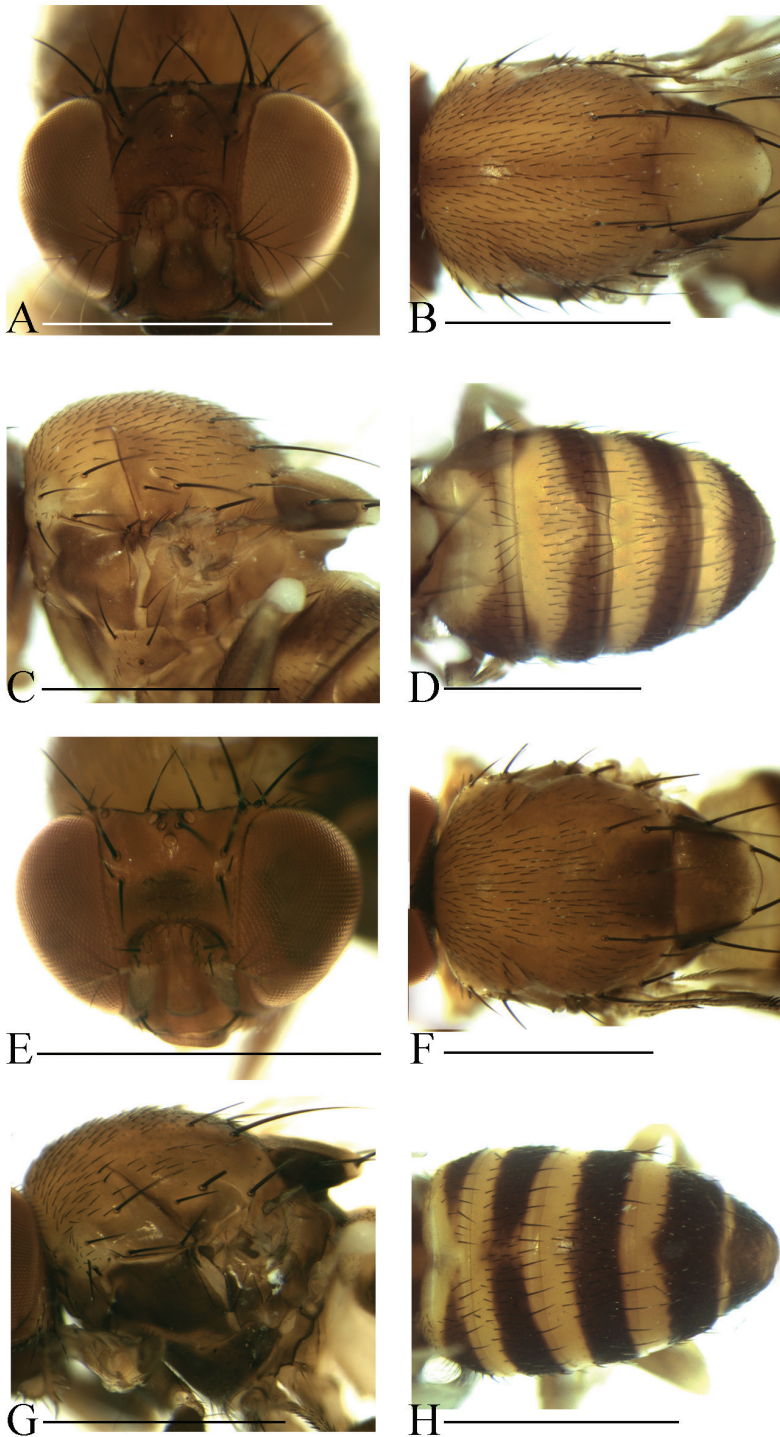
Figure 3. Head, mesonotum, scutellum, pleura and abdomen of male. **A–D** *S. parabrunnea* **E–H** *S. pressobrunnea*. Scale bars 1 mm.

Measurements (in mm). BL = 3.07, ThL =1.47, WL =3.13, WW =1.13.

Indices: arb = 4/3, avd = 0.90, adf = 2.50, flw = 2.00, FW/HW = 0.43, ch/o = 0.05, prorb = 0.50, rcorb = 0.27, vb = 0.33, dcl = 0.45, presctl = 0.29, sctl = 0.80, sterno = 0.71, orbito = 0.50, dcp = 0.39, sctlp = 0.75, C = 2.05, 4c = 0.95, 4v = 2.00, 5x = 1.67, ac = 2.00, M = 0.52, C3F = 0.83.

Distribution. China* (Yunnan), Indonesia (Java, Sumatra).

Scaptodrosophila pressobrunnea (Tsacas & Chassagnard, 1976)
Figs 3E–H, 9

Drosophila pressobrunnea Tsacas & Chassagnard, 1976: 93.

Specimens examined. CHINA: 1♂, 1♀ (SCAU, Nos 128246, 47), Nonggang, Chongzuo, Guangxi, 25°00'N, 106°51'E, alt. 230 m, 21–24.viii.2004, HW Chen.

Diagnosis. This species is very similar to *S. scutellimargo* in the patterns of abdominal tergites (Fig. 3H) and aedeagus curved dorsal (Fig. 9D), but can be distinguished from the latter by having the paramere slightly broadened distally in lateral view (Fig. 9D); gonopods elliptically expanded dorsally in lateral view (Fig. 9D); see under that species.

Description. Male and female: *Head* (Fig. 3E): frons yellowish brown with a brown band anteriorly. Pedicel brownish; first flagellomere yellowish. Facial carina yellowish brown.

Thorax (Fig. 3F, G): mesonotum yellowish brown, with a brown longitudinal stripe on 1/3 posterior. Acrostichal setulae in ca. 8–10 irregular rows. Scutellum brownish, dark brown near basal scutellar setae, pale at tip. Pleura dark brown.

Abdomen (Fig. 3H): tergites II to V yellow, with dark brown caudal bands, the caudal band on tergite II narrowed medially; tergite VI entirely dark brown.

Male terminalia (Fig. 9A–D): epandrium with ca. 15 setae near posterior and ventral margins per side. Surstylus with 6–7 peg-like prensisetae. Hypandrium with a pair of paramedian setae and pubescence basomedially. Paramere with 12 sensilla, and a small projection basally. Aedeagus lacking pubescence.

Female terminalia (Fig. 9E): oviscapt with one subapical trichoid ovisensillum, 14, 8 and 5 peg-like ovisensilla per side on ventral, dorsal and apical margins, respectively.

Measurements (range in 1♂, 1♀, in mm): BL = (2.89, 2.98), ThL = (1.29, 1.16), WL = (2.62, 2.36), WW = (1.02, 0.93).

*Indices*: arb = 4/3, avd = 0.89–0.94, adf = 3.60, flw = 2.00, FW/HW = 0.40–0.42, ch/o = 0.08–0.09, prorb = 0.65–0.68, rcorb = 0.26–0.35, vb = 0.83–1.00, dcl = 0.59, presctl = 0.38–0.45, sctl = 0.97–1.07, sterno = 0.68–0.70, orbito = 0.44–0.50, dcp = 0.38–0.44, sctlp = 0.79–1.10, C = 1.83–1.89, 4c = 1.33–1.40, 4v = 2.41–2.52, 5x = 1.80–1.90, ac = 3.27–3.50, M = 0.70–0.72, C3F = 0.88–0.90.

Distribution. China* (Guangxi), India, Indonesia (Sumatra).

Scaptodrosophila scutellimargo (Duda, 1924)
Figs 4A–D, 10

Drosophila scutellimargo Duda, 1924: 243; Tsacas & Chassagnard, 1976: 92.

Specimens examined. CHINA: 4♀ (SCAU, Nos 128204–07), Longdong, Guang-zhou, Guangdong, 12°19'N, 113°21'E, alt. 200 m, 1.v.2007, HW Chen; 2♀ (SCAU, Nos 128378–79), Tianluhu Park, Guangzhou, Guangdong, 23°13'N, 113°09'E, alt. 240 m, 6.ix.2015, YL Wang; 1♂ (SCAU, No. 128208), Liuxihe, Conghua, Guang-dong, 23°26'N, 113°30'E, alt. 200 m, 12.v.2010, XY Xu; 9♂, 3♀ (SCAU, Nos 128189–200), Jianfengling, Ledong, Hainan, 18°41'N, 108°52'E, alt. 680–820 m, 23.iv.2007, XP Chen, JJ Gao; 2♂, 3♀ (SCAU, Nos 128377–81), Mulun, Huangjiang, Guangxi, 25°09'N, 108°01'E, alt. 449 m, 19.ix.2015, 26.vii.2015, YQ Liu; 1♂, 2♀ (SCAU, Nos 128382–84), Weng'ang, Libo, Guizhou, 25°13'N, 107°56'E, alt. 754 m, 16.ix.2015, L Zhu; 6♂, 7♀ (SCAU, Nos 128229–40, 128370), Menglun, Mengla, Yunnan, 24°41'N, 101°25'E, alt. 680 m, 17.iv.2007, HW Chen, JJ Gao; 10♂, 10♀ (SCAU, Nos 128209–28), Wangtianshu, Mengla, Yunnan, 24°41'N, 101°25'E, alt. 680 m, 22–25.iv.2007, 9.x.2012, HW Chen, JJ Gao. JAPAN: 1♂, 2♀ (SCAU, Nos 128201–03), Iriomote Island, Okinawa, 24°32'N, 123°88'E, alt. 150 m, 12.v.2001, HW Chen.

Diagnosis. Paramere distally broadened and pubescent in lateral view (Fig. 10D); gonopods roundly expanded dorsally in lateral view (Fig. 10D). The 5.3% interspecific genetic distance to *S. scutellimargo* is one of the smallest interspecific distances ascer-tained within this group (Table 2).

Description. Male and female: *Head* (Fig. 4A): frons yellowish brown. Pedicel brownish; first flagellomere yellowish. Facial carina yellowish, short, as 1/3 length as face.

Thorax (Fig. 4B, C): mesonotum brown, with three yellowish brown longitudinal stripes. Acrostichal setulae in ca. 8–10 irregular rows. Scutellum yellowish, dark brown near basal scutellar setae, pale at tip. Pleura brownish to brown.

Abdomen (Fig. 4D): all tergites yellow with dark brown caudal bands, the caudal band on tergite II narrowed medially.

Male terminalia (Fig. 10A–D): epandrium with ca. 16 setae near posterior and ventral margins per side. Surstylus with eight peg-like prensisetae. Hypandrium with a pair of paramedian setae and pubescence basomedially. Paramere with eight sensilla medially distally. Aedeagus lacking pubescence.

Female terminalia (Fig. 10E): oviscapt with one subapical trichoid ovisensillum, 17, 14 and 5 peg-like ovisensilla per side on ventral, dorsal and apical margins, respectively.

Measurements (range in 7♂, 3♀, in mm): BL = (2.73–3.20, 3.07–3.33), ThL = (1.29–1.42, 1.07–1.47), WL = (2.53–2.98, 2.87–3.07), WW = (0.93–1.07, 1.00–1.20).

Indices: arb = 4/3, avd = 0.94–1.06, adf = 0.40–0.80, flw = 2.00–2.50, FW/HW = 0.38–0.42, ch/o = 0.06–0.09, prorb = 0.60–0.74, rcorb = 0.20–0.33, vb = 0.83–1.25,
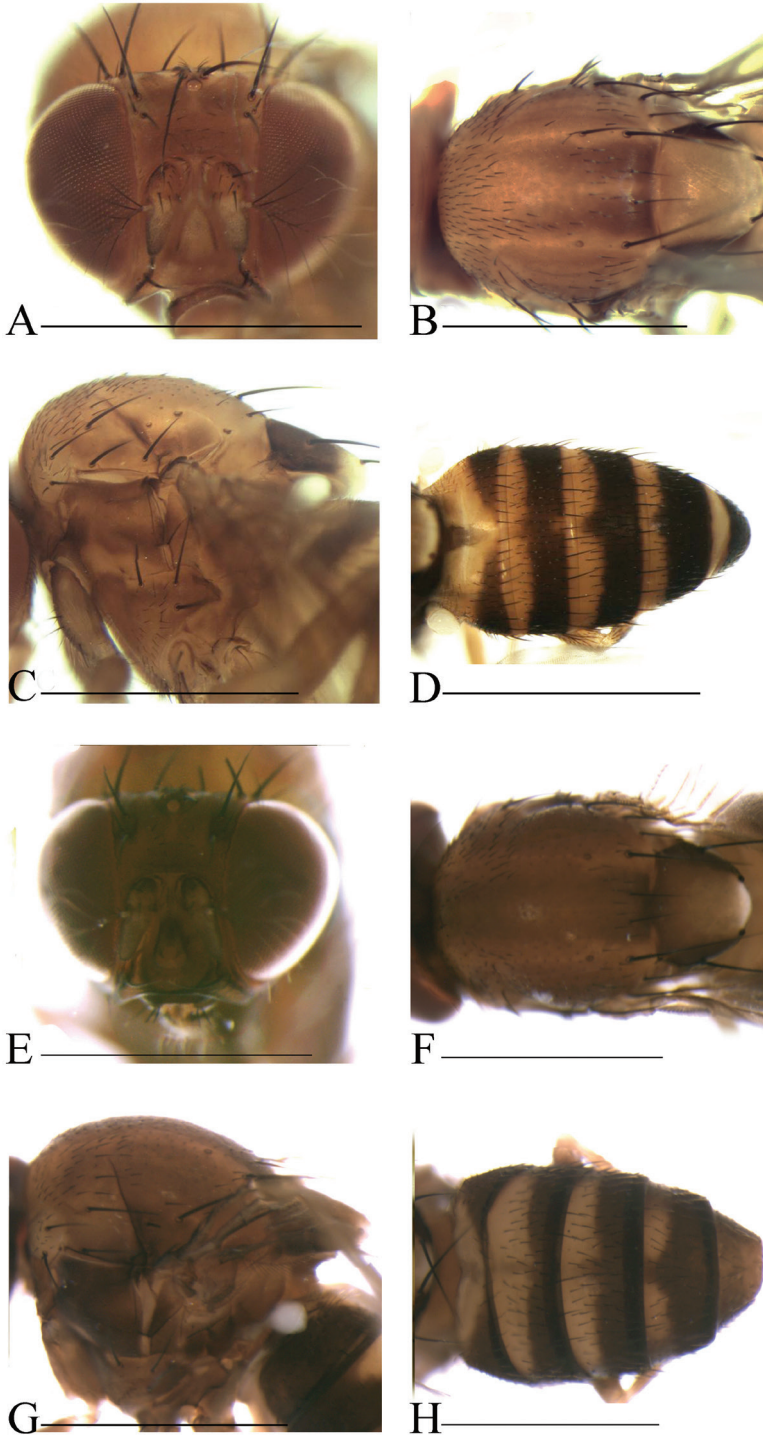
Figure 4. Head, mesonotum, scutellum, pleura and abdomen of male. **A–D** *S. scutellimargo* **E–H** *S. maculata* sp. n. Scale bars 1 mm.

dcl = 0.51–0.59, presctl = 0.31–0.44, sctl = 0.87–1.03, sterno = 0.57–0.69, orbito = 0.40–0.60, dcp = 0.36–0.48, sctlp = 0.86–1.00, C = 1.97–2.20, 4c = 1.00–1.20, 4v = 2.00–2.27, 5x = 1.92–2.20, ac = 2.27–2.92, M = 0.62–0.77, C3F = 0.90–0.94.

Distribution. China (Taiwan, Guangdong, Hainan*, Guangxi*, Guizhou*, Yunnan), Japan* (Ryukyu Is.).

Scaptodrosophila maculata sp. n.
http://zoobank.org/2D412DD1-B660-45B4-AF54-F11970EB111D
Figs 4E–H, 11

Type material. Holotype ♂ (SCAU, No. 128318): CHINA: Wangtianshu, Mengla, Yunnan, 21°47'N, 101°63'E, alt. 760 m, 23.iv.2007, HW Chen. Paratypes: CHINA: 2♂, 6♀ (SCAU, Nos 128319–26), HW Chen, JJ Gao, same data as holotype; 5♂, 8♀ (SCAU, Nos 128329–39, 128371, 72), Wangtianshu, Mengla, Yunnan, 21°47'N, 101°63'E, alt. 760 m, 9.v.2012, HW Chen, JJ Gao; 2♂ (SCAU, Nos 128327–28), Menglun, Mengla, Yunnan, 21°55'N, 101°16'E, alt. 570 m, 3–4.xi.2001, HW Chen.

Diagnosis. Paramere distally curved ventrally, slightly acute apically (Fig. 11D); gonopods not expanded dorsal in lateral view (Fig. 11D). The 3.3% interspecific genetic distance to *S. parabrunnea* is one of the smallest interspecific distances ascertained within this group (Table 2).

Description. Male and female: *Head* (Fig. 4E): frons brownish. Pedicel yellowish brown to brown; first flagellomere yellowish. Facial carina nose-like, brown.

Thorax (Fig. 4F, G): mesonotum brown, with two yellowish brown longitudinal stripes submedially. Acrostichal setulae in ca. 8–10 irregular rows. Scutellum brownish, dark brown near basal scutellar setae, pale at tip. Pleura brownish to dark brown.

Abdomen (Fig. 4H): tergites II to V yellow with dark brown caudal bands, the caudal bands on tergites II and III narrowed medially; tergite VI dark brown.

Male terminalia (Fig. 11A–D): epandrium with ca. 19 setae near posterior and ventral margins per side. Surstylus with ten peg-like prensisetae (Fig. 11B). Hypandrium with a pair of paramedian setae and pubescence medially). Paramere with eight sensilla distally. Aedeagus lacking pubescence.

Female terminalia (Fig. 11E): oviscapt with one subapical trichoid ovisensillum, 18, 13 and 5 peg-like ovisensilla per side on ventral, dorsal and apical margins, respectively.

Measurements [holotype (paratypes range in 4♂, 5♀), in mm]. BL = 3.91 (3.16–3.96, 2.76–3.60), ThL = 1.82 (1.33–1.64, 1.29–1.64), WL = 3.20 (2.49–3.51, 2.40–3.16), WW = 1.38 (1.07–1.11, 1.11–1.33).

Indices: arb = 4/3 (4/3), avd = 1.22 (0.75–1.13), adf = 3.00 (2.67–4.00), flw = 1.67 (1.33–2.50), FW/HW = 0.57 (0.31–0.49), ch/o = 0.10 (0.10–0.18), prorb = 0.79 (0.55–0.78), rcorb = 0.57 (0.23–0.44), vb = 1.00 (0.50–1.00), dcl = 0.83 (0.57–0.95), presctl = 0.50 (0.43–0.52), sctl = 0.91 (0.91–1.29), sterno = 0.77 (0.64–0.92), orbito = 0.50 (0.50–1.00), dcp = 0.53 (0.44–0.53), sctlp = 0.88 (0.83–1.17), C = 2.12

(1.95–2.63), 4c = 1.13 (0.91–1.24), 4v = 2.17 (2.09–2.56), 5x = 1.88 (1.43–2.71), ac = 2.60 (2.10–2.93), M = 0.65 (0.59–0.91), C3F = 0.92 (0.82–0.96).

Etymology. From the Latin word "*maculatus*" (= spotted), referring to the mesonotum with dark patch.

Distribution. China (Yunnan).

Scaptodrosophila melanogaster sp. n.
http://zoobank.org/EDD6A14D-2C1D-453F-AE83-13F275EC9E07
Figs 5A–D, 12

Type material. Holotype ♂ (SCAU, No. 128297): CHINA: Baihualing, Baoshan, Yunnan, 25°17'N, 98°48'E, alt. 1400 m, 7.vi.2011, HW Chen. Paratypes: CHINA: 6♂, 10♀ (SCAU, Nos 128298–313), HW Chen, JJ Gao, same data as holotype; 2♂, 1♀ (SCAU, Nos 128314–15, 128373), Hesong, Menghai, Yunnan, 21°50'N, 100°05'E, alt. 1940 m, 16.iv.2010, 6.v.2012, HW Chen, JM Lu; 1♂ (SCAU, No. 128317), Menglun, Mengla, Yunnan, alt. 570 m, 3, 4.xi.2001, HW Chen.

Diagnosis. This species is similar to *S. rhina* sp. n. in the male terminalia, but can be distinguished from the latter by having the paramere expanded and not divided distally in lateral view (Fig. 12D), the aedeagus distally protruded ventrally in lateral view (Fig. 12D), the mesonotum yellowish brown, with four brown longitudinal stripes sublaterally (Fig. 5B); see under that species.

Description. Male and female: *Head* (Fig. 5A): frons yellowish brown with a brown band anteriorly. Pedicel yellowish brown; first flagellomere yellowish. Facial carina yellowish, short, as 1/3 length as face.

Thorax (Fig. 5B, C): acrostichal setulae in ca. 8–10 irregular rows. Scutellum yellowish brown, dark brown near basal scutellar setae, pale at tip. Pleura dark brown.

Abdomen (Fig. 5D): tergites II to V brown with dark brown caudal bands, the caudal band on tergite II interrupted medially; tergite VI brown.

Male terminalia (Fig. 12A–D): epandrium with ca. 16 setae near posterior and ventral margins per side. Surstylus with 6–7 peg-like prensisetae. Hypandrium with a pair of paramedian setae, lacking pubescence. Paramere with six sensilla subbasally and pubescence distally. Aedeagus lacking pubescence.

Female terminalia (Fig. 12E): oviscapt with one subapical trichoid ovisensillum, 17, 12 and 5 peg-like ovisensilla per side on ventral, dorsal and apical margins, respectively.

Measurements [holotype (paratypes range in 4♂, 5♀), in mm]: BL = 3.60 (3.20–3.47, 3.33–3.78), ThL = 1.64 (1.42–1.64, 1.42–1.78), WL = 3.42 (3.02–3.33, 3.11–3.64), WW = 1.38 (1.20–1.38, 1.24–1.42).

Indices: arb = 4/3 (4/3), avd = 1.06 (0.83–1.11), adf = 2.57 (3.17–3.83), flw = 1.57 (1.57–2.00), FW/HW = 0.43 (0.38–0.45), ch/o = 0.12 (0.08–0.15), prorb = damaged (0.52–0.63), rcorb = damaged (0.25–0.29), vb = 1.20 (0.86–1.20), dcl = damaged (0.68–0.76), presctl = damaged (0.39–0.46), sctl = damaged (0.97–1.07), sterno = 1.23 (0.70–1.22), orbito = 0.56 (0.50–0.60), dcp = 0.56 (0.46–0.55), sctlp = 0.88
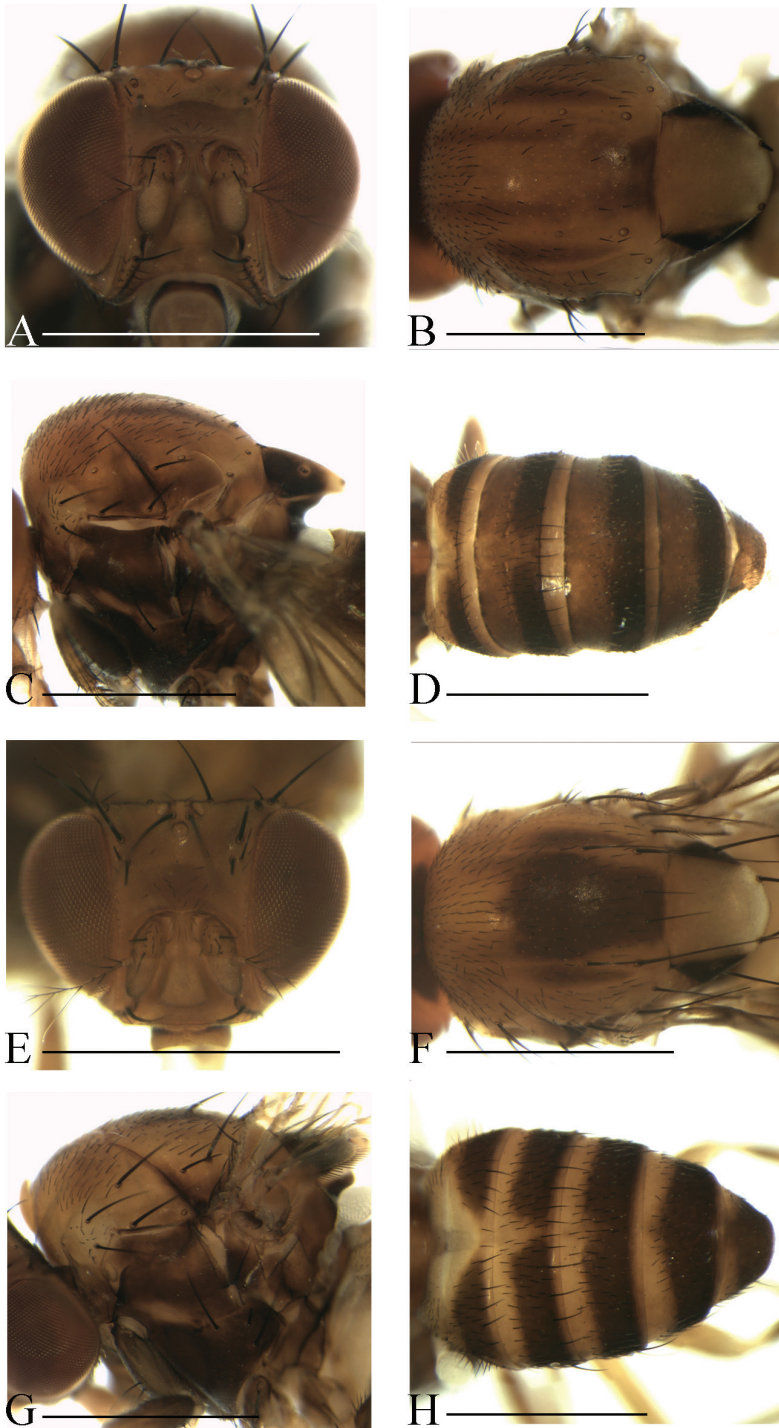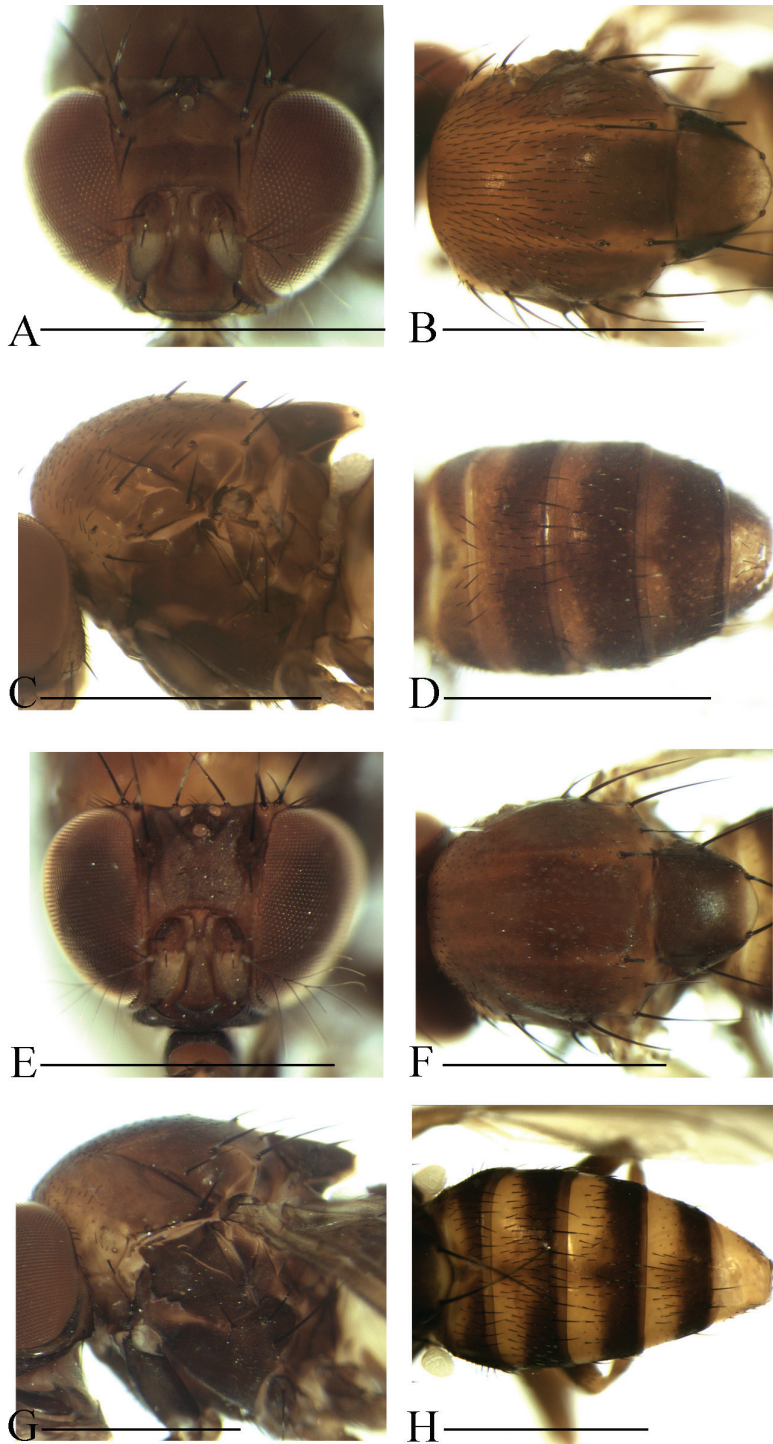
Figure 5. Head, mesonotum, scutellum, pleura and abdomen of male. **A–D** *S. melanogaster* sp. n. **E–H** *S. nigricostata* sp. n. Scale bars 1 mm.

(0.88–1.00), C = 2.28 (1.94–2.16), 4c = 1.02 (0.98–1.24), 4v = 2.02 (1.85–2.32), 5x = 1.33 (1.29–1.73), ac = 2.30 (2.35–2.72), M = 0.53 (0.49–0.68), C3F = 0.91 (0.88–0.98).

Etymology. A combination of the Greek words: "*melas*" (= black) + "*gaster*" (= abdomen), referring to the abdomen nearly black.

Distribution. China (Yunnan).

Scaptodrosophila nigricostata sp. n.
http://zoobank.org/BFBB670B-256F-4F32-AD2A-8E5423C8EF7A
Figs 5E–H, 13

Type material. Holotype ♂ (SCAU, No. 128253): CHINA: Baihualing, Baoshan, Yunnan, alt. 1400 m, 7.vi.2011, ex tussocks, HW Chen. Paratypes: CHINA: 1♂, 4♀ (SCAU, Nos 128248–51, 128374), HW Chen, JJ Gao, same data as holotype; 1♂ (SCAU, No. 128254), Wangtianshu, Mengla, Yunnan, 21°47'N, 101°63'E, alt. 580 m, 23.iv.2007, HW Chen.

Diagnosis. This species is similar to *S. nigripecta* sp. n. in the shape of the paramere and the pattern on the mesonotum (Fig. 13C, D), but can be distinguished from the latter by having the mesonotum mostly yellow (Fig. 5G), and the aedeagus slender and rod-like (Fig. 13C, D); see under that species.

Description. Male and female: *Head* (Fig. 5E): frons yellowish brown with a brown band anteriorly. Pedicel yellowish brown; first flagellomere yellowish brown. Facial carina yellowish brown, short and broad, as 1/3 length as face.

Thorax (Fig. 5F, G): mesonotum with three dark brown longitudinal stripes medially and sublaterally. Acrostichal setulae in ca. 8–10 irregular rows. Scutellum yellowish brown, dark brown near basal scutellar setae, pale at tip. Pleura brown to dark brown.

Abdomen (Fig. 5H): all tergites yellowish brown with dark brown caudal bands, the caudal bands on tergites II and III narrowed medially.

Male terminalia (Fig. 13A–D): epandrium with ca. 15 setae near posterior and ventral margins per side. Surstylus with seven peg-like prensisetae. Hypandrium with a pair of paramedian setae and pubescence medially. Paramere with seven sensilla medially and pubescence distally. Aedeagus lacking pubescence.

Female terminalia (Fig. 13E): oviscapt with one subapical trichoid ovisensillum, 16, 11 and 5 peg-like ovisensilla per side on ventral, dorsal and apical margins, respectively.

Measurements [holotype (paratypes range in 2♂, 4♀), in mm]: BL = 3.38 (2.86–3.33, 2.86–3.29), ThL = 1.60 (1.47–1.64, 1.33–1.56), WL = 3.33 (3.20–3.29, 2.67–3.33), WW = 1.29 (1.20–1.24, 1.07–1.33).

Indices: arb = 4/3 (4/3), avd = 1.00 (0.88–1.43), adf = 2.67 (3.20–4.00), flw = 1.67 (1.83–3.00), FW/HW = 0.42 (0.41–0.47), ch/o = 0.13 (0.05–0.13), prorb = damaged (0.46–0.64), rcorb = damaged (0.27–0.36), vb = 1.00 (0.50–1.00), dcl = 0.77 (0.55–0.69), presctl = 0.44 (0.28–0.43), sctl = damaged (0.88–1.18), sterno = 0.73 (0.56–0.92), orbito = 0.56 (0.44–0.56), dcp = 0.47 (0.40–0.50), sctlp = 0.94 (0.86–

1.00), C = 2.11 (2.20–2.59), 4c = 1.23 (0.90–1.18), 4v = 2.15 (2.11–2.29), 5x = 1.80 (1.67–2.20), ac = 2.37 (2.43–2.57), M = 0.68 (0.50–0.65), C3F = 0.96 (0.89–0.96).

Etymology. A combination of the Latin words: "*niger*" + "*costa*", referring to the black pleura.

Distribution. China (Yunnan).

Scaptodrosophila nigripecta **sp. n.**

http://zoobank.org/8C4FF708-2A9A-4B00-9021-5F0BF170A9A0

Figs 6A–D, 14

Type material. Holotype ♂ (SCAU, No. 128264): CHINA: Wangtianshu, Mengla, Yunnan, 21°47'N, 101°63'E, alt. 760 m, 22.iv.2007, HW Chen. Paratypes: CHINA: 4♂ (SCAU, Nos 128265–68), Wangtianshu, Mengla, Yunnan, 21°47'N, 101°63'E, alt. 760 m, 22.iv.2007, 9.v.2012, HW Chen.

Diagnosis. This species is similar to *S. protenipenis* sp. n. in the aedeagus with pubescence (Fig. 14D), but can be distinguished from the latter by having the paramere apically divided into two triangular lobes in lateral view (Fig. 14D); aedeagus with a cluster of pubescence on small apical part in lateral view (Fig. 14D); see under that species.

Description. Male and female: *Head* (Fig. 6A): frons yellowish brown with a brown band anteriorly (Fig. 6A). Pedicel brown; first flagellomere yellowish. Facial carina brown.

Thorax (Fig. 6B, C): mesonotum brown, with two yellowish brown longitudinal stripes submedially. Acrostichal setulae in ca. 10–12 irregular rows. Scutellum brownish, dark brown near basal scutellar setae, pale at tip. Pleura dark brown.

Abdomen (Fig. 6D): all tergites brownish with dark brown caudal bands, the caudal bands on tergites II and III narrowed medially.

Male terminalia (Fig. 14A–D): epandrium with ca. 17 setae near posterior and ventral margins per side. Surstylus with 6–7 peg-like prensisetae. Hypandrium with a pair of paramedian setae and pubescence medially. Paramere with six sensilla medially and pubescence distally. Aedeagus slightly curved, with thinner pubescence ventrally.

Measurements [holotype (paratypes range in 4♂), in mm]: BL = 2.80 (2.58–2.76), ThL = 1.20 (1.20–1.24), WL = 2.49 (2.40–2.71), WW = 0.89 (0.93–1.02).

Indices: arb = 4/3 (4/3), avd = 0.94 (0.86–0.95), adf = 3.60 (3.40–3.80), flw = 1.60 (1.80–2.00), FW/HW = 0.43 (0.30–0.41), ch/o = 0.09 (0.07–0.12), prorb = 0.59 (0.57–0.71), rcorb = 0.27 (0.32–0.33), vb = 1.00 (1.00–1.17), dcl = damaged (0.62–0.70), presctl = damaged (0.31–0.40), sctl = damaged (0.96), sterno = damaged (1.00–1.05), orbito = 0.50 (0.50–0.63), dcp = 0.46 (0.39–0.50), sctlp = 0.92 (0.85–0.92), C = 1.77 (1.71–1.80), 4c = 1.26 (1.25–1.31), 4v = 2.17 (2.20–2.25), 5x = 2.00 (1.80–2.00), ac = 3.55 (2.71–3.75), M = 0.65 (0.64–0.70), C3F = 0.87 (0.80–0.92).

Etymology. A combination of the Latin words: "*niger*" + "*pectus*", referring to the black thorax.

Distribution. China (Yunnan).

Figure 6. Head, mesonotum, scutellum, pleura and abdomen of male. **A–D** *S. nigripecta* sp. n. **E–H** *S. obscurata* sp. n. Scale bars 1 mm.

Scaptodrosophila obscurata sp. n.
http://zoobank.org/068FE33E-3079-4857-8860-78DFC48EE2CE
Figs 6E–H, 15

Type material. Holotype ♂ (SCAU, No. 128347): CHINA: Wangtianshu, Mengla, Yunnan, 21°47'N, 101°63'E, alt. 760 m, 9.v.2012, HW Chen. Paratypes: CHINA: 1♂ (SCAU, No. 128348), same data as holotype; 20♂, 15♀ (SCAU, Nos 128349–368), Menglun, Mengla, Yunnan, 21°55'N, 101°16'E, alt. 570 m, 3–4.xi.2001, HW Chen; 1♂ (SCAU, No. 128369), Hesong, Menghai, Yunnan, alt. 1940 m, 6.v.2012, HW Chen.

Diagnosis. This species differs from the other known species of this group in having the paramere with a hook-shaped projection basoventrally (Fig. 15D), and the aedeagus apically acute in lateral view (Fig. 15D).

Description. Male and female: *Head* (Fig. 6E): frons brown and glossy. Pedicel brown; first flagellomere yellowish. Facial carina brown and glossy.

Thorax (Fig. 6F, G): mesonotum brown, with two yellowish brown longitudinal stripes submedially. Acrostichal setulae in ca. 10–12 irregular rows. Scutellum brown, dark brown near basal scutellar setae, pale at tip. Pleura dark brown.

Abdomen (Fig. 6H): tergites II to V yellow anteromedially, with black caudal bands; tergite VI yellowish brown.

Male terminalia (Fig. 15A–D): epandrium with ca. 16 setae near posterior and ventral margins per side. Surstylus with 5–6 peg-like prensisetae. Hypandrium with a pair of paramedian setae and pubescence medially. Paramere with four sensilla medially. Aedeagus lacking pubescence.

Female terminalia (Fig. 15E): oviscapt with one subapical trichoid ovisensillum, 15, 11 and 5 peg-like ovisensilla per side on ventral, dorsal and apical margins, respectively.

Measurements [holotype (paratypes range in 6♂, 1♀), in mm]: BL = 3.47 (2.93–3.42, 3.42), ThL = 1.60 (1.38–1.60, 1.64), WL = 2.98 (2.71–2.98, 3.11), WW = 1.16 (1.07–1.20, 1.24).

Indices: arb = 4/3 (4/3), avd = 0.95 (0.94–1.05), adf = 3.50 (3.29–4.00), flw = 1.67 (1.67–2.00), FW/HW = 0.38 (0.38–0.43), ch/o = 0.09 (0.05–0.12), prorb = 0.65 (0.32–0.63), rcorb = 0.23 (0.19–0.38), vb = 1.00 (0.83–1.00), dcl = damaged (0.58–0.73), presctl = damaged (0.23–0.42), sctl =0.88 (0.92–1.06), sterno = 0.65 (0.59–0.85), orbito = 0.50 (0.46–0.67), dcp = 0.43 (0.40–0.46), sctlp = 0.93 (0.88–1.07), C = 2.20 (1.98–2.30), 4c = 1.03 (1.00–1.21), 4v = 1.98 (1.88–2.26), 5x = 1.77 (1.69–2.00), ac = 2.16 (2.10–2.73), M = 0.58 (0.60–0.69), C3F = 0.83 (0.84–0.93).

Etymology. From the Latin word "*obscurata*" (= dark), referring to the thorax dark.

Distribution. China (Yunnan).

Scaptodrosophila protenipenis sp. n.

http://zoobank.org/9A15E25D-846D-41D4-A5A7-DDE46D59A132

Figs 7A–D, 16

Type material. Holotype ♂ (SCAU, No. 128269): CHINA: Hesong, Menghai, Yunnan, alt. 1940 m, 6.v.2012, HW Chen. Paratypes: CHINA: 6♀ (SCAU, Nos 128270–75), HW Chen, JJ Gao, same data as holotype; 12♂, 19♀ (SCAU, Nos 128277–95, 128375), Hesong, Menghai, Yunnan, alt. 1940 m, 16.iv.2010, K Liu, JM Lu, ZF Shao, SJ Yan; 1♂ (SCAU, No. 128276), Baihualing, Baoshan, Yunnan, alt. 1400 m, 7.vi.2011, HW Chen, JJ Gao.

Diagnosis. Paramere apically divided into two round lobes in lateral view (Fig. 16D); aedeagus with dense pubescence in lateral view (Fig. 16D).

Description. Male and female: *Head* (Fig. 7A): frons brownish with a brown band anteriorly. Pedicel brown; first flagellomere yellowish. Facial carina yellowish brown, short, as 1/3 length as face.

Thorax (Fig. 7B, C): mesonotum yellowish brown, with four brown longitudinal stripes. Acrostichal setulae in ca. 10–12 irregular rows. Scutellum yellowish brown, dark brown near basal scutellar setae, pale at tip. Pleura dark brown.

Abdomen (Fig. 7D): tergites II to V brownish with dark brown caudal bands, the caudal bands on tergite II narrowed dorsomedially; tergite VI brownish.

Male terminalia (Fig. 16A–D): epandrium with ca. 17 setae near posterior and ventral margins per side. Surstylus with six peg-like prensisetae. Hypandrium with a pair of paramedian setae and pubescence medially. Paramere with seven sensilla medially and pubescence distally. Aedeagus with pubescence ventrally.

Female terminalia (Fig. 16E): oviscapt with one subapical trichoid ovisensillum, 16, 11 and 5 peg-like ovisensilla per side on ventral, dorsal and apical margins, respectively.

Measurements [holotype (paratypes range in 5♂, 4♀), in mm]: BL = 3.33 (3.16–3.51, 3.33–3.38), ThL = 1.60 (1.56–1.69, 1.60–1.73), WL =3.42 (3.16–3.33, 3.33–3.51), WW = 1.38 (1.29–1.38, 1.33–1.47).

Indices: arb = 4/3 (4/3), avd = 1.00 (0.90–1.00), adf = 3.17 (2.17–3.80), flw = 1.83 (1.43–2.20), FW/HW = 0.41 (0.40–0.44), ch/o = 0.10 (0.09–0.13), prorb = 0.62 (0.50–0.63), rcorb = 0.31 (0.27–0.40), vb = 1.00 (0.67–1.20), dcl = damaged (0.67–0.72), presctl = 0.51 (0.37–0.47), sctl = damaged (0.98–1.15), sterno = 0.73 (0.66–0.79), orbito = 0.56 (0.50–0.60), dcp = 0.46 (0.46–0.53), sctlp = 0.94 (0.81–1.00), C = 1.98 (1.86–2.33), 4c = 1.11 (1.02–1.23), 4v = 2.04 (2.00–2.28), 5x = 1.44 (1.32–1.67), ac = 2.78 (2.21–2.79), M = 0.51 (0.52–0.63), C3F = 0.92 (0.88–0.96).

Etymology. A combination of the Latin words: "*protensus*" + "*penis*", referring to the protruded aedeagus.

Distribution. China (Yunnan).
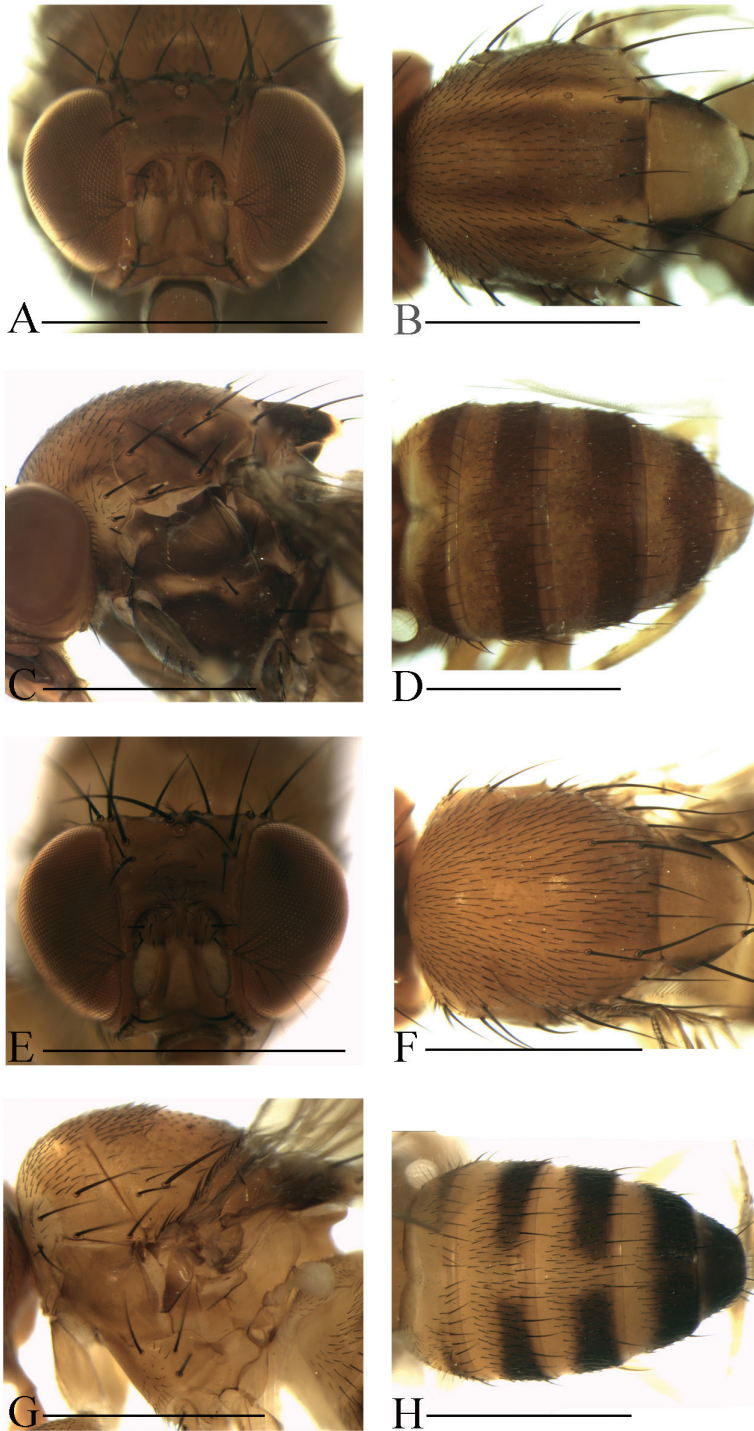
Figure 7. Head, mesonotum, scutellum, pleura and abdomen of male. **A–D** *S. protenipenis* sp. n. **E–H** *S. rhina* sp. n. Scale bars 1 mm.

Scaptodrosophila rhina sp. n.

http://zoobank.org/0AAD1B38-B17E-404C-B5F1-B1BDC732F377

Figs 7E–H, 17

Type material. Holotype ♂ (SCAU, No. 128255): CHINA: Menglun, Mengla, Yunnan, 21°55'N, 101°16'E, alt. 570 m, 3, 4.xi.2001, HW Chen. Paratypes: CHINA: 7♀ (SCAU, Nos 128256–61, 128376), same data as holotype; 1♂ (SCAU, No. 128263), Baihualing, Baoshan, Yunnan, alt. 1400 m, 7.vi.2011, HW Chen.

Diagnosis. This species differs from the other species of the *brunnea* group in the mesonotum being yellowish brown, lacking a longitudinal stripe (Fig. 7F), the pleura being yellowish brown (Fig. 7G), and the paramere distally divided in lateral view (Fig. 17D).

Description. Male and female: *Head* (Fig. 7E): frons yellowish brown with a brown band anteriorly. Pedicel brown; first flagellomere yellowish. Facial carina yellowish brown.

Thorax (Fig. 7F, G): acrostichal setulae in ca. 10–12 irregular rows. Scutellum yellowish brown, dark brown around basal scutellar setae, pale at tip. pleura yellow, with brown patches.

Abdomen (Fig. 7H): tergites II to V yellow, with dark brown caudal bands on tergites III to V, the caudal bands on tergite III and IV interrupted medially; tergite VI dark brown to black.

Male terminalia (Fig. 17A–D): epandrium with ca. 16 setae near posterior and ventral margins per side. Surstylus with five peg-like prensisetae. Hypandrium with a pair of paramedian setae, lacking pubescence. Paramere with five sensilla and pubescence medially. Aedeagus with pubescence ventrally.

Female terminalia (Fig. 17E): oviscapt with three subapical trichoid ovisensilla, 16, 15 and 5 peg-like ovisensilla per side on ventral, dorsal and apical margins, respectively.

Measurements [holotype (paratypes range in 1♂, 1♀), in mm]: BL = 3.33 (3.42, 3.33), ThL = 1.51 (1.60, 1.60), WL = 3.20 (3.20, 3.24), WW = 1.29 (1.20, 1.29).

Indices: arb = 4/3 (4/3), avd = 0.83 (0.80–0.95), adf = 3.00 (3.00–3.80), flw = 1.67 (1.67–1.83), FW/HW = 0.43 (0.42–0.43), ch/o = 0.11 (0.11) , prorb = damaged (damaged), rcorb = 0.31 (damaged), vb = 1.00 (1.00–1.17), dcl = 0.75 (0.64), presctl = 0.40 (0.43), sctl = damaged (damaged), sterno = 0.71 (0.73), orbito = 0.56 (0.44–0.56), dcp = 0.45 (0.47), sctlp = 0.93 (0.88), C = 2.14 (2.10–2.15), 4c = 1.07 (1.02–1.10), 4v = 2.12 (2.07–2.24), 5x = 1.67 (1.79–1.80), ac = 2.44 (2.39–2.56), M = 0.61 (0.60–0.64), C3F = 0.96 (0.91–0.96).

Etymology. From the Greek words: "*rhnios*", referring to the facial carina large and prominent.

Distribution. China (Yunnan).
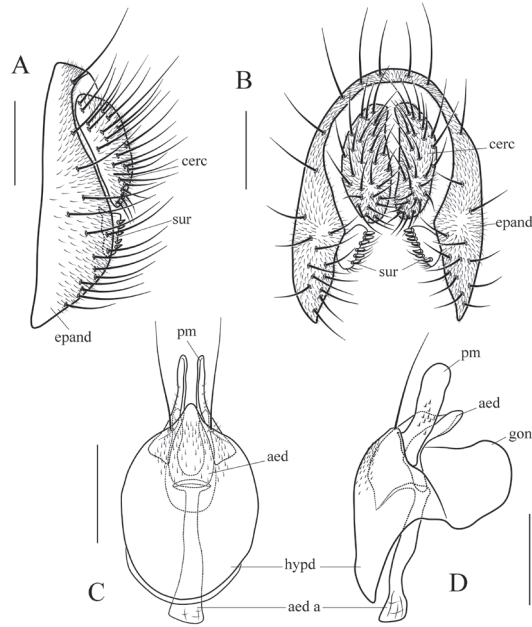
Figure 8. *Scaptodrosophila parabrunnea* (Tsacas & Chassagnard, 1976). **A, B** epandrium (epand), surstylus (sur) and cercus (cerc) (lateral and posterior views) **C, D** hypandrium (hypd), parameres (pm), gonopods (gon), aedeagus (aed) and aedeagal apodeme (aed a) (ventral and lateral views). Scale bars 0.1 mm.
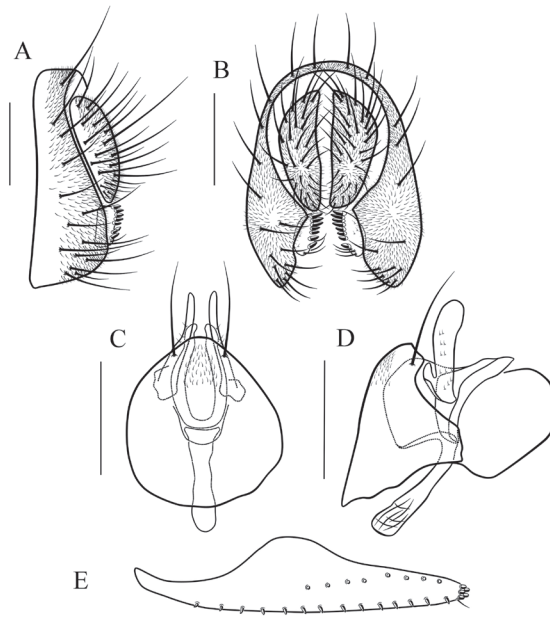
Figure 9. *Scaptodrosophila pressobrunnea* (Tsacas & Chassagnard, 1976). **A, B** epandrium, surstylus and cercus (lateral and posterior views) **C, D** hypandrium, parameres, gonopods, aedeagus and aedeagal apodeme (ventral and lateral views) **E** oviscapt (lateral view). Scale bars 0.1 mm.
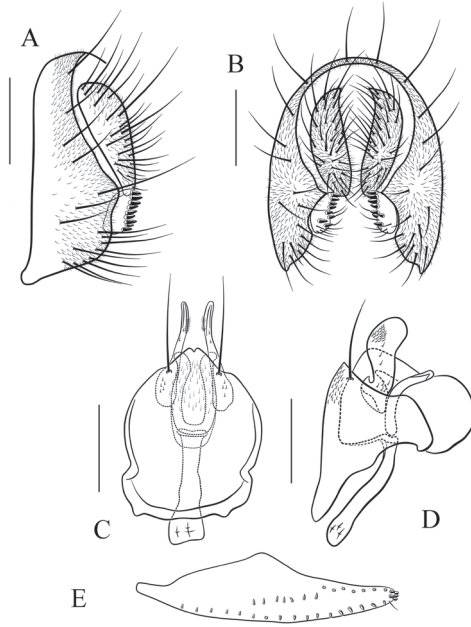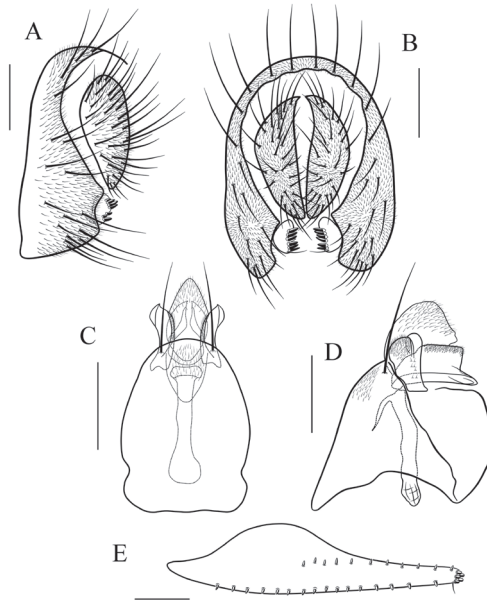
Figure 10. *Scaptodrosophila scutellimargo* (Duda, 1924). **A, B** epandrium, surstylus and cercus (lateral and posterior views) **C, D** hypandrium, parameres, gonopods, aedeagus and aedeagal apodeme (ventral and lateral views) **E** oviscapt (lateral view). Scale bars 0.1 mm.
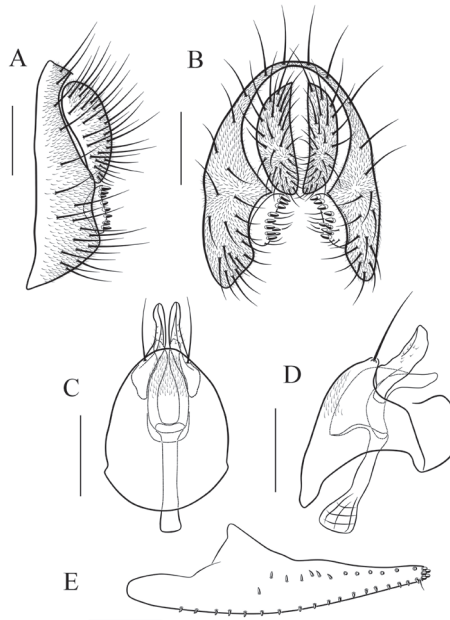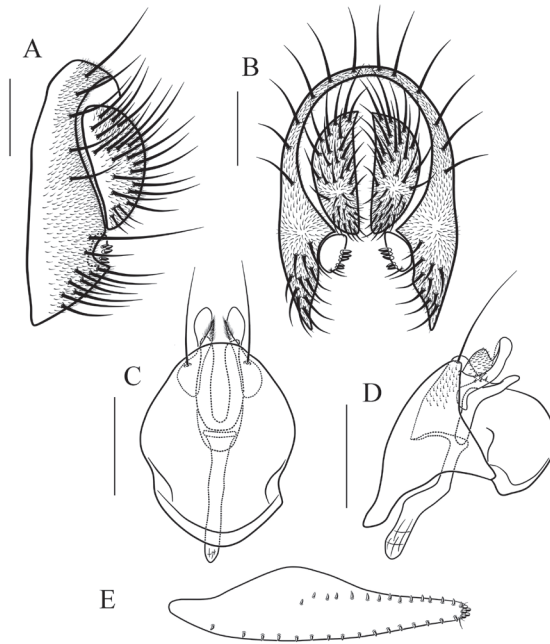

Figure 11. *Scaptodrosophila maculata* sp. n. **A, B** epandrium, surstylus and cercus (lateral and posterior views) **C, D** hypandrium, parameres, gonopods, aedeagus and aedeagal apodeme (ventral and lateral views) **E** oviscapt (lateral view). Scale bars 0.1 mm.
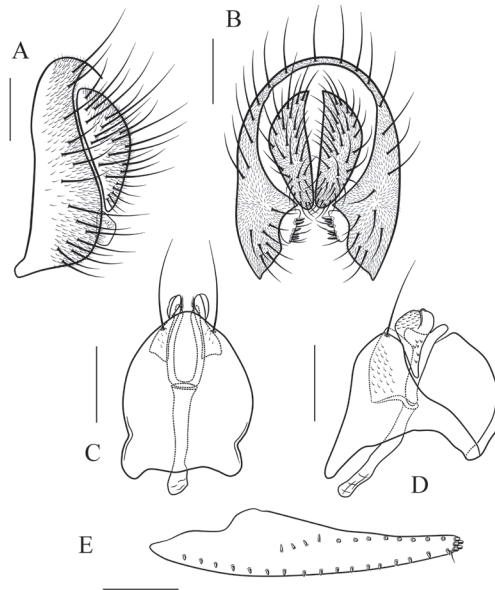
Figure 12. *Scaptodrosophila melanogaster* sp. n. **A, B** epandrium, surstylus and cercus (lateral and posterior views) **C, D** hypandrium, parameres, gonopods, aedeagus and aedeagal apodeme (ventral and lateral views) **E** oviscapt (lateral view). Scale bars 0.1 mm.
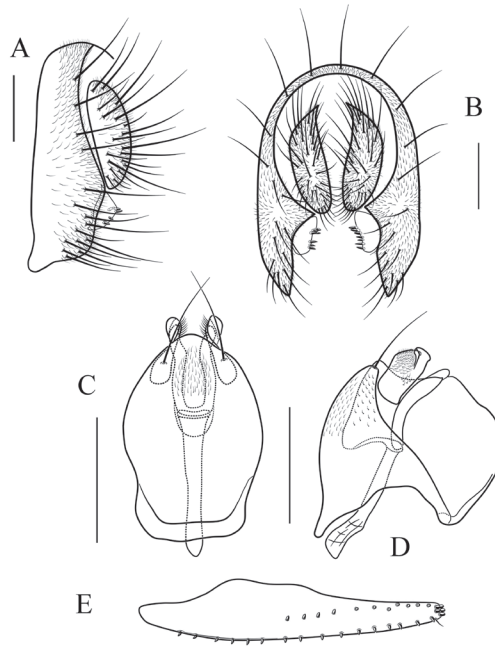
Figure 13. *Scaptodrosophila nigricostata* sp. n. **A, B** epandrium, surstylus and cercus (lateral and posterior views) **C, D** hypandrium, parameres, gonopods, aedeagus and aedeagal apodeme (ventral and lateral views) **E** oviscapt (lateral view). Scale bars 0.1 mm.
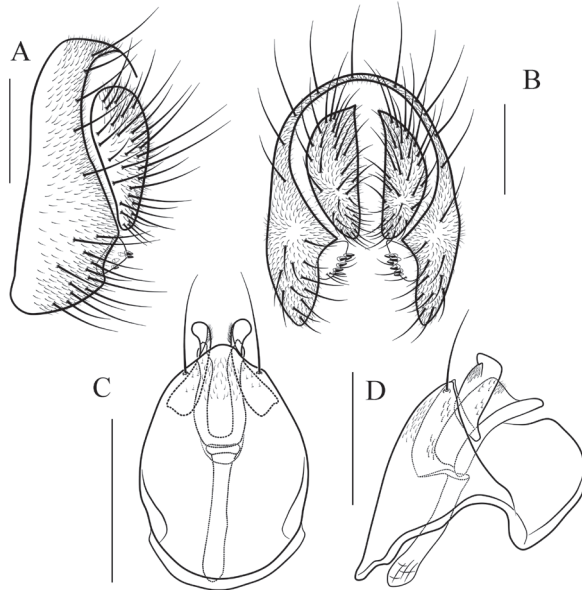
Figure 14. *Scaptodrosophila nigripecta* sp. n. **A, B** epandrium, surstylus and cercus (lateral and posterior views) **C, D** hypandrium, parameres, gonopods, aedeagus and aedeagal apodeme (ventral and lateral views). Scale bars 0.1 mm.
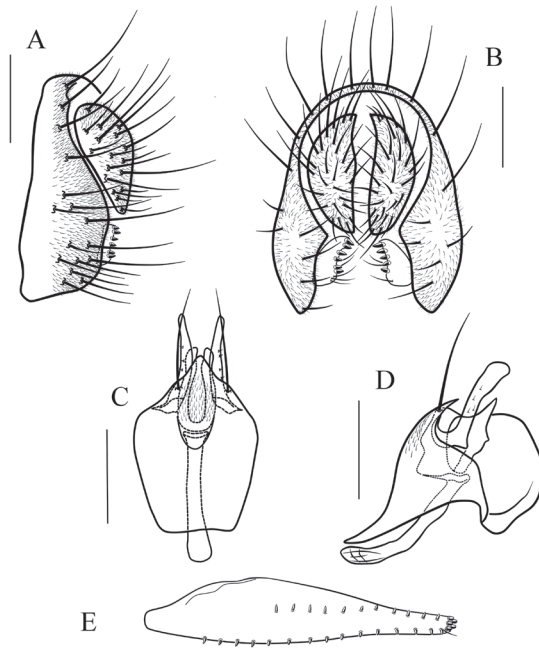
Figure 15. *Scaptodrosophila obscurata* sp. n. **A, B** epandrium, surstylus and cercus (lateral and posterior views) **C, D** hypandrium, parameres, gonopods, aedeagus and aedeagal apodeme (ventral and lateral views) **E** oviscapt (lateral view). Scale bars 0.1 mm.

Figure 16. *Scaptodrosophila protenipenis* sp. n. **A, B** epandrium, surstylus and cercus (lateral and posterior views) **C, D** hypandrium, parameres, gonopods, aedeagus and aedeagal apodeme (ventral and lateral views) **E** oviscapt (lateral view). Scale bars 0.1 mm.

Figure 17. *Scaptodrosophila rhina* sp. n. **A, B** epandrium, surstylus and cercus (lateral and posterior views) **C, D** hypandrium, parameres, gonopods, aedeagus and aedeagal apodeme (ventral and lateral views) **E** oviscapt (lateral view). Scale bars 0.1 mm.

Key to examined species of the *brunnea* group

1   Body brown; carina large; arista exceptionally large, with 4–5 curved long dorsal branches and 3 ventral branches in addition to terminal bifurcation (Figs 3–7A, E) .... *brunnea* **group**...**2**

2   Hypandrium lacking pubescence medially (Figs 12, 17C) **3**

–   Hypandrium pubescent medially (Figs 8–11C, 13–16C)............................**4**

3   Mesonotum yellowish brown, with four brown longitudinal stripes sublaterally (Fig. 5B); pleura dark brown (Fig. 7G); paramere expanded and not divided distally in lateral view (Fig. 12D) ....*S. melanogaster* **sp. n.**

–   Mesonotum yellowish brown, lacking longitudinal stripe (Fig. 7F); pleura yellowish brown (Fig. 7G); paramere distally divided in lateral view (Fig. 17D)..*S. rhina* **sp. n.**

4   Aedeagus pubescent ventrally (Figs 13D, 14D, 16D)................................**5**

–   Aedeagus lacking pubescence (Figs 8–11D, 15D) **7**

5   Mesonotum brown, with two yellowish brown longitudinal stripes submedially (Fig. 6B); paramere apically divided into two triangular lobes in lateral view (Fig. 14D) ....*S. nigripecta* **sp. n.**

–   Mesonotum yellowish brown, with three or four longitudinal stripes (Figs 5F, 7B); paramere apically do not divided into two triangular lobes in lateral view **6**

6   Mesonotum yellowish brown, with four brown longitudinal stripes (Fig. 7B); aedeagus with dense pubescence in lateral view (Fig. 16D)....*S. protenipenis* **sp. n.**

–   Mesonotum yellowish brown, with three dark brown longitudinal stripes medially and sublaterally (Fig. 5F); aedeagus slender rod-like (Fig. 13C, D)...... ....*S. nigricostata* **sp. n.**

7   Mesonotum yellowish brown, with a brownish longitudinal stripe (Fig. 3B, F) **8**

–   Mesonotum brown, with two or three brownish longitudinal stripes (Figs 4B, F, 6F) **9**

8   Mesonotum with a longitudinal stripe on 1/3 posterior (Fig. 3F); pleura dark brown (Fig. 3G); paramere with a small projection basally (Fig. 9D)............ ....*S. pressobrunnea* **(Tsacas & Chassagnard)**

–   Mesonotum yellowish brown, with a brown longitudinal stripe medially (Fig. 3B); paramere lacking projection subbasally (Fig. 8D).......................... ....*S. parabrunnea* **(Tsacas & Chassagnard)**

9   Mesonotum brown, with three yellowish brown longitudinal stripes (Fig. 4B); pleura brownish (Fig. 4C); paramere pubescent distally (Fig. 10D)....... .... *S. scutellimargo* **(Duda)**

–   Mesonotum brown, with two yellowish brown longitudinal stripes (Figs 4F, 6F); pleura dark brown (Figs 4G, 6G); paramere lacking pubescence distally (Figs 11C, D, 15C, D) **10**

10   Frons brown and glossy (Fig. 6E); scutellum brown (Fig. 6F); paramere with
        hook-shaped projection basoventrally (Fig. 15D)............ ***S. obscurata* sp. n.**
–   Frons brownish and dull (Fig. 4E); scutellum brownish (Fig. 4F); paramere
        lacking projection basoventrally (Fig. 11D) ....***S. maculata* sp. n.**

Discussion

The specimens identified as *S. pressobrunnea* and *S. scutellimargo* putatively in this study mostly match the original descriptions, especially in the male terminalia described and illustrated by Tsacas and Chassagnard (1976) and Duda (1924), respectively, while differences are found in the color patterns on mesonotum (lacking longitudinal stripes) in Tsacas and Chassagnard (1976) and Duda (1924). Actually, color patterns of mesonotum can varied intraspecifically in the family Drosophilidae. Similar cases had been reported in *Leucophenga piscifoliacea* Huang & Chen, 2013 and *L. rectifoliacea* Huang & Chen, 2013. Thus, specimens of *S. pressobrunnea* and *S. scutellimargo* putative in this study were recognized as the known species.

The integration of morphological and DNA-based approaches has revealed an effective way to improve accuracy for species identification (Dayrat 2005; Lumleyand Sperling 2010; Padial and De La Riva 2010). In the present study, we try to use the molecular data to text the putative, morpho-species. Each of the new species *S. melanogaster* sp. n., *S. nigricostata* sp. n., *S. nigripecta* sp. n., *S. obscurata* sp. n., *S. protenipeni*s sp. n. and *S. rhina* sp. n. is supported as monophyletic in the NJ tree, and their maximum intraspecific distances are lower than the minimum interspecific distances. In addition, "simple pure characters" are all successfully found in these putative species. Thus, the validity of these seven new species described in the present study was confirmed by the DNA data and morphological research.

It is noteworthy that no "simple pure character" is found for *S. maculata* sp. n. in the character-based analyses, and the smallest interspecific distance in the *brunnea* group is detected between *S. maculata* sp. n. and *S. parabrunnea* (3.3%), which is above the 3% (or 2%) sequence divergence threshold (Hebert et al. 2003a, b, 2004). Actually, the "simple pure character" are not a perfect fix in some case, especially for species in the *brunnea* group with extremely similar *COI* haplotypes, or in cases hybridization and introgression will influence the success of mitochondrial identification methods, which had been observed in turtles of the genus *Graptemys* (Reid et al. 2011), as species often lacked identifying characters simply because of the lack of available variation in *COI*. Although *S. maculata* sp. n. is morphologically similar to *S. parabrunnea*, they can be distinguished easily by the shape of facial carina (Figs 3A, 4E), paramere and aedeagus (Figs 8D, 11D). In the phylogenetic analyses, the NJ tree recovered them as distinct clades (Fig. 1). Therefore, *S. maculata* sp. n. putative was designated as new species.

Dayrat (2005) has previously proposed the use of different sources of evidence in taxonomic practice (i.e. geography, ecology, reproductive isolation, phylogeography,

comparative morphology, population genetics, development, behavior), which is now called 'integrative taxonomy'. In fact, wide overlap between intra- and interspecific distances (0–15.5%) has been repeatedly observed in Diptera (Meier et al. 2006), indicating the necessity of using additional marker(s), and incorporating other sources of information (e.g., geographical and ecological) in species discrimination in this order (Huang et al. 2013).

Acknowledgements

References

Bächli G (2016) The database on Taxonomy of Drosophilidae. http://taxodros.uzh.ch/ [last update: 19 April 2016]

Bock IR, Parsons PA (1978) The subgenus *Scaptodrosophila* (Diptera, Drosophilidae). Systematic Entomology 3: 91–102. https://doi.org/10.1111/j.1365-3113.1978.tb00106.x

Bock IR (1982) Drosophilidae of Australia V. Remaining Genera and Synopsis (Insecta, Diptera). Australian Journal of Zoology (supplementary series) 89: 1–164. https://doi.org/10.1071/AJZS089

Brake I, Bächli G (2008) Drosophilidae (Diptera). In: World Catalogue of Insects (Vol. 9). Brill, 8 pp.

Burla H (1954) Zur Kenntnis der Drosophiliden der Elfenbeinkuste (Französisch West-Afrika). Revue Suisse de Zoologie 61(Supplement): 1–218. https://doi.org/10.5962/bhl.part.75413

Cao HL, Wang XL, Gao JJ, Prigent SR, Watabe H, Zhang YP, Chen HW (2011) Phylogeny of the African and Asian *Phortica* (Drosophilidae) deduced from nuclear and mitochondrial DNA sequences. Molecular Phylogenetics and Evolution 61: 677–685. https://doi.org/10.1016/j.ympev.2011.08.002

Chen HW, Toda MJ (2001) A revision of the Asian and European species in the subgenus *Amiota* Loew (Diptera, Drosophilidae) and establishment of species-groups based on phylogenetic analysis. Journal of Natural History 35: 1571–1563. https://doi.org/10.1080/002229301317067665

Dayrat B (2005) Towards integrative taxonomy. Biological Journal of the Linnean Society 85: 407–415. https://doi.org/10.1111/j.1095-8312.2005.00503.x

de Meijere JCH (1911) Studien uber sudostasiatische Dipteren, VI. Tijdschrift Voor Entomologie 54: 258–432.

DeSalle R, Egan MG, Siddall M (2005) The unholy trinity: taxonomy, species delimitation and DNA barcoding. Philosophical Transactions of the Royal Society B 360: 1905–1916. https://doi.org/10.1098/rstb.2005.1722

Duda O (1924) Die Drosophiliden (Dipteren) des Deutschen Entomologischen Institutes d. Kaiser Wilhelm-Gesellschaft (früheres Deutsches Entomologisches Museum) aus H. Sauter's Formosa-Ausbeute. Arch. Naturgesch 90(A) 3: 235–259.

Duda O (1940) Revision der Afrikanischen Drosophiliden (Diptera). II. Annales Historico-Naturales Musei Nationalis Hungarii 33: 19–53.

Felsenstein J (1985) Confidence limits on phylogenies: an approach using the bootstrap. Evolution 39: 783–791. https://doi.org/10.2307/2408678

Folmer O, Black MB, Hoeh W, Lutz RA, Vrijenhoek RC (1994) DNA primers for amplification of mitochondrial cytochrome *c* oxidase subunit I from diverse metazoan invertebrates. Molecular Marine Biology and Biotechnology 3: 294–299.

Gupta JP, Panigrahy KK (1982) Description of three new species of *Drosophila* (*Scaptodrosophila*) from Orissa. Proceedings: Animal Sciences 91: 631–637. https://doi.org/10.1007/BF03186163

He XF, Gao JJ, Cao HZ, Zhang XL, Chen HW (2009) Taxonomy and molecular phylogeny of the *Phortica hani* species complex (Diptera: Drosophilidae). Zoological Journal of the Linnean Society 157: 359–372. https://doi.org/10.1111/j.1096-3642.2009.00516.x

Hebert PDN, Cywinska A, Ball SL, de Waard JR (2003a) Biological identifications through DNA barcodes. Proceedings of the Royal Society of London Series B 270: 313–321. https://doi.org/10.1098/rspb.2002.2218

Hebert PDN, Ratnasingham S, de Waard JR (2003b) Barcoding animal life: cytochrome c oxidase subunit 1 divergences among closely related species. Proceedings of the Royal Society of London Series B 270: 96–99. https://doi.org/10.1098/rsbl.2003.0025

Hebert PDN, Stoeckle MY, Zemlak TS, Francis CM (2004) Identification of birds through DNA barcodes. PLoS Biology 2: 1657–1663. https://doi.org/10.1371/journal.pbio.0020312

Huang J, Li Tong, Gao JJ, Chen HW (2013) The genus *Leucophenga* (Diptera, Drosophilidae), part II: the *ornata* species group from the East Asia, with morphological and molecular evidence (I). Zootaxa 3701: 101–147. https://doi.org/10.11646/zootaxa.3701.2.1

Kimura M (1980) A simple method for estimating evolutionary rate of base substitutions through comparative studies of nucleotide sequences. Journal of Molecular Evolution 16: 111–120. https://doi.org/10.1007/BF01731581

Kumar S, Stecher G, Tamura K (2016) MEGA7: Molecular Evolutionary Genetics Analysis Version 7.0 for Bigger Datasets. Molecular Biology & Evolution 33(7): 1870. https://doi.org/10.1093/molbev/msw054

Lumley LM, Sperling FAH (2010) Integrating morphology and mitochondrial DNA for species delimitation within the spruce budworm (*Choristoneura fumiferana*) cryptic species complex (Lepidoptera: Tortricidae). Systematic Entomology 35: 416–428. https://doi.org/10.1111/j.1365-3113.2009.00514.x

Mather WB (1955) The genus *Drosophila* (Diptera) in eastern Queensland I. Taxonomy. Australian Journal of Zoology 3: 545–582. https://doi.org/10.1071/ZO9550545

Meier R, Shiyang K, Vaidya G, Ng PKL (2006) DNA barcoding and taxonomy in Diptera: a tale of high intraspecific variability and low identification success. Systematic Biology 55: 715–728. https://doi.org/10.1080/10635150600969864

Nei M, Kumar S (2000) Molecular Evolution and Phylogenetics. Oxford University Press, New York, 333 pp.

Okada T (1968) Addition to the fauna of the family Drosophilidae of Japan and adjacent countries (Diptera): ii. genera *Paramycodrosophila*, *Mycodrosophila*, *Liodrosophila* and *Drosophila*, including a new subgenus *Psilodorha*. Japanese Journal of Entomology 36(4): 324–340.

Padial JM, De La Riva I (2010) A response to recent proposals for integrative taxonomy. Biological Journal of the Linnaean Society 101: 747–756. https://doi.org/10.1111/j.1095-8312.2010.01528.x

Parsons PA, Bock IR (1978) Australian Endemic *Drosophila* III. The *inornata* species group. Australian Journal of Zoology 26: 83–90. https://doi.org/10.1071/ZO9780083

Papp L, Rácz O, Bächli G (1999) Revision of the European species of the *Scaptodrosophila rufifrons* group (Diptera, Drosophilidae). Mitteilungen der Schweizerische Entomologischen Gesellschaft. Bulletin de la Société Entomologique Suisse 72: 105–117.

Reid BN, Le M, Mccord WP, Iverson JB, Georges A, Ergmann T, Amato G, Desalle R, Naro-Maciel E (2011) Comparing and combining distance-based and character-based approaches for barcoding turtles. Molecular Ecology Resources 11(6): 956–67. https://doi.org/10.1111/j.1755-0998.2011.03032.x

Saitou N, Nei M (1987) The neighbor-joining method: A new method for reconstructing phylogenetic trees. Molecular Phylogenetics and Evolution 4: 406–425. https://doi.org/10.1093/oxfordjournals.molbev.a040454

Sarkar IN, Thornton JW, Planet PJ, Figurski DH, Schierwater B, DeSalle R (2002) An automated phylogenetic key for classifying homeoboxes. Molecular Phylogenetics and Evolution 24: 388–399. https://doi.org/10.1016/S1055-7903(02)00259-2

Throckmorton LH (1962) The Problem of Phylogeny in the genus *Drosophila*. University of Texas Publication 6205: 207–343.

Tsacas L, Chassagnard MT (1976) Identité de *Drosophila brunnea* de Meijere et description de nouvelles espèces orientales et africaines à pointe du scutellum blanche (Diptera, Drosophilidae). Bulletin Zoologisch Museum Universiteit van Amsterdam 5: 89–98.

Tsacas L, Chassagnard MT, David JR (1988) A new Afrotropical species-group of anthophilic *Drosophila* in the subgenus *Scaptodrosophila* (Diptera: Drosophilidae). Annales de la Société Entomologique de France 24: 181–202.

Wang BC, Park J, Watabe H, Gao JJ, Xiangyu JG, Aotsuka T, Chen HW, Zhang YP (2006) Molecular phylogeny of the *Drosophila virilis* section (Diptera, Drosophilidae) based on mitochondrial and nuclear sequences. Molecular Phylogenetics and Evolution 40: 484–500. https://doi.org/10.1016/j.ympev.2006.03.026

Wheeler MR (1949) The subgenus *Pholadoris* (*Drosophila*) with descriptions of two new species. University of Texas Publication 492Q: 143–156.

Wheeler MR, Takada H (1966) The Nearctic and Neotropical Species of *Scaptomyza* Hardy (Diptera, Drosophilidae). The University of Texas Publication 6615: 37–78.

Zhao F, Gao JJ, Chen HW (2009) Taxonomy and molecular phylogeny of the Asian *Paraleucophenga* Hendel (Diptera, Drosophilidae). Zoological Journal of the Linnean Society 155: 616–629. https://doi.org/10.1111/j.1096–3642.2008.00450.x

Zhang WX, Toda MJ (1992) A new species-subgroup of the *Drosophila immigrans* species-group (Diptera, Drosophilidae), with description of two new species from China and revision of taxonomic terminology. Japanese Journal of Entomology 60: 839–850.

RESEARCH ARTICLE

Aedes nigrinus (Eckstein, 1918) (Diptera, Culicidae), a new country record for England, contrasted with *Aedes sticticus* (Meigen, 1838)

Ralph E. Harbach[1], Thom Dallimore[2], Andrew G. Briscoe[1], C. Lorna Culverwell[1,3], Alexander G.C. Vaux[4], Jolyon M. Medlock[4]

1 *Department of Life Sciences, Natural History Museum, London, SW7 5BD, UK* **2** *Biology Department, Edge Hill University, Ormskirk, Lancashire, L39 4QP, UK* **3** *Department of Virology, Haartman Institute, University of Helsinki, Helsinki, Finland* **4** *Medical Entomology & Zoonoses Ecology group, Emergency Response Department, Public Health England, Porton Down, Salisbury, SP4 0JG, UK*

Corresponding author: *Ralph E. Harbach* (r.harbach@nhm.ac.uk)

Citation: Harbach RE, Dallimore T, Briscoe AG, Culverwell CL, Vaux AGC, Medlock JM (2017) *Aedes nigrinus* (Eckstein, 1918) (Diptera, Culicidae), a new country record for England, contrasted with *Aedes sticticus* (Meigen, 1838). ZooKeys 671: 119–130. https://doi.org/10.3897/zookeys.671.12477

Abstract

We report the discovery of *Aedes nigrinus* (Eckstein, 1918) in the New Forest of southern England, bringing to 36 the number of mosquito species recorded in Britain. Because it seems that this species has been misidentified previously in Britain as the morphologically similar *Aedes sticticus* (Meigen, 1838), the two species are contrasted and distinguished based on distinctive differences exhibited in the adult and larval stages. The pupa of *Ae. nigrinus* is unknown, but the pupa of *Ae. sticticus* is distinguished from the pupae of other species of *Aedes* by modification of the most recent key to British mosquitoes. The history of the mosquito fauna recorded in the UK is summarized and bionomical information is provided for the two species.

Introduction

The number of mosquito species reported to occur in the United Kingdom has increased significantly since Stephens (1825) recognized the presence of 18 species, 14 of which were incorrectly identified or are currently recognized as synonyms of other species. Nearly a century later, Lang (1920) recorded 20 species, including four that were denoted with names that are currently synonyms of those species. Stephens (1825) recognized only two genera, *Culex* Linnaeus, 1758 for culicine species and *Anopheles* Meigen, 1818, whereas Lang (1920) used a number of generic names that are currently considered to be subgeneric names or synonyms of contemporary genera, including *Culicella* Felt, 1904 (subgenus of *Culiseta* Felt, 1904), *Finlaya* Theobald, 1903 (subgenus of *Aedes* Meigen, 1818), *Ochlerotatus* Lynch Arribálzaga, 1891 (subgenus of *Aedes*), *Taeniorhynchus* Lynch Arribálzaga, 1891 (synonym of subgenus *Ochlerotatus* of *Aedes*) and *Theobaldia* Neveu-Lemaire, 1902 (synonym of *Culiseta*). Following the generic classification of Edwards (1932), except for retaining *Taeniorhynchus*, which Edwards listed as a synonym of *Mansonia* Blanchard, 1901, Marshall (1938) described 29 British species belonging to six genera – *Aedes*, *Anopheles*, *Culex*, *Orthopodomyia* Theobald, 1904, *Taeniorhynchus* and *Theobaldia*. *Theobaldia* Neveu-Lemaire, 1902, being preoccupied by *Theobaldia* Fischer, 1885, was replaced by *Culiseta* Felt, 1904 (see Stone et al. 1959), which was in use by most American authors while *Theobaldia* was being used by European authors. In accordance with the classification of the Culicidae compiled in *A Catalog of the Mosquitoes of the World* (Knight and Stone 1977), Cranston et al. (1987) listed the occurrence of 33 species in Britain, five species of subfamily Anophelinae Grassi, 1900, all in genus *Anopheles*, and 28 species of subfamily Culicinae Meigen, 1818 belonging to five genera, *Aedes* (14 species), *Coquillettidia* Dyar, 1905 (1 species), *Culex* (5 species), *Culiseta* (7 species) and *Orthopodomyia* (1 species). Snow (1990) reduced the list to 32 species by appropriately recognizing *Cx. molestus* Forskål, 1775 as a "form" of *Cx. pipiens*. The list grew to 33 species with the addition of *Anopheles daciae* Linton, Nicolescu & Harbach, 2004 of the Maculipennis Complex based on molecular evidence (Linton et al. 2005), to 34 species with the discovery of *Aedes geminus* Peus, 1970 among museum specimens collected by J.F. Marshall and J. Staley around the Hayling Island area (Medlock and Vaux 2009) and then to 35 species with the recent detection of the invasive *Aedes albopictus* (Skuse, 1895) in southern England (Medlock et al. 2017). In the present paper, we report the discovery of *Aedes nigrinus* (Eckstein, 1918) in the New Forest of southern England, bringing to 36 the number of mosquito species recorded in Britain. Evidence indicates that this species has been misidentified in the past as the morphologically similar *Aedes sticticus* (Meigen, 1838); hence, the two species are contrasted herein. The history of the mosquito fauna recorded in the UK is summarized in Table 1, which includes, for completeness, the nominal species catalogued by Verrall (1901).

Materials and methods

Mosquitoes

Mosquitoes were collected as larvae and individually reared to adults. Larvae of adults identified as *Aedes nigrinus* were collected on 22 May 2016 at Beaulieu Airfield (50°48.53'N; 1°29.79'W and 50°48.11'N; 1°30.83'W), New Forest, Hampshire, England. Larvae of *Ae. sticticus* were collected on 10 May 2011 in Hurcott Wood (32°23.92'N; 2°12.73'W), Kidderminster, Worcestershire, England. The larval and pupal exuviae of *Ae. nigrinus* were lost; those of *Ae. sticticus* were mounted in Euparal on microscope slides. Adults were mounted on points on insect pins. Dissected male genitalia of both species were cleared in 5% NaOH for 2 h at 50°C and slide-mounted in Euparal. The pinned adults were examined under simulated natural light with an Olympus SZ6045 stereomicroscope. The dissected genitalia were studied with an Olympus BX50 compound microscope fitted with differential interference contrast optics. Digital images of wings and genitalia were taken with a Canon 550D digital camera mounted on a Leica M125 stereomicroscope and a Zeiss Axioskop compound microscope, respectively; Helicon Focus version 3.03 software (Helicon Soft Ltd, Kharkov, Ukraine) was used to obtain extended-focus images. The anatomical terminology of Harbach and Knight (1980, 1982), revised and updated in the Anatomical Glossary of the Mosquito Taxonomic Inventory (http://mosquito-taxonomic-inventory.info/node/11027), is used in the descriptions and illustrations.

Abbreviations for morphological structures indicated in figures:

BDL   basal dorsomesal lobe
C   costa
R₁   radius-one
Re   remigium
Sc   subcosta
1A   anal vein

DNA extraction, amplification and sequencing

DNA was extracted from two legs from each of five adults of *Ae. nigrinus* using the DNeasy Blood & Tissue Kit (Qiagen, Hilden, Germany) in accordance to the manufacturer's instructions. Amplification of the mitochondrial cytochrome oxidase subunit I (*COI*) gene and the nuclear internal transcriber spacer 2 (ITS2) region of ribosomal DNA was carried out using the following primers: 5'- GGATTTGGAAATTGATTAGTTCCTT-3' (COIF) and 5'- AAAAATTTTAATTCCAGTTGGAACAGC-3' (COIR) (Chan et al. 2014), 5'- TGTGAACTGCAGGACACATG-3' (ITS2F) and 5'- ATGCTTAAATTTAGGGGGTA-3' (ITS2R) (Walton et al. 2007). PCR was

Table 1. Summary of the history of the mosquito fauna recorded in the UK.

Stephens (1825)	Verrall (1901)	Lang (1920) (20 species)	Marshall (1938) (29 species)	Cranston et al. (1987); Snow (1990) (32 species)	Today (36 species)
Aedes cinereus, Culex nigritulus	Aedes cinereus, Culex nigritulus	Aedes cinereus	Aedes cinereus	Aedes (Aedes) cinereus	Aedes (Aedes) cinereus
					Aedes (Aedes) geminus[1]
Culex cantans; Cx. maculatus	Culex vexans	Ochlerotatus vexans	Aedes vexans	Aedes (Aedimorphus) vexans	Aedes (Aedimorphus) vexans
	Culex annulipes	Ochlerotatus annulipes	Aedes annulipes	Aedes (Ochlerotatus) annulipes	Aedes (Ochlerotatus) annulipes
		Ochlerotatus waterhousei	Aedes cantans	Aedes (Ochlerotatus) cantans	Aedes (Ochlerotatus) cantans
		Ochlerotatus caspius	Aedes caspius	Aedes (Ochlerotatus) caspius	Aedes (Ochlerotatus) caspius
Culex domesticus (in part); Cx. nemorosus	Culex nemorosus	Ochlerotatus nemorosus	Aedes communis	Aedes (Ochlerotatus) communis	Aedes (Ochlerotatus) communis
		Ochlerotatus detritus	Aedes detritus	Aedes (Ochlerotatus) detritus	Aedes (Ochlerotatus) detritus
	Culex dorsalis	Ochlerotatus curriei	Aedes dorsalis	Aedes (Ochlerotatus) dorsalis	Aedes (Ochlerotatus) dorsalis
	Culex lutescens		Aedes flavescens	Aedes (Ochlerotatus) flavescens	Aedes (Ochlerotatus) flavescens
			Aedes leucomelas	Aedes (Ochlerotatus) leucomelas	Aedes (Ochlerotatus) leucomelas
	Culex nigripes (syn. var. sylvae)		Aedes sticticus[2]		Aedes (Ochlerotatus) nigrinus[3]
			Aedes punctor	Aedes (Ochlerotatus) punctor	Aedes (Ochlerotatus) punctor
			Aedes sticticus[2]	Aedes (Ochlerotatus) sticticus	Aedes (Ochlerotatus) sticticus
Culex ornatus (in part)	Culex diversus, Cx. rusticus	Ochlerotatus rusticus	Aedes rusticus	Aedes (Ochlerotatus) rusticus	Aedes (Rusticoidus) rusticus
Culex ornatus (in part)	Culex lateralis, Cx. ornatus	Finlaya geniculata	Aedes geniculatus	Aedes (Finlaya) geniculatus	Aedes (Dahliana) geniculatus
					Aedes (Stegomyia) albopictus[4]
			Anopheles algeriensis	Anopheles (Anopheles) algeriensis	Anopheles (Anopheles) algeriensis
Anopheles maculipennis s.l.[5]	Anopheles maculipennis s.l.[5]	Anopheles maculipennis s.l.[5]	Anopheles maculipennis s.l.[5]	Anopheles (Anopheles) atroparvus	Anopheles (Anopheles) atroparvus
	Anopheles bifurcatus	Anopheles bifurcatus	Anopheles claviger	Anopheles (Anopheles) claviger	Anopheles (Anopheles) claviger
					Anopheles (Anopheles) daciae[6]
				Anopheles (Anopheles) messeae	Anopheles (Anopheles) messeae
	Anopheles nigripes	Anopheles plumbeus	Anopheles plumbeus	Anopheles (Anopheles) plumbeus	Anopheles (Anopheles) plumbeus

Stephens (1825)	Verrall (1901)	Lang (1920) (20 species)	Marshall (1938) (29 species)	Cranston et al. (1987); Snow (1990) (32 species)	Today (36 species)
	Taeniorhynchus richiardii	Taeniorhynchus richiardii	Taeniorhynchus richiardii	Coquillettidia (Coquillettidia) richiardii	Coquillettidia (Coquillettidia) richiardii
			Culex molestus	Culex (Barraudius) modestus	Culex (Barraudius) modestus
				Culex (Culex) pipiens molestus[7]	
Anopheles bifurcatus; Cx. bicolor; Cx. domesticus (in part); Cx. lutescens; Cx. marginalis; Cx. pipiens; Cx. punctatus; Cx. rufus; Cx. sylvaticus	Culex pipiens (syn. Cx. ciliaris)	Culex pipiens	Culex pipiens	Culex (Culex) pipiens	Culex (Culex) pipiens
				Culex (Culex) torrentium	Culex (Culex) torrentium
		Culex apicalis	Culex apicalis	Culex (Neoculex) territans	Culex (Neoculex) territans
				Culiseta (Allotheobaldia) longiareolata	Culiseta (Allotheobaldia) longiareolata
Culex fumipennis	Culex cantans (syn. Cx. fumipennis)	Culicella fumipennis	Theobaldia fumipennis	Culiseta (Culicella) fumipennis	Culiseta (Culicella) fumipennis
			Theobaldia litorea	Culiseta (Culicella) litorea	Culiseta (Culicella) litorea
	Culex morsitans	Culicella morsitans	Theobaldia morsitans	Culiseta (Culicella) morsitans	Culiseta (Culicella) morsitans
			Theobaldia alaskaensis	Culiseta (Culiseta) alaskaensis	Culiseta (Culiseta) alaskaensis
Culex affinis; Cx. annulatus; Cx. calopus	Culex annulatus	Theobaldia annulata	Theobaldia annulata	Culiseta (Culiseta) annulata	Culiseta (Culiseta) annulata
			Theobaldia subochrea	Culiseta (Culiseta) subochrea	Culiseta (Culiseta) subochrea
	Culex pulchripalpis [sic]	Orthopodomyia albionensis	Orthopodomyia pulcripalpis	Orthopodomyia pulcripalpis	Orthopodomyia pulcripalpis

[1] Recorded by Medlock and Vaux (2009).

[2] At least in part, see Discussion.

[3] Recorded herein.

[4] Recorded by Medlock et al. (2017).

[5] Also includes *Anopheles daciae* and *An. messeae*.

[6] Recorded by Linton et al. (2005).

[7] Synonym of *Culex pipiens*; recognized as a "form" of *Cx. pipiens* by Snow (1990).

undertaken using Phusion High-Fidelity PCR Master Mix (New England Biolabs, Ipswich, MA, USA) and products were purified using Isolate II PCR and Gel spin columns (Bioline Reagents Limited, London, UK). Subsequent sequencing reactions were undertaken using the BigDye™ Terminator v. 3.1 Cycle Sequencing Kit (Applied Biosystems Inc., Foster City, CA, USA) and sequenced on a 3500 Series Genetic Analyzer. Analysis of the sequence data was carried out using MEGA7 (Kumar et al. 2016). The exact location and size of the ITS2 region was determined by annotation of the 5.8S/28S flanking regions using the ITS2 database (http://its2.bioapps.biozentrum. uni-wuerzburg.de/).

Results

Adults reared from larvae collected in the New Forest were initially questionably identified as specimens of *Ae. sticticus* using the keys to British mosquitoes provided by Cranston et al. (1987), consequently we ran adults and male genitalia through the keys to European species of *Aedes* and *Ochlerotatus* included in Becker et al. (2010). Based on differential characters of the antennae, wings and abdominal terga of females and characteristics of the apical and basal dorsomesal lobes of the gonocoxites of males, the specimens keyed to *Ae. nigrinus*. This engendered a comparison with specimens collected in Hurcott Wood five years earlier that were identified as *Ae. sticticus* using the keys to adults and larvae contained in Cranston et al. (1987) and Becker et al. (2010). Based on this comparison, there was little doubt that the New Forest specimens were correctly identified as *Ae. nigrinus*. Incidentally, while examining older British mosquito publications, we noted that Marshall (1938) had examined specimens from the New Forest and the male genitalia he illustrated for *Ae. sticticus* appear to be those of *Ae. nigrinus*.

To confirm the morphological identification of *Ae. nigrinus*, we sequenced part of the mitochondrial cytochrome oxidase subunit I gene and the internal transcribed spacer 2 region of ribosomal DNA from specimens collected in the New Forest and Hurcott Wood. Sequences generated in this study were interrogated against the NCBI non-redundant nucleotide database via the BLAST algorithm (Altschul et al. 1990). No ITS2 sequences for *Ae. nigrinus* were available for comparison, but our sequence shared a 95% sequence identity (289/305 bases) to *Ae. sticticus* (KF535079). Following alignment, this difference was accounted for by a number of consistent SNP sites and a six-nucleotide insertion/deletion 207 bases into our sequence. The *COI* sequences of New Forest specimens also returned high BLAST scores for *Ae. sticticus*, but only because the query coverage was higher due to the primer pairs used for amplification. The closest match recognized by identity score was *Ae. nigrinus* (98–99% compared with 96–97% for *Ae. sticticus*). These results support the morphological identification of *Ae. nigrinus* in the UK.
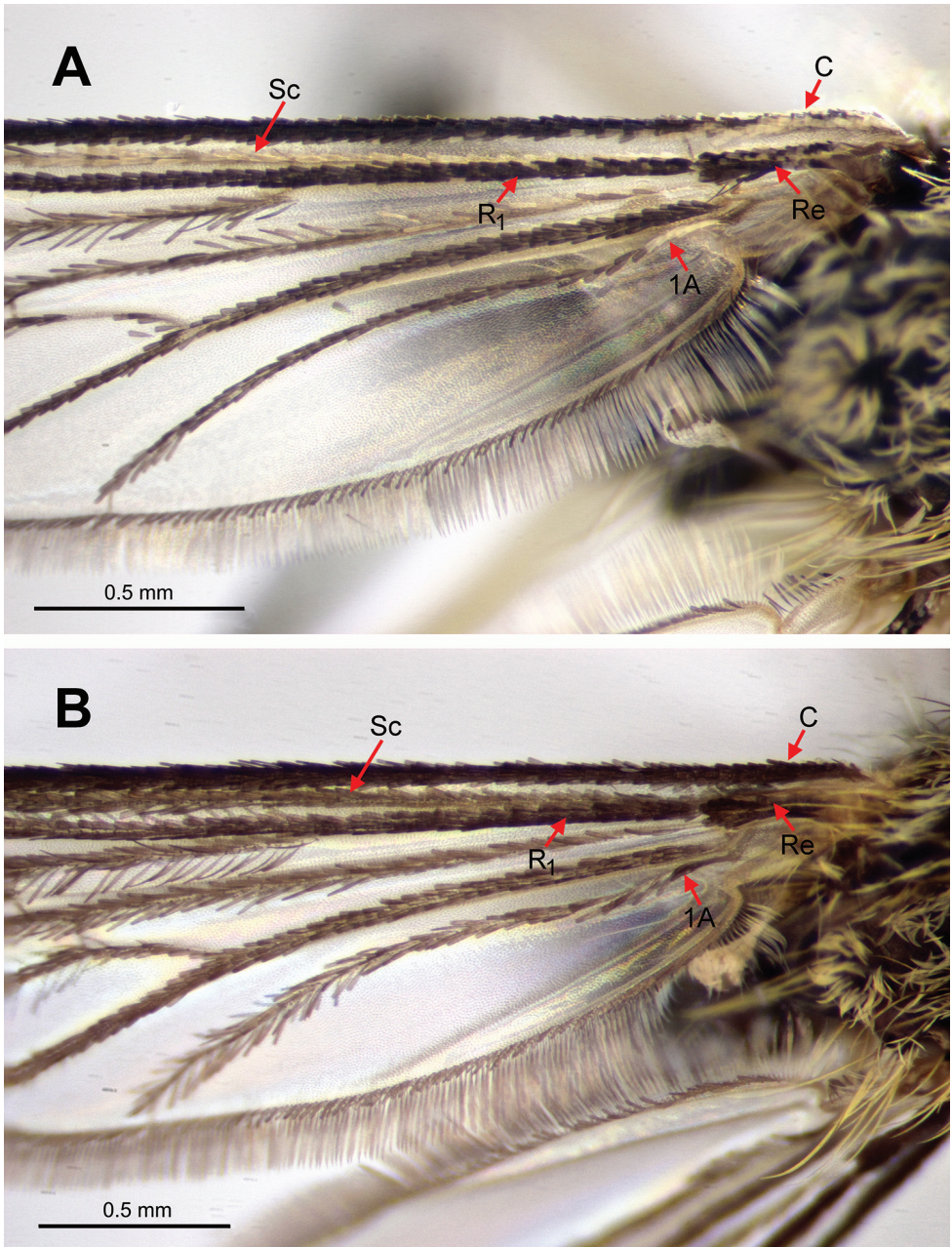
Figure 1. Proximal half of the right wing of female mosquitoes. **A** *Ae. nigrinus*, showing the presence of pale scaling on the costa, subcosta, remigium and anal vein **B** *Ae. sticticus*, showing the absence of pale scaling.

Discussion

Morphology and identification

It is unfortunate that the larval and pupal exuviae of mosquitoes reared from larvae collected in the New Forest were lost as these would have aided the identification of *Ae. nigrinus*. Further field work will be conducted to obtain the immature stages. However, a number of morphological differences are robust enough to distinguish the two species. To aid future identification, the wings and the male genitalia of *Ae. nigrinus* and *Ae. sticticus* are illustrated for comparison in Figures 1 and 2, respectively. The principal features that distinguish the two species are as follows.

Aedes nigrinus. A dark mosquito, integument and dark scaling black, well contrasted with pale scaling. Female: first antennal flagellomere and dorsal surface of pedicel black; wing with pale (white) scaling (Fig. 1A) at base of costa (C), length of subcosta (Sc), on remigium (Re) (not evident in figure), base of radius-one (R_1) (not evident in figure) and base of anal vein (1A); abdominal terga with basal pale bands slightly constricted medially, sometimes reduced to lateral patches on tergum VII. Male genitalia (Fig. 2A): basal dorsomesal lobe of gonocoxite more or less globoid in dorsal (tergal) view. Fourth-instar larva (see Natvig 1948, Becker et al. 2010): setae 5,6-C usually single, rarely double; comb usually with 12–16 scales, rarely with more than 20.

Aedes sticticus. A slightly paler mosquito, integument and dark scaling dark brown to brownish black, less well contrasted with pale scaling. Female: first antennal flagellomere and dorsal surface of pedicel yellowish brown; wing entirely dark-scaled (Fig. 1B); abdominal terga mostly without complete basal pale bands, bands on terga II–IV narrow if present, more distal terga with triangular basolateral pale patches. Male genitalia (Fig. 2B): basal dorsomesal lobe more or less crescentic in dorsal (tergal) view, distomesal surface slightly concave. Fourth-instar larva (see Natvig 1948, Becker et al. 2010): setae 5,6-C usually with 2–4 branches, seta 6-C occasionally single; comb with 19–27 scales.

The female, male and fourth-instar larval stages of *Ae. nigrinus* and *Ae. sticticus* have been described, although not completely (Natvig 1948, Becker et al. 2003, 2010), but no attention has been given to the pupal stage of either species. The pupa of *Ae. nigrinus* remains unknown, but it is possible to distinguish the pupa of *Ae. sticticus* from other species included the key of Cranston et al. (1987) with the following modification of couplet 20 (measurements corrected and wording changed to reflect current usage of morphological terminology).

|		
20(18)	Paddle marginal spicules longer than 10 µm; seta 1-Pa single; paddle length usually greater than 0.85 mm; abdominal length greater than 3.5 mm ....***Ae. punctor***	
–	Paddle marginal spicules shorter than 10 µm; seta 1-Pa single or double; paddle length usually less than 0.85 mm; abdominal length less than 3.5 mm **20a**	
20a (20)	Seta 3-III branched; seta 1-Pa double..***Ae. dorsalis***	
–	Seta 3-III single; seta 1-Pa single...***Ae. sticticus***	
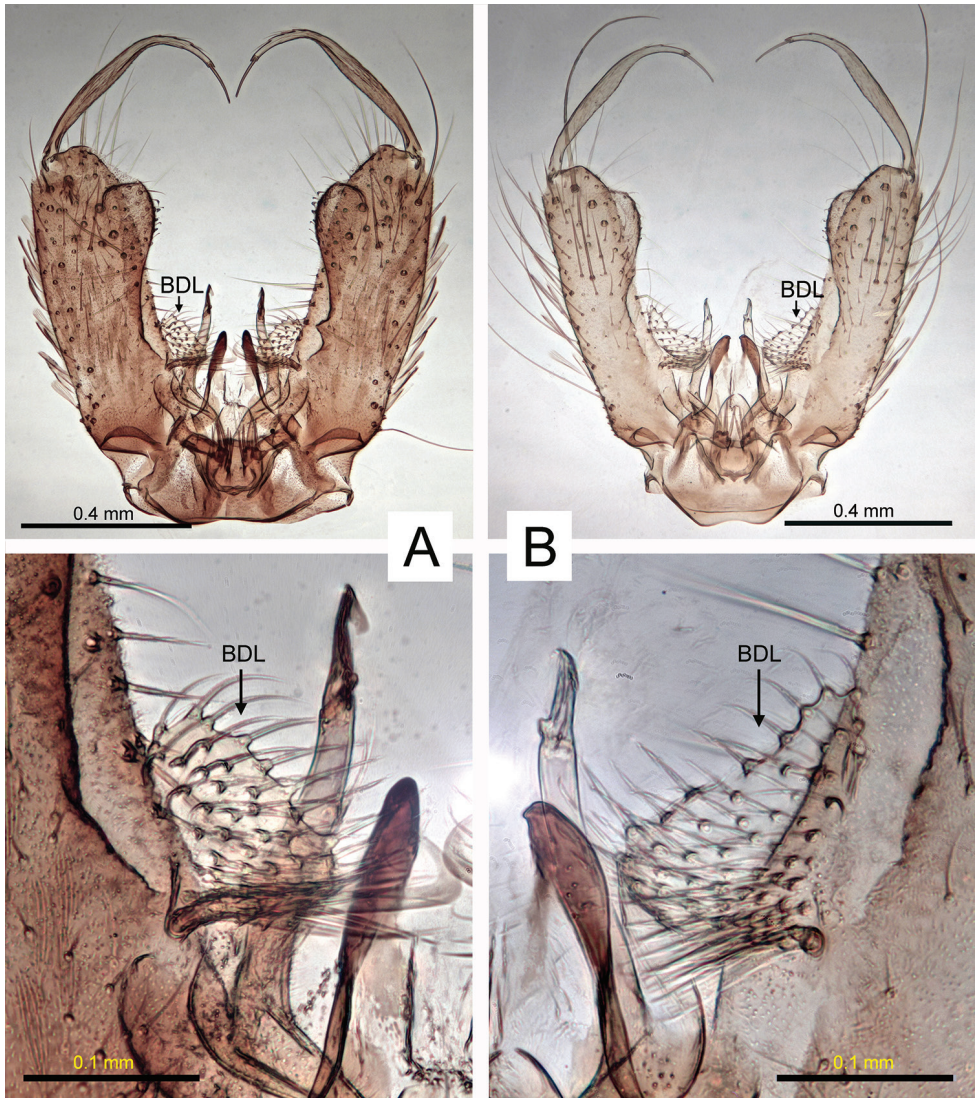
Figure 2. Doral aspects (pre-rotation sense) of the male genitalia of *Ae. nigrinus* (**A**) and *Ae. sticticus* (**B**), which are distinguished by the shape of the basal dorsomesal lobe (BDL).

Bionomics and distribution

Aedes nigrinus and *Ae. sticticus* were both originally described from localities in Germany (Knight and Stone 1977). As far as known, the distribution of *Ae. nigrinus* is limited to an area that extends from southern England (new record reported herein) and France to eastern Russia and from southern Scandinavia and Finland southward to Germany whereas *Ae. sticticus* is broadly distributed in northern areas of the Holarctic Region (Knight and Stone 1977, Becker et al. 2010). According to Cranston et al.

(1987), *Ae. sticticus* has a "patchy distribution" in Europe and "is rare in Britain". The few specimens present in the NHM collection lack basal pale bands with only lateral pale spots present. Such specimens, like most reared from larvae collected in Hurcott Wood, could be misidentified as *Ae. geniculatus* (Olivier, 1791) in the key of Cranston et al. (1987).

The occurrence of *Ae. sticticus* in Britain was first recorded by Marshall (1938), who listed the New Forest among other localities where the species had been collected. The New Forest record was later accepted without question by Cranston et al. (1987) and Snow (1990) and is the only record of the species in southern England (Snow et al. 1998). Since we now know that the New Forest record of Marshall refers to *Ae. nigrinus* (see above), the New Forest should not be listed as an occurrence record for *Ae. sticticus* until this species is definitely known to occur there.

The New Forest became a royal forest more than 950 years ago and is the largest remaining tract of unenclosed pasture land, heathland and forest in England. The land is dominated by gravel, sand and clay that was deposited during the Palaeogene Period of the Cenozoic Era (23.03–65.5 Mya). Many sites near the Beaulieu airfield where *Ae. nigrinus* was collected contain extensive areas of water-logged, marshy bogs and mires where the clay creates an impervious layer of saturated ground. The airfield was established during World War I, closed in 1919, re-opened again in 1942 and operated as an airfield for a further 15 years. Since 1959, the area has returned to an open heathland with open mireland habitat fringing the main airfield site.

Aedes sticticus is primarily associated with floodplains of rivers in forested areas (Cranston et al. 1987, Wood et al. 1979, Becker et al. 2010). In parts of Sweden, it contributes to a significant biting issue and is the subject of an extensive aerial mosquito control programme (Schäfer and Lundström 2009). In other parts of its range in central Europe, it also contributes to significant biting, along with *Aedes vexans* (Meigen, 1830), in floodwater areas along the Dyje River on the border of the Czech Republic and Austria, and is implicated in the transmission of Tahyna virus (Hubálek et al. 2010, Berec et al. 2014). Larvae of this species were found in a shallow floodwater pool in Hurcott Wood in early May and a few adults were collected in June in forest at Woodwalton Fen, Cambridgeshire. In contrast, *Ae. nigrinus* is mainly associated with floodwaters in more open terrain, such as meadows (Becker et al. 2010). Larvae of this species were found at the margins of small ponds in an open area of heath within the New Forest National Park in May, and a single adult male was collected in the same area in September.

Acknowledgements

References

Altschul SF, Gish W, Miller W, Myers EW, Lipman DJ (1990) Basic local alignment search tool. Journal of Molecular Biology 215: 403–410. https://doi.org/10.1016/S0022-2836(05)80360-2

Becker N, Petrić D, Zgomba M, Boase C, Dahl C, Lane J, Kaiser A (2003) Mosquitoes and their control. Kluwer Academic/Plenum Publishers, New York. xxi + 498 pp. https://doi.org/10.1007/978-1-4757-5897-9

Becker N, Petrić D, Zgomba M, Boase C, Madon M, Dahl C, Kaiser A (2010) Mosquitoes and their control. Second edition. Springer-Verlag, Berlin Heidelberg. xxx + 577 pp. https://doi.org/10.1007/978-3-540-92874-4

Berec L, Gelbič I, Šebesta O (2014) Worthy of their name: how floods drive outbreaks of two major floodwater mosquitoes (Diptera: Culicidae). Journal of Medical Entomology 51: 76–88. https://doi.org/10.1603/ME12255

Chan A, Chiang L-P, Hapuarachchi HC, Tan C-H, Pang S-C, Lee R, Lee K-S, Ng L-C, Lam-Phua S-G (2014) DNA barcoding: complementing morphological identification of mosquito species in Singapore. Parasites & Vectors 7: 569. https://doi.org/10.1186/s13071-014-0569-4

Cranston PS, Ramsdale CD, Snow KR, White GB (1987) Keys to the adults, male hypopygia, fourth-instar larvae and pupae of the British mosquitoes (Culicidae) with notes on their ecology and medical importance. Freshwater Biological Association Scientific Publication 48: 1–152.

Edwards FW (1932) Genera Insectorum. Diptera, Fam. Culicidae. Fascicle 194. Desmet-Verteneuil, Brussels. 258 pp. + 5 pls.

Harbach RE, Knight KL (1980) Taxonomists' glossary of mosquito anatomy. Plexus Publishing, Marlton, New Jersey. xi + 415 pp.

Harbach RE, Knight KL (1982) Corrections and additions to *Taxonomists' glossary of mosquito anatomy*. Mosquito Systematics (for 1981) 13: 201–217.

Hubálek Z, Rudolf I, Bakonyi T, Kazdová K, Halouzka J, Šebesta O, Šikutová S, Juřicová Z, Nowotny N (2010) Mosquito (Diptera: Culicidae) surveillance for arboviruses in an area endemic for West Nile (lineage Rabensburg) and Tăhyně viruses in central Europe. Journal of Medical Entomology 4: 466–472. https://doi.org/10.1093/jmedent/47.3.466

Knight KL, Stone A (1977) A catalog of the mosquitoes of the world (Diptera: Culicidae). Second edition. The Thomas Say Foundation. Volume VI. Entomological Society of America, College Park, Maryland. xi + 611 pp.

Kumar S, Stecher G, Tamura K (2016) MEGA7: Molecular evolutionary genetics analysis Version 7.0 for Bigger Datasets. Molecular Biology and Evolution 33: 1870–1874. https://doi.org/10.1093/molbev/msw054

Lang WE (1920) A handbook of British mosquitoes. London: Printed by order of the Trustees of the British Museum; sold by Longmans, Green & Co. vi[i] + 125 pp., 5 pls.

Linton Y-M, Lee AS, Curtis C (2005) Discovery of a third member of the Maculipennis Group in SW England. European Mosquito Bulletin 19: 5–9.

Marshall JF (1938) The British mosquitoes. Printed by order of the Trustees of the British Museum, London. xi + 341 pp., 20 pls.

Medlock JM, Vaux A GC (2009) *Aedes* (*Aedes*) *geminus* Peus (Diptera, Culicidae) – an addition to the British mosquito fauna. Dipterists Digest 16: 1–4.

Medlock JM, Vaux AGC, Cull B, Schaffner F, Gillingham E, Pfluger V, Leach S (2017) Detection of the invasive mosquito species *Aedes albopictus* in southern England. Lancet Infectious Diseases 17: 140. https://doi.org/10.1016/S1473-3099(17)30024-5

Natvig LR (1948) Contributions to the knowledge of the Danish and Fennoscandian mosquitoes: Culicini. Norsk Entomologisk Tidsskrift Suppl. 1: xxiii + 567 pp., 12 pls, 1 map.

Schäfer ML, Lundström JO (2009) The present distribution and predicted geographic expansion of the floodwater mosquito *Aedes sticticus* in Sweden. Journal of Vector Ecology 34: 141–147. https://doi.org/10.1111/j.1948-7134.2009.00017.x

Snow KR (1990) Mosquitoes. Naturalists' Handbooks 14. Richmond Publishing Co. Ltd, Slough, England. vi + 66 pp.

Snow KR, Tees AT, Bulbeck SJ (1998) A provisional atlas of the mosquitoes of Britain. University of East London. 50 pp.

Stephens JF (1825) Some observations on the British Tipulidae, together with descriptions of the species of *Culex* and *Anopheles* found in Britain. Zoological Journal 1: 448–457.

Stone A, Knight KL, Starcke H (1959) A synoptic catalog of the mosquitoes of the world (Diptera, Culicidae). The Thomas Say Foundation. Volume VI. Entomological Society of America, College Park, Maryland. vi + 358 pp.

Verrall GH (1901) A list of British Diptera. Second edition. The University Press, Cambridge. 47 pp. https://doi.org/10.5962/bhl.title.20297

Walton C, Somboon P, O'Loughlin SM, Zhang S, Harbach RE, Linton Y-M, Chen B, Nolan K, Duong S, Fong M-Y, Vythilingam I, Mohammed ZD, Ho DT, Butlin RK (2007) Genetic diversity and molecular identification of mosquito species in the *Anopheles maculatus* group using the ITS2 region of rDNA. Infection, Genetics and Evolution 7: 93–102. https://doi.org/10.1016/j.meegid.2006.05.001

Wood DM, Dang PT, Ellis RA (1979) The insects and arachnids of Canada. Part 6. The Mosquitoes of Canada. (Diptera: Culicidae). Canadian Government Publishing Centre, Supply and Services Canada, Hull, Quebec. 390 pp.

RESEARCH ARTICLE

New records and description of two new species of carideans shrimps from Bahía Santa María-La Reforma lagoon, Gulf of California, Mexico (Crustacea, Caridea, Alpheidae and Processidae)

José Salgado-Barragán[1], Manuel Ayón-Parente[2], Pilar Zamora-Tavares[2]

1 *Laboratorio de Invertebrados Bentónicos, Unidad Académica Mazatlán, Instituto de Ciencias del Mar y Limnología, Universidad Nacional Autónoma de México, México* **2** *Centro Universitario de Ciencias Agropecuarias, Universidad de Guadalajara, México*

Corresponding author: *José Salgado-Barragán* (salgado@ola.icmyl.unam.mx)

Citation: Salgado-Barragán J, Ayón-Parente M, Zamora-Tavares P (2017) New records and description of two new species of carideans shrimps from Bahía Santa María-La Reforma lagoon, Gulf of California, Mexico (Crustacea, Caridea, Alpheidae and Processidae). ZooKeys 671: 131–153. https://doi.org/10.3897/zookeys.671.9081

Abstract

Two new species of the family Alpheidae: *Alpheus margaritae* **sp. n.** and *Leptalpheus melendezensis* **sp. n.** are described from Santa María-La Reforma, coastal lagoon, SE Gulf of California. *Alpheus margaritae* **sp. n.** is closely related to *A. antepaenultimus* and *A. mazatlanicus* from the Eastern Pacific and to *A. chacei* from the Western Atlantic, but can be differentiated from these by a combination of characters, especially the morphology of the scaphocerite and the first pereopods. *Leptalpheus melendezensis* **sp. n.** resembles *L. mexicanus* but can be easily differentiated because *L. melendezensis* **sp. n.** has the anterior margin of the carapace broadly rounded and has only one spine on the mesial margin of ischium in the major cheliped, versus an acute rostrum and an unarmed major cheliped. Additionally, a phylogenetic analysis was used to explore the relationships of these two new taxa. These results show that *Alpheus margaritae* **sp. n.** and *Leptalpheus melendezensis* **sp. n.** are indeed related to the species against which we are comparing them, and demonstrate that they can be considered as different species. Additional specimens of *Leptalpheus* cf. *mexicanus*, *Ambidexter panamensis* and *A. swifti* are recorded for the first time in the Santa María-La Reforma coastal lagoon.

Keywords

Caridea, Crustacea, genetic analysis, Mexican Pacific, new species

Introduction

Caridea is the second most species-rich taxon amongst decapod crustaceans (De Grave and Fransen 2011) including approximately 3450 marine, brackish and freshwater living species. In the Eastern Tropical Pacific (ETP) this group is very well studied and it is the most diversified group of shrimps with a total of 204 species recorded in 2003 (Wicksten and Hendrickx 2003). Since then, at least 26 new species have been described in this region belonging to the genera *Alpheus* Fabricius, 1798 (Anker et al. 2007a; 2007b; 2009; Anker and Pachelle 2013; 2015; Bracken-Grissom and Felder 2014), *Bathystylodactylus* Hanamura & Takeda, 1996 (Wicksten and Martin 2004), *Glyphocrangon* A. Milne-Edwards, 1881 (Hendrickx 2010), *Leptalpheus* Williams, 1965 (Anker 2011; Salgado-Barragán et al. 2014; Anker and Lazarus 2015a), *Leslibetaeus* Anker, Poddoubtchenko & Wehrtmann, 2006 (Anker et al. 2006), *Lysmata* Risso, 1816 (Anker et al. 2009), *Ogyrides* Stebbing, 1914 (Ayón-Parente and Salgado-Barragán 2013), *Pontonia* Latreille, 1829 (Marin and Anker 2008), *Prionocrangon* Wood-Mason,1891 *in* Wood-Mason and Alcock 1891 (Hendrickx and Ayón-Parente 2012), *Salmoneus* Holthuis, 1955 (Anker and Lazarus 2015b), *Synalpheus* Spence Bate, 1888 (Hermoso and Alvarez 2005; Hermoso-Salazar and Hendrickx 2006), *Triacanthoneus* Anker, 2010 (Anker 2010) and *Typton* Costa, 1844 (Ayón-Parente et al. 2015). Despite the knowledge of caridean species recorded in the ETP, there remains a lack of knowledge about the biogeography, distribution and ecology of the group (Hendrickx and Wicksten 2011), particularly regarding infaunal and lagoon species.

The phylogenetic relationships of Alpheidae have been previously assessed in several studies (Knowlton et al. 1998; Williams et al. 2001; Mathews et al. 2002; Anker 2012; Anker et al. 2007; 2008a; 2008b; 2008c; Mathews and Anker 2009; Bracken-Grissom and Felder 2014; Bracken-Grissom et al. 2014). These studies have focused on the resolution of the relationships between species complexes within *Alpheus*. With regards to *Leptalpheus* species, there are no previous phylogenetic analyses. The application of molecular analyses has changed the way of describing and cataloging biological diversity. The use of these approaches has led to new inferences in the evolutionary dynamics of lineages and the role of morphological and genetic evolution (Mathews and Anker 2009).

The Santa María-La Reforma coastal lagoon is one of the largest coastal systems along the NW coast of Mexico. This coastal complex has been identified as one of the richest and most productive in the region, with great considerable importance for the shrimp and fish captures in the Gulf of California (Amezcua et al. 2006; Ruiz-Luna et al. 2010) and also as a support system for seabird populations, as it includes the largest breeding site of several species in Western Mexico (Castillo-Guerrero et al. 2014). Notwithstanding its importance, information about the carcinological fauna of this lagoon is limited and restricted to commercially harvested species (*Callinectes* spp. and penaeid shrimps) (Ruiz-Luna et al. 2010; Rodríguez-Domínguez et al. 2012).

A number of specimens of caridean shrimps were collected during surveys of infaunal invertebrates at several locations of the Bahía Santa María-La Reforma lagoon. After a detailed review of the specimens, we determined that they belong to five species of the

genus *Alpheus*, *Leptalpheus* and *Ambidexter* Manning & Chace, 1971. The morphological analysis of the organisms and DNA sequences obtained from two regions: 16S and COI helped us to confirm that two species are undescribed species, which are herein described and illustrated. *Alpheus margaritae* sp. n. is related to the *A. antepaenultimus* species complex in the Eastern Pacific and to *A. chacei* in the western Atlantic. On the other hand, *Leptalpheus melendezensis* sp. n. seems to be related to *L. forceps* and *L. mexicanus*. The other species comprise new distribution records in the Mexican Pacific.

Materials and methods

From June 2013 to March 2015, a series of surveys was carried out in Bahía Santa María-La Reforma lagoon (SE Gulf of California), in order to collect infaunal crustaceans. Collecting sites were characterized by mud, sand and sandy-mud bottoms with profuse burrow openings of mud shrimps identified as *Neotrypaea tabogensis* (Sakai, 2005), *Neotrypaea* sp., and *Callichirus* cf. *major* Stimpson, 1866. The organisms were collected using a yabby type suction pump operated at intertidal level (0–40 cm depth). Specimens were preserved in 75% alcohol and deposited in the Regional Collection of Marine Invertebrates, Instituto de Ciencias del Mar y Limnología, Universidad Nacional Autónoma de México, in Mazatlán, Sinaloa, Mexico (**EMU**). One male and one female paratypes of *A. margaritae* sp. n. were deposited in the Colección Nacional de Crustáceos, Instituto de Biología, Universidad Nacional Autónoma de México, Ciudad de México, Mexico (**CNCR**). Carapace length of all organisms (**CL**), in mm, was measured from the apex of the rostrum to the median posterior margin of carapace.

Total genomic DNA of alpheids from Bahía Santa María-La Reforma and from the Regional Collection of Marine Invertebrates was extracted from muscle tissue of the walking legs. DNA sequences were obtained from two regions, 16S and COI. The Internal Transcribed Spacer (ITS) sequences were used to estimate the phylogenetic relationships of *L. melendezensis* sp. n. and *L.* cf. *mexicanus* Ríos and Carvacho, 1983 and COI for *A. margaritae* sp. n. The ITS was amplified with the primers 16SH2 (5'-AGATAGAAACCAACCTGG-3') and 16Sar (5'-CGCCTGTTTATCAAAAACAT-3'), and the following thermal cycler conditions 10 min at 94 °C; annealing for 38–42 cycles: 1 min at 94 °C, 1 min at 45–48 °C, 2 min at 72 °C; final extension of 10 min at 72 °C. For the COI region we used the universal primers LCO1490 and HCOI 2198 (Folmer et al. 1994). The PCR took place in a final volume of 20 µL consisting of 12.1 µL of H_2O, 2 µL of reaction buffer, 0.8 µL of dNTPs, 0.5 µL of each primer, 0.5 µL of $MgCl_2$, 0.3 µL Platinum Taq, and 2 µL total DNA. The thermal cycler program was 95 °C for 2 minutes; followed by six cycles at 95 °C for 15 seconds, 45 °C for 15 seconds, 72 °C for 1 minute, then 30 cycles at 95 °C for 15 seconds, 48 °C for 15 seconds, 72 °C for 1 minute, and a final extension step of 72 °C for 3 minutes. The outgroup *Alpheopsis trigona* (Rathbun, 1901) and some sequences of the in-group, for the two regions, were obtained from GenBank (Table 1). Amplification products

Table 1. Sequence data of *Alpheus* and *Leptalpheus* species, voucher number, and Genbank accession.

	16S		COI				
Alpheopsis trigonus	EU868633[+]		AF309946*				
Alpheus antepaenultimus			AF309873*	AF309874*	AF309875*	AF309876*	AF308989*
Alpheus chacei	JX286606[¥]		AF309884*				
Alpheus cylindricus			AY344733*	AF309882*	AF309891*		
Alpheus colombiensis			AF309886*	AF309885*	AF308981*		
Alpheus estuariensis			AF309894*	AF309895*	AF309896*		
Alpheus floridanus			KP100633[§]	KP100634[§]	KP100635[§]		
Alpheus hephaestus			KP100629[§]	KP100630[§]	KP100631[§]		
Alpheus latus			AF309909*				
Alpheus lottini			AF309910*	KJ155615	KJ155539		
Alpheus panamensis			AF309923*				
Alpheus margaritae sp. n.	KY780077[£]	KY780078[£]	KY780079[£]	KY780080[£]			
Alpheus saxidomus			AF309934*	AF309935*			
Leptalpheus axianassae	EU868764[+]						
Leptalpheus corderoae	KY674509[£]						
Leptalpheus forceps	EU868763[+]						
Leptalpheus hendrickxi	KY674510[£]						
Leptalpheus melendezensis sp. n.	KY674512[£]		KY780076[£]				
Leptalpheus mexicanus	KY674511[£]						

Sequences authors: * Williams et al., 2001; [+] Bracken et al., 2009; [¥] Almeida et al., 2013; [§] Bracken-Grissom et al., 2014; [£] this study.

were purified with the enzyme Exosap IT at a volume of 1 μL per 10 μL amplified. These samples were sequenced with the TaqBigDye Terminator Cycle Sequencing kit (Perkin Elmer Applied Biosystems, Foster City, USA), purified with Illustra Autoseq G50 columns and visualized on a 310ABI DNA Sequencer (Perkin Elmer Applied Biosystems, Foster City, USA). The DNA sequences were edited with Chromas Pro 1.41 (McCarthy 1996-1998). Matrices with the DNA sequences for each of the regions were generated using PhyDE 0.9971 (Müller et al., 2011). DNA sequences were aligned using SEAVIEW 4 (Gouy and Gascuel, 2010) with the MUSCLE algorithm (Edgar 2004). Aligned sequences were analyzed using jModelTest 0.1.1 (Posada 2008) to obtain the best-fit nucleotide substitution models to the data, based on the Akaike Information Criterion (Posada and Crandall 1998). Molecular data were analyzed using maximum likelihood (ML) in RAxML 7.0.0 (Stamatakis et al. 2006) using the CIPRES platform, which has the advantage of reducing the execution time of the analysis (Miller et al. 2010). The ML tree was obtained and to assess nodal support a resampling of 1,000 rapid bootstrap inferences was done.

Systematic account

Family Alpheidae Rafinesque, 1815
Genus *Alpheus* Fabricius, 1798

***Alpheus margaritae* sp. n.**
http://zoobank.org/6956A091-E7C7-4313-975F-5DC82A4CC409
Figs 1–5

Material examined. Holotype: Male (CL 4.6 mm), Costa Azul Island, Santa María-La Reforma, Sinaloa, Mexico, 25°5'56"N, 108°7'58"W, 0.1–0.3 m, mudflat with gravel at neap tide, March 30, 2015, (EMU- 10580). Paratypes: all same locality and data as holotype, 5 females (CL 3.0–5.7), 2 ovigerous females (CL 4.3–5.6 mm), 1 juvenile (CL 2.3 mm), (EMU-10581); paratypes, same locality and data as holotype, 1 male (CL 6.5 mm), 1 ovigerous female (CL 5.8 mm), (CNCR 32595).

Diagnosis. Ocular hoods unarmed. Antepenultimate segment of third maxilliped broad. Scaphocerite with concave lateral margins, distolateral tooth overreaching the distal margin of the inner blade, inner blade almost reaching the distal end of antennular peduncle. Major cheliped markedly compressed, with grooves on both dorsal and ventral margins. Pereopods 3–5 with dactylus subspatulate; ischium of third and fourth pereopods with ventral spine.

Description. *Carapace* glabrous (Fig. 2A, B), rostrum triangular, sharp, exceeding anterior margin of ocular hood, reaching 0.33 of visible portion of first antennular segment; rostral carina low and narrow, barely overpassing posterior end of eye; orbital hoods inflated dorsally and produced anteriorly, anterior margin convex, unarmed; orbitorostral groove shallow; pterygostomial margin slightly produced anteriorly below basis of basicerite. First antennular segment (Fig. 2A, B, E) bearing subtriangular carina on ventromesial margin, posterior margin of ventromesial carina convex, anterior margin concave, ventral margin with acute tip, directed anteriorly; second antennular segment approximately 2.0 times as long as wide, 1.5 times length of visible part of first segment, and 3.0 times as long as third segment; stylocerite almost reaching distal margin of first segment.

Antenna (Fig. 2A, B) with lateral margin of scaphocerite slightly concave; distolateral tooth reaching distal end of antennular peduncle; inner blade falling short of tip of distolateral tooth; cleft between inner blade and distolateral tooth arising from approximately 0.25 of scaphocerite; carpocerite overpassing distal end of antennular peduncle by 0.4 length of third antennular segment; basicerite with acute lateral tooth.

Third maxilliped (Fig. 2C, D) reaching distal margin of carpocerite; last segment tapering distally, mesial surface setose, almost twice as long as penultimate segment; penultimate segment approximately twice as long as broad; antepenultimate segment fairly enlarged and flattened, approximately 2.6 times as long as broad, longer than the sum of preceding two segments; lateral surface smooth, mesial surface with sinuous

Figure 1. *Alpheus margaritae* sp. n. Female paratype from Isla Costa Azul, Santa María-La Reforma costal lagoon, Sinaloa, Mexico (EMU-10581), lateral view, color in life.

carina bearing long setae; exopod falling near to median part of penultimate segment in holotype and two female paratypes, shorter than penultimate segment in males and the rest of females; precoxa with one arthrobranch near distal end and small supplementary arthrobranch near proximal end.

Major cheliped of first pereopods (Fig. 3A–D) narrow, 2.4 times as long as broad and with trace of fine granules at anterior half; fingers clearly narrower than palm, occupying the distal 0.4 of chela (0.35 in juveniles); movable finger with superior margin slightly arched at proximal two thirds and then right angled, tip narrow and acute; pollex acute at tip, inferior margin almost straight along proximal two thirds and convex along distal third; palm with superior and inferior transverse grooves; superior transverse groove broad and low, continuing to shallow elongated triangular depression on mesial face and continuing to shallow broad rectangular depression on lateral face; mesial superior depression continuing to proximal portion of palm; lateral superior depression continuing to linea impressa; linea impressa continuing with mesial upper longitudinal depression; inferior transverse groove fairly deep and broad with proximal shoulder slightly projecting, connecting to inverse V-shaped inferior lateral palmar depression; lateral palmar face with shallow depression below superior palmar depression and behind inferior palmar depression, and with median depression between the above two depressions and continuing to below proximal portion of dactylus; mesial palmar surface with elongate depression near inferior margin; a slightly depressed area between upper and lower longitudinal depressions and lower areas between and in front of upper and inferior transverse grooves; ventromesial margin of merus with trace of fine granules, bearing two minute movable teeth at proximal half, unarmed distal end; ventral surface with trace of fine granules in largest specimens.

Figure 2. *Alpheus margaritae* sp. n. Paratype male, CL 6.5 mm (**D, H, I**), (CNCR 32595), Female paratype, CL 7.4 mm (**A–C, E–G**) (EMU-10581); **A** anterior portion of carapace and cephalic appendages, dorsal view **B** same in lateral view (setae omitted) **C, D** third maxilliped **E** antennular carina **F** abdomen, lateral view (setae omitted) **G** telson and uropods, dorsal view (setae partially omitted) **H** second pleopod **I** detail of appendices interna and masculina. Scale bars: **A–D, F–H** 1 mm; **E, I** 0.2 mm
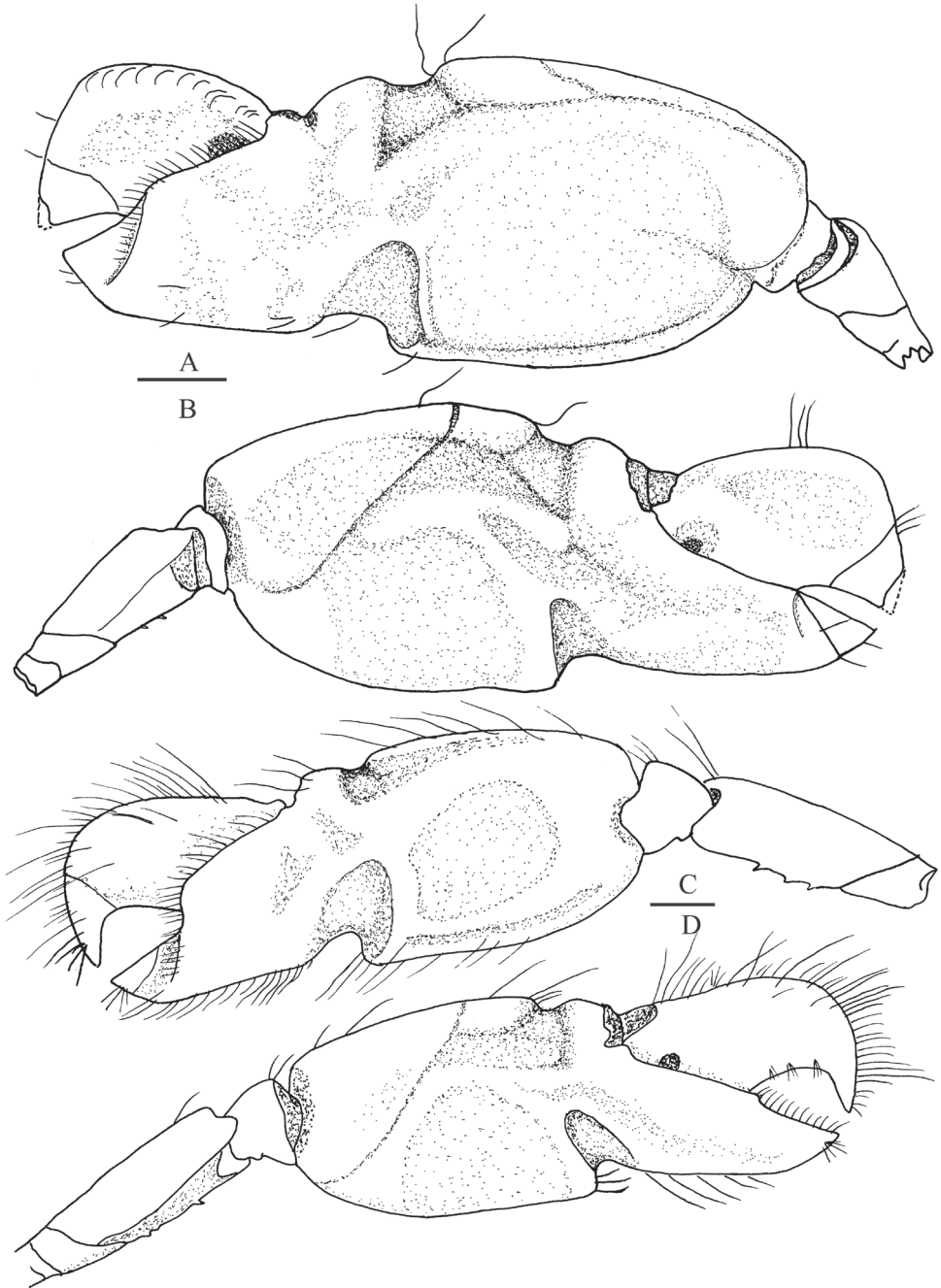
Figure 3. *Alpheus margaritae* sp. n. Female paratype, CL 7.4 mm (**A, B**) (EMU-10581); male paratype, CL 6.5 mm (**C, D**), (CNCR 32595); **A, C** major first pereopod, mesial view **B, D** same, lateral view. Scale bars 1 mm.
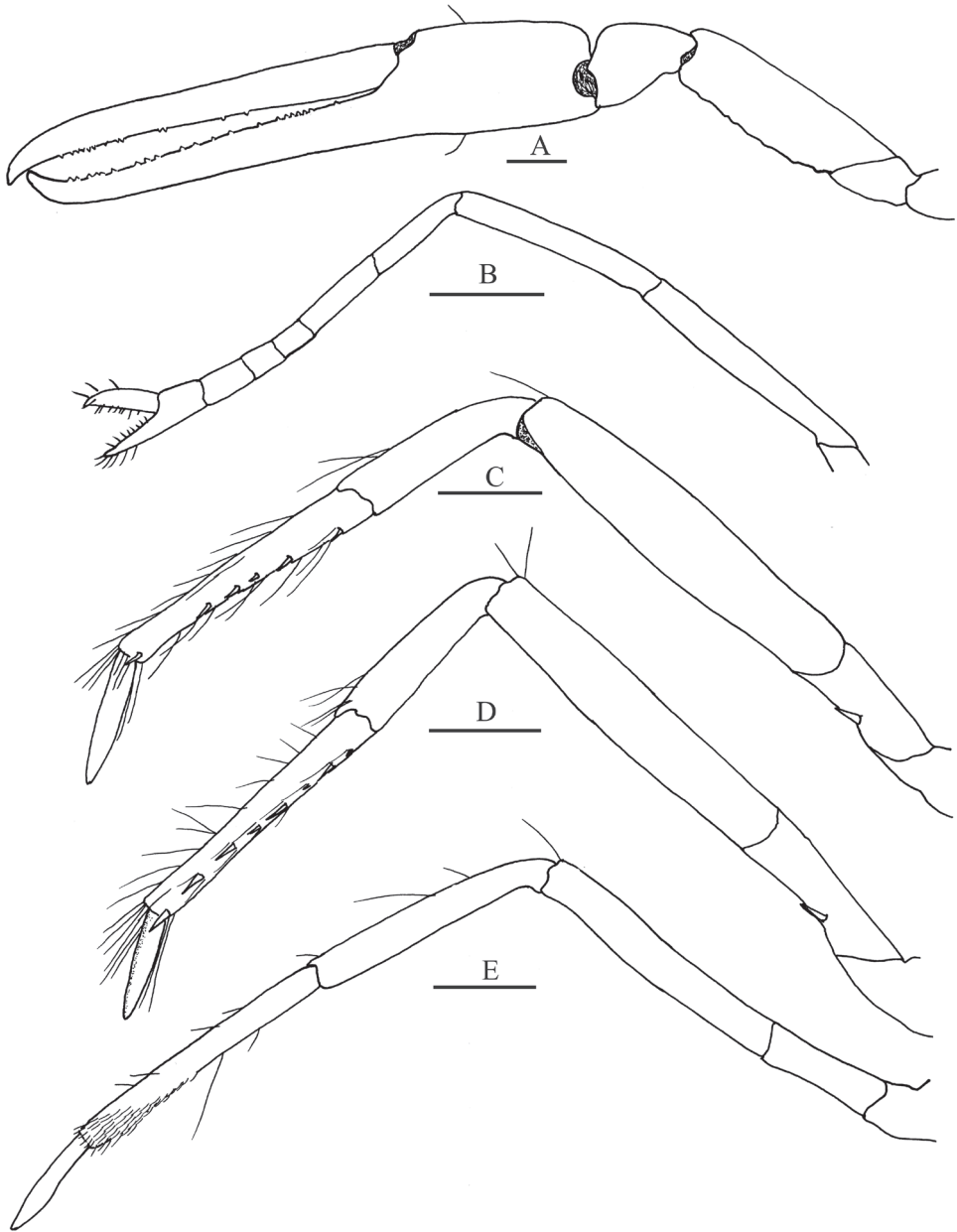
Figure 4. *Alpheus margaritae* sp. n. Female paratype, CL 7.4 mm, (EMU-10581); **A** minor first pereopod, mesial view **B** left second pereopod, lateral view **C** left third pereopod, lateral view **D** left fourth pereopod, lateral view **E** left fifth pereopod, lateral view. Scale bars 1 mm.

Minor chela of first pereopods (Fig. 4A) elongate, 5.6 times as long as broad, with trace of fine granules inferiorly; fingers occupying 0.7 of chela; cutting edges barely serrated, subparallel when closed, apex deflexed inward; movable finger longer than immovable finger in most specimens; tips of fingers blunt to acute. Palm lacking sculpturing, with trace of fine granules on mesial face, swollen laterally and thicker than fingers. Merus with ventromesial margin bearing short setae, with two small movable teeth at proximal half.

Second pereopod (Fig. 4B) reaching distal end of carpocerite beyond distal end of first segment of carpus. Chela shorter than the sum of three distal segments of carpus. Fingers of chela 1.4 times as long as palm. First segment of carpus 1.4 times as long as second; second segment 2.6 times as long as third; fourth segment almost as long as third; fifth segment 1.7 times as long as fourth.

Dactylus of *third pereopod* (Fig. 4C) subspatulate, 0.5 times as long as propodus; propodus 1.4 times as long as carpus, with inferior margin bearing six small spines along its extension. Merus 5.6 times as long as broad and 1.8 times as long as carpus; ischium with ventral spine.

Fourth pereopod (Fig. 4D) similar to third pereopod; ischium with ventral spine.

Ischium of fifth pereopod (Fig. 4E) unarmed; propodus setose distally, setae increasing in number distally; dactylus subspatulate.

Pleura of first to fourth abdominal somites rounded ventrally, not overlapping each other much on ventral regions, that of fifth somite subtriangular on posterior ventral margin (Fig. 2F). Abdominal sternite unarmed at midline. Appendix masculina (Fig. 2H, I) slightly shorter than appendix interna.

Telson (Fig. 2G) Approximately 1.5 times as long as broad at anterior end, armed with two pairs of dorsal spines and low longitudinal median depression on dorsal surface; posterior margin very convex, with two pairs of postero-lateral spines, inner spine stronger, twice as long as outer. Uropodal endopod with fairly distinct mesial depression at anterior half; uropodal exopod bearing movable spine outside of transverse suture, movable spine flanked laterally by short immovable tooth and internally by round lobe; suture forming almost two straight lobes.

Habitat. Soft mud with gravel composed of shells and rocks, in intertidal.

Color in life. Creamy-white with irregular sparse olive green to light brown patches on dorsal surface of carapace, abdomen and telson; uropodal endopodite and distal lobe of exopodite olive green to light brown, proximal lobe of exopodite creamy-white; patches on abdominal plates tend to be more dense towards the rear; first pereopod olive green. No clear differences were observed between sexes (Fig. 1).

Distribution. Only known from Bahía Santa María-La Reforma coastal lagoon, Sinaloa, Mexico.

Etymology. The species is named after Dr. Margarita Hermoso Salazar in recognition of her contributions to the knowledge of Mexican carideans.

Variations. Body structures in *Alpheus margaritae* sp. n. are similar between sexes; sculpture in major cheliped becomes deeper in larger specimens. Disparities among the specimens are:

In nine of the twelve specimens the antepenultimate segment of the third maxilliped is approximately 2.5 times as long as broad, with a sinuous carina on the inner surface bearing long setae and the exopod not reaching the distal end of the antepenultimate segment (Fig. 2D), in three females the shape of that appendage is quite different; the antepenultimate segment of the third maxilliped is slender, without a well-defined inner carina and sparse long setae; the exopod is longer, reaching the middle of the penultimate segment (Fig. 2C); all specimens, with exception of the largest female, bear two spines on proximal half of inferior inner margin of merus of both major and minor chelae and no distal spines are present. In the largest female those proximal spines are absent, although there are some marks in the place where the spines should be located, that likely indicates that spines were lost; relative length of fingers in minor first pereopod increases with the size of the specimens; ranging from 64% in the smallest juvenile to 72% in one of the largest females, with exception of one female (CL = 5.0 mm) whose fingers occupied only 45% of minor chela length. The latter chela does not seem to be damaged and does not appear to represents a case of regeneration.

Remarks. *Alpheus margaritae* sp. n. is morphologically similar to *A. antepaenultimus*, *A. mazatlanicus*, and *A. chacei*. These species share the absence of teeth on the ocular hoods, the antepenultimate segment of the third maxilliped being broad, the major cheliped markedly compressed with grooves on both dorsal and ventral margins, and pereopods 3–5 with subspatulate dactylus.

The new species and *A. antepaenultimus* have the inferior inner margin of merus with spines, while in *A. chacei* the merus lacks these spines. *Alpheus margaritae* sp. n. can be differentiated from *A. antepaenultimus* as in the former the scaphocerite has concave lateral margins, the distolateral tooth overreaches the distal margin of the inner blade, and the inner blade almost reaches the distal end of the antennular peduncle, whereas in *A. antepaenultimus* the lateral margins of the scaphocerite are almost straight, the distal spine almost reaches the distal margin of the inner blade, and the inner blade overpasses the distal end of antennular peduncle. In large specimens of the new species (CL > 5.0 mm) the superior transverse groove of the major cheliped is deeper and the sculpture is more conspicuous than in *A. antepaenultimus*. The proximodorsal margin of the movable finger of *A. margaritae* sp. n. is almost straight and the tip is narrow and acute, while in *A. antepaenultimus* the dorsal margin of the movable finger is arched along all its longitude and bluntly rounded at tip. Also, the number of spines on inferior inner margin of merus of major first pereopods in *A. antepaenultimus* is greater than in the new species (3 or 4 vs. 1 or 2).

Alpheus margaritae sp. n. can be differentiated from *A. mazatlanicus* as in the new species the second antennular segment is proportionally much shorter than wide (2 times vs. 4 times) and the lateral margin of the scaphocerite is slightly concave instead of straight; *A. margaritae* has a hook-like carina on the ventromesial face of the first article of antennular peduncle whereas in *A. mazatlanicus* this carina is broadly triangular; besides, *A. margaritae* has the inner margin of merus of the first pereopod with movable spines on proximal half while in *A. mazatlanicus* such spines are absent; and the ratio of the fingers in relation to the palm in the minor chela is shorter (60%) in *A. mazatlanicus* than in the new species (approximately 70%).
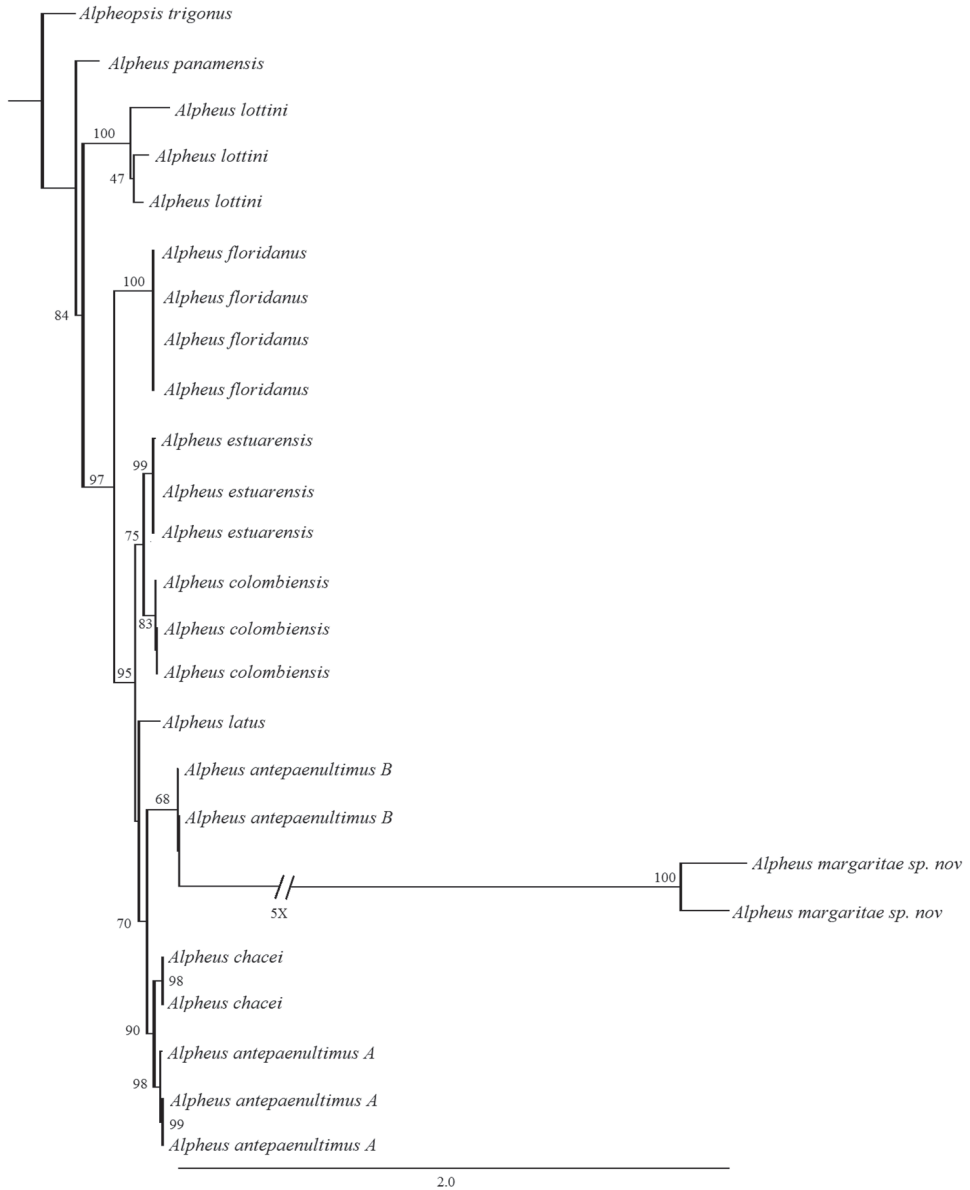
Figure 5. ML tree for *Alpheus* COI sequences. Numbers above each branch are MP bootstrap values. GeneBank accession numbers of *Alpheus chacei*, *A. antepaenultimus* A and *A. antepaenultimus* B as in Williams et al. (2001).

Alpheus margaritae is more related to *A. antepaenultimus* B. The latter is part of a species complex from the Eastern Pacific which include *A. floridanus* specimens from Eastern Pacific sensu Williams et al. 2001 and *A. hephaesthus* (Braken-Grissom et al. 2014). *A. antepaenultimus* A, *A. antepaenultimus* B, and *A. chacei* form a clade

consistent with the morphological traits previously described. This clade could be the result of an ecological radiation, probably associated to the species flexibility to inhabit in tropical and subtropical conditions (Williams et al. 2001). The position of *A. margaritae* within the *A. antepaenultimus* complex suggests that this group of species, and probably *A. mazatlanicus,* could have been subject to such ecological radiation.

Phylogenetics relationships. The COI matrix of *Alpheus* molecular data consisted of 668 characters. The ML phylogenetic hypothesis shows that *Alpheus margaritae* sp. n. is more related to *A. antepaenultimus* B with a bootstrap support of 63. On the other hand, *A. margaritae* sp. n. shows an important mutational distance that differentiates it from *A. antepaenultimus* B. This pair of species is grouped together in the clade formed by *A. chacei* and *A. antepaenultimus* (Fig. 5). COI matrix of *Alpheus* shows that *A. margaritae* sp. n. belongs to the species complex formed by *A. antepaenultimus* A, B, and *A. chacei*. This complex corresponds to the mangrove group (type a) of the clade I proposed by Williams et al. (2001). The *A. antepaenultimus* complex is characterized by the combination of: 1) the absence of spines on the occular hoods, 2) the antepenultimate segment of the third maxilliped is broadened, 3) major cheliped compressed, with transverse groove on superior and inferior margins proximal to fingers, 4) immovable finger of minor chela never balaeniceps, and fingers occupying more than 0.6 of chela, 5) pereopod 3-5 with subspatulate dactylus, 6) ischium of pereopods 3-4 with spine on the ischium, 7) uropodal spines not colored.

Genus *Leptalpheus* Williams, 1965

Leptalpheus melendezensis sp. n.
http://zoobank.org/2DE36886-5588-43C2-B031-10FD45C1EEBA
Figs 6–9

Material examined. Holotype: Male (CL 4.1 mm), Meléndez Island, Santa María-La Reforma, Sinaloa, Mexico, 24°48'07"N, 108°03'22.3"W, sand, 0.2 m at low tide, January 18, 2015, (EMU-10582). Paratype: 1 male (CL 2.9 mm), same data as holotype, (EMU-10583).

Diagnosis. Frontal margin of carapace broadly rounded, weakly produced, without dorsal crests. Antenna with carpocerite longer than scaphocerite, slightly shorter than antennular peduncle. Major cheliped slender; ischium armed with strong ventromesial spine directed upward; fingers slightly twisted laterally, not gaping when closed; without adhesive discs; dactylus with strong proximal tooth on cutting edge, tip acute, crossing distally with tip of pollex; propodus of pereopods 3 and 4 with two ventral spines; propodus of fifth pereopod with two distal rows of setae on ventral margin.

Description. Frontal margin of *carapace* (Fig. 6A) broadly rounded, obtuse, weakly produced, carapace smooth, without dorsal crests or carina; eyestalks with anteromesial margin rounded.
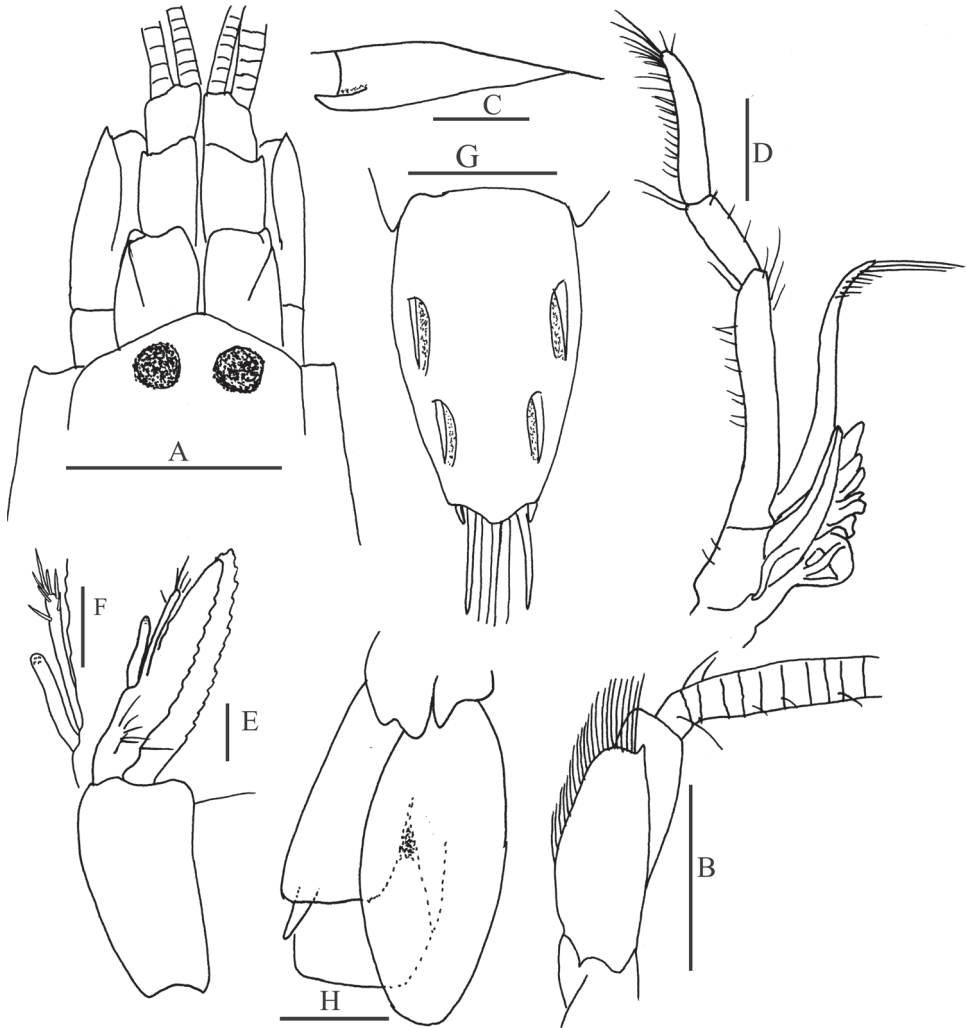
Figure 6. *Leptalpheus melendezensis* sp. n. Holotype male, CL 4.1 mm (EMU10582); **A** anterior portion of carapace and cephalic appendages, dorsal view **B** right antenna, lateral view **C** tooth on ventromesial carina of first segment of antennular peduncle, mesial view **D** third maxilliped **E** second pleopod **F** detail of masculina and internal appendix **G** telson, dorsal view **H** left uropod, dorsal view. Scale bars **A, B** 1 mm; **C, E** 0.2 mm; **D, G, H** 0.5 mm.

Antennular peduncles (Fig. 6A) moderately stout, flattened dorsoventrally; second article longer than broad; stylocerite appressed, not reaching distal margin of first article of the antennular peduncle; ventromesial carina (Fig. 6C) terminating in an upward curving tooth projected beyond the carina; lateral flagellum with two articles.

Antenna (Fig. 6B) with stout basicerite bearing strong distoventral tooth. Scaphocerite (Fig. 6A, B) ovate, with acute distolateral tooth reaching beyond the anterior
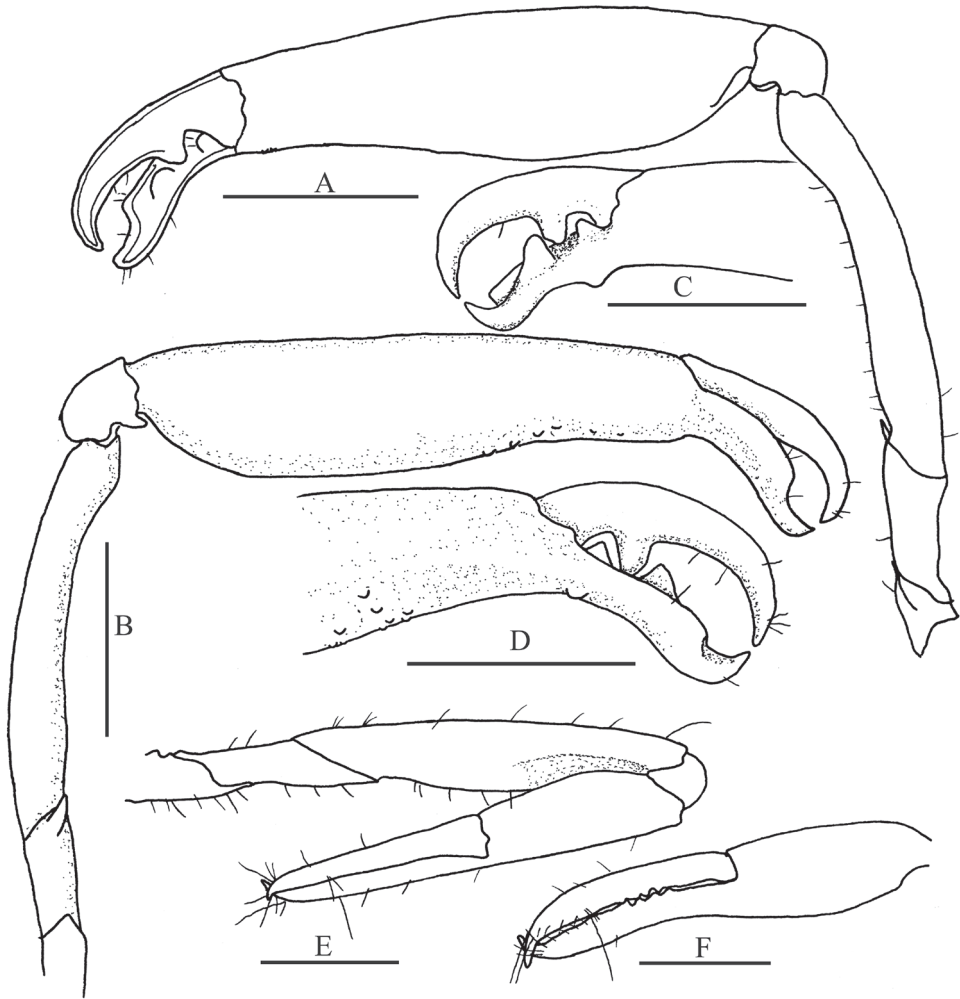
Figure 7. *Leptalpheus melendezensis* sp. n. Holotype male, CL 4.1 mm (EMU-10582); **A** major first pereopod, outer view **B** same, inner view **C** detail of distal portion of same cheliped, outer view **D** same, inner view **E** minor first pereopod, outer view **F** detail of same cheliped, outer view. Scale bars **A, B** 1 mm; **C–F** 0.5 mm.

margin of blade, blade with mesial margin curved; carpocerite longer than scaphocerite, slightly shorter than antennular peduncle.

Mouthparts not dissected, typical for genus in external view. Third maxilliped (Fig. 6D) with lateral plate on coxa produced upward, not reaching the distal margin of the branchiae; ultimate article with rows of brush-like setae increasing in size distally; exopod longer than first article.

Major cheliped (Fig. 7A–D) slender; ischium armed with strong ventromesial spine directed upward; merus slender, with concave depression along ventral margin, ventral
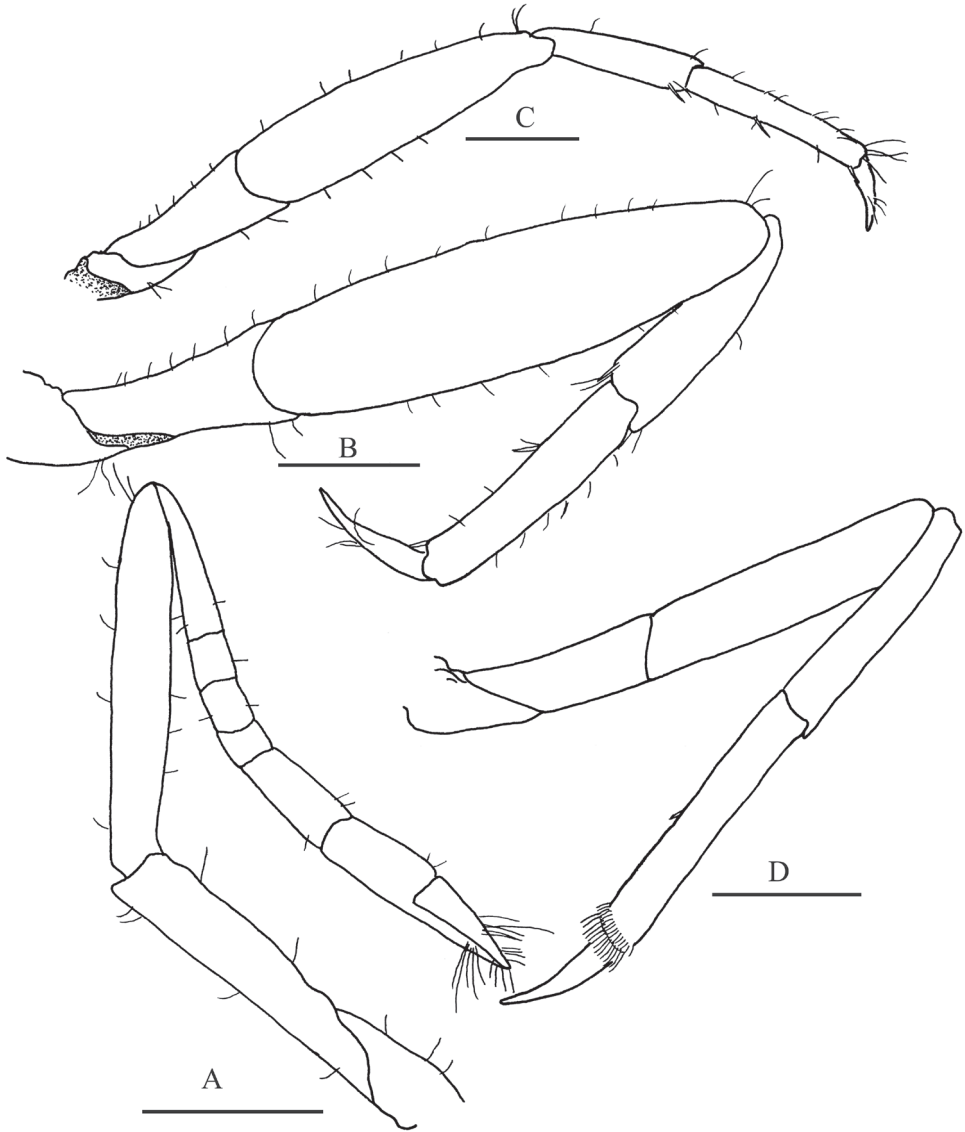
Figure 8. *Leptalpheus melendezensis* sp. n. Holotype male, CL 4.1 mm (EMU-10582); **A** second pereopod, lateral view **B** third pereopod, lateral view **C** fourth pereopod, lateral view **D** fifth pereopod, lateral view. Scale bar 0.5 mm.

margin minutely granulated; carpus short, cup-shaped, dorsally convex, with two distoventral processes, the external blunt and the mesial tooth-like; chela robust, longer than merus; palm 2.5 times as long as fingers, ventrally depressed, narrowing distally, ventral margin with sparse tubercles, dorsal margin smooth; without adhesive discs; fingers slightly twisted laterally, not gaping when closed; pollex with proximal half

ventrally deflexed, outer cutting edge (Fig. 7C) armed with two teeth, distal stronger, mesial margin with proximoventral low tubercle and a shallowly excavated projection along proximal two thirds, tip acute, directed upward; dactylus noticeably curved, dorsum smooth, cutting edge with strong proximal tooth, tip acute, crossing distally with tip of pollex.

Minor cheliped (Fig. 7E, F) with segments unarmed; merus almost as long as chela; carpus short; fingers pointing, slightly longer than palm, median portion of cutting edges armed with 4–5 small, irregularly spaced teeth, tips crossing distally.

Second pereopod (Fig. 8A) unarmed; ischium 0.75 as long as merus; merus shorter than carpus; carpus 5-articulated, articles ratio from proximal to distal approximately 6:2:2:1:4; distal portion of chela with long setae.

Third and fourth pereopods (Fig. 8B, C) similar, compressed; third pereopod slightly longer and stouter than fourth, merus slightly longer than combined length of carpus and propodus, ventrodistal margin of carpus with ventrodistal spine, propodus with 2 spines on median and distal ventral margin and sparse long setae along margins; dactylus curve, slender, acute distally, nearly half as long as propodus.

Fifth pereopod (Fig. 8D) slender, not compressed, ventral margin of propodus with 1 median spiniform seta and distal margin with two rows of setae, distalmost larger; dactylus acute, curved.

Male second pleopod (Fig. 6E) with slender appendix masculina, with two subterminal and four terminal setae; appendix interna 0.75 length of appendix masculina (Fig. 6F).

Telson (Fig. 6G) widest in proximal third, slightly tapering distally, dorsal surface with two pairs of strong spines inserted in deep pits close to lateral margins, posterior margin rounded, with two pairs of spiniform setae at posterolateral angles, lateral one much shorter than mesial one, posterior margin with 4 plumose setae.

Uropod (Fig. 6H) with lateral lobe of protopod ending in two small lobes; exopod with posterodistal margin straight, deeply incised, with a large spine near mesial margin.

Habitat. Sandy beach, associated with burrows of *N. tabogensis*.

Distribution. Known only from Meléndez Island, Bahía Santa María-La Reforma, Sinaloa, Mexico.

Etymology. The name of the species is derived from Meléndez Island, the type locality.

Remarks. *Leptalpheus melendezensis* sp. n. seemed to be related to *L. mexicanus* because the general plan of major cheliped of both species is similar; they both have a curved, slender merus, short carpus and ventrally depressed manus, narrowing distally, with sparse ventral tubercles and convex dactylus with a strong proximal tooth. However, a detailed analysis reveals differences between the species. The ischium of the major cheliped in *L. melendezensis* sp. n. bears a noticeable ventromesial spine, while in *L. mexicanus* it is absent; pollex and dactylus of the major cheliped do not gape in the new species but form a wide open gape in *L. mexicanus*; the pollex of the major cheliped in *L. mexicanus* is ventrally convex and spoon-shaped at distal end, whereas in the new species it is ventrally concave, with a lateral projection along proximal two
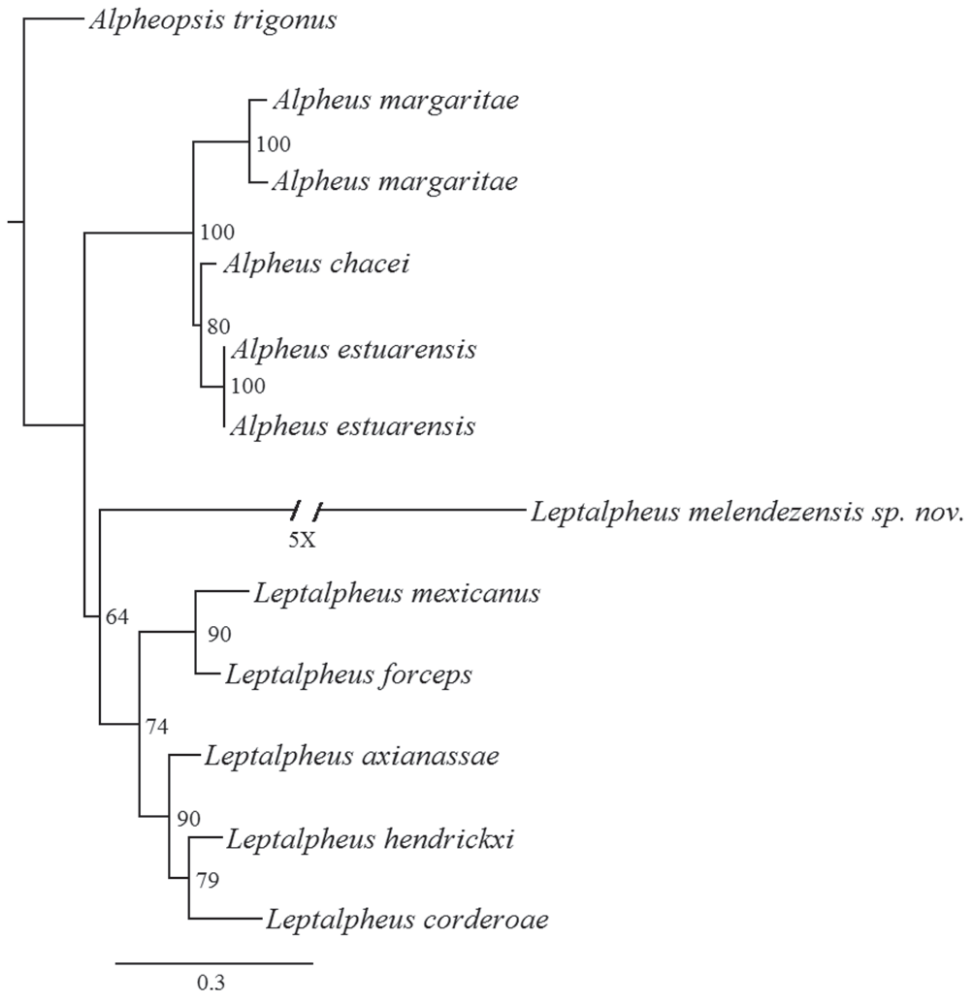
Figure 9. ML tree for *Leptalpheus* 16S sequences. Numbers in the nodes are 1000 bootstrap iterations result values.

thirds and acute at its distal end. Other differences are that the carapace of *L. mexicanus* has an acute, carinate triangular rostrum and two small orbital crests above the eyes, whereas in *L. melendezensis* sp. n. the carapace has a blunt, scarcely projected rostrum without a median carina and without supraocular crests; the tooth on the antennular ventromesial carina is more anteriorly projected in the new species; the propodus of pereopods 3 and 4 of *L. melendezensis* sp. n. bears only two ventral spines as opposed to three in *L. mexicanus*; and the fifth pereopod has two distal rows of setae instead of four as in *L. mexicanus.*

Leptalpheus melendezensis sp. n. is the eighth species assigned to the genus in the eastern Pacific and the fourth recorded from the Pacific coasts of Mexico, and is the

only eastern Pacific species of *Leptalpheus* that presents a major cheliped without adhesive disks and isquium armed with a ventromesial spine.

Phylogenetic relationships. The 16S matrix of *Leptalpheus* molecular data consisted of 688 characters. This relationship had a bootstrap support of 64 (Fig. 9). Also an insertion of five base pairs (TATTT) was identified which was not found in other *Leptalpheus* sequences.

The phylogenetic analysis presented here is a partial contribution to establish a phylogeny of the genus due to the almost total absence of genetic information from other species described in previous works, however this approach and morphological analysis provide sufficient information to recognize that *L. melendezensis* represent a species new to science.

Leptalpheus cf. *mexicanus* Ríos and Carvacho, 1983

Material examined. Two males (CL 3.4 and 3.7 mm) and 4 ovigerous females (CL 2.9–3.6 mm), SE Talchichilte Island, Bahía Santa María-La Reforma, Sinaloa, Mexico, 24°50'5.71"N, 108°03'4.23"W, muddy sand, 0.2 m at low tide, October 5, 2014, (EMU-10584).

Habitat. Previous work and this study agree that this species appears to be associated with mangrove forest (Ríos and Carvacho 1983; Salgado-Barragán et al. 2014). In Santa María-La Reforma, the species was collected in muddy sand, associated with burrows of *N. tabogensis*, near mangrove forest

Distribution. Estero Mulegé, Baja California Sur (type locality), Bahía Santa María-La Reforma and Mazatlán, Sinaloa, and Manzanillo, Colima, Mexico, to Bahía Málaga, Colombia (Salgado-Barragán et al. 2014; present study).

Remarks. We could only observe very small crests on carapace of the two males, which were absent in all females. In our opinion, the presence of these structures could be related to the size of the specimens. Specimens of *L.* cf. *mexicanus* and *L. melendezensis* sp. n. were collected in *N. tabogensis* burrows, but *L.* cf. *mexicanus* was found in muddy sand substrata, whereas the new species was found in a beach of fine sand.

Family Processidae Ortmann, 1896
Genus *Ambidexter* Manning & Chace, 1971

Ambidexter panamensis Abele, 1972

Material examined. 1 female (CL 3.7 mm), 1 ovigerous female (CL 4.2 mm), Garrapata Island, 25°9'13"N, 108°15'25"W, silty sand, 0–0.2 m at low tide, June 25, 2013, (EMU-10585A); 2 females (CL 3.9 mm) and 2 ovigerous females (CL 5.2–5.3 mm), same locality, January 29, 2014, (EMU-10585B); 2 females (CL 3.5–3.6 mm) and 1 ovigerous female (CL 3.9 mm), same locality, March 30, 2015, (EMU-10585C); 1 male

(CL 4.5 mm), Talchichilte Island, Sta. 1, 25°1'15"N, 108°7'6"W, silty sand, 0.1–0.3 m at low tide, January 18, 2015, (EMU-10585D); 1 female (CL 3.2 mm) and 2 ovigerous females (CL 3.5–3.9 mm), Sta. 2, (24°56'36"N, 108°2'54"W), mud-sand, 0.1–0.3 m at low tide, October 05, 2014, (EMU-10585E); 1 male (CL 3.3 mm), same locality, January 18, 2015, (EMU-10585F); 1 male (CL 3.6 mm) and 1 ovigerous female (CL 4.8 mm), 24°44'46"N, 107°59'41"W, mud-sand with gravel, 0.1–0.3 m at neap tide, January 18, 2015, (EMU-10585G); 1 female (CL 2.7 mm) and 1 ovigerous female (CL 4.2 mm), Saliaca Island, 25°8'55"N, 108°16'13"W, sand, 0.1–0.3 m at neap tide, March 30, 2015, (EMU-10585H); 4 ovigerous females (CL 4.7–5.6 mm), Meléndez Island 24°48'6"N, 108°3'21"W, sand, 0.1–0.3 m at neap tide, January 18, 2015, (EMU-10585I); 1 female (CL 3.4 mm) and 2 ovigerous females (CL 4.8–5.1 mm), Costa Azul Island, 25°5'56"N, 108°7'58"W, mud with gravel, 0.1–0.3 m at neap tide, March 30, 2015, (EMU-10585J).

Distribution. Recorded from San Diego, California, and Gulf of California to Naos Island, Panama and Galapagos Islands (Wicksten and Hendrickx 2003)

Remarks. According to Abele (1972), specimens of *A. panamensis* commonly inhabit sandy-muddy substrates with burrows of larger invertebrates. In the type locality, one specimen was found in the tube of a polychaete worm, but other crustaceans, such as callianasids, brachyurans and stomatopods were present in the same site. During our samplings, several specimens of callianassids were also collected together with, or near sites where *A. panamensis* was found. This is the first record of the species at Bahía Santa María-La Reforma, Sinaloa.

Ambidexter swifti Abele, 1972

Material examined. One female (CL 3.9 mm), Meléndez Island, 24°48'6"N, 108°3'21"W, sand, 0.1–0.3 m at neap tide, January 18, 2015: (EMU-10586).

Distribution. Recorded from San Benito Island, Baja California and the Gulf of California including Bahía Santa María-La Reforma to Paitilla, Panama and Galapagos Islands (Wicksten and Hendrickx 2003; this study). This species has been found intertidally in sandy substrate (Abele 1972; Wicksten 1991; this study).

Remarks. This is the second record of the species from the Gulf of California, and the first record of a specimen found inhabiting together with a callianasid shrimp (*N. tabogensis*).

Acknowledgements

References

Abele LG (1972) A review of the genus *Ambidexter* (Crustacea: Decapoda: Processidae) in Panama. Bulletin of Marine Science 22(2): 365–380.

Amezcua F, Madrid-Vera J, Aguirre-Villaseñor H (2006) Efecto de la pesca artesanal de camarón sobre la ictiofauna en el sistema lagunar de Santa María-La Reforma, suroeste del Golfo de California. Ciencias Marinas 32(1B): 97–109.

Anker A (2010) A new genus and three new species of alpheid shrimps (Crustacea, Decapoda, Caridea) from the tropical American coasts. Zootaxa 2652: 47–63.

Anker A (2011) Six new species and three new records of infaunal alpheid shrimps from the genera *Leptalpheus* Williams, 1965 and *Fenneralpheus* Felder and Manning, 1986 (Crustacea, Decapoda). Zootaxa 3041: 1–38.

Anker A, Baeza JA, De Grave S (2009) A new species of *Lysmata* (Crustacea, Decapoda, Hippolytidae) from the Pacific coast of Panama, with observations of its reproductive biology. Zoological Studies 48: 682–692.

Anker A, Hurt C, Knowlton N (2007a) Revision of the *Alpheus nuttingi* (Schmitt) complex (Crustacea: Decapoda: Alpheidae), with description of a new species from the tropical eastern Pacific. Zootaxa 1577: 41–60.

Anker A, Hurt C, Knowlton N (2007b) Three transisthmian snapping shrimps (Crustacea: Decapoda: Alpheidae: *Alpheus*) associated with innkeeper worms (Echiura: Thalassematidae) in Panama. Zootaxa 1626: 1-23.

Anker A, Lazarus JF (2015a) Description of two new associated infaunal decapod crustaceans (Axianassidae and Alpheidae) from the tropical Eastern Pacific. Papéis Avulsos de Zoologia 55(8):115–129. https://doi.org/10.1590/0031-1049.2015.55.08

Anker A, Lazarus JF (2015b) On two new species of the shrimp genus *Salmoneus* Holthuis, 1955 (Decapoda, Caridea, Alpheidae) from the tropical eastern Pacific. Zootaxa 3957(5): 520–534.

Anker A, Pachelle PPG (2013) Re-examination of the eastern Pacific and Atlantic material of *Alpheus malleator* Dana, 1852, with the description of *Alpheus wonkimi* sp. n. (Crustacea: Decapoda: Alpheidae). Zootaxa 3637: 412–431. https://doi.org/10.11646/zootaxa.3637.4.2

Anker A, Pachelle PPG (2015) Two new snapping shrimps (Decapoda: Caridea: Alpheidae: *Alpheus*) from the tropical Eastern Pacific. Arthropoda Selecta 24(3): 247–258.

Anker A, Poddoubtchenko D, Wehrtmann IS (2006) *Leslibetaeus coibita*, n. gen., n. sp., a new alpheid shrimp from the Pacific coast of Panama (Crustacea: Decapoda). Zootaxa 1183: 27–41.

Ayón-Parente M, Hendrickx ME, Galván-Villa CM (2015) A new species of the genus *Typton* Costa (Crustacea: Decapoda: Palaemonidae: Pontoniinae) from the eastern tropical Pacific. Zootaxa 3926(3): 430–438. https://doi.org/10.11646/zootaxa.3926.3.7

Ayón-Parente M, Salgado-Barragán J (2013) A new species of the caridean shrimp genus *Ogyrides* Stebbing, 1914 (Decapoda: Ogyrididae) from the eastern tropical Pacific. Zootaxa 3683(5): 589–594. https://doi.org/10.11646/zootaxa.3683.5.7

Bracken-Grissom HD, Felder DL (2014) Provisional revision of American snapping shrimp allied to *Alpheus floridanus* Kingsley, 1878 (Crustacea: Decapoda: Alpheidae) with notes on *A. floridanus africanus*. Zootaxa 3895(4): 451–491. https://doi.org/10.11646/zootaxa.3895.4.1

Castillo-Guerrero JA, González-Medina E, Fernández G (2014) Seabird colonies of the small islands of Bahía Santa María-La Reforma, Sinaloa, Mexico. Waterbirds 37(4): 439–445. https://doi.org/10.1675/063.037.0412

Carvacho A (1979) Les crevettes carides de la mangrove guadeloupéenne. Bulletin du Muséum National d´Histoire Naturelle, Paris. 4e série 1: 445–470.

De Grave S, Fransen CHJM (2011) Carideorum catalogus: the recent species of the dendrobranchiate, stenopodidean, procarididean and caridean shrimps (Crustacea: Decapoda). Zoologische Mededelingen, Leiden 89(5): 195–589.

Edgar RC (2004) MUSCLE: multiple sequence alignment with high accuracy and high throughput. Nucleic Acids Research 32: 1792–1797. https://doi.org/10.1093/nar/gkh340

Fabricius JC (1798) Supplementum Entomologiae Systematicae. Hafniae, Proftet Storch, 572 pp.

Gouy M, Guidon S, Gascuel O (2004) Sea View versión 4: A graphical user interface for sequence alignment and phylogenetic tree building. Molecular Biology and Evolution 27: 221–224. https://doi.org/10.1093/molbev/msp259

Hendrickx ME (2010) A new species of *Glyphocrangon* (Decapoda: Caridea: Glyphocrangonidae) from off the coast of Western Mexico. Zootaxa 2372: 358–366.

Hendrickx ME, Ayón-Parente M (2012) First record of *Prionocrangon* Wood-Mason and Alcock, 1891 (Crustacea: Decapoda: Caridea: Crangonidae) in the East Pacific and description of a new species from western Mexico. Zootaxa 3205: 63–68.

Hendrickx ME, Wicksten MK (2011) New distribution ranges and records of caridean shrimps (Crustacea: Decapoda: Caridea) from the west coast of Mexico. Hidrobiológica 21(1): 26–33.

Hermoso M, Alvarez F (2005) *Synalpheus lani*, a new species from the Mexican Pacific (Crustacea: Caridea: Alpheidae). Proceedings of the Biological Society of Washington 118: 522–527. https://doi.org/10.2988/0006-324X(2005)118[522:SLANSF]2.0.CO;2

Hermoso-Salazar M, Hendrickx ME (2006) Two new species of *Synalpheus* Bate, 1888 (Decapoda, Caridea, Alpheidae) from the SE Gulf of California, Mexico. Crustaceana 78: 1099–1116. https://doi.org/10.1163/156854005775361061

Manning RB, Chace FA (1971) Shrimps of the family Processidae from the Northwestern Atlantic Ocean (Crustacea: Decapoda: Caridea). Smithsonian Contributions to Zoology 89: 1–41. https://doi.org/10.5479/si.00810282.89

Marin I, Anker A (2008) A new species of *Pontonia* Latreille, 1829 (Crustacea, Decapoda, Palaemonidae) associated with sea squirts (Tunicata, Ascidiacea) from the Pacific coast of Panama. Zoosystema 30: 501–515. https://doi.org/10.1093/molbev/msn083

McCarthy C (1996–1998) Chromas vs. 1.45 (32 bit). School of Health Science, Griffith University, Queensland, Australia. http://technelysium.com.au./chromas.html

Miller MA, Pfeiffer W, Schwartz T (2010) Creating the CIPRES Science Gateway for inference of large phylogenetic trees in Proceedings of the Gateway Computing Environments Workshop (GCE), 14 N. 2010, New Orleans, LA, 1–8.

Posada D (2008) JModelTest: phylogenetic model averaging. Molecular Biology and Evolution 25: 1253–1256. https://doi.org/10.1093/molbev/msn083

Posada D, Crandall KA (1998) Model test: Testing the model of DNA substitution. Bioinformatics 14: 817–818. https://doi.org/10.1093/bioinformatics/14.9.817

Rodríguez-Domínguez G, Castillo-Vargasmachuca SG, Pérez-González R, Aragón-Noriega EA (2012) Estimation of the individual growth parameters of the brown crab *Callinectes bellicosus* (Brachyura, Portunidae) using a multi-model approach. Crustaceana 85(1): 55–69. https://doi.org/10.1163/156854012X623700

Ruiz-Luna A, Meraz-Sánchez R, Madrid-Vera J (2010) Abundance distribution patterns of commercial shrimp off northwestern Mexico modeled with geographic information systems. Ciencias Marinas 36(2): 107–120. https://doi.org/10.7773/cm.v36i2.1619

Salgado-Barragán J, Ayón-Parente M, Hendrickx ME (2014) A new species of *Leptalpheus* Williams, 1965 and new records of *L. mexicanus* Ríos and Carvacho, 1983 and *L. hendrickxi* Anker, 2011 (Crustacea: Decapoda: Alpheidae) from the Pacific coast of Mexico. Zootaxa 3835(4): 573–582. https://doi.org/10.11646/zootaxa.3835.4.8

Stamatakis A (2006) RAxML-VI-HPC: Maximum likelihood based phylogenetic analyses with thousands of taxa and mixed models. Bioinformatics 22: 2688–2690. https://doi.org/10.1093/bioinformatics/btl446

Wicksten MK (1991) Caridean and stenopodid shrimp of the Galápagos Islands. In: James MJ (Ed) Galapagos. Plenum Publications, New York, 147–156. https://doi.org/10.1007/978-1-4899-0646-5_7

Wicksten MK, Hendrickx ME (2003) An updated checklist of benthic marine and brackish water shrimps (Decapoda: Penaeoidea, Stenopodidea, Caridea) from the Eastern Tropical Pacific. In: Hendrickx ME (Ed.) Contributions to the Study of East Pacific Crustaceans. 2. [Contribuciones al Estudio de los Crustáceos del Pacífico Este. 2]. Instituto de Ciencias del Mar y Limnología, UNAM, 49–76.

Wicksten MK, Martin JW (2004) A new species of caridean shrimp of the family Stylodactylidae from the eastern Pacific Ocean. Proceedings of the Biological Society of Washington 117: 377–384.

Corrigenda: Iorgu IȘ, Iorgu EI, Puskás G, Ivković S, Borisov S, Gavril VD, Chobanov DP (2016) Geographic distribution of *Gryllotalpa stepposa* (Insecta, Orthoptera, Gryllotalpidae) in South-eastern Europe, with first records for Romania, Hungary and Serbia. ZooKeys 605: 73-82, doi: 10.3897/zookeys.605.8804

Ionuț Ștefan Iorgu[1], Elena Iulia Iorgu[1], Gellért Puskás[2], Slobodan Ivković[3], Simeon Borisov[4], Viorel Dumitru Gavril[5], Dragan Petrov Chobanov[6]

1 *"Grigore Antipa" National Museum of Natural History, Kiseleff Blvd. 1, Bucharest, Romania* **2** *Department of Zoology, Hungarian Natural History Museum, Baross u. 13, H–1088, Budapest, Hungary* **3** *Lovačka 14, 21410 Futog, Serbia* **4** *"St. Kliment Ohridski" University, Faculty of Biology, Dragan Tsankov Blvd. 8, Sofia, Bulgaria* **5** *Institute of Biology, Romanian Academy, Independenței Blvd. 296, Bucharest, Romania* **6** *Institute of Biodiversity and Ecosystem Research, Bulgarian Academy of Sciences, Tsar Osvoboditel Blvd. 1, Sofia, Bulgaria*

Corresponding author: *Ionuț Ștefan Iorgu* (ionut.iorgu@antipa.ro)

Several errors came to our attention after the manuscript was published, which we address here. We regret these and offer our corrections (in font style **Bold**) to help resolve this situation:

First, in the key to identification of South-east European species of genus *Gryllotalpa*, we misplaced the figure citations and these should be corrected as follows:

2	Epiphallus short and wide (less than 2× longer than its widest part), apically more flattened, with a shallow ventral slot (**Fig. 1J**). Distal part of the median vein (♂) opposite to the radial branch 1 (transverse radio-cubital vein) weak and poorly visible (Fig. 1H) .... ***G. gryllotalpa***

–	Epiphallus long and slender (its length 2–2.3× larger than its widest part and over 3 time the width of apex), apically thicker, with a deep slot (**Fig. 1K**). Distal part of the median vein (♂) opposite to the radial branch 1 (transverse radio-cubital vein) well visible, dark (Fig. 1G) **3**

In Figure 1 caption, the following corrections have to be made:

Figure 1. Inner part of hind tibia: **A** *Gryllotalpa unispina* **B** *G. stepposa* **C** *G. gryllotalpa*. Dorsal view of male tegminae: **D** *Gryllotalpa unispina* **E** *G. stepposa* **F** *G. gryllotalpa*. Distal part of the median vein (♂): **G** *Gryllotalpa stepposa* **H** *G. gryllotalpa*. Epiphallus: **I** *Gryllotalpa unispina* **J** *G. gryllotalpa* **K** *G. stepposa*. Locations: *Gryllotalpa unispina* – Letea; *G. stepposa* – Șura Mare; *G. gryllotalpa* – Pașcani (Romania). Scale bars: 1 mm.

Finally, we have to correct a figure citation in the following phrase:

With the current study, we prove the range of this species is significantly wider, covering Romania (thus making the connection with the range of the species in Moldova and Ukraine), all the territory of Bulgaria and Eastern Macedonia (as high as 1000–1200 m asl), North–eastern Greece (on the territory of the district of East Macedonia and Thrace), the lowland of Northern (possibly also Central and South) Serbia, and some areas of Hungary (**Figure 2**).